THE DEVELOPMENT OF A NONEQUILIBRIUM RADIATIVE HEAT TRANSFER COMPUTATIONAL MODEL FOR HIGH ALTITUDE ENTRY VEHICLE FLOWFIED METHODS

Final Report

TEES Report No. 42890-95-1

August 1995

NASA Grant No. NAG 9-680

Leland A. Carlson

Professor of Aerospace Engineering

Texas A&M University

College Station, TX 77843-3141

THE DEVELOPMENT OF A NONEQUILIBRIUM RADIATIVE HEAT TRANSFER COMPUTATIONAL MODEL FOR HIGH ALTITUDE ENTRY VEHICLE FLOWFIELD METHODS

I. Project Synopsis

This final report will attempt to concisely summarize the activities and accomplishments associated with NASA Grant NAG 9-680 and to include pertinent documents in an appendix. The project officially started on June 1, 1993 and officially terminated on May 31, 1995 with a total funding of $55,563.

The project initially had one primary and several secondary objectives. The original primary objective was to couple into the NASA Johnson Space Center (JSC) nonequilibrium chemistry Euler equation entry vehicle flowfield code, INEQ3D, the Texas A&M University (TAMU) local thermodynamic nonequilibrium (LTNE) radiation model. This model had previously been developed and verified under NASA Langley and NASA Johnson sponsorship as part of a viscous shock layer entry vehicle flowfield code. The secondary objectives were: (1) to investigate the necessity of including the radiative flux term in the vibrational-electron-electronic (VEE) energy equation as well as in the global energy equation, (2) to determine the importance of including the small net change in electronic energy between products and reactants which occurs during a chemical reaction, and (3) to study the effect of atom-atom impact ionization reactions on entry vehicle nonequilibrium flowfield chemistry and radiation. For each of these objectives, it was assumed that the code would be applicable to lunar return entry conditions, i.e. altitude above 75 km, velocity greater than 11 km/sec, where nonequilibrium chemistry and radiative heating phenomena would be significant. In addition, it was tacitly assumed that as part of the project the code would be applied to a variety of flight conditions and geometries.

Originally it was anticipated by both JSC and TAMU researchers that this project would be straight forward. Fundamentally, it appeared that the primary tasks were to modify INEQ3D to include radiative

flux in the global and VEE energy equations, make minor modifications in the vibrational coupling, chemistry, and electron-electronic models in INEQ3D, and to make INEQ3D and the nonequilibrium radiation model compatible. Subsequently, the secondary objectives could be studied and a variety of flight conditions investigated to verify the code. Since INEQ3D and its companion Navier-Stokes code had previously been applied to shuttle and other orbital return situations, it was believed that the project could be completed in one year.

Initially, some difficulties were encountered in the development of suitable computational grids and test cases. However, these were overcome by the acquisition of the grid generator, GRIDGEN, and the helpful suggestions and training by Michael An of Lockheed and Chuck Campbell of JSC. Further, it was determined that the changes required in the thermodynamic, chemistry, and vibrational-dissociation coupling models of INEQ3D to make them suitable for lunar return conditions were more extensive than originally believed. Nevertheless the changes were determined and the code was modified to include the TAMU LTNE radiation model in both coupled and uncoupled modes. These changes are discussed Appendix I and the code changes are detailed in Appendix II. The latter also includes standard input files, sample output files, and listings of all modified subroutines and include files. Appendix II along with original user's guides associated with INEQ3D and the TAMU radiation model should enable an individual to utilize the modified code.

Unfortunately, when attempts were made to apply the code to lunar return conditions, significant difficulties were encountered. These problems were associated with extremely slow convergence and frequent numerical instability and solution divergence. As a result, the primary task and challenge of the project shifted to determining methods for achieving acceptable solutions and to discovering the origin of the inefficiency of the code.

Progress at overcoming these difficulties was extremely slow but eventually a procedure was developed which led to reasonable and converged solutions. This process involved a chemical production rate

relaxation procedure and a stop restart process. Initially, solutions were started with a CFL number of two. However, as the solution progressed and fast electron-atom impact ionization reactions became important near the end of the nonequilibrium region when the flow approaches thermal equilibrium, the CFL number had to be reduced. Typically, every 4000 iterations the solution was examined. If instabilities were present then the CFL number was halved and the solution was rerun with the previous restart file from the time before any instabilities appeared. If the solution were stable for two runs at the same CFL number, the CFL number was doubled for the next run. Usually, convergence required approximately 40,000 total iterations, not counting those which had to be discarded because of instabilities; and the final CFL number was about 0.0625.

While this procedure worked, it was not efficient. On the TAMU Cray Y-MP (2-16), radiatively uncoupled cases required 1.084×10^{-4} CPU sec/iteration/grid point while radiatively coupled cases were almost four times slower. For a typical 50 x 70 two dimensional grid, this meant that each solution required over 15,000 seconds per plane. Since INEQ3D requires at least two planes, a typical solution required over eight hours of CPU time. Thus, the present solution algorithm appears to be inefficient at lunar return conditions.

To solve or even propose a solution for this lack of efficiency, the origin of the problem needed to be determined. The solution algorithm in INEQ3D is an implicit approach which for the inviscid terms leads to a diagonal system. Unfortunately, the chemical source terms associated with the nonequilibrium chemistry lead in general in a fully implicit scheme to a full chemical source Jacobian matrix. To decrease the computational effort, INEQ3D uses a diagonal form of the chemical source Jacobian, which for orbital entry conditions appeared to work well.

To examine the impact of diagonalizing the chemical source term, chemical relaxation in quiescent oxygen was examined using both fully implicit and various diagonalization approaches for the chemical source term. These results showed that a negative diagonal scheme could easily become unstable for

reasonable CFL numbers and that a positive diagonal scheme as used in INEQ3D, while stable for small CFL numbers did not necessarily conserve elemental species. It was concluded that for large reaction systems with many species, diagonalization of the chemical source Jacobian could lead to significant time step restrictions and instability.

It should be noted that previously INEQ3D had primarily been applied to orbital return conditions with chemistry models only involving five or seven species and very limited ionization. For lunar return cases, the present studies utilized eleven species and 26 chemical reactions. These reactions contain many involving ionization, and the time scales for the reactions vary widely. The latter, particularly the fast electron-atom impact ionization reactions, tend to make the governing equations numerically stiff and appear to be the origin of the numerical difficulties. Fundamentally, it appears that the diagonalization of the chemical source Jacobian is inappropriate for lunar return conditions. A fully implicit chemistry scheme or a point implicit approach might be more suitable; and consideration could be given to modifying INEQ3D appropriately in the future.

As a result of these difficulties the project required twice as long as anticipated; and only two flowfield conditions and configurations were extensively investigated, both of which were two dimensional. The first configuration was a 10 cm radius cylinder at 11.36 km/sec at 76.42 km, while the second was a two dimensional blunt body approximating the Fire II vehicle at 11.37 km/sec at 81.86 km. While the latter corresponds to the 1632 sec data point of the Fire II flight, the two dimensional body was about one-third size since the computational model was two dimensional and not axisymmetric. Other flight conditions and three dimensional configurations were not studied due to the extensive computational difficulties.

Nevertheless, the code was modified, nonequilibrium radiation gasdynamic coupling was incorporated, methods for obtaining results were developed, and results were obtained. In addition, the secondary objectives were investigated and some significant accomplishments were achieved by the project. These are summarized below and discussed in detail in the Appendices.

II. Accomplishments, Conclusions, and Recommendations

The accomplishments, conclusions, and recommendations resulting from this research project are as follows:

1. The TAMU LTNE air radiation model has been incorporated into the NASA nonequilibrium thermo-chemical inviscid flowfield solver, INEQ3D. The radiation model can be used in either an uncoupled or coupled mode. In the uncoupled mode, the radiative heating to the body is computed after the flowfield is converged and the effects of the radiative losses on the flowfield are not determined. In coupled operation, the consequences of radiative energy losses are included in an iterative manner; and the final solution accounts for the effects of radiative cooling and coupling on the final flowfield solution and radiative heat transfer.

2. The reaction chemistry model and vibration-dissociation coupling model has been modified. It now includes the option of using a $T^pT_v^q$ model for the effective temperature for dissociation reactions, the electron-electronic temperature for electron impact ionization and dissociation reactions, and the forward rate temperature in the local equilibrium constant. In addition, the vibrational relaxation time for individual species has been modified to include a collision cross section cutoff and to account for the diffusive nature of vibrational relaxation.

3. A chemical production rate relaxation process has been incorporated to mitigate the numerical stiffness associated with the onset of very fast reactions such as electron-atom impact ionization.

4. The vibrational-electron-electronic energy equation has been modified to more correctly account for phenomena associated with lunar return. The free electron - heavy particle energy exchange has been modified to include all heavy particles and to utilize collision cross sections appropriate for the collision partner. In addition, terms accounting for the change in average electronic energy due to chemical reactions and for energy losses associated with radiative transfer have been included. Very few models have included

these terms in the vibration-electron-electronic energy equation in the past. Note that the radiative flux term has also been included in the overall energy equation.

5. While the present solution scheme is inefficient for lunar return conditions, procedures have been developed that lead to converged solutions.

6. It appears that changes in electronic energy due to chemical reactions has a negligible effect on the overall vibrational-electron-electronic energy.

7. It has been demonstrated that while a solution may appear to be converged and subsequent iterations may predict only small changes in temperatures and chemical composition, these small changes can cause significant changes in the predicted radiative heat transfer. In the cases studied, changes in flowfield properties between 20,000 and 40,000 iterations were barely visible on plots, but during these iterations the radiation in the 2 - 4 eV range decreased, indicating strong sensitivity to molecular concentrations, while the radiation above 10 eV increased significantly. The latter was due to small changes in electron-electronic temperatures and in the atom, ion, and electron concentrations. Thus, for high altitude lunar return conditions, the predicted radiative heating as well as equation residuals and flowfield properties must be monitored to determine acceptable convergence.

8. Studies have determined that atom-atom impact ionization reactions such as $N + N = N+ + e + N$ might be very important in seeding subsequent electron-impact ionization reactions in air. The importance of these reactions has never been definitively determined. Some investigators have ignored the reactions, assuming them to be unimportant for air where other ionization reactions could seed the flow with electrons, while others have included them using estimates for the reaction rate. These estimates could easily be in error by an order of magnitude. In the current studies decreasing the estimated forward rate by an order of magnitude had only a minor effect, but increasing the rate by an order of magnitude dramatically decreased the shock standoff distance while significantly increasing the amount of the shock layer in thermal and near chemical equilibrium. Consequently, the predicted radiative heat transfer increased by a

factor of approximately 2.5. This strong sensitivity to a single reaction rate and its consequence of a larger equilibrium zone is interesting, particularly considering that in many cases the Fire II experiment has been better predicted using equilibrium methods in regions where it would be anticipated that the flow is almost entirely in nonequilibrium. **Thus, it is believed that further studies of the sensitivity of radiative heating to "estimated" reaction rates are needed and that particular emphasis should be placed upon those reactions, such as atom-atom impact, which seed the flow with electrons prior to electron avalanche.**

9. Comparison of the present results with those obtained previously using the TAMU radiation model in a viscous shock layer code for similar flight conditions indicate differences in the electron-electronic temperature in the nonequilibrium region. While all the codes used identical chemistry, the previous codes used either a three temperature (T, T_v, $T_{e\text{-}elec}$) or a multiple vibrational temperature (T, T_{vN2}, T_{vO2}, ..., $T_{e\text{-}elec}$) model with a MCVDV vibration dissociation coupling model. The present method uses only two temperatures (T, $T_{vib\text{-}e\text{-}elec}$) and a Park like vibration dissociation coupling model. In general, the present method yielded electron-electronic temperatures in the nonequilibrium zones lower than the MCVDV methods. **Thus, it appears that vibration-dissociation coupling is important even at lunar return conditions and that further study of the influence and accuracy of vibration-dissociation models on radiative heat transfer in this flight regime is needed.**

10. Studies to determine the importance of including radiative flux terms in both the global energy equation and in the vibration-electron-electronic energy equation were inconclusive. **Further studies of the importance of the radiative flux term in the VEE equation are needed.**

11. It is believed that the origin of the convergence and stability difficulties encountered at lunar return conditions is due to the use of a diagonal implicit scheme to approximate the chemical source Jacobian. For lunar return conditions involving many species, significant ionization and radiation, and reactions having disparate time scales, it may be necessary to use either fully implicit chemistry or a point implicit

approach. Further studies on methods to efficiently handle the ionization chemistry associated with lunar return conditions are needed.

III. Personnel

The individuals who have been associated with the project are as follows:

Leland A. Carlson, Professor of Aerospace Engineering -- Dr. Carlson served as the principal investigator for the project. At various times, Dr. Carlson was partially supported by the project.

Christopher J. Roy, Graduate Research Assistant -- Chris Roy joined the project at its inception and earned his Masters' degree using research associated with the project for his thesis.

IV. Acknowledgments

The technical monitors for this project were Dr. Carl Scott and Mr. Joe Caram, Aerosciences Branch, NASA Johnson Space Center. Their assistance, comments, and helpful suggestions contributed significantly to the project and is truly appreciated. Further, Dr. Luen Tam and Michael An of Lockheed along with Chuck Campbell of NASA JSC provided invaluable assistance with the INEQ3D flowfield solver and the GRIDGEN grid generator. The individuals associated with this project wish to express their heartfelt appreciation to all of these NASA JSC and Lockheed personnel.

APPENDIX I

VIABILITY OF THE DIAGONAL IMPLICIT ALGORITHM FOR HYPERSONIC FLOWFIELDS WITH FINITE RATE CHEMISTRY

Christopher J. Roy

VIABILITY OF THE DIAGONAL IMPLICIT ALGORITHM FOR HYPERSONIC FLOWFIELDS WITH FINITE RATE CHEMISTRY

A Thesis

by

CHRISTOPHER JOHN ROY

Submitted to the Office of Graduate Studies of
Texas A&M University
in partial fulfillment of the requirements for the degree of

MASTER OF SCIENCE

December 1994

Major Subject: Aerospace Engineering

ABSTRACT

Viability of the Diagonal Implicit Algorithm for Hypersonic Flowfields with Finite Rate Chemistry. (December 1994)

Christopher John Roy, B.S.E., Duke University;

M.S., Texas A&M University

Chair of Advisory Committee: Dr. Leland A. Carlson

The diagonal implicit algorithm has been examined for high speed, moderate density flows. In this flight regime, nonequilibrium thermal, chemical, and radiative effects are important and the determination of these finite rate processes, coupled with a three dimensional flowfield solver, can require large computational resources. In order to minimize computational costs, Imlay et al. proposed a diagonal implicit solution algorithm. For the extreme conditions of planetary return examined in this report, the avalanche ionization phenomenon gave rise to fast chemical reactions in the stagnation region. The diagonal implicit algorithm was found to give unsatisfactory convergence rates in this region due to numerical instabilities, even at reduced CFL numbers. Thus, the diagonal implicit approximation is not feasible for flows with fast chemical reactions. In addition, changes in the atom impact ionization rates for nitrogen were found to significantly affect the flowfield properties and radiative heat transfer.

ACKNOWLEDGEMENTS

The author would like to thank Dr. Leland Carlson for his guidance and patience during the writing of this thesis. Thanks go to project monitors Dr. Carl Scott and Joe Caram of NASA-Johnson Space Center as well as Dr. Luen Tam of Lockheed, whose flowfield code formed the basis for this research. Special thanks to Michael An of Lockheed and Chuck Campbell of NASA-JSC, who provided invaluable assistance with the INEQ3D flowfield solver. The author would also like to thank Dr. Jack Edwards of North Carolina State University for the discussions on numerical stiffness of reacting flows.

TABLE OF CONTENTS

TABLE OF CONTENTS (CONTINUED)

LIST OF TABLES

LIST OF FIGURES

LIST OF FIGURES (CONTINUED)

LIST OF FIGURES (CONTINUED)

LIST OF FIGURES (CONTINUED)

LIST OF FIGURES (CONTINUED)

NOMENCLATURE

A,B,C	inviscid flux Jacobians
C_p,C_v	specific heat at constant pressure, volume
D_k	Damkohler number
F,G,H	inviscid flux vectors
F^+,F^-	positive, negative components of the inviscid flux
G	Gibb's free energy
G°	Gibb's free energy evaluated at 1 atmosphere
I	identity matrix
J	Jacobian of the coordinate transformation
K_c	equilibrium constant based on concentrations
K_p	equilibrium constant based on partial pressures
M	molecular weight
Q	vector of primitive variables
Q	partition function
Q_{rad}	radiative source vector
R	universal gas constant
$R_{f,b}$	forward, backward reaction rates
$\Re$	residual
T	temperature
T_a	Park's effective temperature
Vol	cell volume
a_f	frozen speed of sound
c	mass fraction
e	internal energy per unit mass
g_i	degeneracy of electronic level i
h°	heat of formation
k	Boltzmann constant
$k_{f,b}$	forward, backward reaction rate coefficient
m	mass per particle
n	number density
p	pressure
q	temperature exponent for Park's TTV model
q_r	radiative flux
u,v,w	cartesian components of velocity
x,y,z	cartesian coordinates
$[x]$	molar density of species x
Δ	shock standoff distance
θ_{lim}	flux limiter
θ_v	characteristic temperature of vibration
Λ	diagonal matrix of eigenvalues
χ	chemical rate relaxation factor

NOMENCLATURE (CONTINUED)

Ω	chemical source vector
δ_{ROE}	Roe's higher order characteristic based flux
ϵ_i	excitation energy of electronic level i
μ	reduced molecular weight
ν', ν''	stiochiometric coefficients of reactants, products
ν_{es}	effective collision frequency
ξ, η, ζ	curvilinear coordinates
ρ	density
σ	effective cross section for vibrational relaxation
σ_{es}	effective energy exchange cross section
τ	average vibrational relaxation time
$\dot{\omega}$	mass production rate

Subscripts

T	translational-rotational
V	vibrational-electron-electronic
e	free electron
el	electronic
rot	rotational
s	species s
tr	translational
v	vibrational

Superscripts

MW	Millikan and White
P	Park
n,n+1	iterative time level

INTRODUCTION

In the future it will be increasingly necessary to accurately model high speed low density flows since this flight regime is encountered in situations such as aeroassisted orbital transfer and aerobraking for planetary/lunar return. During such maneuvers, significant energy savings can be achieved via a combination of aerobraking and retrobraking.[1] Originally, in the mid-1980's, interest in this flight regime focused on Orbital Transfer Vehicle (OTV) maneuvers for achieving the large drop in energy associated with changing from high Earth orbit (HEO) to low Earth orbit (LEO). More recently, however, NASA has been concerned with the high speed aerobraking associated with Martian and lunar return.

One method of aeroassisted orbital transfer involves a series of high altitude passes to change from a hyperbolic re-entry or elliptical orbital trajectory to the desired orbit. This method is energy efficient and results in low thermal and structural loads to the vehicle; but the large amount of time required for such multipass aerobraking precludes it from being used for manned missions, where a premium is placed on minimizing mission time. A more time efficient alternative is aerocapture where the vehicle makes a single pass deep into the planet's atmosphere. Vehicles in this flight regime have large velocities at low density altitudes, causing chemical, thermal and radiative nonequilibrium phenomena to become important. These nonequilibrium processes must be properly modeled in order to accurately predict the heat transfer and aerodynamic forces acting on the entry vehicle.

Journal model is *AIAA Journal.*

Numerical solutions to hypersonic reacting flows can encounter numerical stiffness difficulties due to the disparity in the chemical time scale vs. the convective time scale. To overcome this stiffness problem, many researchers employ implicit solution schemes which allow large computational time steps. These schemes can be computationally intensive per iteration since the procedure requires computation of both flux and chemical source Jacobians. To reduce the per iteration workload, Imlay and Eberhardt[2] introduced a diagonal implicit algorithm which approximates the chemical source Jacobian by a diagonal matrix and is significantly less computationally intensive.

The main goal of this thesis is to examine the applicability of the diagonal implicit algorithm for nonequilibrium flowfields where radiative heat transfer is important. In addition, there are a number of secondary goals. In a two temperature model, some investigators[3,4] argue that the energy loss or gain due to radiative phenomena should be included not only in the global energy conservation equation, but also in the vibrational-electron-electronic (VEE) energy equation. In addition, when a chemical reaction occurs, there is generally a small net change in electronic energy between the products and reactants. The effect of including these two phenomena in the VEE energy equation will also be evaluated. Finally, the effect of atomic impact ionization on the electron avalanche phenomenon will be examined, since it is included by some investigators and ignored by others.

In this investigation, the flowfield solver is INEQ3D, an inviscid, upwinding scheme developed by Tam.[5] This hypersonic CFD code includes both thermal nonequilibrium effects and finite rate chemistry. For the radiative heat transfer a

nonequilibrium radiative transport model developed at Texas A&M University (TAMU) by Gally and Carlson[6,7] is utilized; and, as part of this investigation, this radiative model has been coupled with INEQ3D.

Test Configurations

Two flowfield conditions and configurations are investigated in this study, both of which are two dimensional. The first configuration is a 10 centimeter radius cylinder at a free stream velocity of 11.36 km/sec (Mach 40.5) and an altitude of 76.42 kilometers. The second configuration is a two dimensional blunt body approximating the Fire 2 radiation experiment[8] vehicle, and the flowfield conditions correspond to conditions at 1632 seconds in the Fire 2 flight. At that time, the velocity was 11.37 km/sec at an altitude of 81.86 kilometers, corresponding to a free stream Mach number of 39.0. However, the two dimensional body is modified to one third scale to account for the larger shock stand-off distance associated with two dimensional versus three dimensional flow. Since the conditions for the cylinder occur at a lower altitude and hence a higher density, the first case will be used for the coupled radiation calculations.

BACKGROUND

There are three main types of hypersonic low density continuum flows: equilibrium, frozen, and nonequilibrium flow, whose regimes are determined by the relative magnitude of the flowfield time scale versus the chemical and/or thermal time scale. The flowfield time scale is related to the time it takes a particle to traverse the region of interest; and for the blunt bodies considered here, the flowfield time scale, or particle residency time, is approximately the time required for a particle to travel from the shock to the vicinity of the body surface. On the other hand, the thermal time scale is related to the amount of time it takes for the internal modes of energy to equilibrate with each other, while the chemical time scale is different for each chemical reaction and is related to the rate at which the chemical reactions, both forward and backward, take place.

In equilibrium flow, a particle undergoes a large number of collisions as it traverses the flowfield, which allows the chemistry and temperatures to adjust almost instantaneously to large perturbations. In this situation, the chemistry is simply a function of two state variables and all energy modes can be characterized by a single temperature. These energy modes include the random kinetic energy of heavy particles (heavy particle translational energy), the random kinetic energy of free electrons (free electron energy), the energy of bound electrons (electronic energy) and the energy associated with the rotation and vibration of polyatomic species (rotational and vibrational energy).

Chemically frozen flow occurs when a particle encounters very few collisions as

it passes through the flowfield, and as a result the chemical composition remains relatively constant during large flowfield perturbations such as shock waves. In a thermally frozen flow, the vibrational and electron-electronic temperatures are often held constant, while the translational-rotational temperature is permitted to vary. In this case, since the translational and rotational modes take only a few collisions to become excited, they are usually considered to be in equilibrium with each other and described by a single temperature, T. Note that when the temperature associated with an energy mode is assumed constant, the net energy exchange with that mode is considered to be zero.

When the chemical and/or thermal relaxation times are approximately the same order of magnitude as the particle residency time, the flow is said to be in nonequilibrium. In such a flow, it is important to account for the details of the collisional processes in order to correctly model the energy exchange between internal energy modes.

Furthermore, at high temperatures, the internal energy modes of the particles can become excited, which creates new degrees of freedom that can accept energy. At low temperatures, a gas has only two modes of energy, translational and rotational. Both monatomic and polyatomic particles have translational energy associated with the random kinetic energy of the gas (i.e. the classical concept of temperature). Since the particles are free to translate in three different directions, there are three degrees of freedom associated with this mode. Polyatomic particles can also store significant amounts of energy in the rotation of the molecule, and when fully excited, which typically occurs at temperatures over 300 K, the rotational excitation for diatomic particles such as N_2,

N_2^+, NO, etc. adds only two degrees of freedom since rotation about the internuclear axis has a very small moment of inertia. At still higher temperatures, the diatomic species vibrate in a manner analogous to two masses connected by a spring which adds two additional degrees of freedom. At even higher temperature, the electrons bound to particle nuclei are excited to levels above the electronic ground state, which adds two more degrees of freedom.

When all of the energy modes of the particles are in equilibrium with each other, their internal energies can be characterized by a single temperature. However, particles moving through a large flowfield disturbance such as a shock wave must obey total energy conservation, and thus, across a shock wave, the large drop in directed kinetic energy of the free stream particles must be distributed into the internal energy modes. Since the translational energy mode of a gas requires only one or two collisions, or mean free paths, to become excited, most of the free stream kinetic energy is absorbed into this mode during the passage throughout the shock wave. Further, since it takes on the order of only ten collisions to excite molecules rotationally, the rotational energy mode is almost always considered to be in equilibrium with the translational mode.

On the other hand, the vibrational and electronic modes take significantly longer to become excited due to the geometry of vibrational collisions and the inefficient energy exchange between bound electrons and heavy particles. Although collisions between bound and free electrons are more efficient that those between bound electron and heavy particles, significant numbers of free electrons occur only at very high temperatures and usually only after a phenomena called avalanche ionization, which will be discussed in

detail in a later section. This disparity between the excitation rates of the internal modes of energy means that vibrational and electron-electronic energy cannot be characterized by the same temperature as translational energy.

Thermal nonequilibrium occurs when the temperatures characterizing the various energy modes are different. Thus, the vibrational energy mode is commonly described by a separate temperature, T_v, and the electronic energy by the electronic temperature, T_e. When free electrons are present in the gas, the efficient energy exchange between the free and bound electrons allows the random kinetic energy of the free electrons to be in thermal equilibrium with the bound electrons. Thus the free electron energy can also be characterized by the electronic temperature, T_e. Note that the temperatures associated with the various modes of energy are defined such that they are equal to one another at thermal equilibrium, which occurs when there is no net energy transfer from one mode to another.

In addition to simple vibrational or electronic excitation, these modes can receive enough energy during a collision to break the molecular bond between the vibrating particles and cause dissociation or to cause a bound electron to break away from its nucleus (ionization). These and other types of chemical reactions complicate the determination of the thermodynamic state of the gas. Instead of simply having the diatomic nitrogen and oxygen found in free stream air, the chemical composition of the gas changes as it moves through the flowfield. Further, the flowfield dynamics affect the amount of energy exchanged in the relaxation and chemical processes, which in turn affects the flowfield. Thus, there can be strong chemical- and thermal-gasdynamic

coupling in nonequilibrium flows.

In regions of local thermodynamic equilibrium (LTE), the allocation of electronic excitation is described by a Boltzmann distribution. However, for atomic species there is a large energy gap between the lower two or three electronic energy levels (called ground states) and the upper energy levels (excited states). In low density flows, there are more low energy collisional partners available to excite the electrons within the ground or excited states or to ionize atoms with electrons in excited states than there are high energy collisional partners available to cause the electrons to transition from the ground to the excited states or to ionize directly from the ground states. Thus, in such flows ionization from the excited states occurs rapidly,[7] and the populations of the ground and excited states may not necessarily follow a Boltzmann distribution. This phenomenon is known as Local Thermodynamic Nonequilibrium (LTNE), and it is included in the TAMU radiation model for both atoms and molecules.

FLOWFIELD THEORY

The flowfield solver used in the present studies is the inviscid, nonequilibrium three dimensional code INEQ3D developed by Tam,[5] and the following discussion closely follows his flowfield theory development. This code uses a cell centered finite volume discretization of the governing partial differential equations with a high order total variant diminishing (TVD) scheme based on Van Leer's flux-vector splitting (FVS) and Roe's characteristic based flux-difference splitting (FDS). The code is currently capable of handling up to an eleven species air model with an arbitrary number of chemical reactions. The matrix solver utilizes a Lower-Upper Symmetric Gauss-Seidel (LU-SGS) implicit scheme based on the work of Jameson and Turkel.[9]

Governing Equations

The Euler equations given in generalized curvilinear coordinates (ξ, η, ζ) for chemically reacting flows are:

$$\frac{\partial \boldsymbol{Q}}{\partial \tau} + \frac{\partial \boldsymbol{F}}{\partial \xi} + \frac{\partial \boldsymbol{G}}{\partial \eta} + \frac{\partial \boldsymbol{H}}{\partial \zeta} = \boldsymbol{\Omega} \qquad (1)$$

The vector **Q** is composed of the conservative variables, **F**, **G**, and **H** are the inviscid flux vectors, and $\boldsymbol{\Omega}$ is the source vector which includes chemical production terms, energy coupling between internal modes, and energy gained or lost due to inelastic chemical reactions.

The above vectors are defined as follows:

$$Q = \frac{1}{J}\begin{Bmatrix} \rho_1 \\ \rho_2 \\ \vdots \\ \rho_{ns-(q+1)} \\ \rho \\ \rho u \\ \rho v \\ \rho w \\ \rho e \\ \rho e_v \end{Bmatrix}, \quad F = \frac{|\nabla\xi|}{J}\begin{Bmatrix} \rho_1 \tilde{u} \\ \rho_2 \tilde{u} \\ \vdots \\ \rho_{ns-(q+1)} \tilde{u} \\ \rho \tilde{u} \\ \rho u \tilde{u} + \xi_x p \\ \rho v \tilde{u} + \xi_y p \\ \rho w \tilde{u} + \xi_z p \\ (\rho e + p)\tilde{u} \\ \rho e_v \tilde{u} \end{Bmatrix}$$

$$G = \frac{|\nabla\eta|}{J}\begin{Bmatrix} \rho_1 \tilde{v} \\ \rho_2 \tilde{v} \\ \vdots \\ \rho_{ns-(q+1)} \tilde{v} \\ \rho \tilde{v} \\ \rho u \tilde{v} + \eta_x p \\ \rho v \tilde{v} + \eta_y p \\ \rho w \tilde{v} + \eta_z p \\ (\rho e + p)\tilde{v} \\ \rho e_v \tilde{v} \end{Bmatrix}, \quad H = \frac{|\nabla\zeta|}{J}\begin{Bmatrix} \rho_1 \tilde{w} \\ \rho_2 \tilde{w} \\ \vdots \\ \rho_{s-(q+1)} \tilde{w} \\ \rho \tilde{w} \\ \rho u \tilde{w} + \zeta_x p \\ \rho v \tilde{w} + \zeta_y p \\ \rho w \tilde{w} + \zeta_z p \\ (\rho e + p)\tilde{w} \\ \rho e_v \tilde{w} \end{Bmatrix} \quad \text{(2a) - (2e)}$$

$$\Omega = \begin{Bmatrix} \dot{\omega}_1 \\ \dot{\omega}_2 \\ \vdots \\ \dot{\omega}_{s-(q+1)} \\ 0 \\ 0 \\ 0 \\ 0 \\ 0 \\ Q_{T-V} + Q_{T-e} + \sum \dot{n}_{e,s} \hat{I}_s - \sum \dot{\omega}_s \hat{D}_s \end{Bmatrix}$$

The contravariant velocities are given by

$$\begin{pmatrix} \tilde{u} \\ \tilde{v} \\ \tilde{w} \end{pmatrix} = \begin{pmatrix} \xi_x & \xi_y & \xi_z \\ \eta_x & \eta_y & \eta_z \\ \zeta_x & \zeta_y & \zeta_z \end{pmatrix} \begin{pmatrix} u \\ v \\ w \end{pmatrix} \tag{3}$$

where ξ, η, and ζ refer to the curvilinear coordinate directions. The Jacobian of the transformation, J, is defined by:

$$J = \frac{\partial(\xi, \eta, \zeta)}{\partial(x, y, z)} \tag{4}$$

Elemental species conservation allows for the removal of q equations from the species conservation equations, where q is the number of elementary particles. For the eleven species air model, q = 2 since air is fundamentally composed of nitrogen and oxygen atoms. Further, assuming there are no external magnetic fields present, another equation may be eliminated by imposing local charge neutrality. Therefore, instead of solving for ns species conservation equations where ns is the total number of species, only ns - (q + 1) equations have to be solved.

For a two temperature model, the governing equations are supplemented by two energy relations, discussed later, as well as the equation of state given by

$$p = \sum_{s=hp} \rho_s \frac{R}{M_s} T + \rho_{e^-} \frac{R}{M_{e^-}} T_V \tag{5}$$

where hp denotes heavy particles only and e^- the free electrons.

The variables in the above equations can be non-dimensionalized as follows:

$$x=\frac{\bar{x}}{\bar{L}};\ y=\frac{\bar{y}}{\bar{L}};\ z=\frac{\bar{z}}{\bar{L}};\ \tau=\frac{\bar{t}}{\bar{L}}\sqrt{\frac{\bar{p}_\infty}{\bar{\rho}_\infty}};$$

$$u=\frac{\bar{u}}{\sqrt{\frac{\bar{p}_\infty}{\bar{\rho}_\infty}}};\ v=\frac{\bar{v}}{\sqrt{\frac{\bar{p}_\infty}{\bar{\rho}_\infty}}};\ w=\frac{\bar{w}}{\sqrt{\frac{\bar{p}_\infty}{\bar{\rho}_\infty}}};\ Q_{rad}=\frac{\bar{Q}_{rad}}{\bar{p}_\infty}\sqrt{\frac{\bar{\rho}_\infty}{\bar{p}_\infty}}\bar{L}; \tag{6}$$

$$\rho=\frac{\bar{\rho}}{\bar{\rho}_\infty};\ \rho_i=\frac{\bar{\rho}_i}{\bar{\rho}_\infty};\ p=\frac{\bar{p}}{\bar{p}_\infty};\ T=\frac{\bar{T}}{\bar{T}_\infty};\ T_v=\frac{\bar{T}_v}{\bar{T}_\infty};$$

$$e=\frac{\bar{e}}{\frac{\bar{p}_\infty}{\bar{\rho}_\infty}};\ e_v=\frac{\bar{e}_v}{\frac{\bar{p}_\infty}{\bar{\rho}_\infty}};\ h=\frac{\bar{e}+\bar{p}/\bar{\rho}}{\frac{\bar{p}_\infty}{\bar{\rho}_\infty}};\ C_p=\frac{\bar{C}_p}{\frac{R_u}{M_\infty}}$$

where the overbar denotes dimensional quantities.

Solution Scheme

The present solution scheme utilizes upwind-differencing and flux splitting to determine the inviscid fluxes at the cell interfaces. The first order fluxes at the interfaces are of the form

$$F^1_{i+\frac{1}{2}}=F^+(Q)+F^-(Q) \tag{7}$$

where the interface flux is split using Van Leer flux-vector splitting[10] (FVS), which yields continuously differentiable fluxes at sonic and stagnation points. Here Q^- and Q^+ are determined via upwind extrapolation.

The higher order terms of the interface fluxes are then computed by using Roe's characteristic based flux-difference splitting[11] (FDS). This higher order term is then

added to the first order FVS term to get the total flux at the interface

$$F^H_{i+\frac{1}{2}} = F^1_{i+\frac{1}{2}} + \delta^H_{Roe} \tag{8a}$$

where,

$$\delta^H_{Roe} = \frac{1}{2} R \theta_{lim} |\Lambda| R^{-1} \frac{(Q_R - Q_L)}{\delta} A . \tag{8b}$$

Here, R and R^{-1} are the matrices composed of the right and left eigenvectors of A respectively, and **A** is the matrix whose diagonal terms are the eigenvalues. While the present method includes options for a number of flux limiters and TVD schemes, results presented in this report use Chakravarthy and Osher's[12] formulation for the flux limiter and a fully one-sided, second-order upwinding TVD scheme.

The governing equations are then formulated into an implicit solution scheme, which in delta notation is given by

$$[I\frac{Vol}{\delta t} + (D_\xi A + D_\eta B + D_\zeta C)]\Delta Q - \frac{\partial \Omega}{\partial Q}\Delta Q = -\Re \tag{9}$$

where D_ξ, D_η, and D_ζ are the difference operators approximating the derivatives ∂_ξ, ∂_η, and ∂_ζ. The term $\Re$ is the residual given by equation (1) without the time derivative, and **A**, **B**, and **C** are the inviscid flux Jacobians

$$A = \frac{\partial F}{\partial Q}; \quad B = \frac{\partial G}{\partial Q}; \quad C = \frac{\partial H}{\partial Q} \tag{10}$$

which are linearized by the method of Jameson[9,13] and result in diagonal matrices for the inviscid flux Jacobians. The matrix solver utilizes a block LU decomposition coupled

with forward and backward sweeps.

Following the work Imlay,[2] the chemical source Jacobian, Ω, is approximated by a diagonal matrix. The implications of this approximation will be examined in a later section.

In order to include radiative coupling, the following radiative source term must be added to the right hand side of equation (1):

$$Q_{rad} = \begin{bmatrix} 0 \\ 0 \\ \vdots \\ 0 \\ -\dfrac{\partial q_{r,tot}}{\partial n} \\ -\dfrac{\partial q_{r,v}}{\partial n} \end{bmatrix} \tag{11}$$

where q_r is the radiative flux and n is normal to the body (η direction). Further, to couple the radiation in a fully implicit manner, the radiative flux at time level n+1 in the implicit procedure should be formulated as

$$Q_{rad}^{n+1} = Q_{rad}^{n} + \left.\frac{\partial Q_{rad}}{\partial Q}\right|_{n} \Delta Q \tag{12}$$

This approach would add a $-(\partial Q_{rad}/\partial Q)\Delta Q$ term to the left hand side of equation (9). However, since the radiative terms are only updated approximately every 500 iterations, it is approximately correct to neglect the radiative Jacobian, $\partial Q_{rad}/\partial Q$. This approximation simplifies the implicit procedure while retaining the effect of radiation coupling in the final converged solution via the inclusion of Q_{rad} on the right hand side of the solution scheme presented in equation (9). The radiation calculations are therefore

only loosely coupled with the flowfield solver during the iterative solution process.

Two Temperature Model

In general, nonequilibrium flows can be modeled with three distinct temperatures. One temperature characterizes the translational and rotational energy of the heavy particles (T), another temperature describes the vibrational energy of the molecules (T_v), and the third temperature represents both the electronic energy of the bound electrons and the translational energy of the free electrons (T_e). Park[14] notes that there is strong coupling between the N_2 vibrational energy mode and the free electron translational energy; and it is known that for atoms there is rapid equilibration between the low electronic states (ground states) and the free electrons. This strong coupling and possible equilibration between the vibrational, electron, and electronic energy modes suggests that for many cases their energies can be approximately represented by a single temperature, T_V.

Gnoffo[15] points out that although it may be important to characterize each vibrational species with its own temperature, such modeling is limited by the lack of knowledge concerning vibration-vibration coupling between different vibrating species. Further, McGough[16] has examined the use of multiple vibrational temperatures with the assumption of no vibration-vibration coupling between diatomic species and found that results with a single vibrational temperature match experimental data better than those obtained with multiple vibrational temperatures without vibration-vibration coupling.

Thus, in the current work, a single vibrational temperature is used to characterize

the vibrational energy of all diatomic species. This model is used due to its relative simplicity as well as the limited information available on vibration-vibration coupling. Further, following the logic of Park above, the vibrational energy is assumed to be in equilibrium with both the electronic energy and the translational energy of the free electrons; and thus these modes are characterized by a single vibrational-electron-electronic temperature, T_V. Note that the capital V subscript refers to vibrational, free electron, and electronic energy modes whereas the lower case υ denotes the vibrational mode only. Finally, the translational and rotational modes of all species are characterized by a single temperature, T.

Thermodynamic Model

In a thermally perfect gas, the internal energy and specific heats are found for each species by summing over the contributions from all the energy modes, but for cases with thermal nonequilibrium, the internal energies are functions of two or more temperatures. Thus, the total internal energy for the two temperature model is defined as

$$e = e_{tr} + e_{rot} + e_V + \Delta e^o + \frac{1}{2}\vec{u}\cdot\vec{u}\,. \qquad (13)$$

The term Δe^o is the heat of formation accounting for the energy stored and released in chemical reactions. The translational and rotational contributions are determined by assuming these modes are fully excited with each degree of freedom contributing ½kT. The quantity e_V is the vibrational-electron-electronic energy given by

$$e_V = \frac{\rho_{e^-} e_{e^-} + \sum_{s=hp} \rho_s (e_{v,s} + e_{el,s})}{\rho} \qquad (14)$$

where e_{e^-}, e_v, and e_{el} are the free electron, vibrational, and electronic energies respectively, which can be found from statistical mechanics via

$$e_v = \frac{\partial (\ln Q_v)}{\partial T} \qquad (15a)$$

and

$$e_{el} = \frac{\partial (\ln Q_{el})}{\partial T} + \frac{C_4}{3} T_e^3 - \frac{C_5}{T_e} . \qquad (15b)$$

The vibrational and electronic partition functions Q_v and Q_{el} are given by

$$Q_v = \frac{\theta_v}{\exp^{-\theta_v / T_e} - 1} \qquad (16a)$$

and

$$Q_{el} = g_0 + g_1 \exp^{-\epsilon_1 / T_e} + g_2 \exp^{-\epsilon_2 / T_e} . \qquad (16b)$$

In equation (15b), C_4 and C_5 are curve fit constants that account for electronic energy levels higher than the third electronic state. See the Appendix for tabulated values.

The thermodynamic quantity, Gibb's free energy, can be used to calculate effective temperatures for reaction rates and is needed for computing the equilibrium constant, K_C, associated with each chemical reaction. In the present model its determination utilizes the curve fits of Gupta[17] to get the total free energy. Then the vibrational and rotational contributions are calculated via partition functions and

subtracted from the total value. These results are then used to determine curve fits of the translational, rotational, and heat of formation contributions to the total free energy as a function of temperature. This procedure has been performed for each heavy particle species as well for the free electrons, and the curve fits are of the form:

$$\left.\frac{G}{RT}\right|_{tr+rot+\Delta h^\circ} = C_1*(1-\ln T) + \frac{C_2}{T} - C_3 \qquad (17)$$

The constants C_1, C_2, and C_3 are given in the Appendix for each species.

CHEMICAL KINETICS

The nonequilibrium chemical and thermal effects enter into the governing equations through the energy exchange and loss terms in the energy equations and through the species production rates in the species continuity equations. With the radiative coupling terms, the global energy conservation equation in Cartesian coordinates is given by:

Global Energy Conservation

$$\frac{\partial \rho e}{\partial t} + \frac{\partial (\rho e + p) u}{\partial x} + \frac{\partial (\rho e + p) v}{\partial y} + \frac{\partial (\rho e + p) w}{\partial z} = -\frac{\partial q_{r,tot}}{\partial n} \quad (18)$$

The first term on the left hand side is the rate of change of total energy per unit volume. The next three terms are the convective energy fluxes, and the term on the right hand side is the rate of energy loss or gain due to all radiative processes.

With a two temperature model, it is necessary to insure the conservation of the energies characterized by the vibrational-electron-electronic temperature, T_V. Thus the vibrational-electron-electronic (VEE) energy equation is given as:

Vibrational-Electron-Electronic Energy Conservation

$$\frac{\partial \rho e_V}{\partial t} + \frac{\partial \rho e_V u}{\partial x} + \frac{\partial \rho e_V v}{\partial y} + \frac{\partial \rho e_V w}{\partial z} = Q_{T-V} + Q_{T-e}$$

$$- \sum_{s=6}^{10} \dot{n}_{e,s} \hat{I}_s + \sum_{s=mol} \dot{\omega}_s \hat{D}_s + \sum_{s=1}^{10} \dot{\omega}_s e_{el,s} - \frac{\partial q_{r,V}}{\partial n} \quad (19)$$

The first term on the left hand side of equation (19) is the rate of change of the vibrational-electron-electronic energy per unit volume, and the remaining terms on the

left hand side account for the convective flux of vibrational-electron-electronic energy. Terms one and two on the right hand side account for translational-vibrational energy exchange and translational-free electron energy exchange, respectively, due to elastic collisions. These terms will be discussed in detail in the subsection entitled Relaxation Processes. The third term on the right hand side accounts for the loss of free electron energy due to electron impact ionization, while term four accounts for the change in average vibrational energy due to dissociation or recombination. The fifth term models the change in average electronic energy due to chemical reactions, and the final term is the rate of VEE energy loss due to radiative processes involving electron transitions and vibrational energy changes. The current radiation coupling model assumes that this radiative term is approximately equal to the total radiative term found in the global energy equation. Terms three through six are discussed in a later subsection labeled Chemical and Radiative Coupling.

For the present studies, an air model composed of eleven species, N_2, O_2, NO, NO^+, N_2^+, O_2^+, N^+, O^+, N, O, and e^-, along with the 26 chemical reactions listed in Table I is used. Most of this model is based on the work of Park,[18,19,20] but modifications include changing the electron impact atomic ionization rates to newly derived values of Carlson and Gally[6,7,21] and using the heavy particle atom ionization rates of Carlson.[22]

Table I. Reaction System for 11 Species Air

	Reaction					A		B	E
1	N_2	+M1	=N	+N	+M	3.00	$x10^{22}$	-1.6	113200
2	N_2	+M2	=N	+N	+M	7.00	$x10^{21}$	-1.6	113200
3	O_2	+M1	=O	+O	+M	1.00	$x10^{22}$	-1.5	59500
4	O_2	+M2	=O	+O	+M	2.00	$x10^{21}$	-1.5	59500
5	NO	+M3	=N	+O	+M	1.10	$x10^{17}$	0.0	75500
6	NO	+M4	=N	+O	+M	5.00	$x10^{15}$	0.0	75500
7	O	$+e^-$	$=O^+$	$+e^-$	$+e^-$	6.35	$x10^{15}$	0.0	106200
8	N	$+e^-$	$=N^+$	$+e^-$	$+e^-$	5.08	$x10^{16}$	0.0	121000
9	NO	+O	=N	$+O_2$		8.40	$x10^{12}$	0.0	19450
10	N_2	+O	=NO	+N		6.40	$x10^{17}$	-1.0	38400
11	N_2	$+e^-$	=N	+N	$+e^-$	3.00	$x10^{24}$	-1.6	113100
12	N	+O	=NO	$+e^-$		5.30	$x10^{12}$	0.0	31900
13	N	+N	$=N2^+$	$+e^-$		2.00	$x10^{13}$	0.0	67500
14	NO^+	+O	$=N^+$	$+O_2$		1.00	$x10^{12}$	0.5	77200
15	N^+	$+N_2$	$=N_2^+$	+N		1.00	$x10^{12}$	0.5	12200
16	O^+	+NO	$=N^+$	$+O_2$		1.40	$x10^5$	1.9	26600
17	NO^+	+N	$=O^+$	$+N_2$		3.40	$x10^{13}$	-1.08	12800
18	O^+	$+N_2$	$=N_2^+$	+O		9.10	$x10^{11}$	0.36	22800
19	NO^+	+N	$=N2^+$	+O		7.20	$x10^{13}$	0.0	35500
20	O	+O	$=O_2^+$	$+e^-$		1.10	$x10^{13}$	0.0	80600
21	O_2^+	+N	$=N^+$	$+O_2$		8.70	$x10^{13}$	0.14	28600
22	O_2^+	$+N_2$	$=N_2^+$	$+O_2$		9.90	$x10^{12}$	0.0	40700
23	O_2^+	+O	$=O^+$	$+O_2$		4.00	$x10^{12}$	-0.09	18000
24	NO^+	$+O_2$	$=O_2^+$	+N		2.30	$x10^{13}$	0.41	32600
25	NO^+	+O	$=O_2^+$	+N		7.20	$x10^{12}$	0.29	48600
26	N	+M5	$=N^+$	$+e^-$	+M	2.34	$x10^{11}$	0.5	120000

Rates in the form $k_f = AT^B\exp(-E/T)$.
$T=T_e$ in electron impact reactions.
M1 = N,N^+,O,O^+
M2 = $N_2,N_2^+,O_2,O_2^+,NO,NO^+$
M3 = N,N^+,O,O^+,NO
M4 = N_2,N_2^+,O_2,O_2^+,NO^+
M5 = N,N^+

Chemical Rate Model

The forward reaction rate coefficients are based on the Arrhenius equation and take the form

$$k_f = AT^B \exp(-E/T) \qquad (20)$$

where A, B and E are the constants found in Table I and T is an appropriate temperature. It is generally agreed that for dissociation reactions, the forward reaction rates should take into account the amount of vibrational energy in the molecular collision partners. In addition, the electron impact ionization and electron impact dissociation reactions should be modified to account for the energy available in the translational mode of the free electrons. Tam and Li's chemical rate model,[23] as originally formulated in INEQ3D, accounts for all energies present in the reacting partners by replacing the temperature in equation (20) with an effective temperature, T_{eff}, for each reaction. This effective temperature is found by calculating the Gibb's free energy of each of the internal energy modes and is of the form:

$$\frac{1}{T_{eff}} = \sum_{all\ i} \frac{f_i}{T_i} \qquad (21a)$$

where the statistical factors, f_i, are found by

$$\left\{ f_i = \frac{T_i \Delta G_i^\circ}{\sum_{all\ i} T_i \Delta G_i^\circ} \right\} \qquad \sum_{all\ i} f_i = 1 \qquad (21b)$$

The subscript i denotes each internal energy mode and for a given reaction, $\Delta G_{i,s}^\circ$ is the

change in Gibb's free energy (products minus reactants) for energy mode i, given by:

$$\Delta G_i^\circ = \sum_{s=1}^{ns} (\nu_s'' G_{i,s}^\circ) - \sum_{s=1}^{ns} (\nu_s' G_{i,s}^\circ) \qquad (22)$$

The variables ν_s'' and ν_s' are the stoichiometric coefficients of the products and the reactants respectively and ns is the total number of chemical species. The quantity $G_{i,s}^\circ$ is the Gibb's free energy of species s evaluated at one atmosphere for energy mode i. Determination of the Gibb's free energies is explained in the subsection entitled Thermodynamic Model.

For a given reaction, the reverse reaction rate coefficient can be found by calculating the equilibrium constant, K_C, in terms of the Gibb's free energies and then using the relation

$$\frac{k_f(T)}{k_b} = K_C(T) \; . \qquad (23)$$

This equation is true for equilibrium and follows from the law of mass action.[24] Although it does not necessarily hold precisely for nonequilibrium conditions, equation (23) is approximately correct in this region.[25] In the original model, the reverse reaction rate coefficient was found by substituting the effective temperature T_{eff} into equation (23), with the equilibrium constant given by:

$$K_C = K_p (RT_{eff})^{-\Delta n} = \exp\left(- \sum_{all\ i} \frac{\Delta G_i^\circ}{RT_i} \right) (RT_{eff})^{-\Delta n} \; . \qquad (24)$$

Here, K_p is the equilibrium constant based on partial pressures and Δn is the difference in stoichiometric coefficients between the products and reactants.

Unfortunately, for free stream Mach numbers greater than 30, Tam's effective temperature does not exhibit physically correct temperature dependence for certain reactions, particularly the electron impact reactions which should depend heavily on the electron-electronic temperature. Since the electron impact reactions and avalanche ionization are very important for the conditions studied herein, Tam's effective temperature model was replaced with Park's TTV model.[18,26,27] In this model, an effective temperature for dissociation reactions is calculated based upon a geometric average of the translational and vibrational temperatures using

$$T_a = T_v^q T^{1-q} \tag{25}$$

where q typically ranges from 0.2 to 0.5. An exception is the electron impact dissociation of N_2 ($N_2 + e^- \rightarrow N_2^+ + e^- + e^-$), where T_a is replaced with T_d (or T_V in the case of a two temperature model) to account for the free electron translational energy.[18] Based on similar logic, the electron impact ionization reactions utilize the free electron temperature T_d in the calculation of the forward rates. In all cases the equilibrium constant is evaluated using the temperature used in the forward rate. An alternative approach for determining the backward rate would be to calculate a local equilibrium constant based on the local characteristic temperatures of each internal energy mode.[6,21]

Chemical Production Rates

The forward and reverse reaction rates are summed over all reactions to determine the net change in each species in a given cell volume. This mass production rate of species s per unit volume is given by

$$\dot{\omega}_s = M_s \sum_{r=1}^{nr} (\nu''_{s,r} - \nu'_{s,r}) (R_{f,r} - R_{b,r}) \qquad (26)$$

where $\nu'_{s,r}$ and $\nu''_{s,r}$ are the stoichiometric coefficients of the reactants and the products respectively, and nr refers to the total number of reactions. The forward and reverse reaction rates for a given reaction r are given by

$$R_{f,r} = k_{f,r} \prod_{s=1}^{ns} \left(\frac{\rho_s}{M_s} \right)^{\nu'_{s,r}} \qquad (27a)$$

and

$$R_{b,r} = k_{b,r} \prod_{s=1}^{ns} \left(\frac{\rho_s}{M_s} \right)^{\nu''_{s,r}} \qquad (27b)$$

where $k_{f,r}$ and $k_{b,r}$ are the forward and reverse reaction rate coefficients respectively.

Chemical Production Rate Relaxation

Recall that chemical nonequilibrium exists when chemical processes occur on approximately the same time scale as the particle residence time. In an equilibrium region of the flow, the forward and reverse chemical reaction rates often are very fast, and thus, the local time step required to characterize the fast chemical reactions can become very small. The presence of two or more disparate time scales in a numerical scheme is referred to as numerical stiffness, and some authors[18,28] suggest that implicit schemes are generally less susceptible to numerical stiffness problems than explicit schemes. Although INEQ3D utilizes an implicit solution scheme, the source Jacobian, $\partial\Omega/\partial Q$, is diagonalized; and it is possible that this diagonalization significantly changes

the eigenvalues associated with the chemistry, leading to numerical instability. Such instability, if it occurred, would probably initially occur in the chemical species concentrations in the stagnation point region of the flowfield.

In order to mitigate the potentially serious numerical stiffness problems, a method is needed to slow down the chemical rates while still converging to the correct steady state solution. Thus, a chemical production rate time relaxation is proposed of the form:

$$\omega_s^{n+1} = \omega_s^n + \chi\,(\overline{\omega}_s^{n+1} - \omega_s^n) \qquad (28)$$

where ω_s^{n+1} is the new time relaxed production rate for species s, $\overline{\omega}_s^{n+1}$ is the actual species production rate found via the forward and reverse reaction rates, and ω_s^n is the value of the production rate at time level n found from equation (28). The relaxation factor χ typically takes on values between 0.1 and 0.5, with the smaller value indicating more chemical relaxation. This time relaxation slows down the production of a species when the change in production rates between iterations is large, which should enhance stability; but it gives the correct rate when the solution nears convergence (i.e. $\Delta\omega_s^{n+1} = 0$ when $\Delta\overline{\omega}_s^{n+1} = 0$).

Relaxation Processes

Thermal relaxation occurs when two or more energy modes are out of equilibrium with each other and there is a net transfer of energy, via collisions, from one mode to another. The first two terms on the right hand side of the vibrational-electron-electronic energy equation, equation (19), account for the elastic energy transfer between energy modes.

The energy exchange between translational and vibrational modes can be modeled as

$$Q_{T-V} = \sum_{s=mol} \rho_s \frac{[e_{V,s}(T) - e_{V,s}(T_V)]}{\langle \tau_s \rangle} \tag{29}$$

where the term $\langle \tau_s \rangle$ is the vibrational relaxation time for species s. Millikan and White[29] suggested a vibrational relaxation time for species s given by:

$$\tau_s^{MW} = \frac{\sum_{j=hp} \{n_j \exp[A_s(T^{-1/3} - 0/015\mu_{sj}^{1/4}) - 18.42]\}}{p \sum_{j=hp} n_j} \tag{30}$$

where n_j is the number density of species j and A_s is an empirical constant for the vibrating species s with values for N_2, O_2, and NO of 220, 129, and 168 respectively.[15] The term μ_{sj} is the reduced molecular weight of the colliding species. In the current version of INEQ3D, τ_s^{MW} is approximated by a collision partner independent form:

$$\tau^{MW} = 5.9E\text{-}12 \exp\left(\frac{A}{T^{1/3}}\right) \tag{31}$$

where A is assumed to be the value given for N_2 above (220).

Park[30] determined that above 8000 K, the relaxation times of Millikan and White yield collision cross sections that are too large by an order of magnitude. Thus he determined that $\langle \tau_s \rangle$ may be better modeled as

$$\langle \tau_s \rangle = \tau_s^{MW} + \tau_s^{P} \tag{32}$$

where

$$\tau_s^P = \frac{1}{\sigma_s n_s \left(\frac{8kT}{\pi m_s}\right)^{1/2}} \tag{33}$$

and σ_s is an effective cross section for vibrational relaxation. In addition to the modification to τ_s^{MW} and approximation of equation (31), a correction factor is included to account for the diffusion-like nature of vibrational relaxation giving

$$Q_{T-v} = \frac{\left[\frac{|T_{sh}-T_V|}{T_{sh}-T_{sh,v}}\right]^{S-1}}{\langle\tau\rangle} \sum_{s=mol} \rho_s [e_{V,s}(T) - e_{V,s}(T_V)] \tag{34}$$

where $S = 3.5\exp(-5000/T_{sh})$ and T_{sh} is the translational temperature immediately after the normal shock.

The second term on the right hand side of equation (19) accounts for the change in free electron translational energy due to elastic collisions with heavy particles and was originally approximated by:

$$Q_{T-e^-} = 2\rho_{e^-}\frac{3}{2}\overline{R}(T-T_{el})\sum_{s=4}^{10}\frac{\nu_{es}}{M_s} \tag{35}$$

Here, the summation from 4 to 10 includes all atoms and ions, but it omits the neutral molecules. The variable ν_{es} is the effective collision frequency of an electron with species s found from:

$$\nu_{es} = n_s \sigma_{es}\left(\frac{8kT_{el}}{\pi m_{e^-}}\right)^{1/2} \tag{36}$$

where T_{el} is the electron-electronic temperature equal to T_V for the two temperature model, m_{e^-} is the electron mass, and σ_{es} is the effective energy exchange cross section.

However, for the conditions studied in this research, it is important to include all heavy particles in the evaluation of the translational-free electron elastic energy exchange. Thus, the free electron translational coupling model has been modified to that of Gnoffo[15] based on the work of Appleton and Bray.[31] This model utilizes equation (35) summed over all heavy particles and uses different effective collision cross sections than those utilized originally. For collisions between electrons and neutral particles, ν_{es} is given by equation (36), but the effective energy exchange cross section σ_{es} is defined by curve fits for each neutral species given by:

$$\sigma_{es} = \tilde{a}_s + \tilde{b}_s T_{el} + \tilde{c}_s T_{el}^2 \qquad (37)$$

The constants[15] used in equation (37) can be found in the Appendix.

Further, the effective collision frequency between electrons and charged heavy particles must take into account the Coulomb forces between the oppositely charged particles. This effect can be modeled as

$$\nu_{es} = \frac{8}{3}\left(\frac{\pi}{m_{e^-}}\right)^{1/2} n_s e^4 \frac{1}{(2kT_{el})^{3/2}} \ln\left(\frac{k^3 T_{el}^3}{\pi n_{e^-} e^6}\right) \qquad (38)$$

where k is Boltzmann's constant and e is the electronic charge equal to 1.5188E-4 esu in the mks system of units (1 esu^2 equals 1 kg m^3/s^2).

Chemical and Radiative Coupling

Chemical reaction effects also appear as energy sources and sinks in the vibrational-electron-electronic (VEE) energy equation (equation (19)). Recall the third term on the right hand side of the VEE energy equation:

$$-\sum_{s=6}^{10} \dot{n}_{e,s} \hat{I}_s \tag{39}$$

which represents the free electron energy lost due to electron impact ionization. The variable $\dot{n}_{e,s}$ is the molar rate of ionization of species s via electron impact, and the energy per unit mole lost by a free electron in producing species s through electron impact ionization is given as I_s. Here it is assumed that the particle ionizes from the electronic ground state; and, thus, I_s is taken as the first ionization energy of the species. Although ionization usually occurs from the excited states, this assumption is still valid since electron transitions from the ground states to the excited states occur mainly from high speed collisions with free electrons. Thus, the total free electron energy lost in electron impact ionization is approximately the same.

The fourth term is the vibrational energy lost or gained due to dissociation or recombination of the molecular species of the form:

$$\sum_{s=mol} \dot{\omega}_s \hat{D}_s \tag{40}$$

The quantity $\hat{D}_s$ is the average vibrational energy which is created or destroyed due to such reactions. Currently INEQ3D assumes that $\hat{D}_s$ is the average vibrational energy, e_v, of species s. It should be noted that larger values of $\hat{D}_s$ will cause dissociation to preferentially occur, given a sufficiently energetic collision, from the upper vibrational levels which have higher vibrational energies; but this approach is not to be confused with the preferential Coupled Vibration-Dissociation-Vibration (CVDV) model proposed by Treanor and Morrone[32,33] which keeps a detailed account of the amount of energy

gained and lost in each reaction involving diatomic species.

The fifth term on the right hand side of the vibrational-electron-electronic energy equation is the change in average electronic energy due to chemical reactions. This term has the form

$$\sum_{s=1}^{10} \dot{\omega}_s e_{el,s} \tag{41}$$

where $e_{el,s}$ is the average electronic energy of species s. Few researchers have accounted for this change in electronic energy; and, thus, its effect on the flowfield will be examined as part of this research.

The last term in the global energy equation, $-\partial q_r/\partial n$, accounts for the loss or gain of energy due to radiative transitions. This total radiative flux term can be separated into the contributions from the various radiative phenomena. These processes, in decreasing order of importance, are radiation used to break chemical bonds (photo-ionization and photo-dissociation), electronic state transitions, excess ionization energy imparted to freed electrons, free-free electron transitions, changes in vibrational states, and changes in rotational states.[6] The correct form of the radiative heat flux in the vibrational-electron-electronic energy equation would require detailed information on the amount of radiation exchanged in each of the above processes. However, since all of the above processes are accounted for in the VEE energy equation except rotation, and since rotation is the smallest of those contributions, it is approximately correct to include the total radiation term in the VEE energy equation. The effect of including the total radiation term, $\partial q_{r,tot}/\partial n$, in the vibrational-electron-electronic energy equation will also be examined.

RADIATION THEORY

The TAMU nonequilibrium radiation model developed by Gally and Carlson[6,7] is based on the equilibrium radiation code RADICAL developed by Nicolet.[34,35] There are four types of radiative processes included in the current TAMU model. Atomic continuum radiation (bound-free) occurs when an atom gains or loses an electron in a photo-deionization or ionization process. Atomic line radiation (a bound-bound process) occurs when an electron transitions from one orbit to another within an atom's electronic shell, and these transitions result in distinct lines of radiation. Another bound-bound process is molecular band radiation. This type of radiation occurs when electrons transition from one electronic orbit to another within a molecule's electronic shell and appears as closely grouped lines or bands since there are a number of electronic levels available, each with its own distinct vibrational states. The final type of radiation is Braumstrahlung free-free radiation, which occurs when free electrons pass by the electronic shell of a particle, causing a change in the translational energy of the free electron, thereby emitting or absorbing radiation.

Radiation Correction Factors

Atomic ionization is a two step process involving excitation from the ground to the excited states, which is a slow process, and then ionization from the excited states, which is a fast process. In the region immediately behind the shock front, the high rate of ionization causes the excited states to become depopulated. Thus, the total electronic energy of the atoms can no longer be described by a Boltzmann distribution and it

becomes important to include Local Thermodynamic Nonequilibrium (LTNE) when calculating the radiative fluxes. This feature is included in the present study via a first order model which calculates atomic radiative correction factors to determine the nonequilibrium populations of the excited states. For atoms, the atomic correction factors are found by assuming that the atoms with excited electronic states are in equilibrium with the ions and free electrons. Thus, for nitrogen, the ionization reaction

$$N^* + e^- \rightleftharpoons N^+ + e^- + e^- \tag{42}$$

is assumed to be in equilibrium, where N^* refers to the excited electronic states of nitrogen and N^+ is the ion. This first order atomic LTNE model includes emission, absorption, and induced emission for both the continuum and line processes. For further details, see references 6, 7, and 21.

The first order model for molecular radiation is based on the quasi-steady state method (QSSM) of Park,[30] which determines the populations of the molecular electronic excited states. These populations are then used to calculate similar correction factors for nonequilibrium molecular radiation.

Tangent Slab Approximation

Theoretically, the computation of the radiative flux terms involve, at every point, an integration over the entire flowfield as well as over all frequencies, but realistically, such a computation is impractical. Thus, to simplify the radiation calculations, a tangent slab approximation is used. In cases where the shock standoff distance is much smaller than the body's radius of curvature, the body and the shock wave approximate two

parallel or tangent infinite planes. Fortunately, this situation is true for the high speed, blunt body flows under consideration. Thus, in the tangent slab model it is assumed locally that the radiating flow is invariant in the ξ and σ directions and only varies in the η direction; and hence the net radiative flux can be computed via integration only normal to the body. For further details see references 6, 7, and 21.

NUMERICAL ISSUES

For planetary return, the high vehicle speeds attained relatively deep into the atmosphere can cause large equilibrium regions in the shock layer preceded by an exponential increase in free electron density known as avalanche ionization. It is well known that in regions of equilibrium the numerical solution for a finite rate chemistry model coupled with a fluid dynamic solver will exhibit numerical stiffness. On a physical basis, this problem occurs when the time scales for two or more phenomena are orders of magnitude different.

The relative time scale for two physical processes is given by the Damkohler number, D_k, which for the cases examined herein, relates the characteristic time for a fluid element to traverse the flowfield to the characteristic time for a given chemical reaction:

$$D_k = \frac{t_{fluid}}{t_{chemistry}} \tag{43}$$

Finite rate chemistry is applicable for Damkohler numbers near unity, while equilibrium chemistry is associated with Damkohler numbers much greater than one. For planetary return, the region immediately after the shock front has a Damkohler number near unity while the presence of avalanche ionization in the stagnation zone leads to much larger Damkohler numbers.

Avalanche ionization contributes to the numerical stiffness since the ionization production rate for the electron impact ionization reactions is sensitive to both the electron temperature and the number density of free electrons. When the electron

temperature and the electron number density gets sufficiently high, the electron impact ionization reactions are triggered, creating yet more free electrons. The electron number density thus increases logarithmically[18] and leads to a decrease in the electron, and due to coupling, the electronic and vibrational temperatures. Thus, the phenomenon of avalanche ionization decreases the chemical and thermal nonequilibrium region immediately after the shock front. The drop in temperature induces a corresponding rise in the density, which increases the number of collisions and therefore also forces the chemistry to equilibrate faster.

In the INEQ3D model, the local time step is based on the CFL number, which is a function of the local eigenvalues of the flux Jacobians. These eigenvalues are related to the speed of propagation of pressure waves in the flow which depend on the frozen speed of sound given by

$$a_f = \sqrt{\frac{\gamma p}{\rho}} \ . \tag{44}$$

As the density increases due to avalanche ionization, the local speed of sound decreases, thereby allowing a larger local time step. Conversely, the characteristic time for the chemical reactions decreases in the presence of avalanche ionization and the beginning of equilibrium, and thus requires a smaller time step.

A fully implicit method can mitigate the effects of numerical stiffness by allowing CFL numbers much greater than one. This situation is true if the linearization of the chemistry and flux Jacobians is performed consistently and if the resulting block tri-diagonal matrix is inverted exactly. These two conditions are difficult to achieve for

reacting flow calculations because the linearization is complex and the exact inversion of large block tri-diagonal matrices is costly. Since the flux Jacobian linearization of Jameson[9] results in diagonal matrices, the need for matrix inversions can be eliminated entirely by diagonalizing the source Jacobian. The number of operations required to invert an nxn matrix exactly is on the order of n^3 while the inversion of an nxn diagonal matrix requires approximately n operations. The solution scheme utilized in the current version of INEQ3D, which approximates the chemical source Jacobian with a diagonal matrix, is referred to as the diagonal implicit algorithm.

Chemical Relaxation in Quiescent Oxygen: A Test Case

In order to examine the diagonal implicit scheme in detail, the simplified case of chemical relaxation in quiescent oxygen is examined. The vibrational energy mode is neglected for this example; and the assumption of no mass flux into or out of the system is imposed for simplicity, forcing the total density to remain constant.

The following reactions will be modeled:

$$\begin{aligned} \textit{reaction}\ \#1: &\quad O_2 + O_2 \rightleftharpoons 2O + O_2 \\ \textit{reaction}\ \#2: &\quad O_2 + O \rightleftharpoons 2O + O \end{aligned} \tag{45}$$

The equations governing this model for coupled chemical relaxation are

$$\frac{dc_{O_2}}{dt} = F_1(c_{O_2}, c_O) \tag{46}$$

$$\frac{dc_O}{dt} = F_2(c_{O_2}, c_O) \tag{47}$$

where F_1 and F_2 are the chemical production rate equations for O_2 and O, respectively, which are functions of the mass fractions as well as the forward and reverse reaction rates for the two given reactions. The rate equation for O_2, in terms of the molar densities, is given by:

$$\frac{d[O_2]}{dt} = -(k_{f,1}[O_2]^2 - k_{b,1}[O_2][O]^2 + k_{f,2}[O_2][O] - k_{b,2}[O]^3) \tag{48}$$

A similar expression can be found for the molar production rate of O.

The total energy is constant for this system and is found by:

$$e_{tot} = \sum_s c_s c_{v_s} T + \sum_s c_s h_s^0 \tag{49}$$

The temperature T is found by taking the translational and rotational contributions to the total energy and dividing by the specific heats:

$$T = \frac{e_{total} - \sum_s c_s h_s^0}{\sum_s c_s c_{v_s}} \tag{50}$$

Discretizing the governing equations and linearizing according to the implicit Euler formulation gives the following linear systems:

$$\frac{\Delta c_{O_2}}{\Delta t} = F_1^n + \left.\frac{\partial F_1}{\partial c_{O_2}}\right|_n \Delta c_{O_2} + \left.\frac{\partial F_1}{\partial c_O}\right|_n \Delta c_O \qquad (51)$$

and

$$\frac{\Delta c_O}{\Delta t} = F_2^n + \left.\frac{\partial F_2}{\partial c_{O_2}}\right|_n \Delta c_{O_2} + \left.\frac{\partial F_2}{\partial c_O}\right|_n \Delta c_O \qquad (52)$$

where

$$\Delta c_s = c_s^{n+1} - c_s^n \ . \qquad (53)$$

Using matrix algebra, this equation can be rewritten as:

$$\frac{1}{\Delta t} I \Delta \mathbf{Q} = \frac{\partial \boldsymbol{\Omega}}{\partial \mathbf{Q}} \Delta \mathbf{Q} + \boldsymbol{\Omega} \qquad (54)$$

where

$$\mathbf{Q} = \begin{bmatrix} \Delta c_{O_2} \\ \Delta c_O \end{bmatrix}, \quad \boldsymbol{\Omega} = \begin{bmatrix} F_1 \\ F_2 \end{bmatrix} \qquad (55)$$

and $\partial\Omega/\partial Q$ is the chemical source Jacobian. In matrix form, equation (54) becomes

$$\begin{bmatrix} \left(\frac{1}{\Delta t} - \left.\frac{\partial F_1}{\partial c_{O_2}}\right|_n\right) & -\left.\frac{\partial F_1}{\partial c_O}\right|_n \\ -\left.\frac{\partial F_2}{\partial c_{O_2}}\right|_n & \left(\frac{1}{\Delta t} - \left.\frac{\partial F_2}{\partial c_O}\right|_n\right) \end{bmatrix} \begin{bmatrix} \Delta c_{O_2} \\ \Delta c_O \end{bmatrix} = \begin{bmatrix} F_1 \\ F_2 \end{bmatrix} . \qquad (56)$$

To simplify the linearization, the rate equations F_1 and F_2 are assumed to be functions of the mass fractions only, and the dependence on the forward and backward rate coefficients is neglected. Although this simplification puts limitations on the

effective time step, it is representative of the level of approximation found in INEQ3D. The derivatives of F_1 with respect to the mass fractions are:

$$\frac{\partial F_1}{\partial C_{O_2}} = -\frac{M_{O_2}}{\rho}\left[2k_{f,1}\left(\frac{\rho}{M_{O_2}}\right)^2 C_{O_2} - k_{b,1}\left(\frac{\rho}{M_O}\right)^2\left(\frac{\rho}{M_{O_2}}\right)C_O^2 + k_{f,2}\left(\frac{\rho}{M_{O_2}}\right)\left(\frac{\rho}{M_O}\right)C_O\right] \tag{57}$$

$$\frac{\partial F_1}{\partial C_O} = -\frac{M_{O_2}}{\rho}\left[-2k_{b,1}\left(\frac{\rho}{M_O}\right)^2\left(\frac{\rho}{M_{O_2}}\right)C_O C_{O_2} + k_{f,2}\left(\frac{\rho}{M_{O_2}}\right)\left(\frac{\rho}{M_O}\right)C_{O_2} - 3k_{b,2}\left(\frac{\rho}{M_O}\right)^3 C_O^3\right] \tag{58}$$

Similar expressions can be found for the F_2 derivatives.

When a large number of chemical species and reactions are used, the chemical source Jacobian can become expensive to invert due to the presence of the off-diagonal terms in equation (56). Consequently, Imlay[2] has suggested approximating this source Jacobian by a diagonal matrix, thereby eliminating the source matrix inversion. Note that in such a formulation, the chemistry is only loosely coupled with the flowfield solver. In a later section, the diagonal implicit algorithm approach will be compared to the full implicit scheme for this simple test case.

Diagonal Implicit Scheme

At this point, consider a system with an arbitrary number of chemical species which has chemical source terms only. Then, the fully implicit formulation for the chemical source Jacobian is given by:

$$\frac{\partial \Omega}{\partial Q} = \begin{bmatrix} \frac{\partial \omega_1}{\partial \rho_1} & \frac{\partial \omega_1}{\partial \rho_2} & \cdots & \frac{\partial \omega_1}{\partial \rho_n} \\ \frac{\partial \omega_2}{\partial \rho_1} & \frac{\partial \omega_2}{\partial \rho_2} & \cdots & \frac{\partial \omega_2}{\partial \rho_n} \\ \vdots & \vdots & \ddots & \vdots \\ \frac{\partial \omega_n}{\partial \rho_1} & \frac{\partial \omega_n}{\partial \rho_2} & \cdots & \frac{\partial \omega_n}{\partial \rho_n} \end{bmatrix} \tag{59}$$

In order to decrease the computational effort of solving this matrix, Imlay suggests diagonalizing the source Jacobian by:

$$\frac{\partial \Omega}{\partial Q} = \begin{bmatrix} \frac{\partial \omega}{\partial \rho_1} & 0 & \cdots & 0 \\ 0 & \frac{\partial \omega}{\partial \rho_2} & \cdots & 0 \\ \vdots & \vdots & \ddots & \vdots \\ 0 & 0 & 0 & \frac{\partial \omega}{\partial \rho_n} \end{bmatrix} \tag{60}$$

where

$$\frac{1}{\tau_i} = \frac{\partial \omega}{\partial \rho_i} = \frac{1}{M_i}\left[\sum_{j=1}^{n}\left(\frac{\partial \omega_i}{\partial \rho_j}\right)^2\right]^{\frac{1}{2}} \tag{61}$$

With this diagonalized source Jacobian, the solution scheme becomes diagonal implicit and the chemistry is only loosely coupled with the flowfield solver.

By replacing the source Jacobian of the quiescent oxygen text case with the above diagonal implicit approximation, equation (56) becomes:

$$\begin{bmatrix} \left(\frac{1}{\Delta t}-\frac{1}{\tau_1}\right) & 0 \\ 0 & \left(\frac{1}{\Delta t}-\frac{1}{\tau_2}\right) \end{bmatrix} \begin{bmatrix} \Delta C_{O_2} \\ \\ \Delta C_O \end{bmatrix} = \begin{bmatrix} F_1 \\ \\ F_2 \end{bmatrix} \qquad (62)$$

However, since the τ_i terms are always positive, the diagonalized source Jacobian subtracts from the diagonal terms making this scheme unconditionally unstable when τ_1 or τ_2 is less than Δt. Upon examination, the diagonal terms of the full source Jacobian were found to have both positive and negative values and, thus, the approximate Jacobian may not retain the proper sign on the diagonal terms. If the diagonal terms are instead added, effectively changing the sign on the approximate Jacobian, diagonal dominance is enhanced. This modification is allowed since, for steady state cases, the implicit operator is simply the means for obtaining a converged solution and the left hand side of equation (62) will approach zero as the solution converges and the change in the mass fractions approaches zero. In the next section, diagonal implicit results will be presented for this test case with the approximate Jacobian both added to and subtracted from the diagonal terms. Note that the current version of INEQ3D utilizes the positive diagonal formulation where the diagonal terms of the source Jacobian increase the diagonal dominance of the implicit operator.

DISCUSSION OF RESULTS

In this research, two different two dimensional re-entry configurations were examined, corresponding to 1634 and 1632 seconds in the Fire 2 vehicle flight trajectory.[8] These two dimensional test cases utilized scaled down bodies in order to more closely match the shock standoff distances of the corresponding three dimensional cases, but the size of the nonequilibrium region immediately behind the shock front should not be affected by this scaling. Unfortunately, the numerical problems described in the last section seemingly prohibited the study of flows with large equilibrium regions; and although this difficulty limits the validation of the radiation model, it does provide a starting point for future work. The two test configurations are summarized in Table II below.

Table II. Hypersonic Flowfield Case Summary

Case	Altitude (km)	Speed (km/sec)	R_{nose} (cm)	Notes
Cylinder	76.42	11.36	10	Fire 2 1634 Conditions
2-D Fire 2	81.86	11.37	31.2	Fire 2 1632 Conditions

For all cases where radiation calculations were performed, the wall temperature was assumed to be 2000 K, which corresponds to the current maximum temperature for a reusable, non-ablating heat shield. In addition, for all cases examined in this report,

the chemical rate relaxation factor was 0.3, Park's $T_v^{0.3} T^{0.7}$ effective temperature model was utilized for dissociation reactions, and the translational-electronic coupling term of Gnoffo was employed.

Numerical calculations with the modified version of INEQ3D were performed on Texas A&M's Cray-YMP for the test cases, and both radiatively coupled and uncoupled situations were investigated. Typical radiatively uncoupled cases required 1.084×10^{-4} CPU seconds/iteration/grid point, while radiative coupled runs, where the radiation was updated every 1000 iterations, required 3.848×10^{-4} CPU seconds/iteration/grid point. A large number of iterations (between 30,000 and 40,000) were needed in order to achieve a significant drop in the residuals due to time step limitations that arose from two sources. First, the equations governing hypersonic flow become numerically stiff when the chemical reaction rates get fast and equilibrium regions appear; and significant equilibrium occurs in situations where radiation transport becomes important. Second, the time step was further limited by the diagonal implicit scheme which loosely couples the chemistry with the flowfield solver.

The flowfield grids were constructed to minimize mesh cell size in the stagnation region and thus mitigate the effects of numerical stiffness. The mesh for the cylinder case used 50x70 grid points and is shown in Figure 1. Note that while there is some clustering for the bow shock, the main clustering occurs near the body in the thermo-chemical equilibrium region. The mesh for the two dimensional 1632 case used 50x80 grid points and is given in Figure 2. Again, the majority of clustering occurs near the wall. Results are presented for both cases along the constant i grid lines shown in

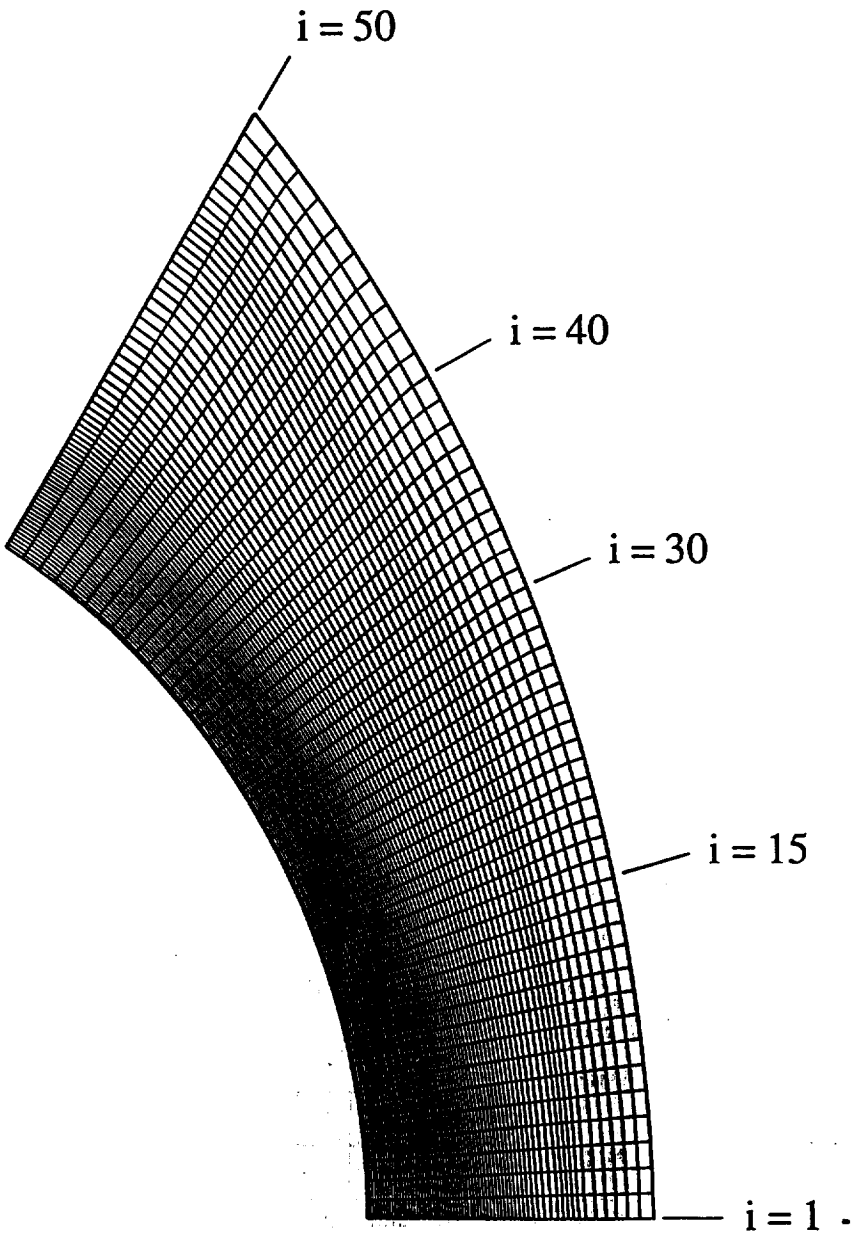

Figure 1: Cylinder Grid - 50x70 Grid Points

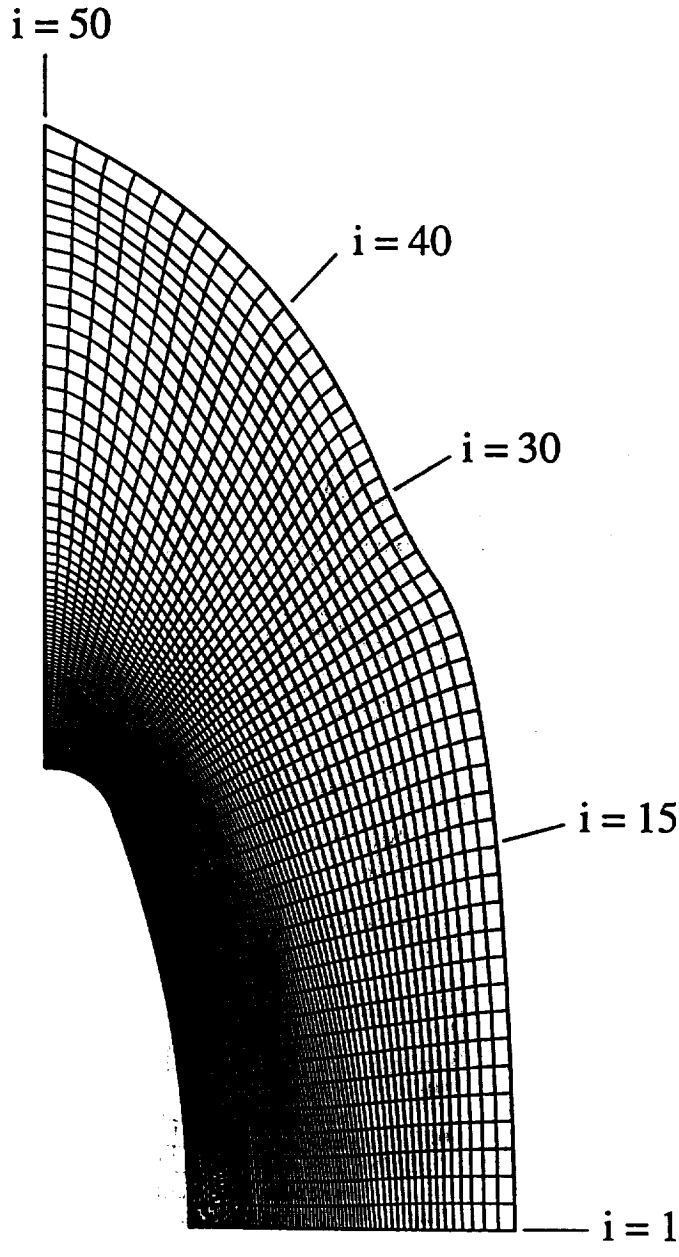

Figure 2: 2D Fire 2 Grid - 50x80 Grid Points

Figures 1 and 2 as well as along the body. All other results presented in this report are along the stagnation streamline.

Cylinder Flowfield Results

The first set of results is for the cylinder with no radiative coupling. This flowfield converged in approximately 20,000 iterations with CFL numbers between 2 and 0.25. As the solution progressed, the electron number density increased in the stagnation zone and avalanche ionization led to an increase in the total density. The density increase had the effect of both decreasing the speed of sound, which increased the allowable time step, as well as forcing the chemistry to equilibrium faster, which decreased the maximum allowable chemical time step. Thus, to converge the chemistry, an additional 20,000 iterations were required with maximum allowable CFL numbers between 0.5 and 0.0625. These additional iterations allowed the N_2 mole fraction near the wall to drop from $7x10^{-3}$ to $4x10^{-4}$ which had little effect on the rest of the flowfield. The temperatures are given in Figure 3 and the profiles show that the only major change between the two iteration conditions is a temperature drop within one centimeter of the wall. A change in this region is also seen in the pressure and density plots shown on Figure 4. Further insight into this phenomenon can be gained by examining the mole fractions, Figures 5 and 6, which show that the major changes occur in the concentrations of the diatomic species. As the electron avalanche phenomenon is encountered near 0.5 cm, the maximum allowable time step must be reduced to maintain stability, and this time step reduction virtually halts the relatively slow dissociation reactions. Thus, the

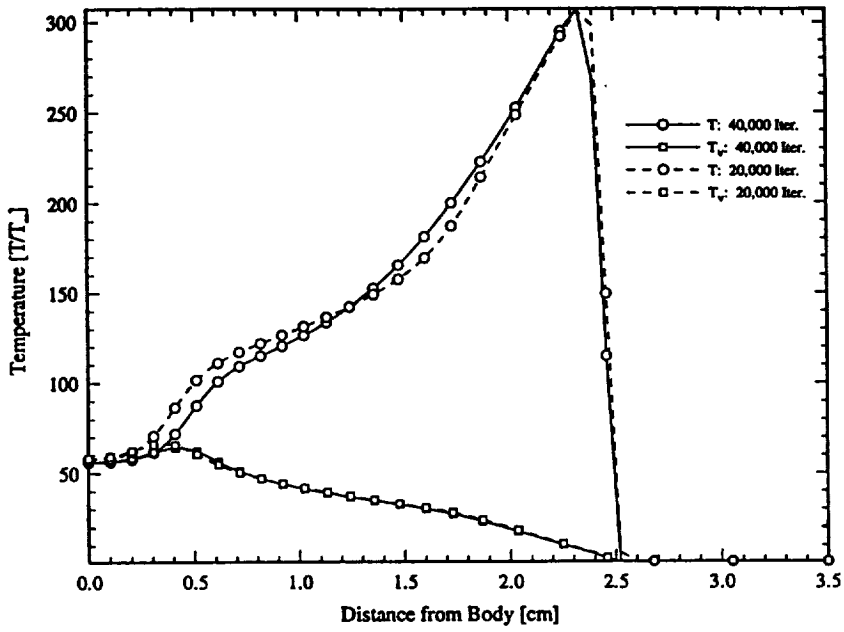

Figure 3: Cylinder Case - Thermal Profile without Radiative Coupling, 20,000 and 40,000 Iterations

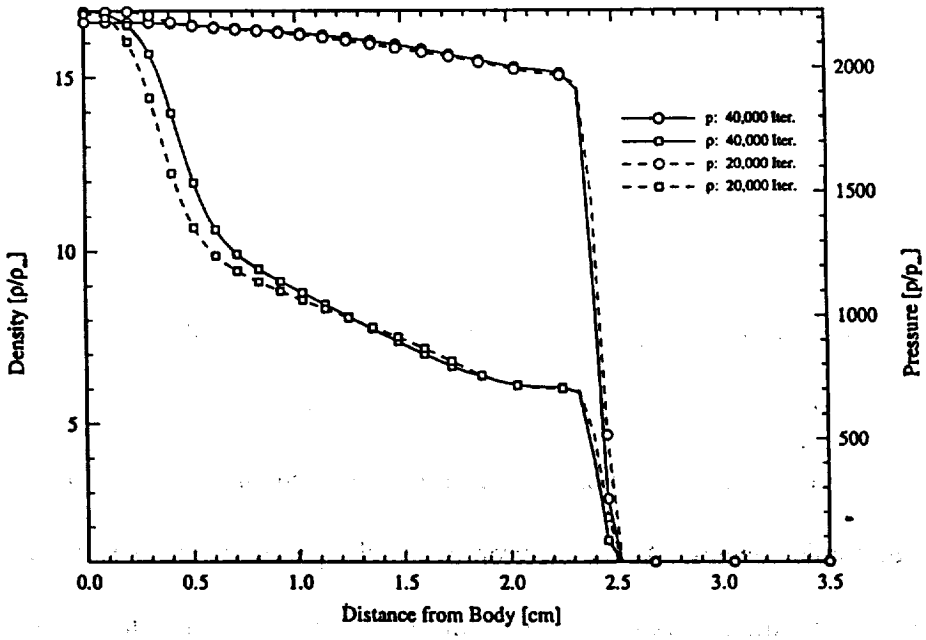

Figure 4: Cylinder Case - Density and Pressure Profiles without Radiative Coupling, 20,000 and 40,000 Iterations

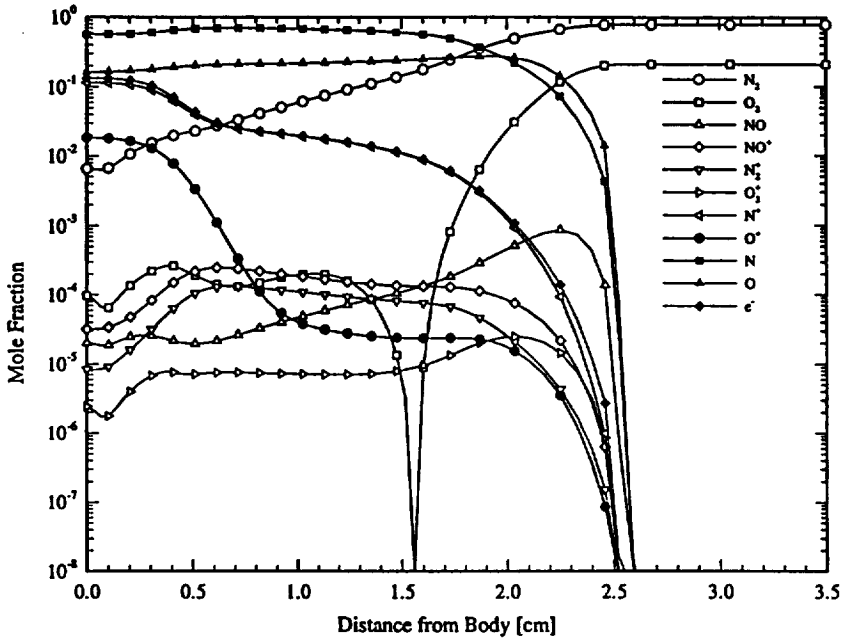

Figure 5: Cylinder Case - Mole Fractions at 20,000 Iterations without Radiative Coupling

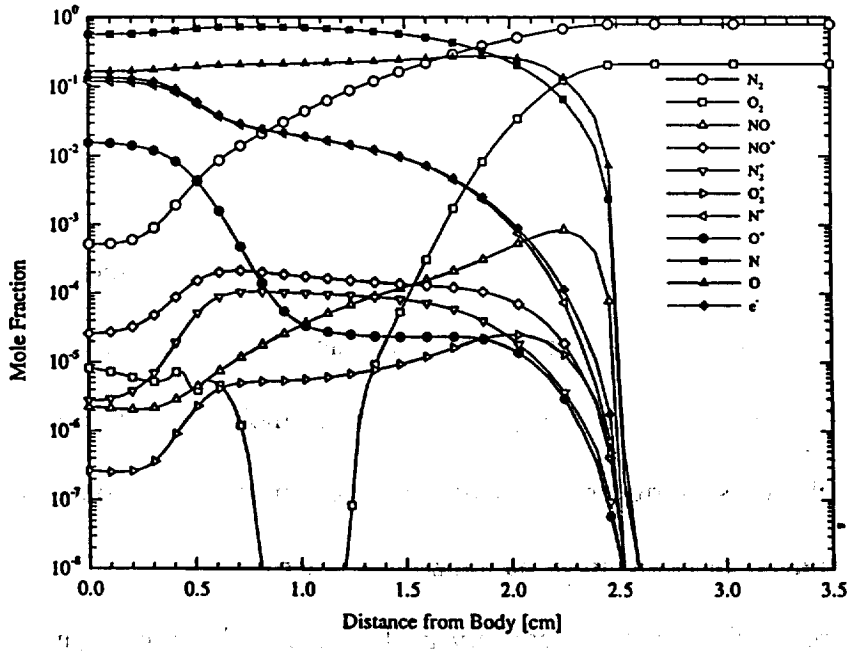

Figure 6: Cylinder Case - Mole Fractions at 40,000 Iterations without Radiative Coupling

changes in chemical composition between the two time levels occur mainly in N_2, O_2, and NO, the primary dissociating species.

Grouped and detailed radiation frequency spectra for this uncoupled case are shown in Figures 7 and 8. The atomic line radiation in the 0-2 eV and 8-12 eV region increased between 20,000 and 40,000 cycles, while the molecular continuum radiation between 2-4 eV decreased. For this case the total radiative heat transfer to the stagnation point was found to be 3.35 W/cm^2.

In Figures 9 through 16, results are presented for four different stations along the body corresponding to the i grid lines designated in Figure 1. Note that high free electron concentrations are present along the entire body. The thermodynamic variables along the body are also plotted versus the i station and are presented in Figures 17 and 18 and show a significant drop in density and pressure as the gas expands around the body.

Modified Atom-Atom Impact Ionization Rates

Many current researchers either ignore atomic impact ionization, such as reaction 26 in Table I, or use reaction rates that are uncertain. These reactions may be important in seeding the avalanche ionization phenomena since molecular ionization may produce insufficient electrons to trigger avalanche. In order for avalanche ionization to occur, a significant number of atoms must be ionized by other means.

As previously stated, a secondary goal of this study is to evaluate the effect of atom impact ionization rate coefficients on the overall structure and radiative heat

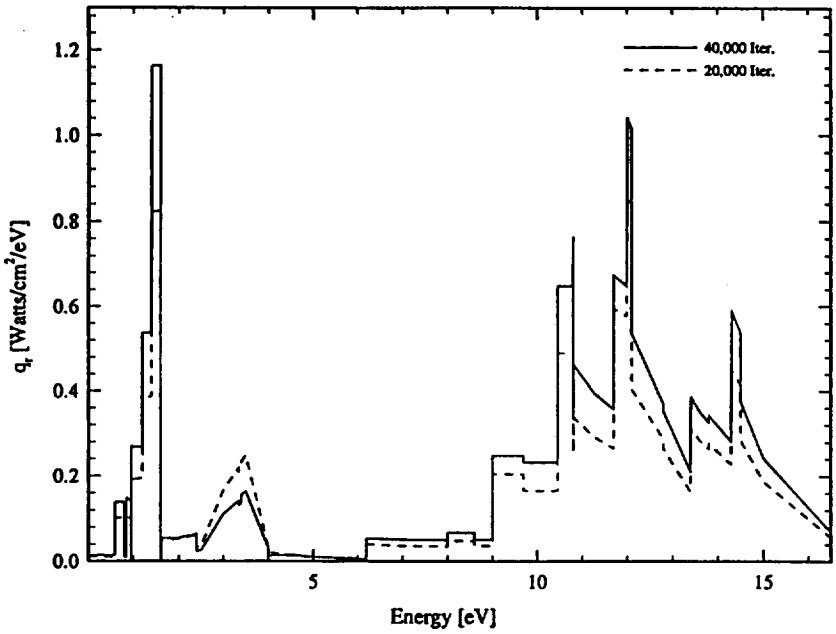

Figure 7: Cylinder Case - Grouped Radiative Spectra without Radiative Coupling, 20,000 and 40,000 Iterations

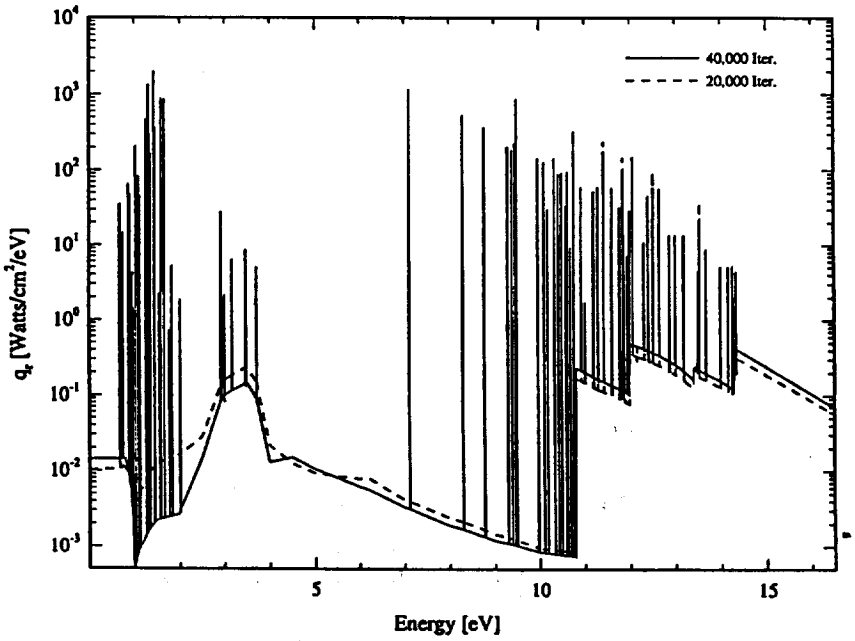

Figure 8: Cylinder Case - Detailed Radiative Spectra without Radiative Coupling, 20,000 and 40,000 Iterations

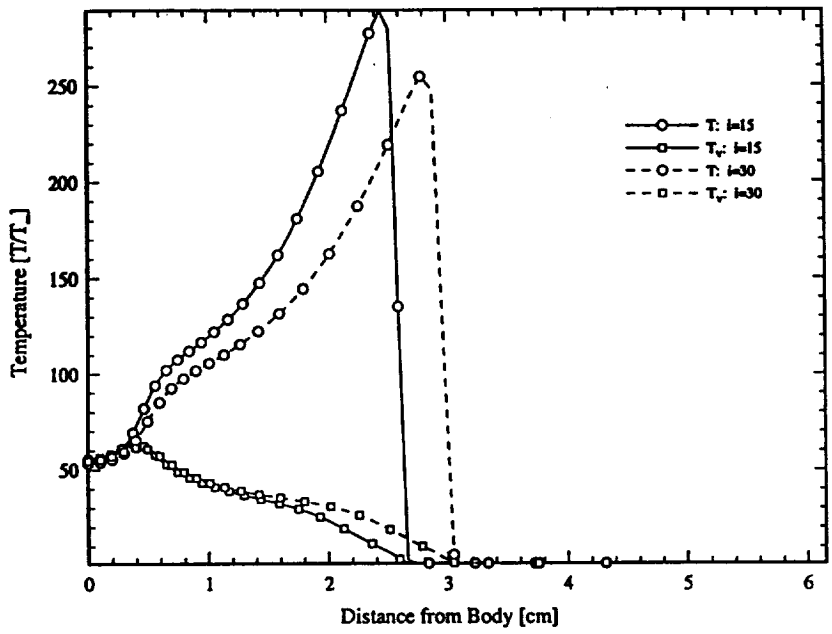

Figure 9: Cylinder Case - Thermal Profile without Radiative Coupling Along Grid Lines i = 15 and i = 30

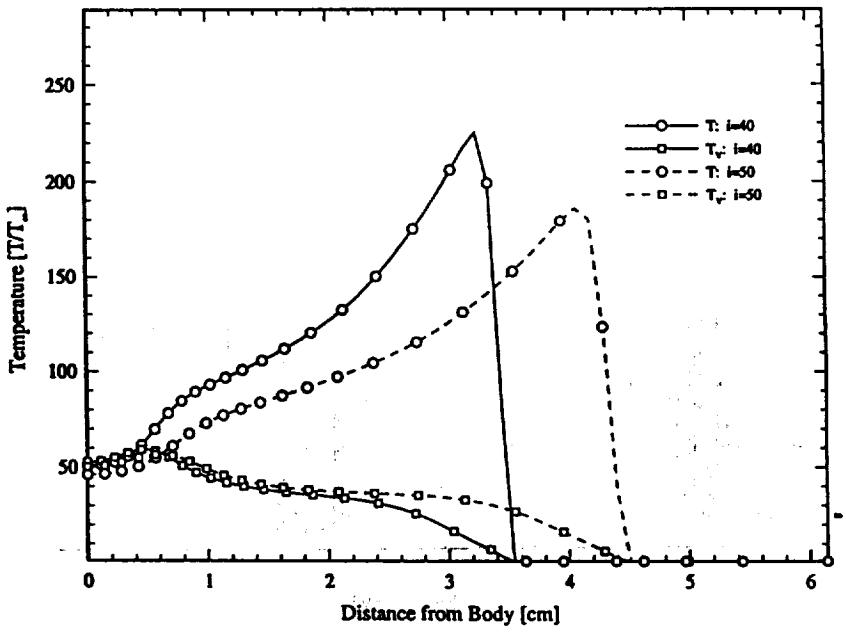

Figure 10: Cylinder Case - Thermal Profile without Radiative Coupling Along Grid Lines i = 40 and i = 50

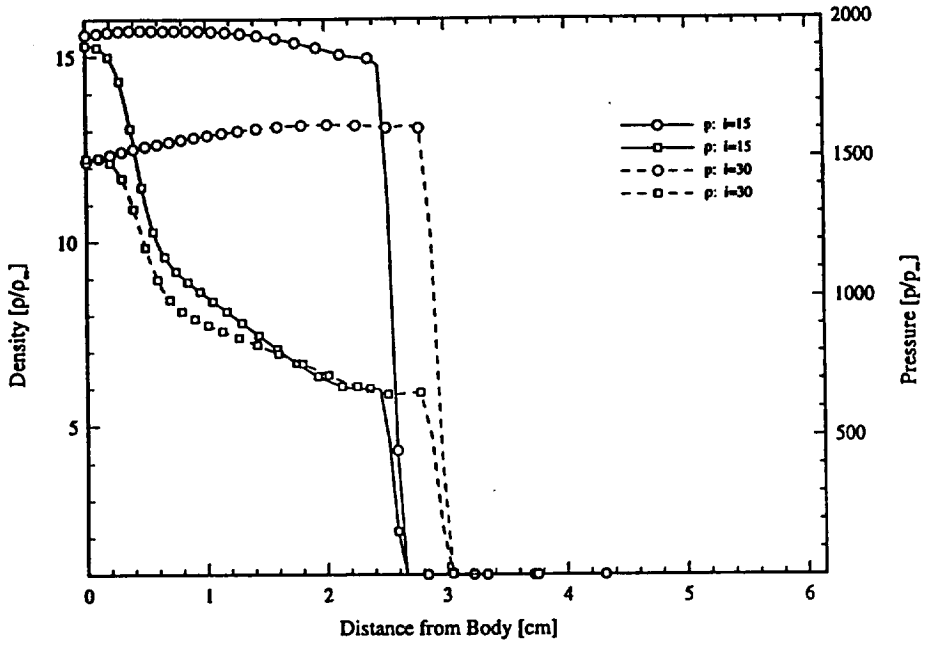

Figure 11: Cylinder Case - Density and Pressure Profiles without Radiative Coupling Along Grid Lines i = 15 and i = 30

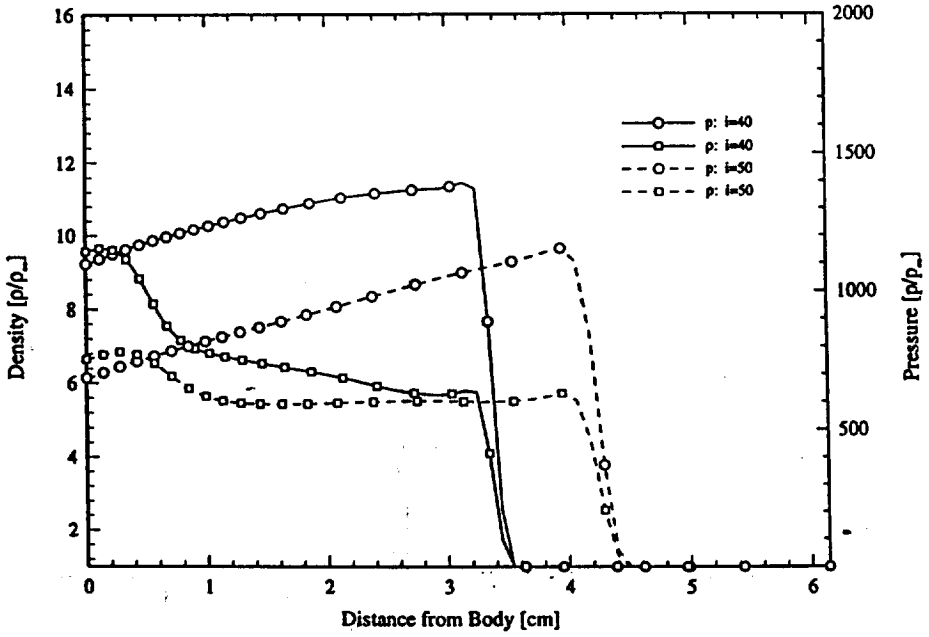

Figure 12: Cylinder Case - Density and Pressure Profiles without Radiative Coupling Along Grid Lines i = 40 and i = 50

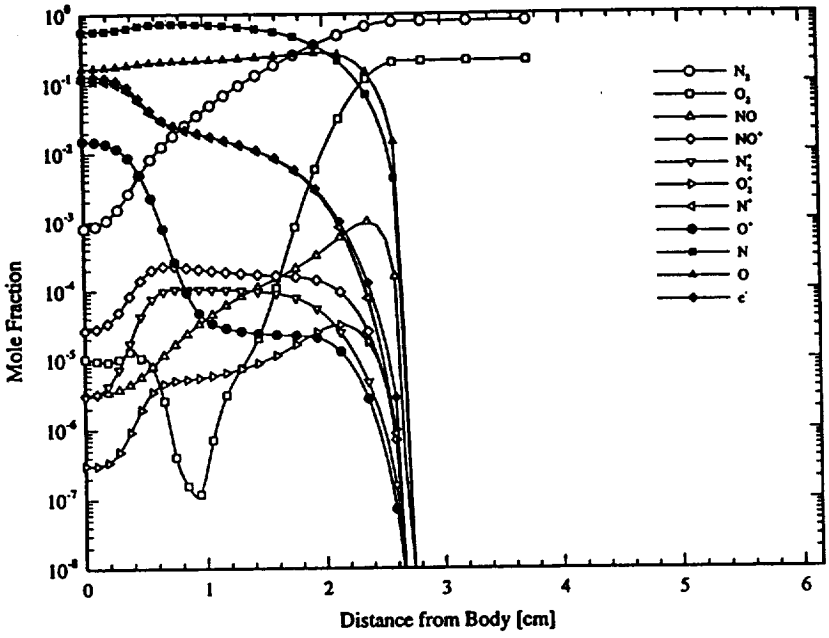

Figure 13: Cylinder Case - Mole Fractions without Radiative Coupling Along Grid Line i = 15

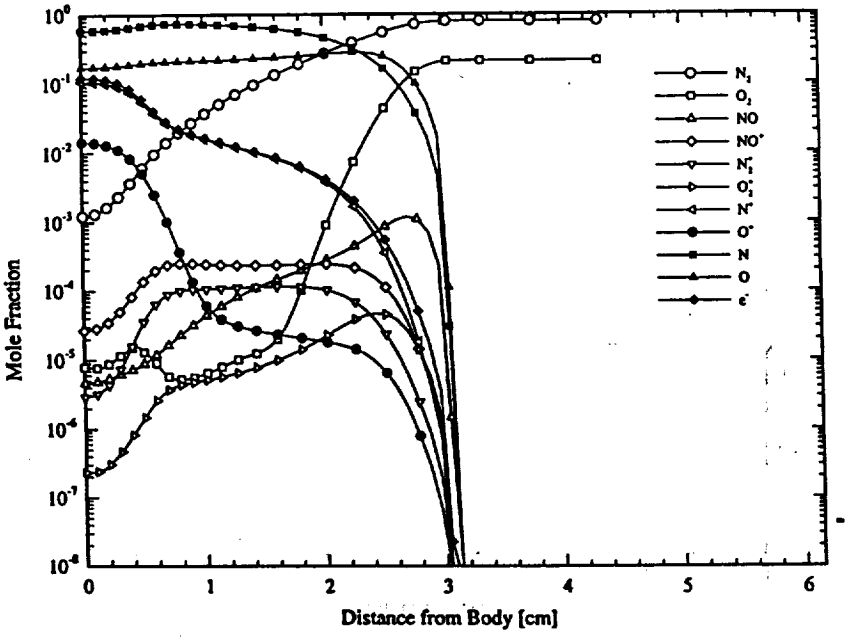

Figure 14: Cylinder Case - Mole Fractions without Radiative Coupling Along Grid Line i = 30

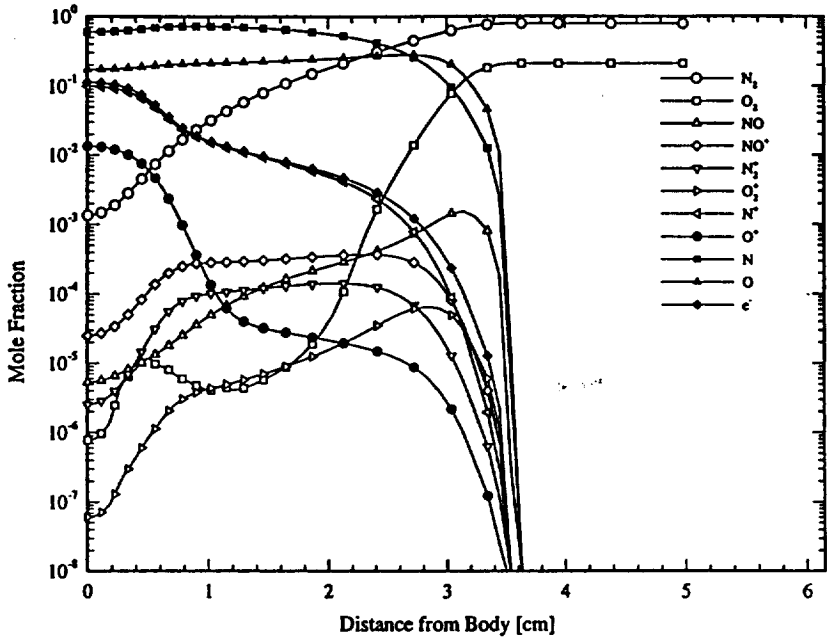

Figure 15: Cylinder Case - Mole Fractions without Radiative Coupling Along Grid Line i = 40

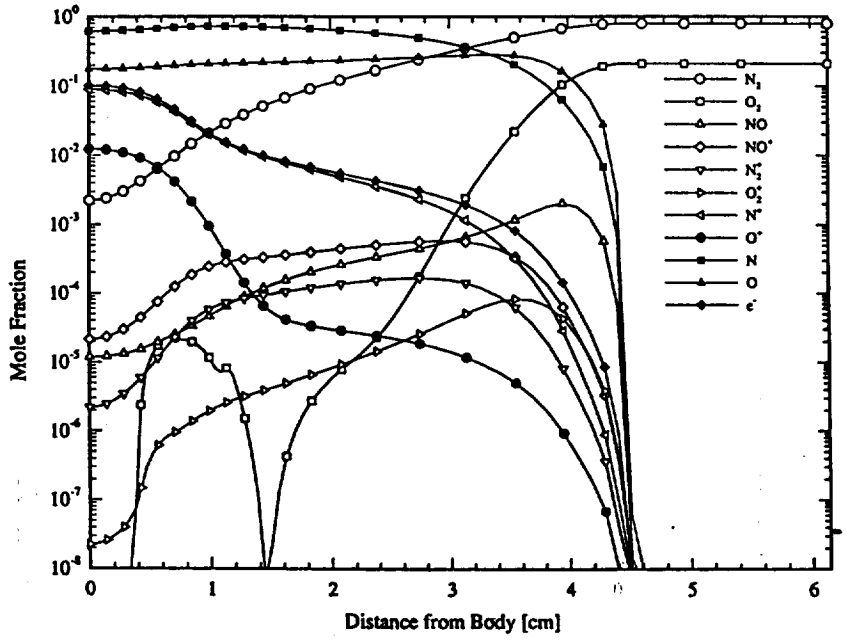

Figure 16: Cylinder Case - Mole Fractions without Radiative Coupling Along Grid Line i = 50

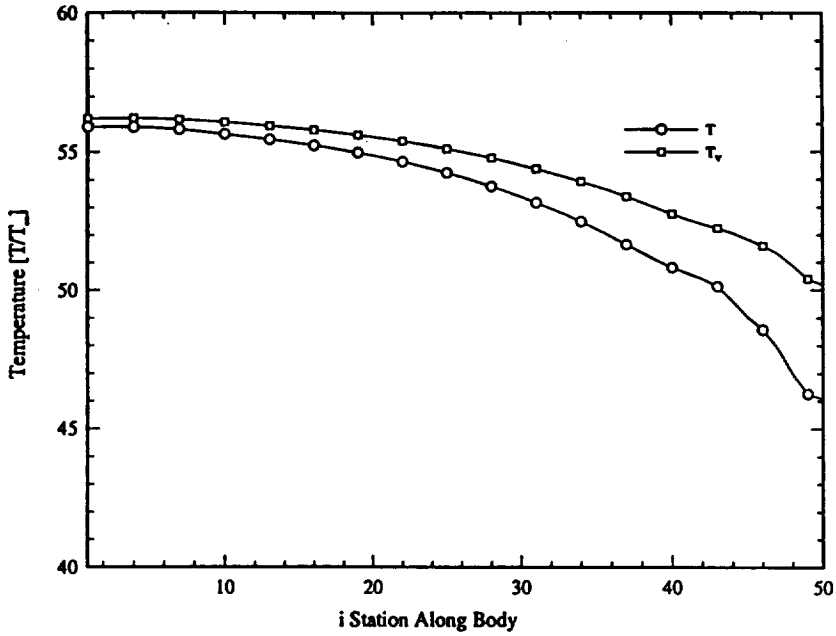

Figure 17: Cylinder Case - Thermal Profile without Radiative Coupling Along the Body

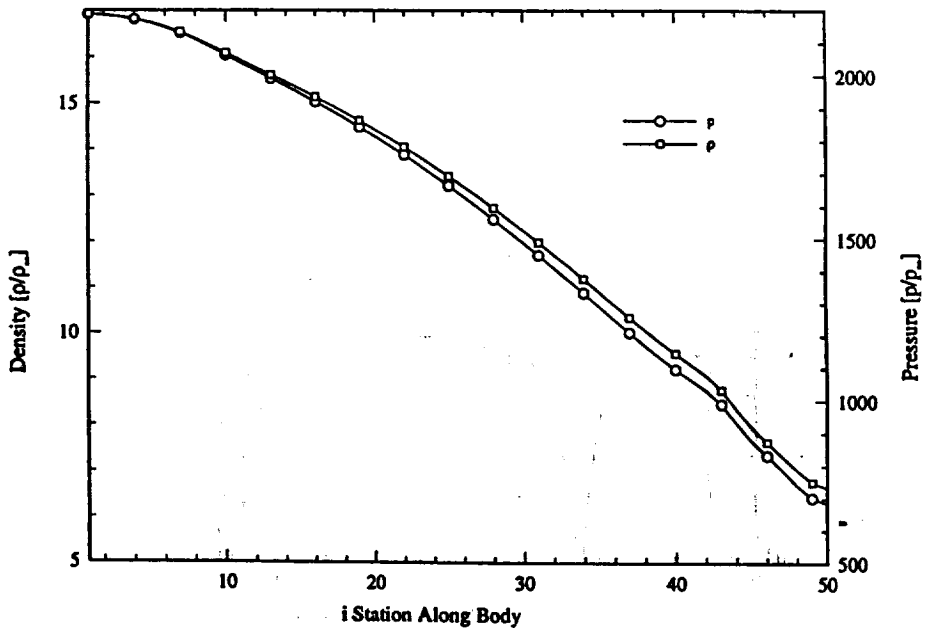

Figure 18: Cylinder Case - Density and Pressure Profiles without Radiative Coupling Along the Body

transfer in the shock layer of a high speed re-entry body. Many years ago, Carlson[22] estimated these rates assuming that ionization is a two step process which is rate limited by electronic excitation from the ground states to the excited states and by using an excitation cross-section approximately one tenth of the theoretical maximum. However, the work of Zel'dovich and Razier,[36] implies that the excitation cross-section could be an order of magnitude smaller than Carlson's estimate; and, thus, the rates for the ionization of atomic nitrogen due to atom impact by both neutral and ionized atomic nitrogen could be significantly different.

Results using Carlson's rates have been first compared to those obtained by reducing the forward rates for reaction 26 by a factor of ten. Figure 19 gives the thermal profile through the shock layer for both Carlson's rates and the reduced rates. Note that the shock standoff distance has increased by 0.2 cm compared to the results with the original rates, and that the translational and vibrational modes do not equilibrate as rapidly. Figure 20 gives the pressure and density for this case, while Figures 21 and 22 give the chemical composition for Carlson's rates and the lowered rates, respectively. As expected, the ionization of atomic nitrogen proceeds much slower, and many of the molecular profiles, particularly N_2, O_2, and NO are significantly different near the wall. Obviously the amount of atomic impact ionization affects the chemistry in significant and subtle ways.

The grouped and detailed radiation frequency spectra for the two rates are compared on Figures 23 and 24, and they show a significant decrease in the atomic line radiation for the case with decreased rates. The net radiative flux to the wall calculated

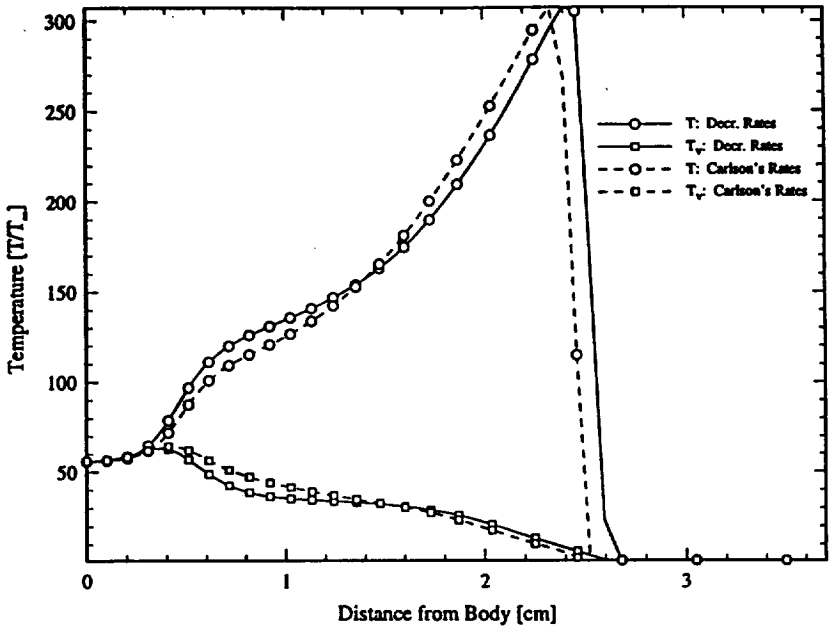

Figure 19: Cylinder Case - Thermal Profile, Decreased Atom Impact Ionization Rates Versus Carlson's Rates

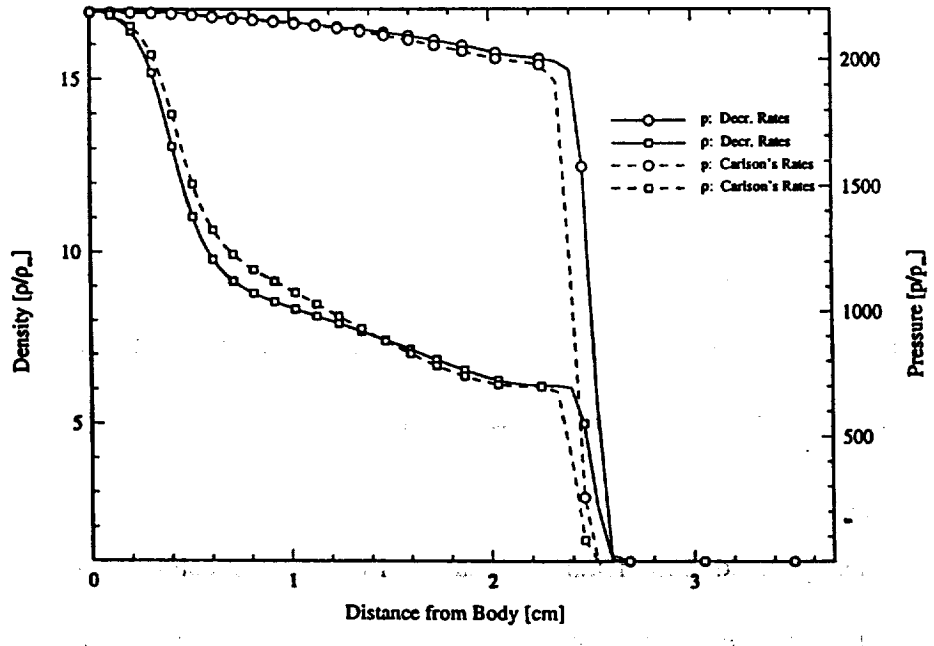

Figure 20: Cylinder Case - Density and Pressure Profiles, Decreased Atom Impact Ionization Rates Versus Carlson's Rates

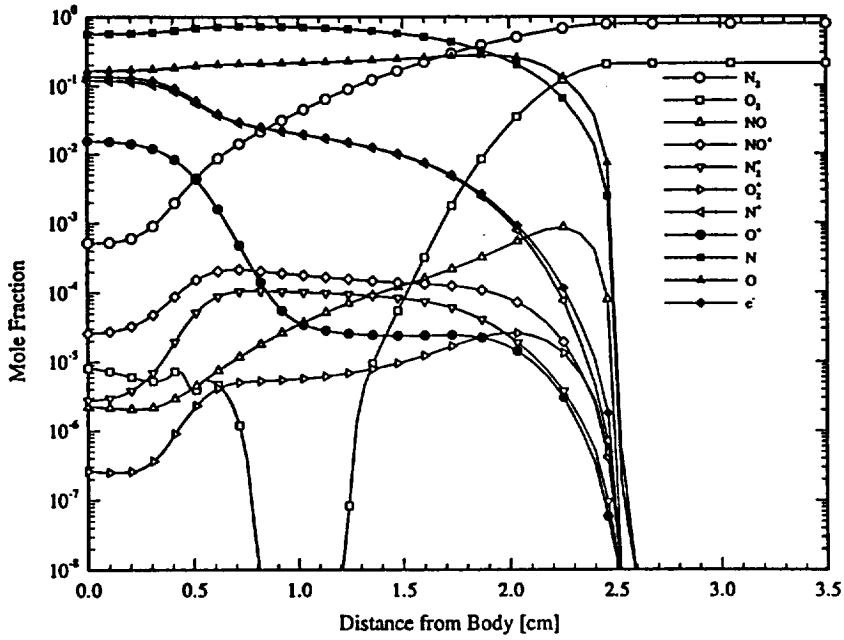

Figure 21: Cylinder Case - Mole Fractions for Carlson's Atom Impact Ionization Rates

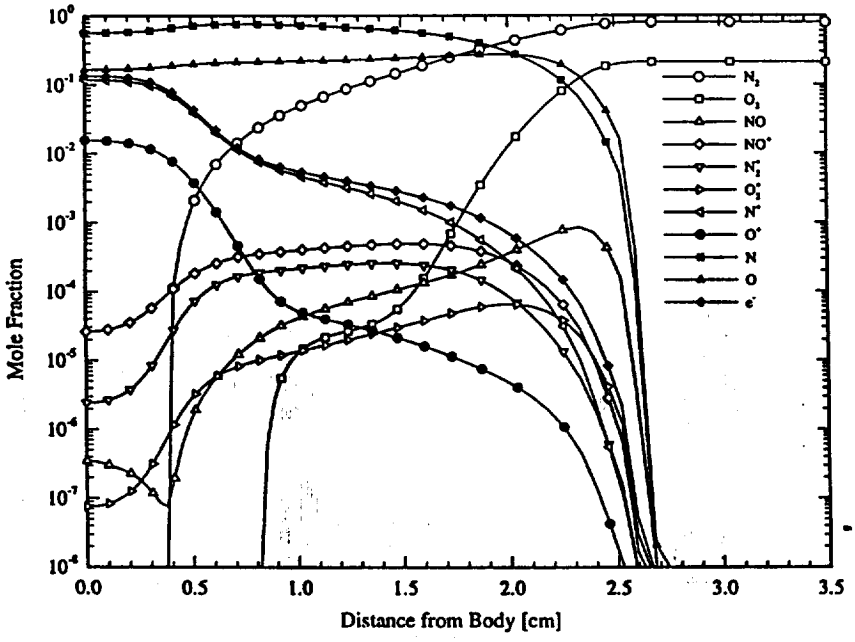

Figure 22: Cylinder Case - Mole Fractions for Decreased Atom Impact Ionization Rates

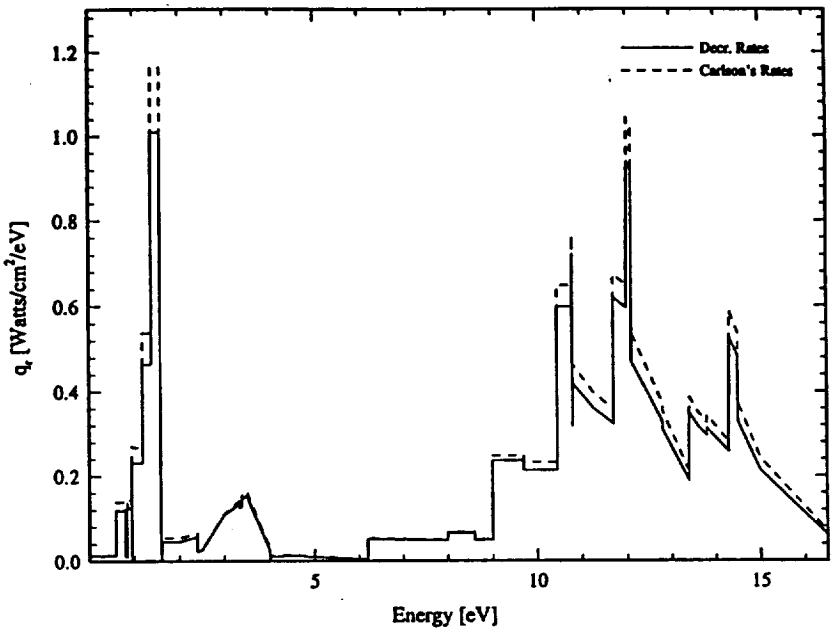

Figure 23: Cylinder Case - Grouped Radiative Spectra, Decreased Atom Impact Ionization Rates Versus Carlson's Rates

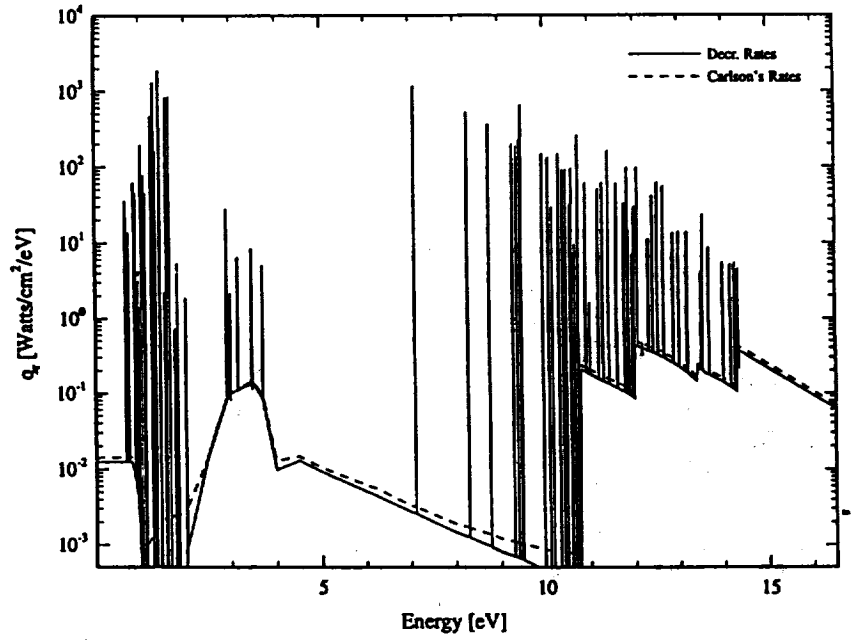

Figure 24: Cylinder Case - Detailed Radiative Spectra, Decreased Atom Impact Ionization Rates Versus Carlson's Rates

with decreased rates is 3.02 W/cm^2 compared to 3.35 W/cm^2 for the unmodified rates. It should be noted that these results assume no radiative coupling.

In order to further examine flowfield dependence on the atomic impact ionization rates, these rates were also increased by an order of magnitude. As shown on Figure 15, the shock standoff distance for this case decreased from 2.5 cm to 1.7 cm, and the temperature profiles exhibited a lower translational-rotational temperature immediately after the shock than found with the original rates. In addition, the thermal equilibrium region increased to almost one centimeter compared to 0.4 cm originally. The reduced shock standoff distance is caused by the shorter nonequilibrium zone and the corresponding faster rise in the total density after the shock (Figure 16).

A comparison of the chemistry profiles in Figures 17 and 18 shows that the utilization of the increased atomic impact ionization rates has greatly increased the chemical relaxation rate of the major species behind the shock front. In addition, this larger equilibrium region and the presence of more free electrons immediately behind the shock front has greatly increased the atomic line and continuum radiation, as shown on Figures 19 and 20, changing the total radiative heat transfer to the wall from 3.35 to 8.22 W/cm^2. Therefore, contrary to some investigators' assumptions, atomic impact ionization may be very important in the immediate post shock region.

Radiatively Coupled Solutions

The cylinder configuration was investigated using the present model with the radiation loosely coupled with the flowfield solver. In other words, the radiation was

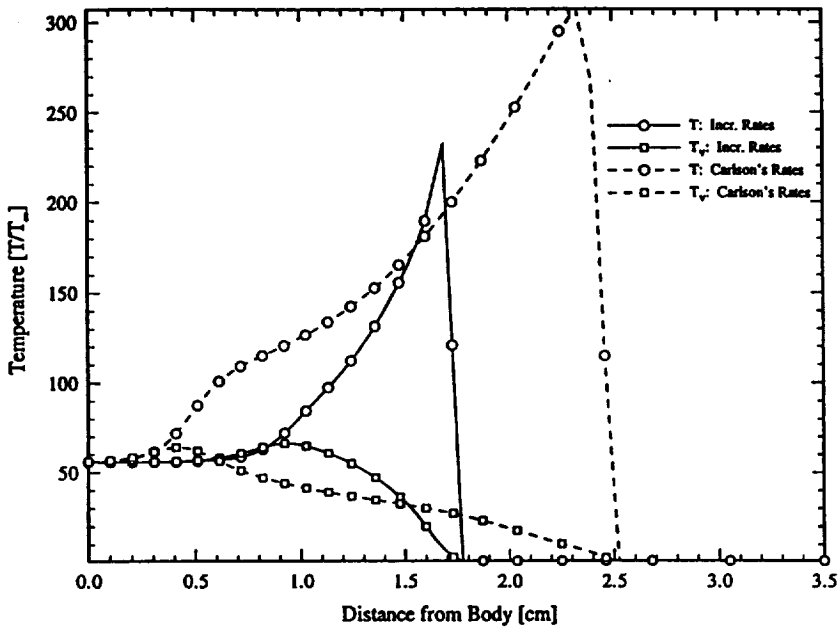

Figure 25: Cylinder Case - Thermal Profile, Increased Atom Impact Ionization Rates Versus Carlson's Rates

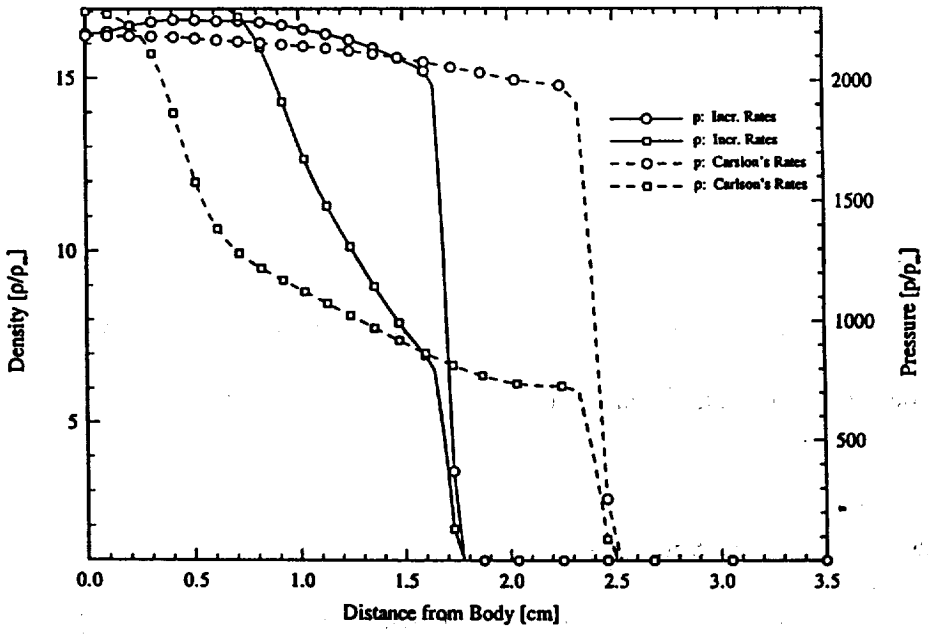

Figure 26: Cylinder Case - Density and Pressure Profiles, Increased Atom Impact Ionization Rates Versus Carlson's Rates

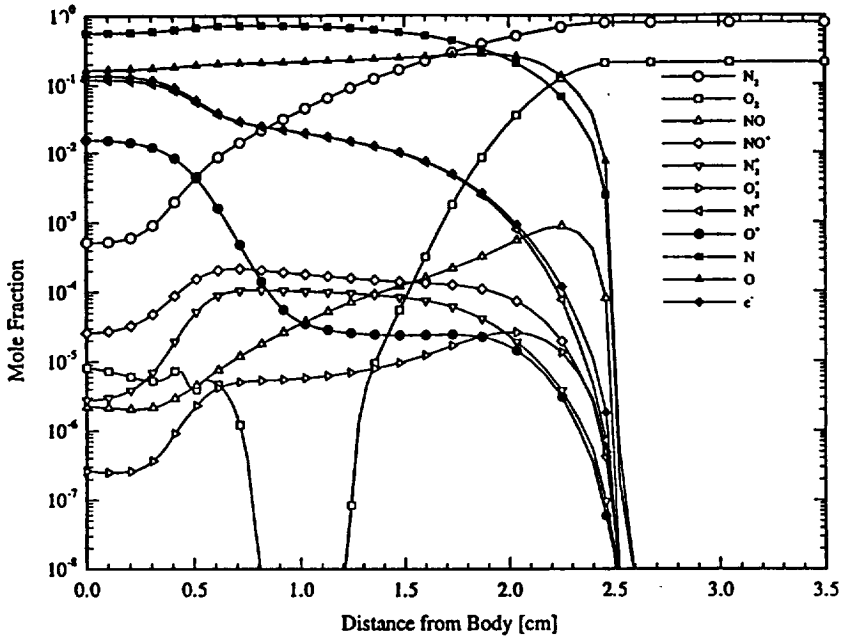

Figure 27: Cylinder Case - Mole Fractions for Carlson's Atom Impact Ionization Rates

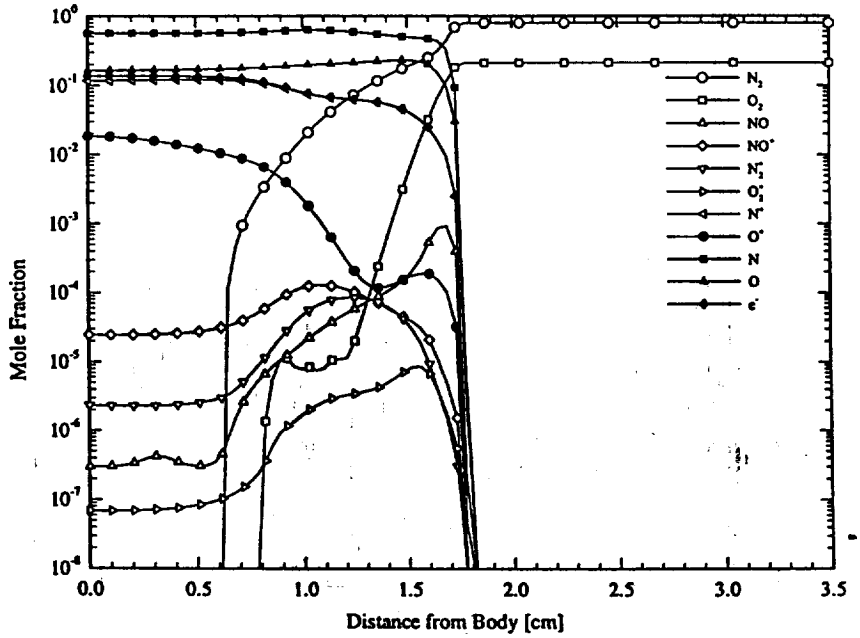

Figure 28: Cylinder Case - Mole Fractions for Increased Atom Impact Ionization Rates

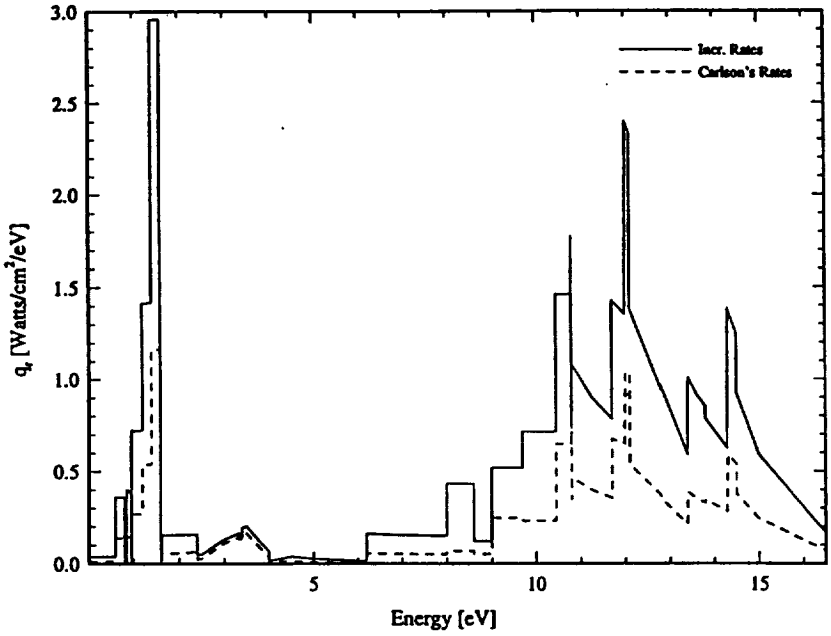

Figure 29: Cylinder Case - Grouped Radiative Spectra, Increased Atom Impact Ionization Rates Versus Carlson's Rates

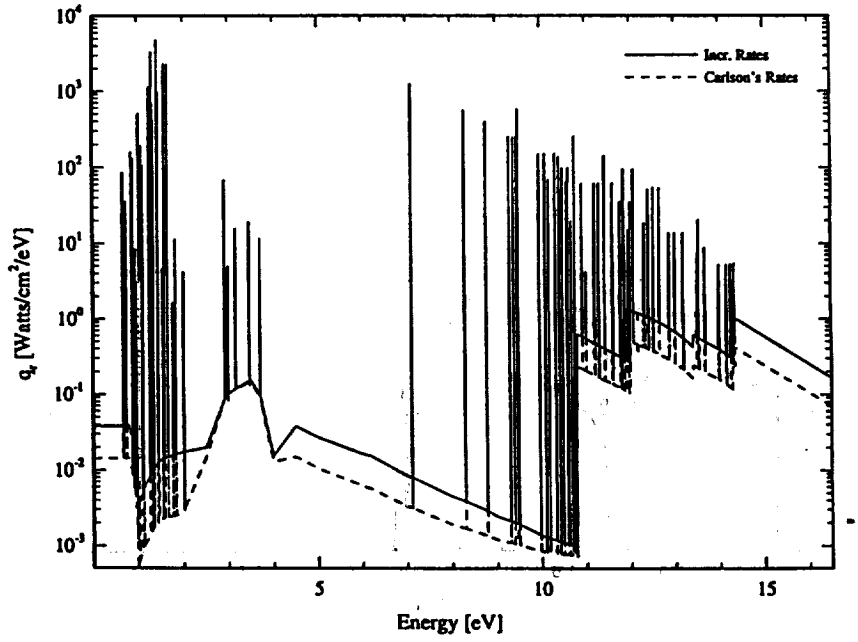

Figure 30: Cylinder Case - Detailed Radiative Spectra, Increased Atom Impact Ionization Rates Versus Carlson's Rates

added explicitly to the right hand side of the energy equations while neglecting the radiative Jacobian. Thermal and chemical stagnation profiles are presented in Figures 21 and 22; and obviously, for this case, the radiation coupling has no noticeable effect as the solutions are almost identical. In addition, the net radiative flux to the wall for this case was found to be 3.34 W/cm^2, which is only slightly less than the uncoupled result.

In order to verify the qualitative aspects of the radiation coupling, the radiative coupling terms, which are added to the energy equations, were increased by an order of magnitude. It was observed that increasing the radiation coupling did not have a significant effect on the thermodynamic variables in the shock layer and the radiative heat transfer to the stagnation point dropped by only one percent, as shown in Table II. Thus, the radiation coupling effects were found to be inconclusive due to two factors. First, the amount of radiative coupling for the flight condition examined was likely very small. Second, the difference in radiative flux values may simply reflect the level of solution convergence.

This case was also computed with radiation coupling only in the global energy equation in order to see the consequences of excluding the radiation term in the VEE energy equation. The effect on the flowfield variables, chemistry, and radiation was found to be negligible. Unfortunately, since radiation coupling for this case was small, these results do not definitively establish that the radiative coupling term can be neglected in the VEE energy equation, and further study is needed.

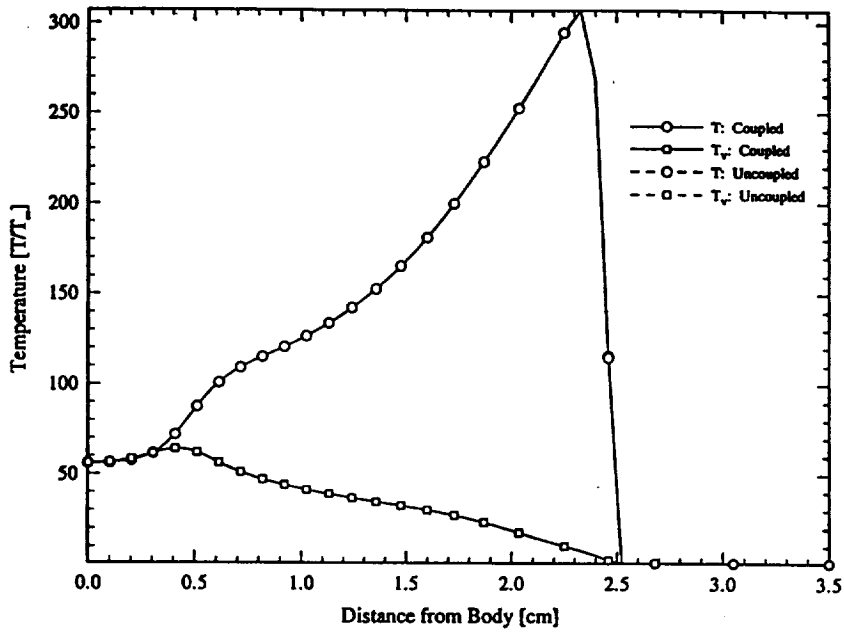

Figure 31: Cylinder Case - Thermal Profile, Radiative Coupling in the Global and VEE Energy Equations Versus Uncoupled

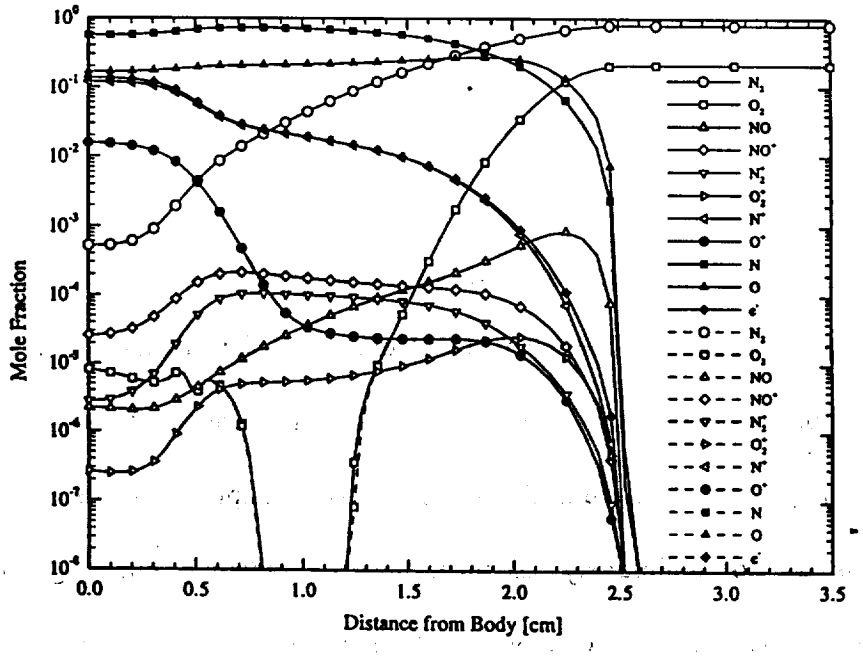

Figure 32: Cylinder Case - Mole Fractions, Radiative Coupling in the Global and VEE Energy Equations Versus Uncoupled

Effect of $\Sigma\omega_s e_{el,s}$ Term

As discussed earlier, there is question concerning the importance of the $\Sigma\omega_s e_{el,s}$ term in equation (19) which accounts for the change in average electronic energy due to a chemical reaction. Thus, the cylinder configuration was computed both with and without this term; and it was found to have no discernible effect on the solution. Since this case has significant ionization, the exclusion of this term should have produced different results if it were important. However, since its inclusion does not appear to affect either the results or the effort required to obtain a solution, it probably should be retained. The present results for the cylinder case are all summarized in Table III.

Table III. Summary of Flowfield Results for the Cylinder Configuration

Case	Shock Standoff Distance, Δ (cm)	Radiative Heat Flux to the Wall (W/cm^2)
Radiatively Uncoupled (20,000 iter.)	2.36	2.69
Radiatively Uncoupled (40,000 iter.)	2.36	3.35
Radiatively Coupled	2.36	3.34
Radiation in Global Energy Eq. Only	2.36	3.32
Radiation Coupling x10	2.36	3.27
Lowered Ionization Rates ($A=2.3\times10^{10}$)	2.42	3.02
Increased Ionization Rates ($A=2.3\times10^{12}$)	1.70	8.22
Removed $\Sigma\omega_s e_{el,s}$ Term from VEE Eq.	2.36	3.35

Fire 2 1632 Flowfield Results

A two dimensional version of the Fire 2 flight experiment at 1632 seconds mission time was examined. As previously mentioned, the body was scaled down to one third size to approximately match the shock standoff distance found in the three dimensional case. The flowfield variables took longer to converge than the cylinder case due to the larger region of equilibrium. The maximum CFL numbers which still forced the solution towards convergence were used and varied between 2.0 and 0.0625. The smaller CFL values were needed after avalanche ionization began, which started at approximately 12,000 iterations as the two temperatures converged in pseudo-time. Stagnation streamline thermal profiles are given in Figure 33 for 19,000 and 38,000 iterations. Although the temperature plots are similar, a large number of iterations were needed to resolve the chemistry in the stagnation region; and as a result, for the two times shown, the temperature dropped in the stagnation region from approximately 12500 K to 10500 K. This temperature drop is caused by the energy sink of the dissociation and ionization chemical reactions in the stagnation region. The pressure and density, shown on Figure 34, both exhibit corresponding increases.

Figures 37 and 38 give the chemistry profiles at the two iteration stages. At 38,000 cycles the avalanche ionization region has increased in size and the diatomic oxygen and nitrogen near the wall has dissociated several orders of magnitude further. The oscillations in the O_2 concentrations are numerical effects caused by large gradients or possibly species conservation problems associated with the diagonal implicit algorithm (to be discussed later). The radiative transfer spectral results in Figures 37 and 38 show

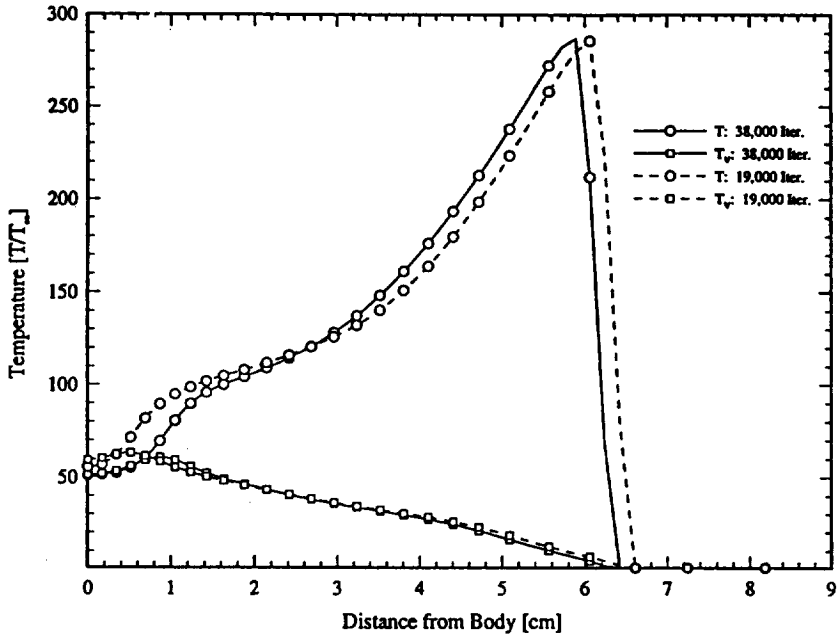

Figure 33: Fire 2 1632 Case - Thermal Profile without Radiative Coupling, 19,000 and 38,000 Iterations

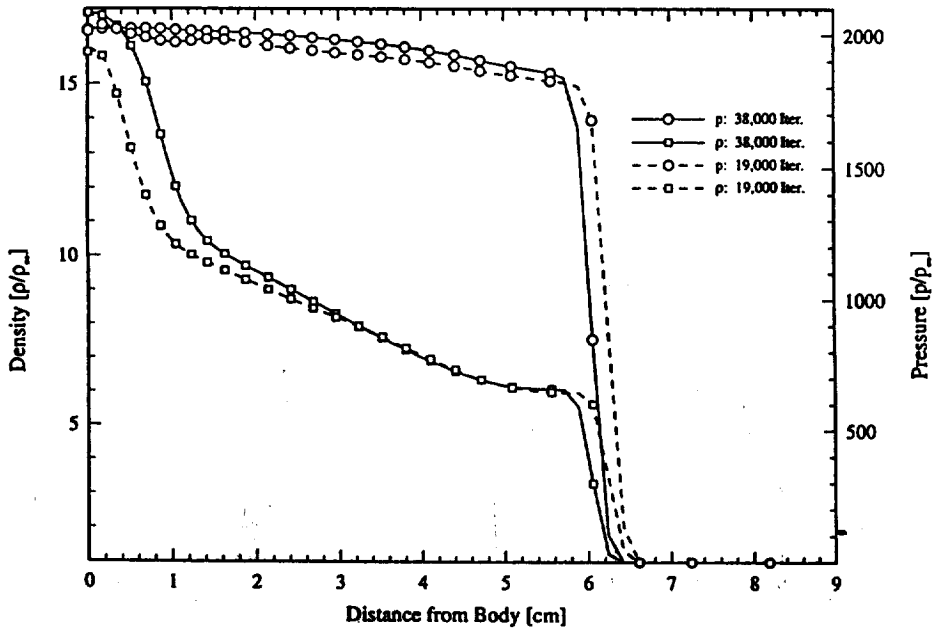

Figure 34: Fire 2 1632 Case - Density and Pressure Profiles without Radiative Coupling, 19,000 Iterations and 38,000 Iterations

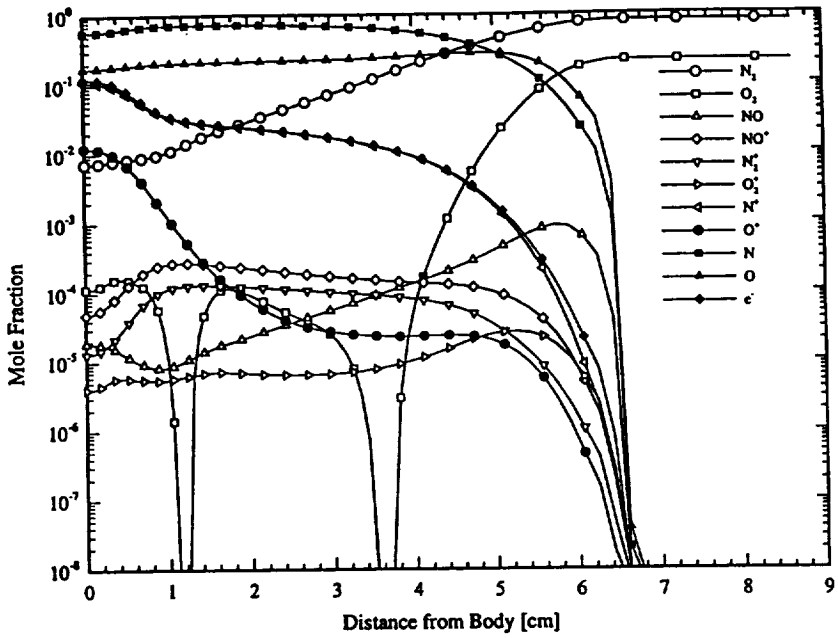

Figure 35: Fire 2 1632 Case - Mole Fractions at 19,000 Iterations without Radiative Coupling

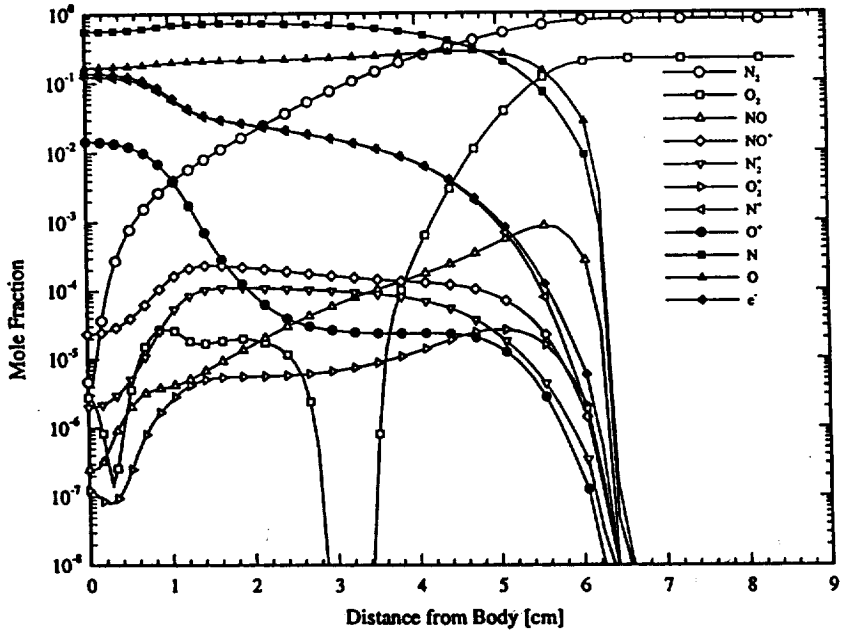

Figure 36: Fire 2 1632 Case - Mole Fractions at 38,000 Iterations without Radiative Coupling

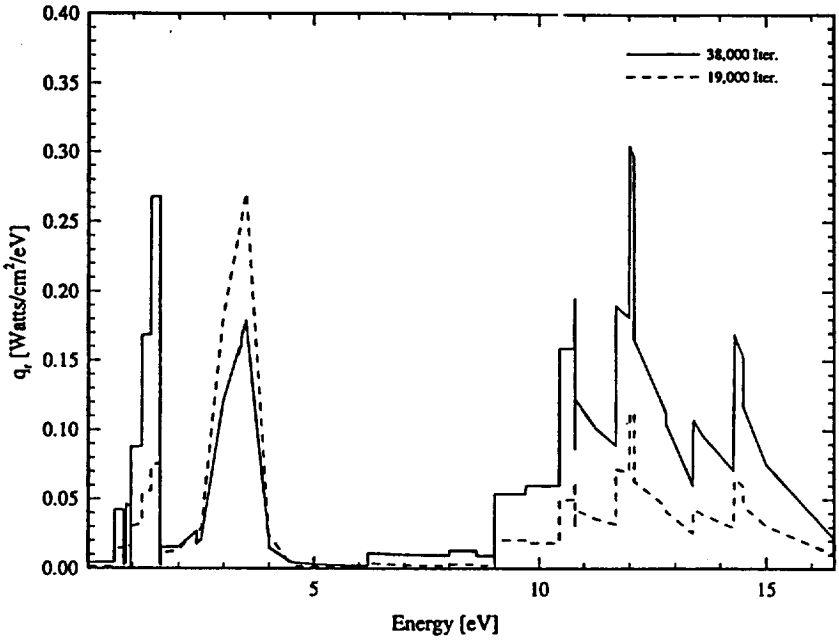

Figure 37: Fire 2 1632 Case - Grouped Radiative Spectra without Radiative Coupling, 19,000 Iterations and 38,000 Iterations

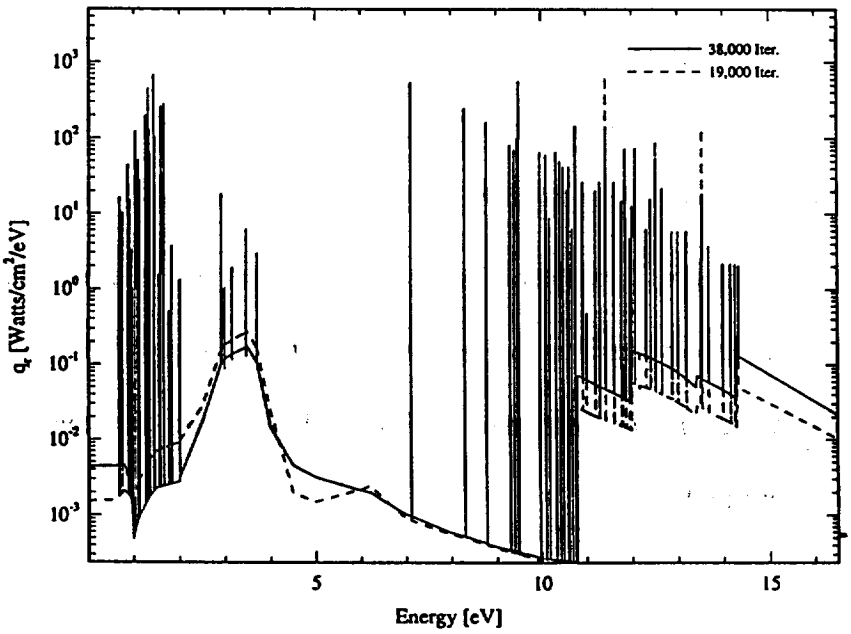

Figure 38: Fire 2 1632 Case - Detailed Radiative Spectra without Radiative Coupling, 19,000 Iterations and 38,000 Iterations

hat due to the increase in the size of the equilibrium region, the radiative flux to the wall has increased between the two iterative levels from 0.58 W/cm^2 to 1.03 W/cm^2 due to the increase in contributions from atomic lines above 9 eV and the decrease in $N_2^+(1^-)$ in the 2-4 eV region.

Results along the constant i lines noted in Figure 2 are presented in Figures 39 through 46. High free electron mole fractions are evident in the avalanche ionization region until the flow encounters the relatively sharp corner near the outflow plane. Here, the gas rapidly expands around the corner causing the translational temperature, density, and pressure to drop dramatically. The vibrational temperature requires many more collisions to reach equilibrium, and, thus, the vibrational temperature remains relatively constant, as shown in Figures 47 and 48.

Modified Atom-Atom Impact Ionization Rates

Results using the original atomic impact rates are compared to those using the decreased rates in Figures 49 through 54. Although the shock standoff distance increased by approximately 0.1 cm, it is clear that the overall effect on the flowfield was small. Thus, the flowfield is less sensitive to changes in the atomic impact ionization rates when the flight conditions are less extreme. All preceding results for the 1632 case are summarized below in Table IV.

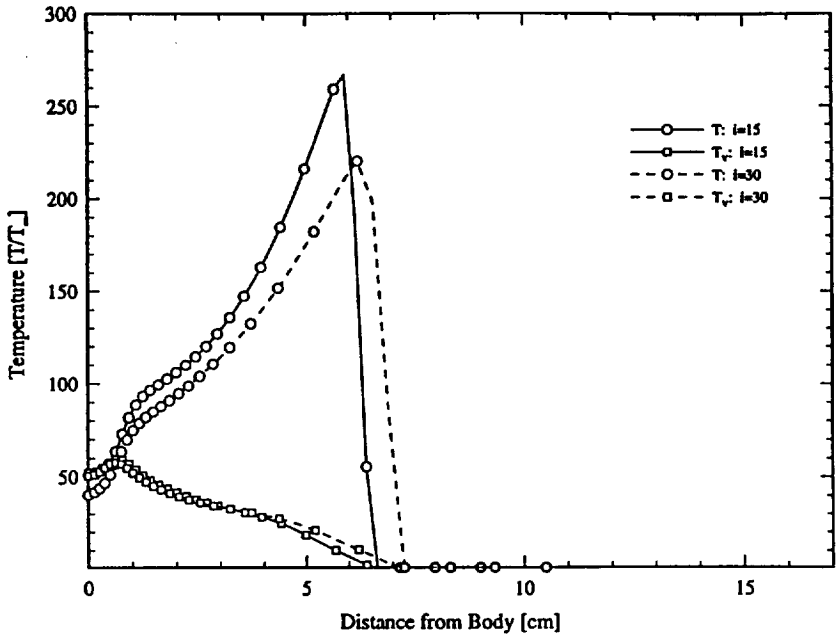

Figure 39: Fire 2 1632 Case - Thermal Profile without Radiative Coupling Along Grid Lines i = 15 and i = 30

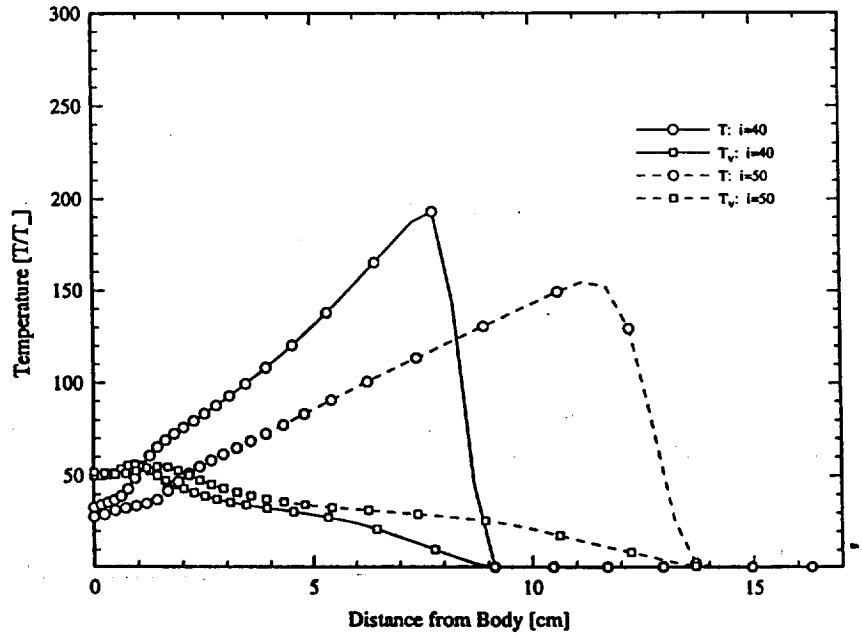

Figure 40: Fire 2 1632 Case - Thermal Profile without Radiative Coupling Along Grid Lines i = 40 and i = 50

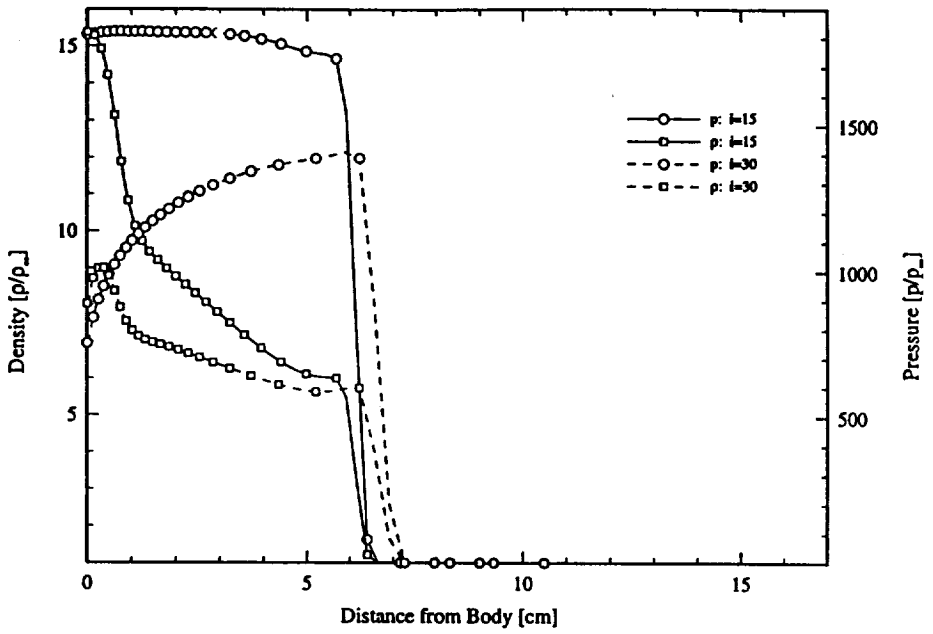

Figure 41: Fire 2 1632 Case - Density and Pressure Profiles without Radiative Coupling Along Grid Lines i = 15 and i = 30

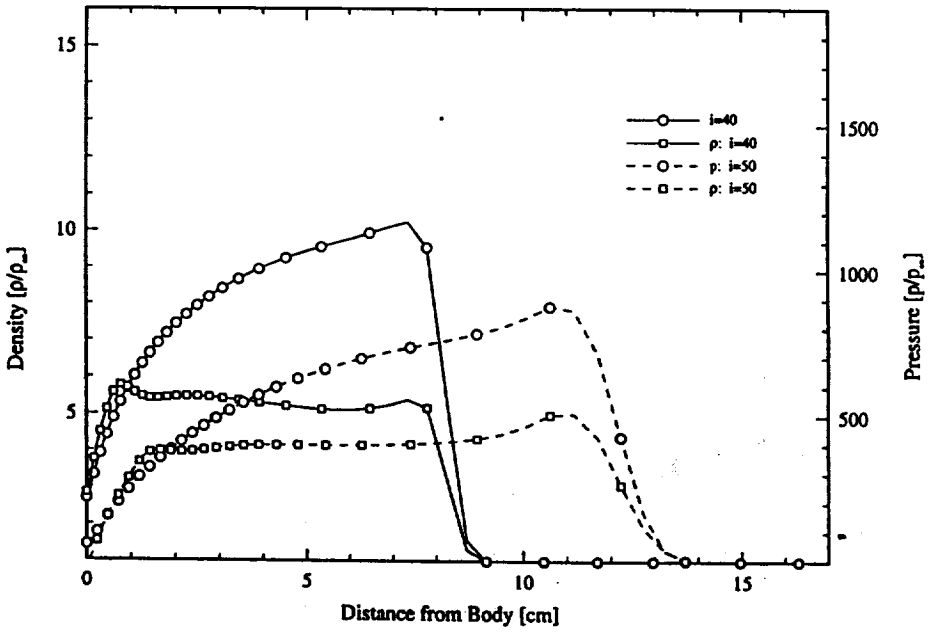

Figure 42: Fire 2 1632 Case - Density and Pressure Profiles without Radiative Coupling Along Grid Lines i = 40 and i = 50

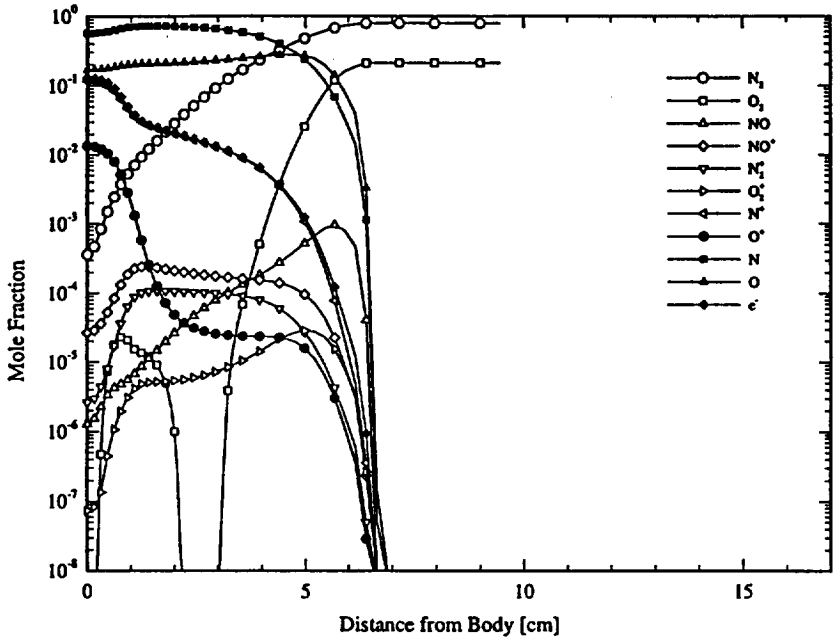

Figure 43: Fire 2 1632 Case - Mole Fractions without Radiative Coupling Along Grid Line i = 15

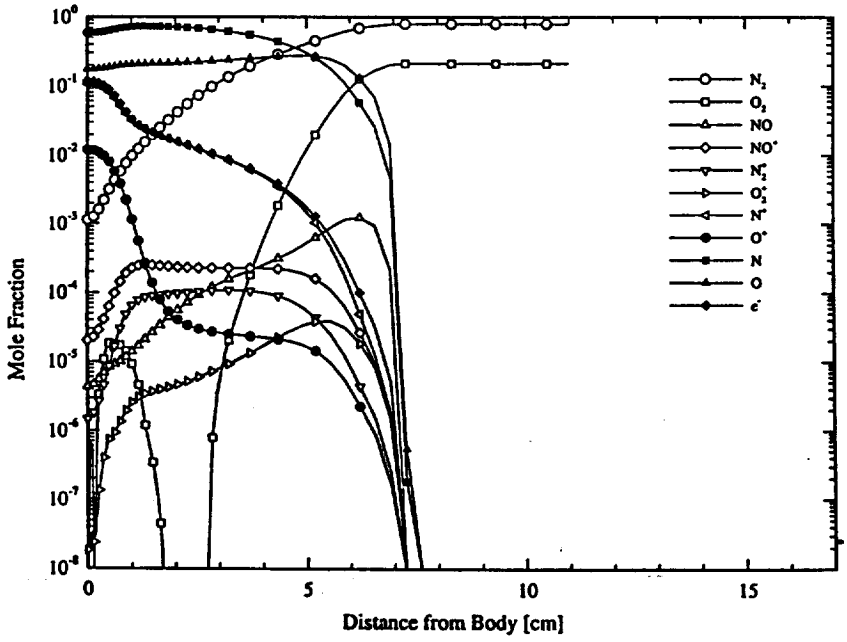

Figure 44: Fire 2 1632 Case - Mole Fractions without Radiative Coupling Along Grid Line i = 30

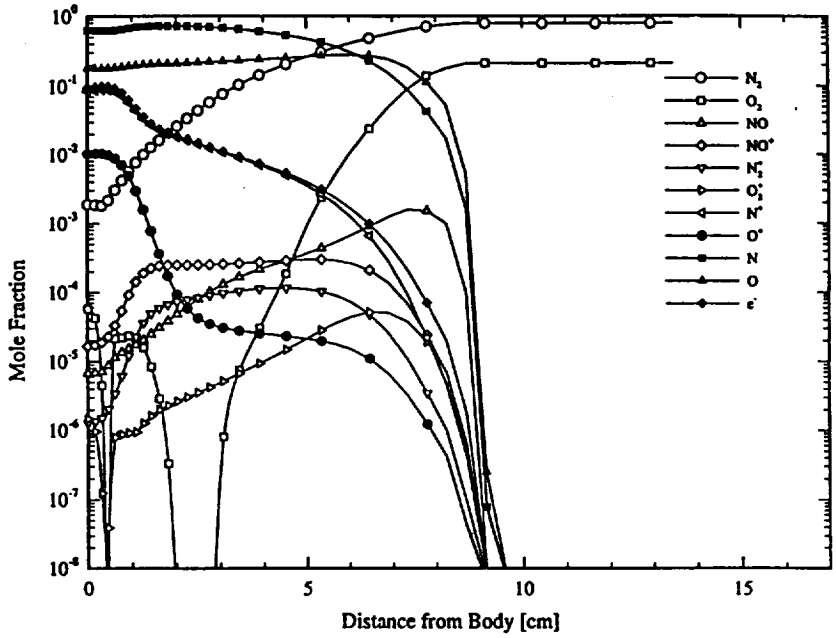

Figure 45: Fire 2 1632 Case - Mole Fractions without Radiative Coupling Along Grid Line i = 40

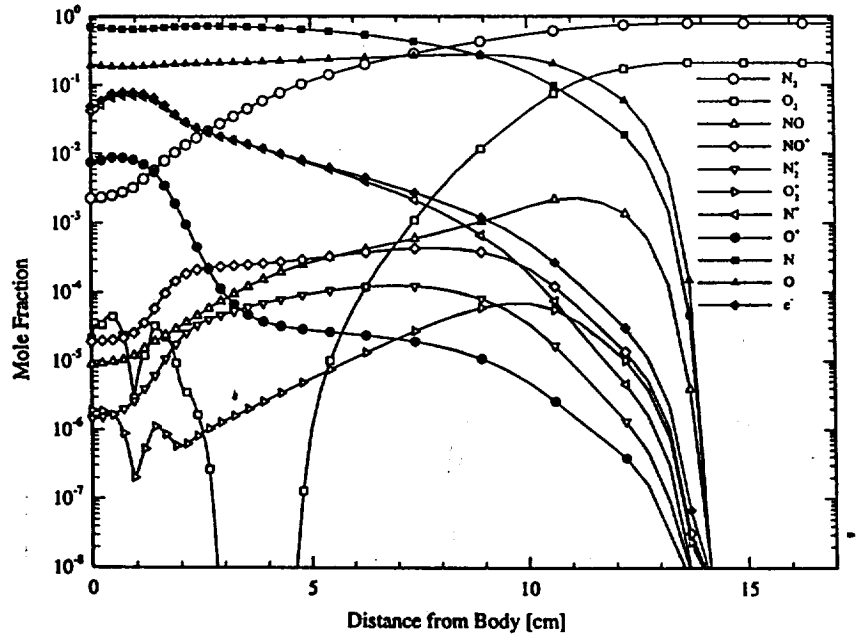

Figure 46: Fire 2 1632 Case - Mole Fractions without Radiative Coupling Along Grid Line i = 50

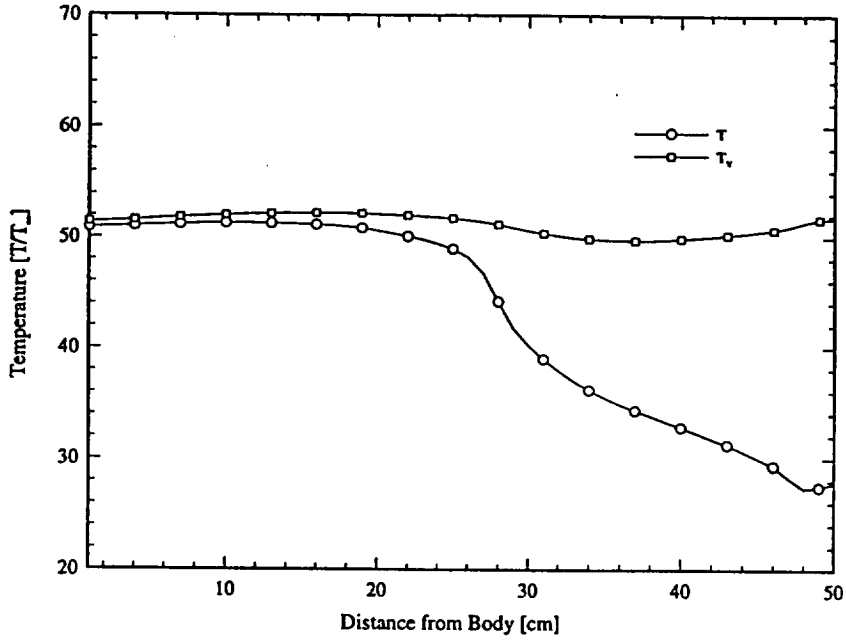

Figure 47: Fire 2 1632 Case - Thermal Profile without Radiative Coupling Along the Body

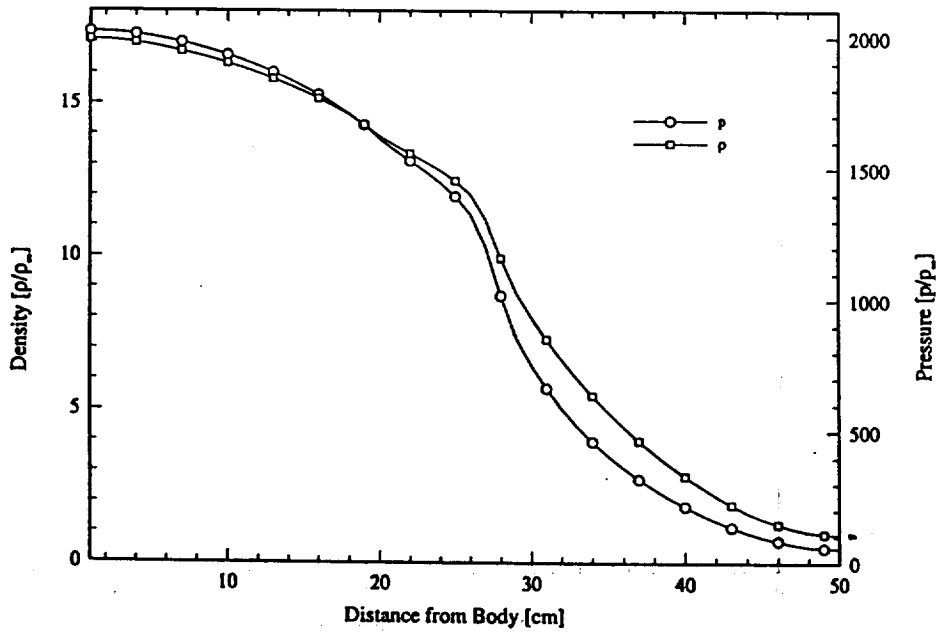

Figure 48: Fire 2 1632 Case - Density and Pressure Profiles without Radiative Coupling Along the Body

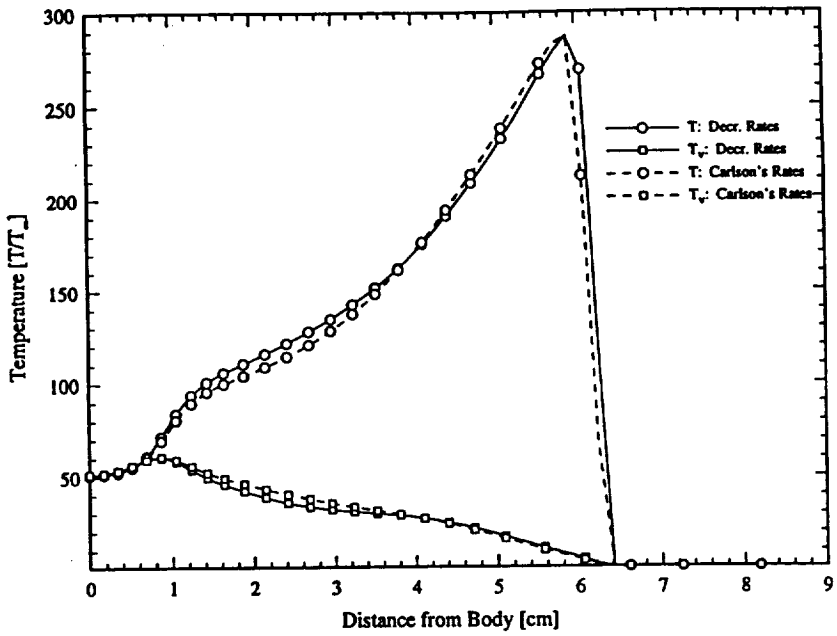

Figure 49: Fire 2 1632 Case - Thermal Profile, Decreased Atom Impact Ionization Rates Versus Carlson's Rates

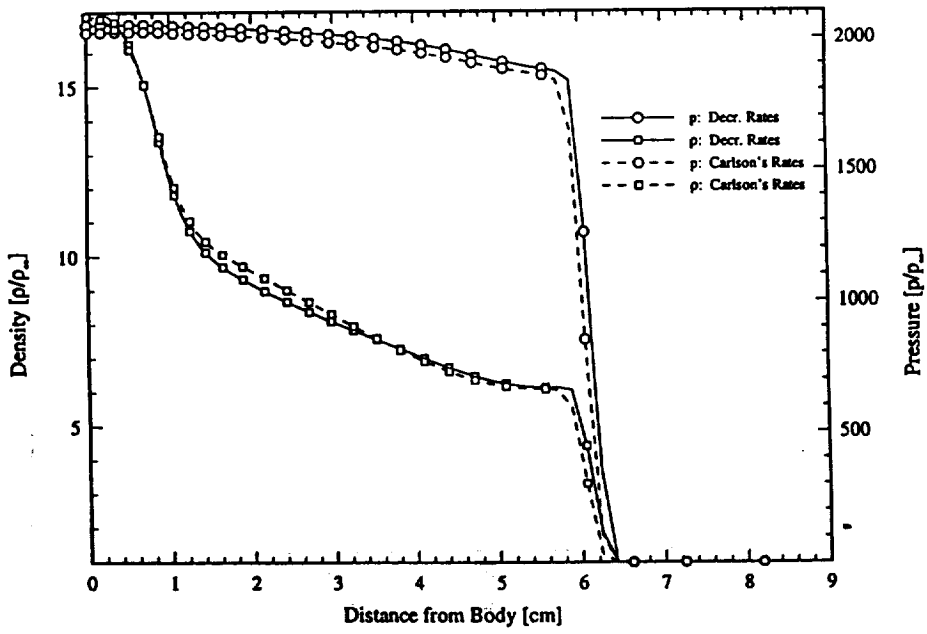

Figure 50: Fire 2 1632 Case - Density and Pressure Profiles, Decreased Atom Impact Ionization Rates Versus Carlson's Rates

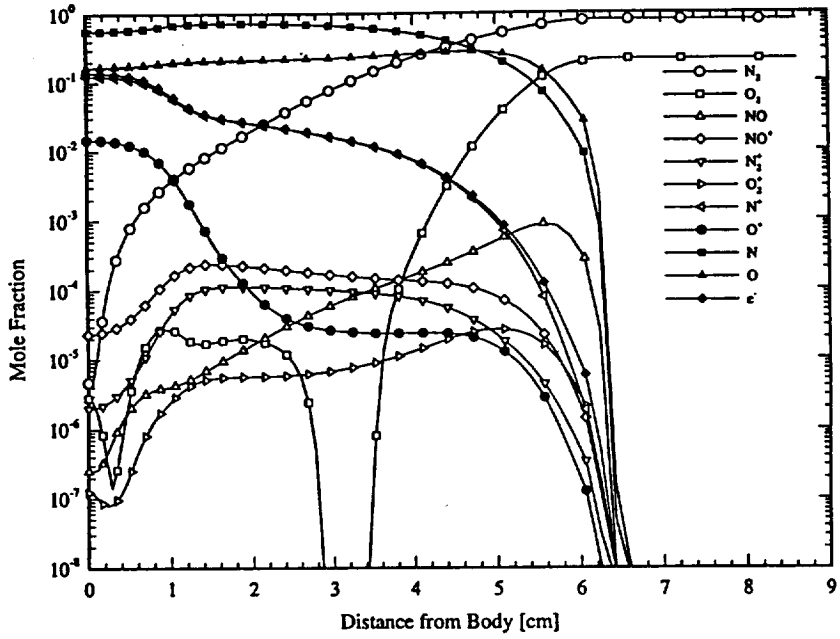

Figure 51: Fire 2 1632 Case - Mole Fractions for Carlson's Atom Impact Ionization Rates

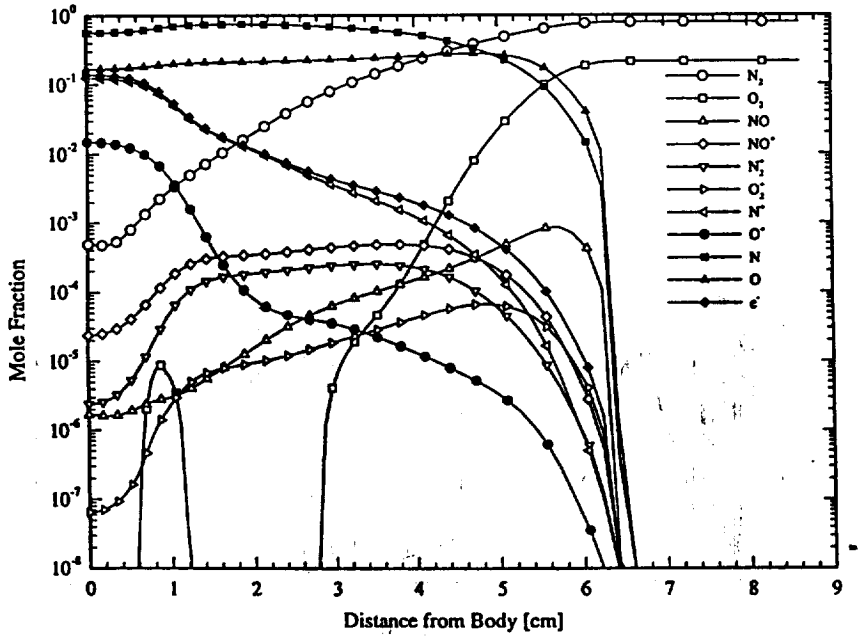

Figure 52: Fire 2 1632 Case - Mole Fractions for Decreased Atom Impact Ionization Rates

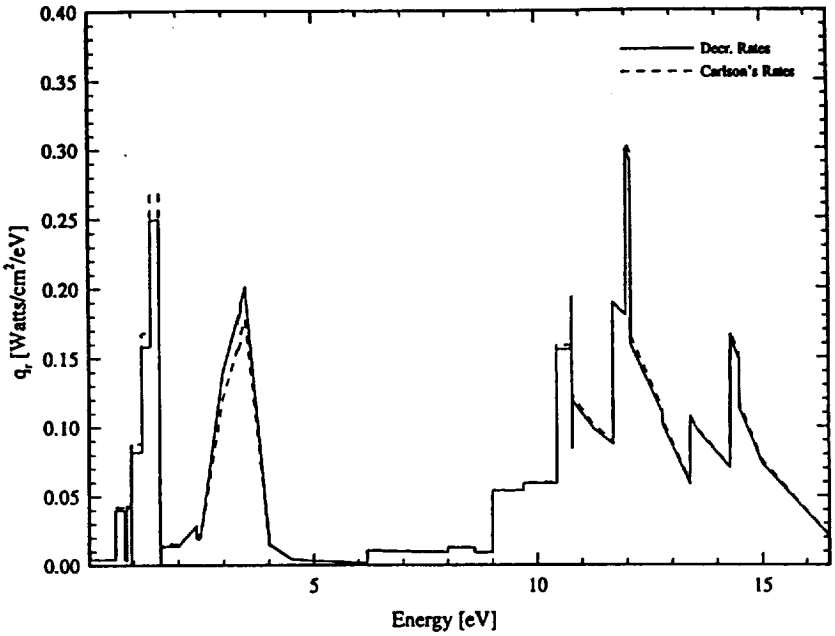

Figure 53: Fire 2 1632 Case - Grouped Radiative Spectra, Decreased Atom Impact Ionization Rates Versus Carlson's Rates

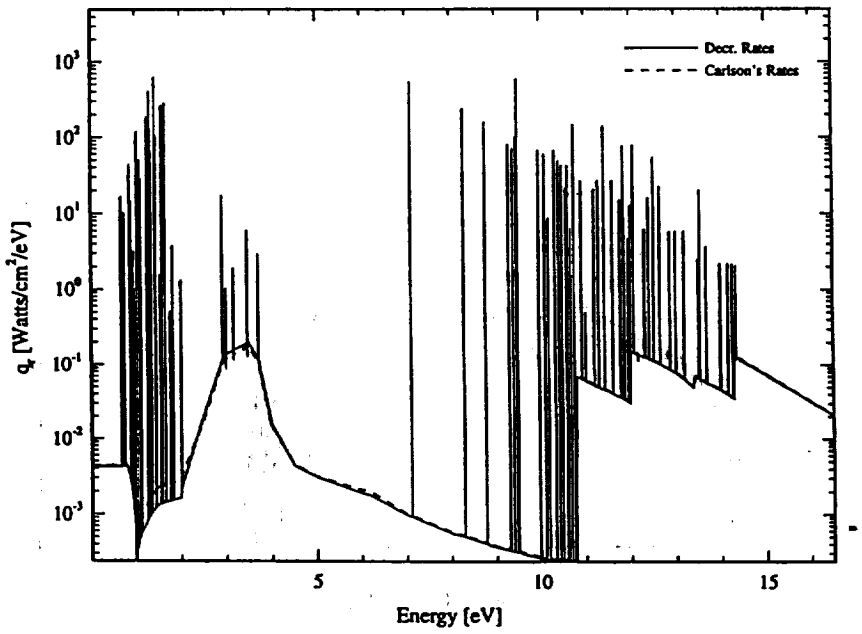

Figure 54: Fire 2 1632 Case - Detailed Radiative Spectra, Decreased Atom Impact Ionization Rates Versus Carlson's Rates

Table IV. Summary of Results for the 1632 Configuration

Case	Shock Standoff Distance, Δ (cm)	Radiative Heat Flux to the Wall, (W/cm^2)
Radiatively Uncoupled (19,000 iter.)	6.14	0.58
Radiatively Uncoupled (38,000 iter.)	5.80	1.03
Lowered Ionization Rates ($A=2.34x10^{10}$)	5.96	1.03

Quiescent Oxygen Results

To investigate further the consequences of diagonalizing the chemical source Jacobian a quiescent oxygen reacting gas was also studied. Results were obtained using a pilot code for both oxygen dissociation and recombination cases. Since for the quiescent situation there is no flow into or out of the control volume, the total density remained constant at the initial value of $2.85x10^{-4}$ kg/m^3. In both cases, the time step was increased exponentially by multiplying the time step at each iteration by the factor 1.1; and the criteria for a converged solution was that the temperature change between successive iterations be less than $1x10^{-4}$ K. These cases were computed with the diagonal implicit approximation of the source Jacobian both added to (+) and subtracted from (-) the left hand side of the solution scheme. These cases correspond to a negative and positive source Jacobian on the right hand side, respectively. In this section, results for these cases are compared to those obtained using a fully implicit algorithm.

Oxygen Dissociation

For this case diatomic oxygen is perturbed from 300 K to 10,000 K at time t_0. Figures 55 and 56 present results with an initial time step of $1x10^{-7}$ seconds, and all cases required 109 iterations to converge. The time step was set initially to a small value due to the fast reaction rates at the initially high temperature. The final equilibrium temperature agrees fairly well for all three cases at approximately 2920 K. The mass fractions for O also agree at 29.1%, but the O_2 mass fractions for the diagonal implicit schemes are 2% low for the diagonal (+) scheme and 4% high for the diagonal (-) scheme as compared to the fully implicit method (70.9%). Obviously, in the current diagonalized formulation, the elemental species are not being perfectly conserved.

The initial time step was then increased to $1x10^{-6}$ seconds. The fully implicit and the positive diagonal implicit each took 85 iterations, while the negative diagonal approach quickly diverged to the imposed limits on mass fraction ($1x10^{-18} < c < 1$). Figures 57 and 58 indicate that although the equilibrium temperatures were close, the O_2 mass fractions were again quite different. In addition, the path to convergence was different for the two solutions from the results shown on Figure 40. Thus, for larger initial values of Δt, it appears that the solution behavior is algorithm dependent.

Oxygen Recombination

The case examining oxygen recombination assumed that the gas was initially in the atomic state at a very high temperature, which then instantaneously dropped to 1000 K. Figures 59 and 60 display the resulting thermal and chemical profiles for an initial

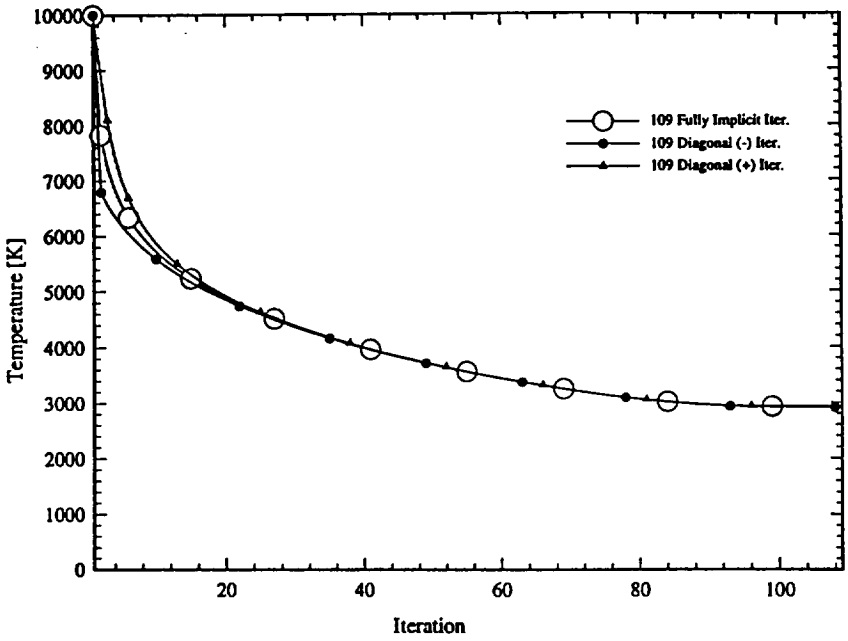

Figure 55: Oxygen Dissociation - Temperature Comparison for Fully Implicit, Diagonal (-), and Diagonal (+), $\Delta t_o = 1x10^{-7}$

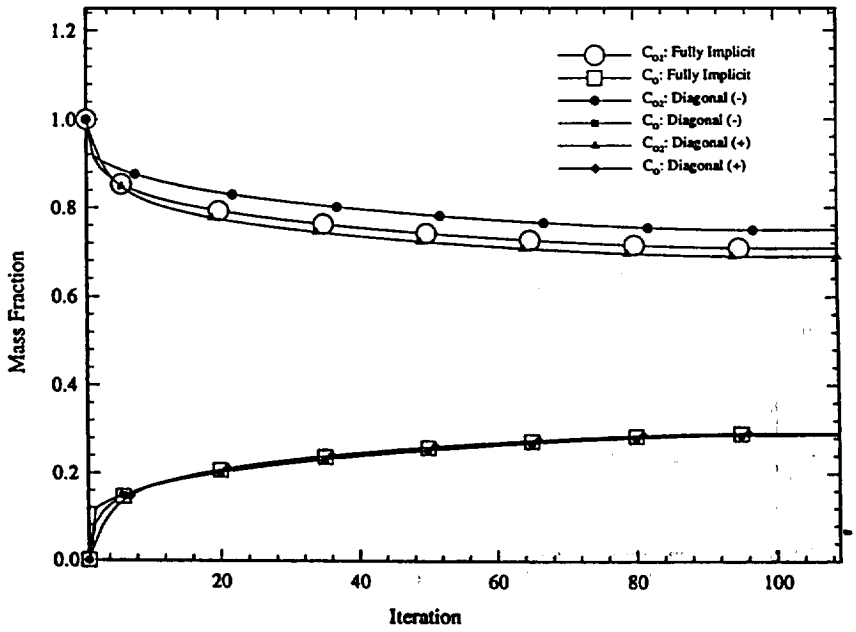

Figure 56: Oxygen Dissociation - Mass Fraction Comparison for Fully Implicit, Diagonal (-), and Diagonal (+), $\Delta t_o = 1x10^{-7}$

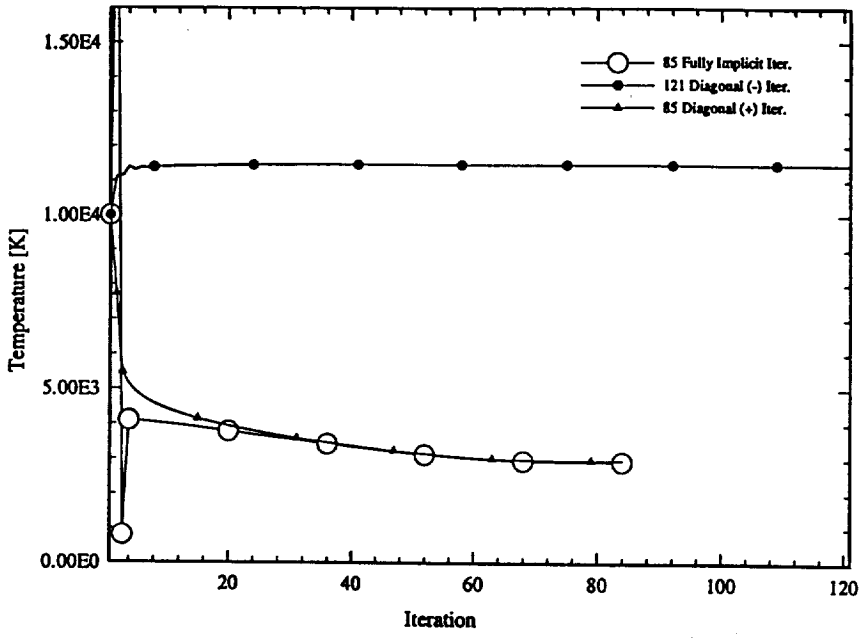

Figure 57: Oxygen Dissociation - Temperature Comparison for Fully Implicit, Diagonal (-), and Diagonal (+), $\Delta t_o = 1x10^{-6}$

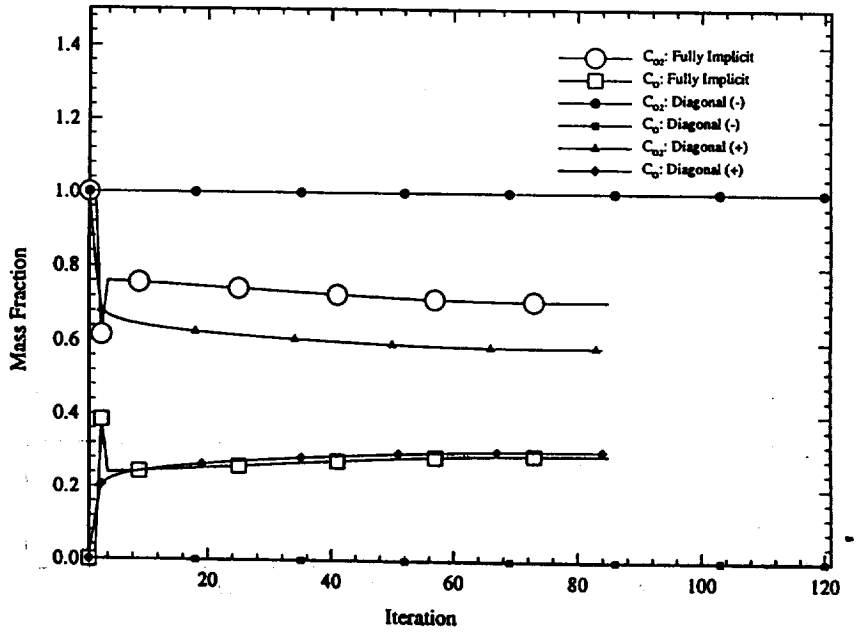

Figure 58: Oxygen Dissociation - Mass Fraction Comparison for Fully Implicit, Diagonal (-), and Diagonal (+), $\Delta t_o = 1x10^{-6}$

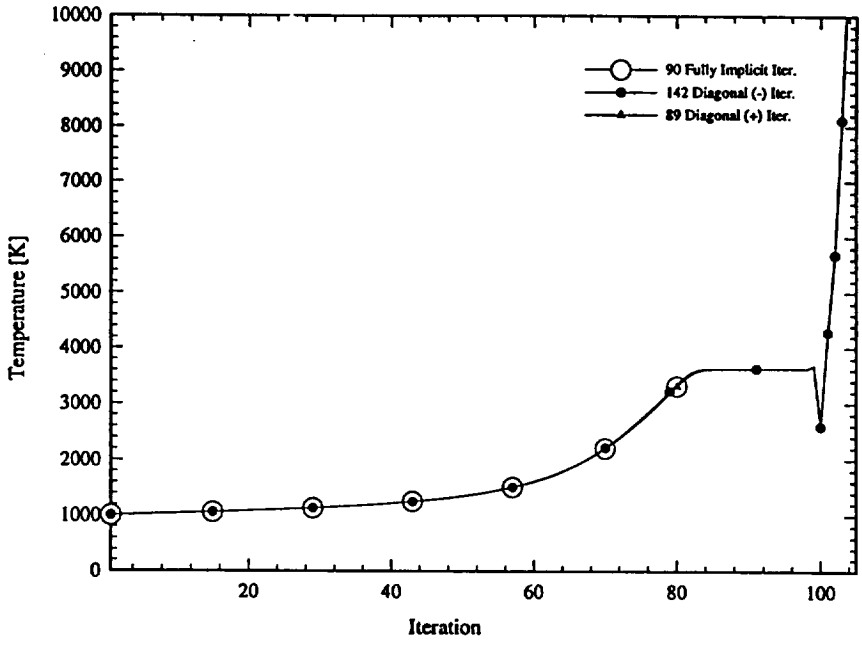

Figure 59: Oxygen Recombination - Temperature Comparison for Fully Implicit, Diagonal (-), and Diagonal (+), $\Delta t_o = 1x10^{-7}$

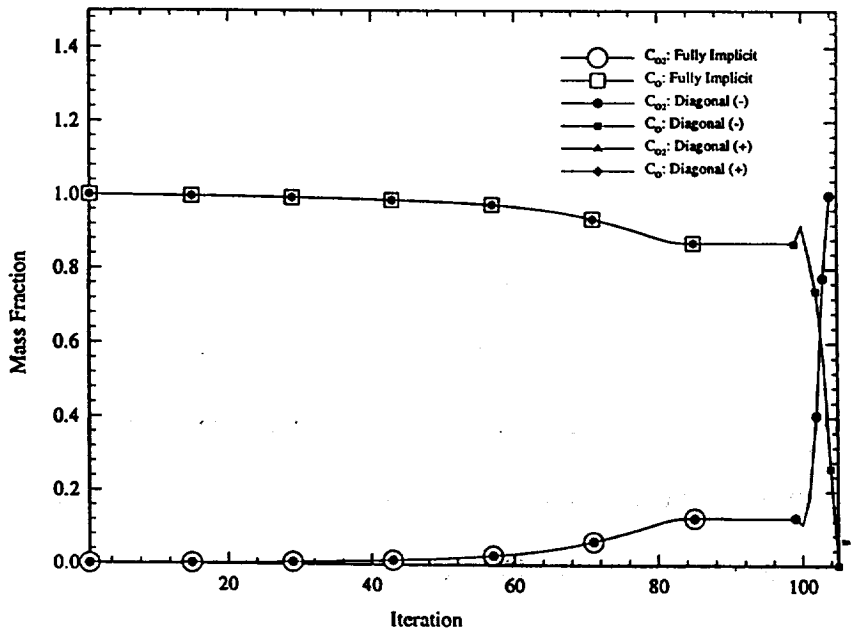

Figure 60: Oxygen Recombination - Mass Fraction Comparison for Fully Implicit, Diagonal (-), and Diagonal (+), $\Delta t_o = 1x10^{-7}$

time step of $1x10^{-7}$ seconds. The fully implicit and diagonal (+) schemes converged in 90 iterations to 3625 K while the negative diagonal scheme went unstable at approximately 100 iterations. This onset of instability corresponds to the point when the magnitude of the source Jacobian terms ($\partial F_1/\partial c_{O2}$ and $\partial F_2/\partial c_O$) becomes larger than $1/\Delta t$; and thus, the chemistry Jacobian forces the solution to proceed in the wrong direction. The mass fractions for the fully implicit and positive diagonal schemes are also nearly equal at 12.9% and 87.1% for O_2 and O respectively, while the negative diagonal scheme diverged.

Figures 61 and 62 show results obtained for an initial time step of $1x10^{-4}$ seconds. Larger initial time steps are allowed for this case since the initial reaction rates are slower at the lower temperatures. The negative diagonal algorithm clearly became unstable very quickly. However, the positive diagonal scheme converged to 3576.7 K at equilibrium, 50 degrees less than the fully implicit scheme. For both cases, the O mass fraction was the same, but the O_2 mass fraction for the diagonal (+) scheme was 16.0% at equilibrium as compared to 12.9% for the fully implicit scheme.

Obviously, the negative diagonal scheme is unstable for large time steps; and the diagonal (+) scheme, while stable, does not necessarily conserve elemental species, especially when the time step becomes large. For large reaction systems with many species, this semi-implicit nature of the chemistry coupling could lead to significant time step restrictions due to numerical stiffness.

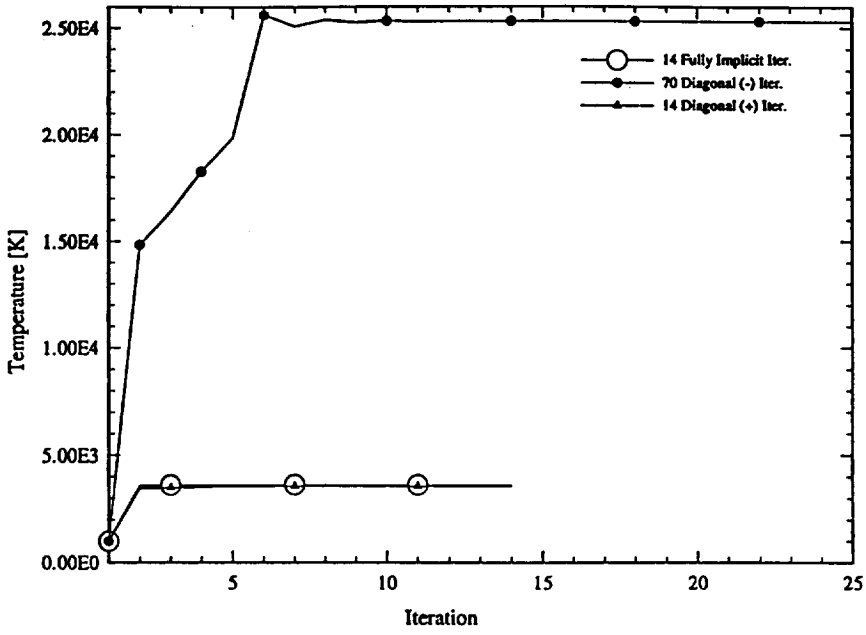

Figure 61: Oxygen Recombination - Temperature Comparison for Fully Implicit, Diagonal (-), and Diagonal (+), $\Delta t_o = 1x10^{-4}$

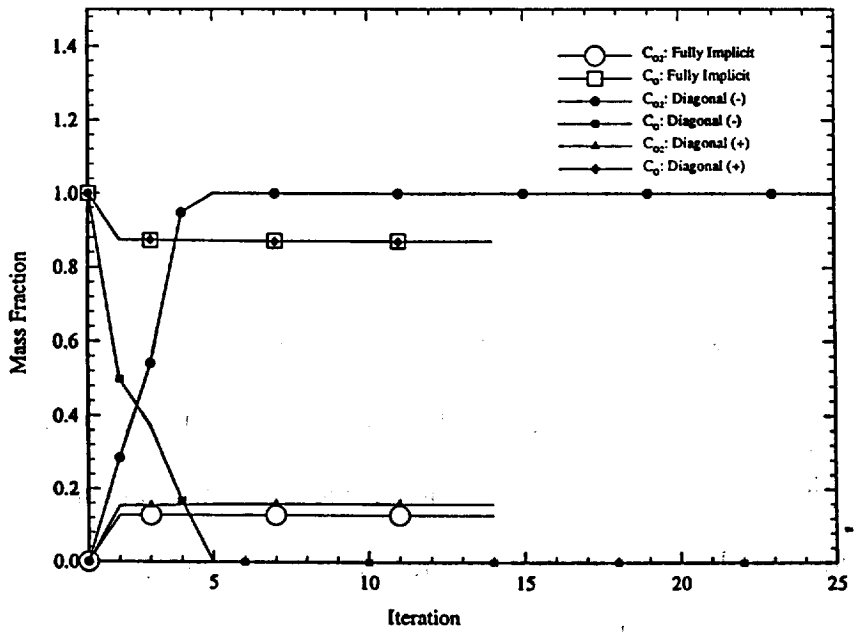

Figure 62: Oxygen Recombination - Mass Fraction Comparison for Fully Implicit, Diagonal (-), and Diagonal (+), $\Delta t_o = 1x10^{-4}$

CONCLUSIONS

A nonequilibrium radiation transport model has been coupled with the nonequilibrium thermo-chemical flowfield solver, INEQ3D. The effective temperature model for calculating the reaction rates of dissociation reactions has been modified to Park's TTV model.[18,26,27] In addition, the free electron-translational coupling model of Gnoffo[15] has been integrated into the solver along with a chemical rate time relaxation factor to mitigate the effects of numerical stiffness. Two cases were successfully studied corresponding to two points in the Fire 2 vehicle flight trajectory.

Studies with these cases showed that the atomic impact ionization rates were very important in seeding avalanche ionization in air for the cylinder case. Decreasing these rate coefficients by an order of magnitude increased the shock standoff distance, while decreasing the net radiative heat transfer by approximately ten percent. Increasing the rates dramatically decreased the shock standoff distance and the stagnation point radiative heating increased by a factor of roughly 2.5. Further investigation is needed since the flowfield properties and radiative heat transfer were found to be extremely sensitive to the rates utilized in the atomic impact ionization reactions.

The studies also showed that the removal of the term which accounts for the net change in electronic energy due to chemical reactions had a negligible effect on the flowfield. However, the effect of including the radiative coupling terms in the vibrational-electron-electronic energy equation were inconclusive due to the numerical stiffness that manifested in flows where radiative phenomena becomes important.

In the above studies, difficulties were encountered in obtaining converged

solutions and very small CFL numbers were required when significant equilibrium existed. It is believed that the possible origin of this difficulty is in the approach used to approximate the chemical source Jacobian. The diagonal implicit scheme, as proposed by Imlay et al.[2] becomes unstable when the diagonal terms of the implicit operator become small (or negative) and diagonal dominance is lost. By switching the sign on the diagonalized chemistry Jacobian diagonal dominance is enhanced, but the approximate nature of the chemistry-flowfield coupling causes the species densities to be updated in an approximate manner. The switched sign positive diagonal scheme used in the present method therefore loosely couples the chemistry with the flowfield. For flows with fast chemical reactions and, therefore, large Damkohler numbers, the numerical stiffness may require fully implicit chemistry in order to achieve the relatively large chemical time steps necessary for satisfactory flowfield convergence.

Radiative heat transfer becomes significant at high speeds and moderate densities where large equilibrium zones occur along with the avalanche ionization phenomenon. When the CFL numbers were large enough to allow the flowfield to converge efficiently, oscillations in the chemistry profiles were observed in the stagnation region where the chemical rates are fastest. Thus the diagonal implicit algorithm may not be practical for the numerical computation of nonequilibrium high speed, re-entry flows involving significant ionization and radiation. In these flight regimes, for example, lunar return, it may be important for the chemistry to be fully implicit within the confines of the numerical solution scheme. Obviously, further study in the use of implicit methods for these cases is needed.

REFERENCES

[1] Walberg, G. D., "A Survey of Aeroassisted Orbit Transfer," *Journal of Spacecraft and Rockets*, Vol. 22, No. 1, 1985, pp. 3-18.

[2] Imlay, S. T., Roberts, D. W., Soetrisno, M., and Eberhardt, S., "Nonequilibrium Thermo-Chemical Calculations Using a Diagonal Implicit Scheme," AIAA Paper 91-0468, Jan. 1990.

[3] Hartung, L. C., Mitcheltree, R. A., and Gnoffo, P. A., "Coupled Radiation Effects in Thermochemical Nonequilibrium Shock-Capturing Flowfield Calculations," AIAA Paper 92-2868, July 1992.

[4] Greendyke, R. B., and Hartung, L. C., "A Convective and Radiative Heat Transfer Analysis for the Fire II Forebody," AIAA Paper 93-3194, July 1993.

[5] Tam, L. T., An, M. Y., and Campbell, C. H., "Nonequilibrium Hypersonic Flow Computation for Weakly Ionized Air and Comparison with Flight Data," AIAA Paper 93-3195, July 1993.

[6] Gally, T. A., and Carlson, L. A., "An Approximate Local Thermodynamic Nonequilibrium Radiation Model for Air," AIAA Paper 92-2972, July 1992.

[7] Gally, T. A., Carlson, L. A., and Green, D., "A Flowfield Coupled Excitation and Radiation Model for Nonequilibrium Reacting Flows," *Journal of Thermophysics and Heat Transfer*, Vol. 7, No. 2, April 1993, pp. 285-293.

[8] Cauchon, D. L., McKee, C. W., and Cornette, E. S., "Spectral Measurements of Gas-Cap Radiation During Project Fire Flight Experiments at Reentry Velocities Near 11.4 Kilometers per Second," NASA TM X-1389, October 1967.

[9] Jameson, A., and Turkel, E., "Implicit Schemes and LU Decompositions," Mathematics of Computation, Vol. 37, No. 156, 1981, pp. 385-397.

[10] Van Leer, B., "Toward the Ultimate Conservation Difference Scheme V, A Second-Order Sequel to Godunov's Method," *Journal of Computational Physics*, Vol. 32, 1979, pp. 101-135.

[11] Roe, P. L., "Characteristio-Based Schemes for the Euler Equations," Annual Review of Fluid Mechanics, 1986, pp. 337-356.

[12] Chakravarthy, S. R., and Osher, S., "High Resolution Applications of the Osher Upwind Scheme for the Euler Equations," AIAA Paper 83-1943, 1983, pp. 363-73.

[13] Sheun S., and Yoon, S., "Numerical Study of Chemically Reacting Flows Using a Lower-upper Symmetric Successive Overrelaxation Scheme," *AIAA Journal*, Vol. 27, No. 12, Dec. 1989, pp. 1752-1760.

[14] Park, C., "Assessment of Two-Temperature Kinetic Model for Ionizing Air," AIAA Paper 87-1547, June 1987.

[15] Gnoffo, P. A., Gupta, R. N., and Shinn, J. L., "Conservation Equations and Physical Models for Hypersonic Air Flows in Thermal and Chemical Nonequilibrium," NASA TP 2867, 1989.

[16] McGough, D. E., "A Preferential Vibration Dissociation Coupling Model for Nonequilibrium Hypersonic Flowfields," Master's Thesis, Texas A&M University, 1993.

[17] Gupta, R. N., Yos, J. M., and Thompson, R. A., "A Review of Reaction Rates and Thermodynamic and Transport Properties for the 11-Species Air Model for Chemical and Thermal Nonequilibrium Calculations to 30000 K," NASA TM-101528, Feb. 1989.

[18] Park, C., *Nonequilibrium Hypersonic Aerothermodynamics*, John Wiley & Sons, New York, 1990, pp. 166-167.

[19] Park, C., "A Review of Reaction Rates in High Temperature Air," AIAA Paper 89-1740, June 1989.

[20] Park, C., Howe, J. T., Jaffe, R. L., and Candler, G. V., "Chemical-Kinetic Problems of Future NASA Missions," AIAA Paper 91-0464, Jan. 1991.

[21] Gally, T. A., "Development of Engineering Methods for Nonequilibrium Radiative Phenomena About Aeroassisted Entry Vehicles," Ph.D. Dissertation, Texas A&M University, 1992.

[22] Carlson, L. A., "Radiative Transfer, Chemical Nonequilibrium, and Two-Temperature Effects Behind a Reflected Shock Wave in Nitrogen," Ph.D. Dissertation, Ohio State University, 1969.

[23] Tam, L. T., and Li, C. P., "Three-Dimensional Thermochemical Nonequilibrium Flow Modeling for Hypersonic Flows," AIAA Paper 89-1860, June 1989.

[24] Vincenti, W. G., and Kruger, C. H., *Introduction to Physical Gas Dynamics*, Robert E. Krieger Publishing Co., Malabar, Florida, 1965, pp. 55-57.

[25] Sharma, S. P., Huo, W., and Park, C., "The Rate Parameters for Coupled Vibration Dissociation in Generalized SSH Theory," AIAA Paper 88-2714, 1988.

[26] Park, C., "Assessment of Two-Temperature Kinetic Model for Dissociating and Weakly-Ionizing Nitrogen," *Journal of Thermophysics and Heat Transfer*, Vol. 2, 1988, pp. 8-16.

[27] Park, C., "Assessment of Two Temperature Kinetic Model for Ionizing Air," AIAA Paper 87-1574, June 1987.

[28] Oran, E. S., and Boris, J. P., *Numerical Simulation of Reactive Flow*, Elsevier Science Publishing Co., New York, 1987, pp. 153-158.

[29] Millikan, R. C. and White, D. R., "Systematics of Vibrational Relaxation," *Journal of Chemical Physics*, Vol. 39, No. 12, Dec. 1963, pp. 3209-3213.

[30] Park, C., "Calculation of Nonequilibrium Radiation in the Flight Regimes of Aeroassisted Orbital Transfer Vehicles," *Thermal Design of Aeroassisted Orbital Transfer Vehicles*, edited by H. F. Nelson, Vol. 96, Progress in Astronautics and Aeronautics, AIAA, New York, 1985, pp. 395-418.

[31] Appleton, J. P., and Bray, K. N. C, "The Conservation Equations for a Nonequilibrium Plasma," *Journal of Fluid Mechanics*, Vol. 20, Pt. 4, Dec. 1964, pp. 659-672.

[32] Treanor, C. E., and Marrone, P. V., "Effect of Dissociation on the Rate of Vibrational Relaxation," *Physics of Fluids*, Vol. 5, No. 9, Sept. 1962, pp. 1022-1026.

[33] Treanor, C. E., and Marrone, P. V., "Vibration and Dissociation Coupling Behind Strong Shock Waves," *Dynamics of Manned Lifting Planetary Entry*, edited by S. M. Scala, John Wiley and Sons, New York, 1963, pp. 160-171.

[34] Nicolet, W. E., "Advanced Methods for Calculating Radiation Transport in Ablation-Product Contaminated Boundary Layers," NASA CR 1656, Sept. 1970.

[35] Nicolet, W. E., "Rapid Methods for Calculating Radiation Transport in the Entry Environment," NASA CR 2528, April 1975.

[36] Zel'dovich, Y. B., and Razier, Y. P., *Physics of Shock Waves and High-Temperature Hydrodynamic Phenomena*, Vol. I, Academic Press, New York, 1966, pp. 398-401.

VITA

Christopher John Roy was born in [redacted]. He spent his childhood in Hopkinsville, Kentucky before moving to Fayetteville, North Carolina where he attended high school. He began his college career at Duke University where he competed on the varsity swimming team while working towards a Bachelors degree in mechanical engineering. After graduating in 1992, Mr. Roy then attended Texas A&M University and received a Masters degree in aerospace engineering in 1994. He is currently pursuing his Ph.D. at North Carolina State University and plans to seek employment in academia or industry conducting research in computational fluid dynamics. Correspondence to Mr. Roy may be sent to 1745 Smoky Canyon Dr., Hope Mills, North Carolina, 28348.

APPENDIX

Table A.1. Thermodynamic Constants

Species	Mol. Wt.	C_1	C_2	C_3	C_4	C_5
N_2	28.016	3.5	-1697.54	4.472	1.203×10^{-10}	1442.60
O_2	32.0	3.5	-1136.12	5.535	-4.812×10^{-10}	-2537.66
NO	30.008	3.5	-1375.50	5.870	-4.143×10^{-10}	82.58
NO^+	30.008	3.5	-1722.15	5.905	-5.407×10^{-11}	-294.97
N_2^+	28.016	3.5	-3810.69	4.520	-5.042×10^{-10}	-3841.10
O_2^+	32.0	3.5	-1316.26	6.289	-7.770×10^{-10}	-989.86
N^+	14.008	2.5	45.85	5.415	9.647×10^{-10}	5664.84
O^+	16.0	2.5	42.71	4.397	4.795×10^{-10}	-55.39
N	14.008	2.5	45.89	5.177	3.748×10^{-9}	-109.28
O	16.0	2.5	13.43	6.026	3.825×10^{-9}	5401.94
e^-	.0005486	2.5	-670.88	-11.69	-	-

TABLE A.2. Curve Fit Constants for Energy Exchange Cross Section, σ_{es}

Species	a_s	b_s	c_s
N	5×10^{-20}	0	0
O	1.2×10^{-20}	1.7×10^{-24}	-2×10^{-29}
N_2	7.5×10^{-20}	5.5×10^{-24}	-1×10^{-28}
O_2	2×10^{-20}	6×10^{-24}	0
NO	1×10^{-19}	0	0

REFERENCES

[1] Walberg, G. D., "A Survey of Aeroassisted Orbit Transfer," *Journal of Spacecraft and Rockets*, Vol. 22, No. 1, 1985, pp. 3-18.

[2] Imlay, S. T., Roberts, D. W., Soetrisno, M., and Eberhardt, S., "Nonequilibrium Thermo-Chemical Calculations Using a Diagonal Implicit Scheme," AIAA Paper 91-0468, Jan. 1990.

[3] Hartung, L. C., Mitcheltree, R. A., and Gnoffo, P. A., "Coupled Radiation Effects in Thermochemical Nonequilibrium Shock-Capturing Flowfield Calculations," AIAA Paper 92-2868, July 1992.

[4] Greendyke, R. B., and Hartung, L. C., "A Convective and Radiative Heat Transfer Analysis for the Fire II Forebody," AIAA Paper 93-3194, July 1993.

[5] Tam, L. T., An, M. Y., and Campbell, C. H., "Nonequilibrium Hypersonic Flow Computation for Weakly Ionized Air and Comparison with Flight Data," AIAA Paper 93-3195, July 1993.

[6] Gally, T. A., and Carlson, L. A., "An Approximate Local Thermodynamic Nonequilibrium Radiation Model for Air," AIAA Paper 92-2972, July 1992.

[7] Gally, T. A., Carlson, L. A., and Green, D., "A Flowfield Coupled Excitation and Radiation Model for Nonequilibrium Reacting Flows," *Journal of Thermophysics and Heat Transfer*, Vol. 7, No. 2, April 1993, pp. 285-293.

[8] Cauchon, D. L., McKee, C. W., and Cornette, E. S., "Spectral Measurements of Gas-Cap Radiation During Project Fire Flight Experiments at Reentry Velocities Near 11.4 Kilometers per Second," NASA TM X-1389, October 1967.

[9] Jameson, A., and Turkel, E., "Implicit Schemes and LU Decompositions," *Mathematics of Computation*, Vol. 37, No. 156, 1981, pp. 385-397.

[10] Van Leer, B., "Toward the Ultimate Conservation Difference Scheme V, A Second-Order Sequel to Godunov's Method," *Journal of Computational Physics*, Vol. 32, 1979, pp. 101-135.

[11] Roe, P. L., "Characteristic-Based Schemes for the Euler Equations," *Annual Review of Fluid Mechanics*, 1986, pp. 337-356.

[12] Chakravarthy, S. R., and Osher, S., "High Resolution Applications of the Osher Upwind Scheme for the Euler Equations," AIAA Paper 83-1943, 1983, pp. 363-73.

[13] Sheun, S., and Yoon, S., "Numerical Study of Chemically Reacting Flows Using a Lower-upper Symmetric Successive Overrelaxation Scheme," *AIAA Journal*, Vol. 27, No. 12, Dec. 1989, pp. 1752-1760.

[14] Park, C., "Assessment of Two-Temperature Kinetic Model for Ionizing Air," AIAA Paper 87-1547, June 1987.

[15] Gnoffo, P. A., Gupta, R. N., and Shinn, J. L., "Conservation Equations and Physical Models for Hypersonic Air Flows in Thermal and Chemical Nonequilibrium," NASA TP 2867, 1989.

[16] McGough, D. E., "A Preferential Vibration Dissociation Coupling Model for Nonequilibrium Hypersonic Flowfields," Master's Thesis, Texas A&M University, 1993.

[17] Gupta, R. N., Yos, J. M., and Thompson, R. A., "A Review of Reaction Rates and Thermodynamic and Transport Properties for the 11-Species Air Model for Chemical and Thermal Nonequilibrium Calculations to 30000 K," NASA TM-101528, Feb. 1989.

[18] Park, C., *Nonequilibrium Hypersonic Aerothermodynamics*, John Wiley & Sons, New York, 1990, pp. 166-167.

[19] Park, C., "A Review of Reaction Rates in High Temperature Air," AIAA Paper 89-1740, June 1989.

[20] Park, C., Howe, J. T., Jaffe, R. L., and Candler, G. V., "Chemical-Kinetic Problems of Future NASA Missions," AIAA Paper 91-0464, Jan. 1991.

[21] Gally, T. A., "Development of Engineering Methods for Nonequilibrium Radiative Phenomena About Aeroassisted Entry Vehicles," Ph.D. Dissertation, Texas A&M University, 1992.

[22] Carlson, L. A., "Radiative Transfer, Chemical Nonequilibrium, and Two-Temperature Effects Behind a Reflected Shock Wave in Nitrogen," Ph.D. Dissertation, Ohio State University, 1969.

[23] Tam, L. T., and Li, C. P., "Three-Dimensional Thermochemical Nonequilibrium Flow Modeling for Hypersonic Flows," AIAA Paper 89-1860, June 1989.

[24] Vincenti, W. G., and Kruger, C. H., *Introduction to Physical Gas Dynamics*, Robert E. Krieger Publishing Co., Malabar, Florida, 1965, pp. 55-57.

[25] Sharma, S. P., Huo, W., and Park, C., "The Rate Parameters for Coupled Vibration Dissociation in Generalized SSH Theory," AIAA Paper 88-2714, 1988.

[26] Park, C., "Assessment of Two-Temperature Kinetic Model for Dissociating and Weakly-Ionizing Nitrogen," *Journal of Thermophysics and Heat Transfer*, Vol. 2, 1988, pp. 8-16.

[27] Park, C., "Assessment of Two Temperature Kinetic Model for Ionizing Air," AIAA Paper 87-1574, June 1987.

[28] Oran, E. S., and Boris, J. P., *Numerical Simulation of Reactive Flow*, Elsevier Science Publishing Co., New York, 1987, pp. 153-158.

[29] Millikan, R. C. and White, D. R., "Systematics of Vibrational Relaxation," *Journal of Chemical Physics*, Vol. 39, No. 12, Dec. 1963, pp. 3209-3213.

[30] Park, C., "Calculation of Nonequilibrium Radiation in the Flight Regimes of Aeroassisted Orbital Transfer Vehicles," *Thermal Design of Aeroassisted Orbital Transfer Vehicles*, edited by H. F. Nelson, Vol. 96, Progress in Astronautics and Aeronautics, AIAA, New York, 1985, pp. 395-418.

[31] Appleton, J. P., and Bray, K. N. C, "The Conservation Equations for a Nonequilibrium Plasma," *Journal of Fluid Mechanics*, Vol. 20, Pt. 4, Dec. 1964, pp. 659-672.

[32] Treanor, C. E., and Marrone, P. V., "Effect of Dissociation on the Rate of Vibrational Relaxation," *Physics of Fluids*, Vol. 5, No. 9, Sept. 1962, pp. 1022-1026.

[33] Treanor, C. E., and Marrone, P. V., "Vibration and Dissociation Coupling Behind Strong Shock Waves," *Dynamics of Manned Lifting Planetary Entry*, edited by S. M. Scala, John Wiley and Sons, New York, 1963, pp. 160-171.

[34] Nicolet, W. E., "Advanced Methods for Calculating Radiation Transport in Ablation-Product Contaminated Boundary Layers," NASA CR 1656, Sept. 1970.

[35] Nicolet, W. E., "Rapid Methods for Calculating Radiation Transport in the Entry Environment," NASA CR 2528, April 1975.

[36] Zel'dovich, Y. B., and Razier, Y. P., *Physics of Shock Waves and High-Temperature Hydrodynamic Phenomena*, Vol. I, Academic Press, New York, 1966, pp. 398-401.

APPENDIX

Table A.1. Thermodynamic Constants

Species	Mol. Wt.	C_1	C_2	C_3	C_4	C_5
N_2	28.016	3.5	-1697.54	4.472	1.203×10^{-10}	1442.60
O_2	32.0	3.5	-1136.12	5.535	-4.812×10^{-10}	-2537.66
NO	30.008	3.5	-1375.50	5.870	-4.143×10^{-10}	82.58
NO^+	30.008	3.5	-1722.15	5.905	-5.407×10^{-11}	-294.97
N_2^+	28.016	3.5	-3810.69	4.520	-5.042×10^{-10}	-3841.10
O_2^+	32.0	3.5	-1316.26	6.289	-7.770×10^{-10}	-989.86
N^+	14.008	2.5	45.85	5.415	9.647×10^{-10}	5664.84
O^+	16.0	2.5	42.71	4.397	4.795×10^{-10}	-55.39
N	14.008	2.5	45.89	5.177	3.748×10^{-9}	-109.28
O	16.0	2.5	13.43	6.026	3.825×10^{-9}	5401.94
e^-	.0005486	2.5	-670.88	-11.69	-	-

TABLE A.2. Curve Fit Constants for Energy Exchange Cross Section, σ_{es}

Species	a_s	b_s	c_s
N	5×10^{-20}	0	0
O	1.2×10^{-20}	1.7×10^{-24}	-2×10^{-29}
N_2	7.5×10^{-20}	5.5×10^{-24}	-1×10^{-28}
O_2	2×10^{-20}	6×10^{-24}	0
NO	1×10^{-19}	0	0

VITA

Christopher John Roy was born in [redacted], [redacted] on [redacted], [redacted]. He spent his childhood in Hopkinsville, Kentucky before moving to Fayetteville, North Carolina where he attended high school. He began his college career at Duke University where he competed on the varsity swimming team while working towards a Bachelors degree in mechanical engineering. After graduating in 1992, Mr. Roy then attended Texas A&M University and received a Masters degree in aerospace engineering in 1994. He is currently pursuing his Ph.D. at North Carolina State University and plans to seek employment in academia or industry conducting research in computational fluid dynamics. Correspondence to Mr. Roy may be sent to 1745 Smoky Canyon Dr., Hope Mills, North Carolina, 28348.

APPENDIX II

RADIATIVE COUPLING USER'S GUIDE FOR INEQ3D

Christopher J. Roy

Radiative Coupling User's Guide for INEQ3D

TEES Report No. 42890-95-03
August 1995

NASA Grant No. NAG 9-680

Christopher J. Roy
Aerospace Engineering Department
Texas A&M University
College Station, TX 77843-3141

Contents

List of Figures

1 Introduction

1.1 Purpose

The purpose of this work was to couple the nonequilibrium flowfield solver INEQ3D [1] with the Texas A&M University (TAMU) local thermodynamic nonequilibrium (LTNE) radiation model [2], [3] to account for the energy sinks and sources associated with high temperature air radiation.

1.2 Flight Conditions

Radiative transport becomes significant in high speed entry flows at velocities associated with Lunar and Martian return. At these conditions nonequilibrium chemistry and nonequilibrium radiation phenomena can interact significantly, particularly via the fast electron impact ionization reactions.

1.3 Problems

The presence of these fast reactions along with convective phenomena which occur at a much slower rate leads to numerical stiffness during the discretized solution of the governing equations. The diagonal implicit approximation [4] for the chemical source Jacobian used in INEQ3D lowers the maximum allowable Courant (CFL) number to the point where a large number of iterations are necessary to advance the convective phenomena in pseudo-time.

1.4 Proposed Solution

Since the CFL number is limited by the fast electron impact reactions, either a fully implicit or a point implicit formulation for both the flowfield solver and the chem-

istry should raise the stability limit. While implicit methods would increase the per-iteration cost the overall cost of achieving a converged solution should be greatly reduced.

2 INEQ3D Minor Modifications

2.1 Electron–Heavy Particle Collisions

The original formulation for energy exchange due to elastic collisions between electrons and heavy particles was given by

$$Q_{T-e} = 2\rho_{e^-}\frac{3}{2}R(T - T_{el})\sum_{s=4}^{10}\frac{\nu_{es}}{M_s} \tag{1}$$

where the summation from 4 to 10 includes all atoms and ions, but omits the neutral diatomic molecules. The variable ν_{es} is the effective collision frequency of an electron with species s and is found from

$$\nu_{es} = n_s\sigma_{es}\left(\frac{8kT_{el}}{\pi m_{e^-}}\right)^{1/2} \tag{2}$$

where σ_{es} is the effective energy exchange cross section.

In order to include all heavy particles in the the evaluation of the translational–free electron elastic energy exchange, the above model was modified to that of Appleton and Bray [5]. This new model utilizes equation (1) summed over all heavy particles and an effective energy exchange cross section for neutrals given by:

$$\sigma_{es} = a_s + b_sT_{el} + c_sT_{el}^2 \tag{3}$$

The constants in equation (3) may be found in the Appendix of reference [6].

For collisions between electrons and the positively charged heavy particles the Coulombic attractive force must be taken into account. This effect can be modeled as

$$\nu_{es} = \frac{8}{3}\left(\frac{\pi}{m_{e^-}}\right)^{1/2} n_s e^4 \frac{1}{(2kT_{el})^{(3/2)}} \ln\left(\frac{k^3T_{el}^3}{\pi n_{e^-}e^6}\right) \tag{4}$$

where e is the electronic charge equal to 1.5188E-4 esu in the m-k-s system of units ($1\ esu^2 = 1\ kg\ m^3/s^2$).

2.2 Effective Temperature Model

The original model [1] for determining chemical rate processes used an effective temperature to determine the forward reaction rate coefficients. This effective temperature was based on the available Gibb's free energy in each energy mode and was of the form

$$\frac{1}{T_{eff}} = \sum_{all\ i} \frac{f_i}{T_i} \tag{5}$$

where the statistical factor f_i is the ratio of free energy in mode i to the total free energy.

It was found that this effective temperature model does not reflect the physically correct temperature dependence for Mach numbers in excess of thirty when used with Park's eleven species air reaction set (see reference [6], page 21), particularly for the electron impact reactions where, in the Park model [7], [8], [9], the effective temperature is replaced by the electron–electronic temperature. Since the electron-atom impact reactions are extremely important for the conditions where radiative heating becomes significant, the above effective temperature model was replaced with Park's TTV model. In this model, the effective temperature for dissociation is calculated based on a geometric average of the translational and vibrational temperatures using

$$T_a = T_v^q T_{tr}^{1-q} \tag{6}$$

where q was taken to be 0.3 for the cases examined in reference [6]. The electron

impact reactions were assumed to be functions of the electron-electroni : temperature to account for the free electron translational energy [7]. For all reactions the equilibrium constant was evaluated using the same temperature found in the forward rate equation.

2.3 Chemical Production Rate Relaxation

In order to reduce the instabilities associated with numerical stiffness, a method for slowing down the chemistry was needed which would not alter the steady state solution. To this end, a chemical production rate time relaxation was introduced of the form

$$\omega_s^{n+1} = \omega_s^n + \chi(\bar{\omega}_s^{n+1} - \omega_s^n) \tag{7}$$

where ω_s^{n+1} is the new time relaxed production rate for species s, $\bar{\omega}_s^{n+1}$ is the actual species production rate, and ω_s^n is the value of the relaxed production rate at time level n found from equation (7). For all cases run in reference [6], the chemistry was under-relaxed with $\chi = 0.3$. To include the above chemical relaxation, it was necessary to store the old value of the production rate at each point. The array WOLD is one of two added to INEQ3D's main program.

3 Radiation Coupling

3.1 Radiation Post-Processing

The array DQDY is the second array added to the the main program and is used to store the radiative flux along a single ξ = constant line. Two new variables were introduced into the main input file to allow radiative post-processing. The variable RSTAG, when enabled, calculates the radiative absorption and emission at each grid point along the stagnation streamline. These results are then sent to the file *fort.25*. This file is used as input for the post-processing fortran code *radnew.f*, which outputs both grouped (*fort.65*) and detailed (*fort.66*) radiative spectra information to the stagnation point.

The variable RBODY, when enabled, allows the calculation of net radiative heat transfer to the body along the surface. The output is sent to *fort.55* which gives both the I location and the net radiative heat transfer to the body in units of W/cm^2. Since this calculation involves integrating the radiation along each ξ = constant grid line normal to the body, this option is computationally expensive and should be turned off when not needed.

Two files are utilized as input for the radiation routines. The file *mexcite.dat* contains molecular excitation and cross-section data and the file *rad.dat* serves as the main input file for the TAMU radiation model. For further information, see references [10] and [11].

3.2 Radiation–Gas Dynamic Coupling

There are several options included for radiation coupling in the supplemental input file *fort.88*. One option allows the radiative energy source term to be included in the global energy equation, while another allows this coupling term to be included in the vibrational-electron-electronic (VEE) energy equation as well. The radiation coupling can be costly for large grids, and thus an option is included for performing the radiation calculations only after a specified number of iterations (eg. every 200 iterations) and starting at a specified iteration number. The general procedure is to allow the flowfield to reach a certain level of convergence and then to slowly introduce the radiative source terms. For example, these last few options allow the user to begin radiation calculations at iteration 1000 with 50% of the full radiation coupling term and then increase this contribution by 10% every 100 iterations, thus allowing the full 100% of the radiative contribution to be counted by iteration 1500 and updated every 100 iterations thereafter.

4 Input Files

4.1 Standard Input

Two variables were added to the main input file (standard input):

RSTAG	Flag for radiation post processing at the stagnation point =.FALSE. for no radiative post processing =.TRUE. for radiative post processing
RBODY	Flag for radiation post processing along the body =.FALSE. for no radiative post processing =.TRUE. for radiative post processing

4.2 Secondary Input File *(fort.88)*

A second input file was created to handle the new parameters governing both the radiation calculations and the other minor modifications:

Record 1, section title (RADIATION COUPLING VARIABLES)

Record 2, free format

RAD	Flag for radiation coupling in Global energy equation =.FALSE. for no radiation coupling =.TRUE. for radiation coupling
RADVEE	Flag for radiation coupling in the vibrational-electron-electronic energy equation (only used if RAD=.TRUE.) =.FALSE. for no radiation coupling in VEE energy equation =.TRUE. for radiation coupling in VEE energy equation

Record 3, free format

IFIRST	First iteration to perform radiation coupling
KRAD	Number of flowfield iterations between radiation coupling updates
RADINC	Amount to increment radiation coupling factor (eg. RADINC=0.10 will increment the radiation factor by 10iterations)
RADFAC	Initial radiation factor (calculated as fraction of total radiation coupling)

Record 4, section title (CHEMICAL RATE TIME RELAXATION)

Record 5, free format

WFAC	Chemical rate relaxation factor =1.0 No chemical rate relaxation =0.0 Frozen chemical rates

Record 6, section title (PARK'S TTV EFFECTIVE TEMPERATURE MODEL)

Record 7, free format

TMODEL	Flag for Park's $T_{eff} = T_v^q T_{tr}^{q-1}$ effective temperature model =.FALSE. for Tam and Li's effective temperature model =.TRUE. for Park's effective temperature model

Record 8, free format

QPARK	Exponent q in $T_{eff} = T_v^q T_{tr}^{q-1}$
IPARK1	Last reaction to use T_{eff} (following reactions will use translational temperature)*
IPARK2	First reaction to use the electronic temperature*

Record 9, section title (GNOFFO'S T-E COUPLING: CURVE FIT CONSTANTS FOR NEUTRALS)

TECPL	Flag for Gnoffo's (Appleton and Bray's) coupling between electrons and heavy particles (valid between 5000 and 15000 Kelvin) =.FALSE. for Tam's T-E coupling =.TRUE. for Gnoffo's T-E coupling

Record 10, free format

KMAX	Number of entries in the following arrays

Records (I=11,KMAX+11), free format

ICCS(I)	Neutral species number for T-E coupling curve fit
CCS(I,1-3)	Curve fit constants for above species

*note: The reaction set must be ordered such that reactions 1 to IPARK1 utilize T_{eff}, reactions IPARK1+1 to IPARK2-1 utilize T_{tr}, and reactions IPARK2 to end utilize T_{el} in rate calculations.

5 Solution Methodology

The instabilities due to fast chemical reactions manifested primarily in the stagnation nose region of the body. In order to mitigate the effects of numerical stiffness in this region, the grid was refined to decrease the time step and thus better capture the fast electron impact reactions.

The Courant (CFL) number was initially set to a relatively large value. After roughly 4000 iterations, the solution was examined. If instabilities were present then the CFL number was halved and the solution was rerun with the previous restart file (before any instabilities appeared). If the solution was stable for two runs at the same CFL number, then the CFL number was doubled for the next run. It was noted that soon after the electron-atom impact ionization phenomenon became prominent, the CFL number had to be reduced, sometimes as low as 1/16th of the initial CFL number.

6 Sample Results

Two dimensional results are presented for a 10 centimeter radius cylinder at a free stream velocity of 11.36 km/sec (Mach 40.5) and an altitude of 76.42 kilometers. These conditions correspond to the the Fire 2 flight experiment [12] at 1634 seconds mission time although the cylinder radius is significantly smaller than the effective nose radius of the Fire 2 vehicle. This scaling was done in order to account for the increased shock stand-off distance for two dimensional bodies and to decrease the size of the equilibrium region where the fast reactions take place.

The computational grid is shown in Figure 1 and utilizes clustering both at the shock location and in the equilibrium region of the flow. Figure 2 gives the thermal profile, pressure, and total density along the stagnation streamline. A large region of thermal nonequilibrium is evident immediately after the flow passes through the shock wave while the thermal equilibrium region is much smaller. The increase in density found in the thermal equilibrium region is due mainly to the dissociation of diatomic nitrogen near the stagnation point (Figure 3). The sharp increase in the electron, O^+, and N^+ mole fractions near thermal equilibrium is a result of the avalanche ionization phenomenon. Initially, as the flow passes through the shock wave, electrons are produced by a variety of relatively slow ionization reactions. As the electron temperature and the electron number density increases, the faster electron-atom impact ionization reactions become the primary source for creating free electrons, causing an exponential increase in the electron number density known as avalanche ionization.

Also shown in Figure 3 is a residual plot giving the L_2 norm residual of four of the chemical species over the entire flowfield. Figure 4 gives the L_2 norm residual of four additional chemical species as well as an example of the CFL number modification scheme. Although the CFL number starts out at a reasonable value, the appearance of the avalanche ionization phenomena forces the stability limit to drop so that the final CFL number has a value of 0.0625.

Both grouped and detailed radiation frequency spectra are presented in Figure 5. The majority of the radiation comes from bound-bound and bound-free transitions in the ultraviolet region (9-16 Ev range) and the total radiative heat transfer to the stagnation point was found to be 3.35 W/cm^2. The magnitude of the radiative heat flux along the cylinder's surface is shown in Figure 6. As expected, the maximum radiative heating occurs at the stagnation point (I=2) for both continuum and line radiative transitions.

Contour plots for the species mass fractions are given in Figures 7 through 11. Oscillations are present in the O_2 mass fraction plot (Figure 7) and are probably numerical effects caused by the presence of strong chemistry gradients as well as numerical stiffness. The avalanche ionization region is clearly depicted in the electron mass fraction contour plot of Figure 12. Also shown is the Mach number based on the local speed of sound and it is apparent that the flow is well into the supersonic regime as the outflow plane is encountered. Presented in Figures 13 and 14 are contour plots for the two temperatures, the density, and the pressure.

7 Conclusions and Recommendations

The TAMU nonequilibrium radiation transport model has been coupled with the nonequilibrium thermo-chemical flowfield solver INEQ3D. The effective temperature model for calculating the reation rates for dissocation has been modified to Park's TTV model [7], [8], [9]. In addiditon, the free electron-translational coupling model of Appleton and Bray [5] has been integrated into the solver along with a chemical rate time relaxation factor to mitigate the effects of numerical stiffness.

Difficulties were encountered in obtaining converged solutions and very small CFL numbers were required when significant equilibrium regions were present. It is believed that the origin of this difficulty is in the approach used to approximate the chemical source Jacobian. The diagonal implicit scheme, as proposed by Imlay et al. [4] handles the chemistry in an approximate manner and therefore only loosely couples the chemistry with the flowfield solution. For flows with fast chemical reactions, the numerical stiffness caused by the disparate time scales in the convective and chemical phenomena may require fully implicit chemistry in order to achieve the relatively large chemical time steps necessary for satisfactory flowfield convergence.

Radiative heat transfer becomes significant at high speeds and moderate densities where large equilibrium zones occur along with the avalanche ionization phenomenon. When the CFL numbers were large enough to allow the flowfield to converge efficiently, oscillations in the chemistry profiles were observed in the stagnation region where the chemical rates are fastest. Thus the diagonal implicit algorithm may not be practical

for the computation of nonequilibrium high speed, re-entry flows involving significant ionization and radiation. In these flight regimes, for example lunar return, it may be important for the chemistry to be fully implicit within the confines of the numerical solution scheme. Further study in the use of implicit methods for these cases is needed.

The variation in the radiative flux terms along the body (ξ direction) is much smaller than the variation normal to the body (η direction). The radiative flux source terms are currently calculated at every constant ξ line. In order to increase the computational efficiency of the code, it is suggested that the radiative terms may only need to be calculated every second or third line along the body. This modification would cut the costly radiation calculations by a factor of two (or three) for two dimensional cases and a factor of four (or nine) for three dimensional cases.

8 References

References

[1] Tam, L. T., and Li, C. P., "Three-Dimensional Thermochemical Nonequilibrium Flow Modeling for Hypersonic Flows," AIAA Paper 89-1860, June 1989.

[2] Gally, T. A., and Carlson, L. A., "An Approximate Local Thermodynamic Nonequilibrium Radiation Model for Air," AIAA Paper 92-2972, July 1992.

[3] Gally, T. A., Carlson, L. A., and Green, D., "A Flowfield Coupled Excitation and Radiation Model for Nonequilibrium Reacting Flows," *Journal of Thermophysics and Heat Transfer*, Vol. 7, No. 2, April 1993, pp. 285-293.

[4] Imlay, S. T., Roberts, D. W., Soetrisno, M., and Eberhardt, S., "Nonequilibrium Thermo-Chemical Calculations Using a Diagonal Implicit Scheme," AIAA Paper 91-0468, Jan. 1990.

[5] Appleton, J. P., and Bray, K. N. C., "The Conservation Equations for a Nonequilibrium Plasma," *Journal of Fluid Mechanics*, Vol. 20, Pt. 4, Dec. 1964, pp. 659-672.

[6] Roy, C. J., "Viability of the Diagonal Implicit Algorithm for Hypersonic Flowfields with Finite Rate Chemistry," Master's Thesis, Texas A&M University, 1994.

[7] Park, C., *Nonequilibrium Hypersonic Aerothermodynamics*, John Wiley & Sons, New York, 1990, pp. 166-167.

[8] Park, C., "Assessment of Two-Temperature Kinetic Model for Dissociating and Weakly-Ionizing Nitrogen," *Journal of Thermophysics and Heat Transfer*, Vol. 2, 1988, pp. 8-16.

[9] Park, C., "Assessment of Two Temperature Kinetic Model for Ionizing Air," AIAA Paper 87-1574, June 1987.

[10] Nicolet, W. E., "Advanced Methods for Calculating Radiation Transport in Ablation-Product Contaminated Boundary Layers," NASA CR 1656, Sept. 1970.

[11] Nicolet, W. E., "Rapid Methods for Calculating Radiation Transport in the Entry Environment," NASA CR 2528, April 1975.

[12] Cauchon, D. L., McKee, C. W., and Cornette, E. S., "Spectral Measurements of Gas-Cap Radiation During Project Fire Flight Experiments at Reentry Velocities Near 11.4 Kilometers per Second," NASA TM X-1389, October 1967.

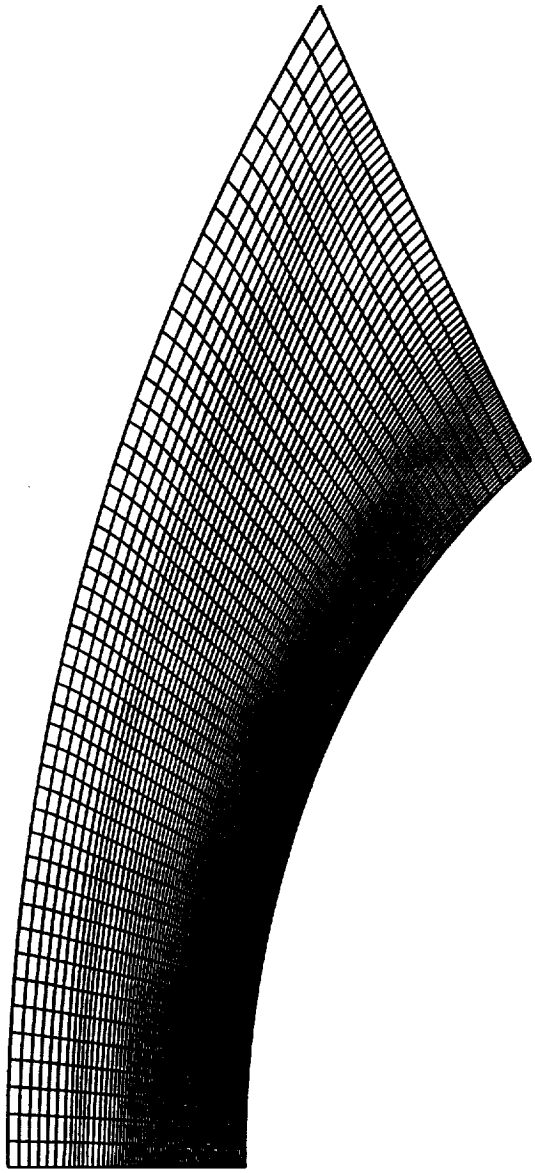

Figure 1: Computational Mesh for Cylinder Case (50x70)

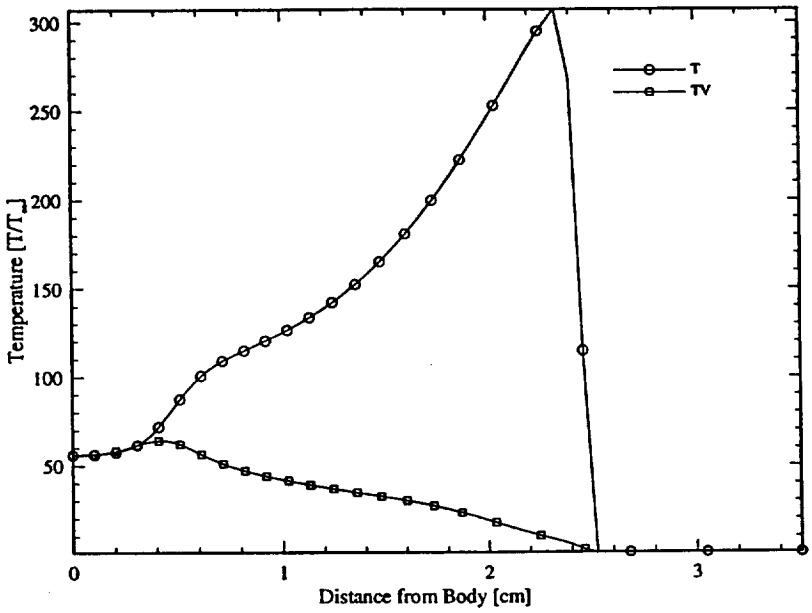

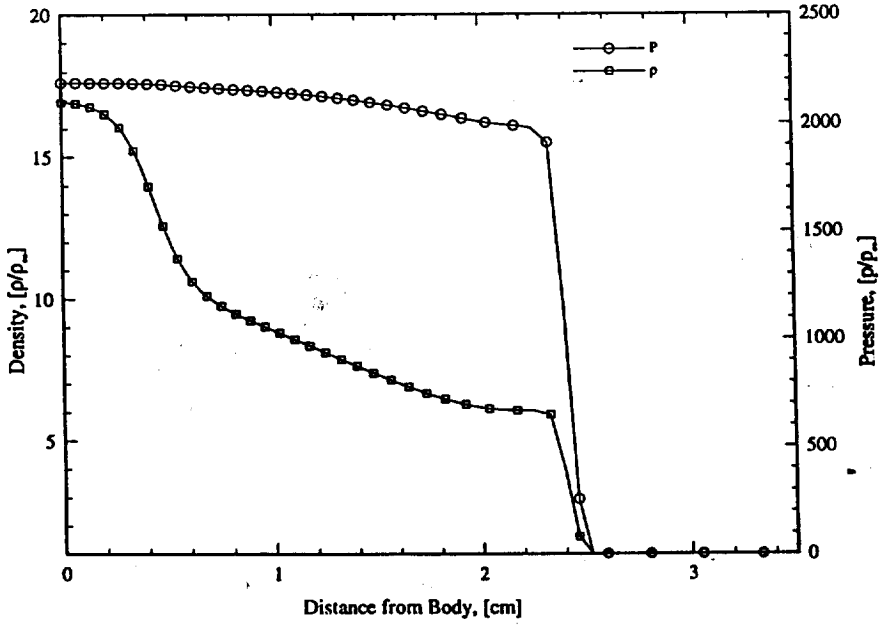

Figure 2: Thermodynamic Properties Along Stagnation Streamline

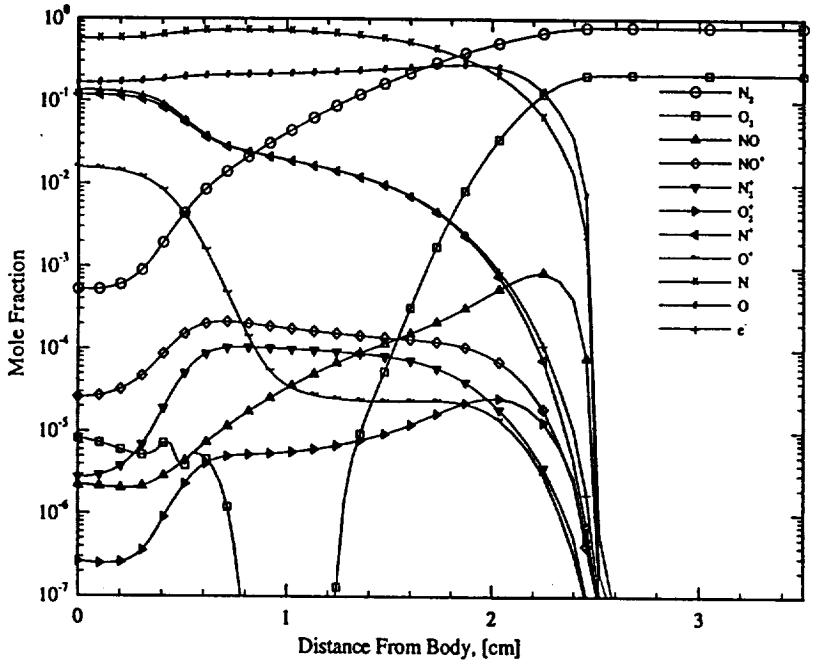

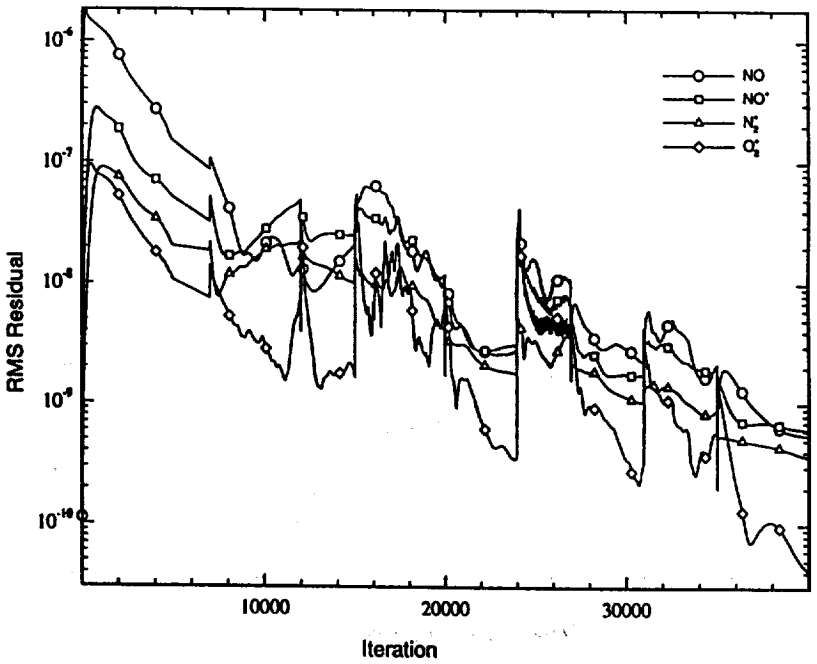

Figure 3: Stagnation Streamline Chemistry and Residual Plot

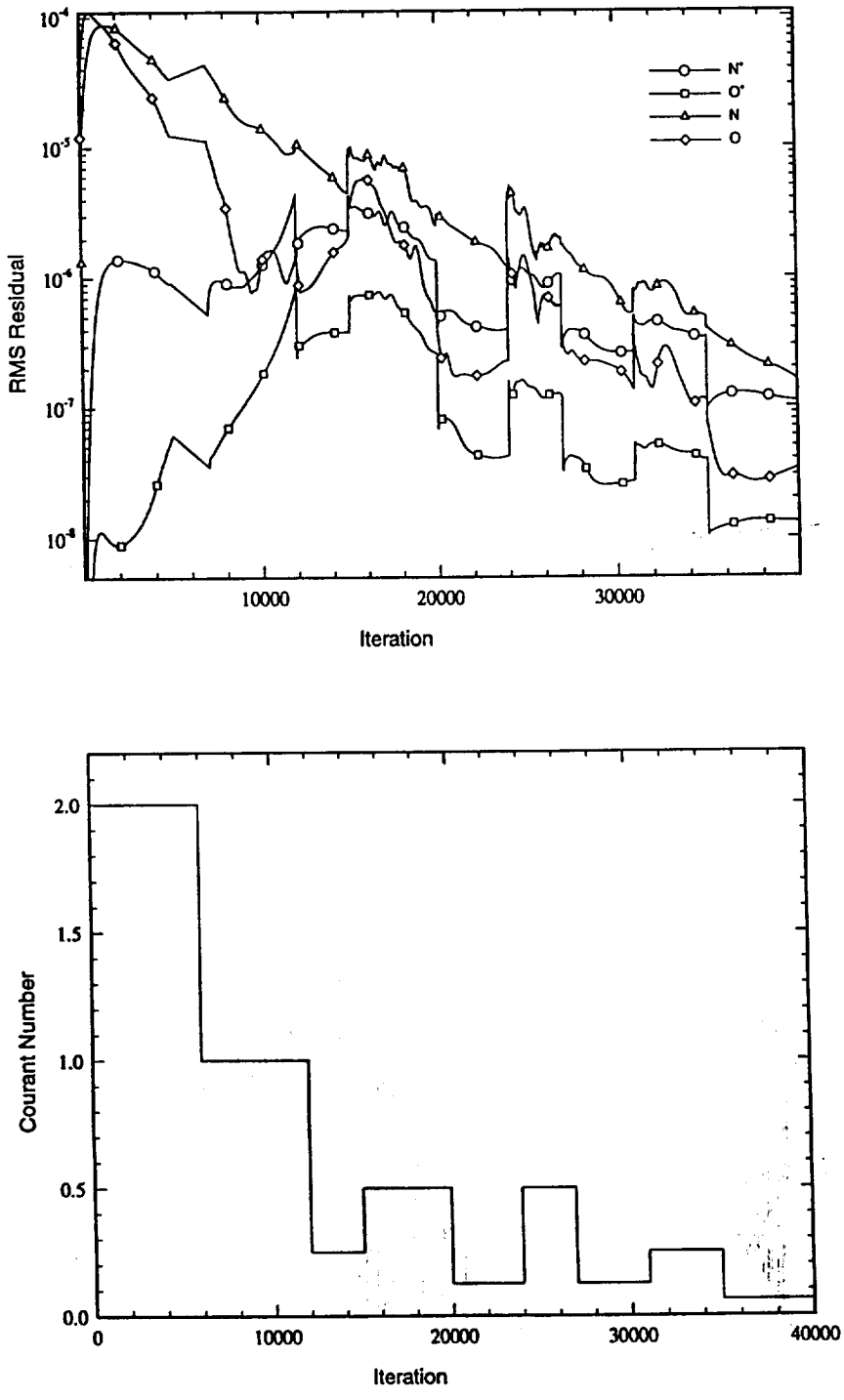

Figure 4: Residual Plot and CFL Modification Scheme

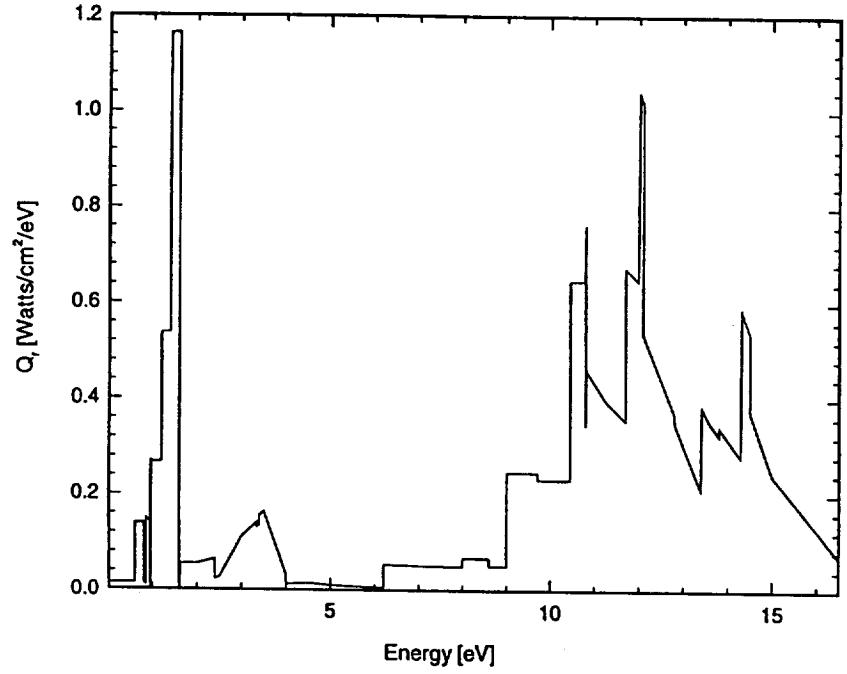

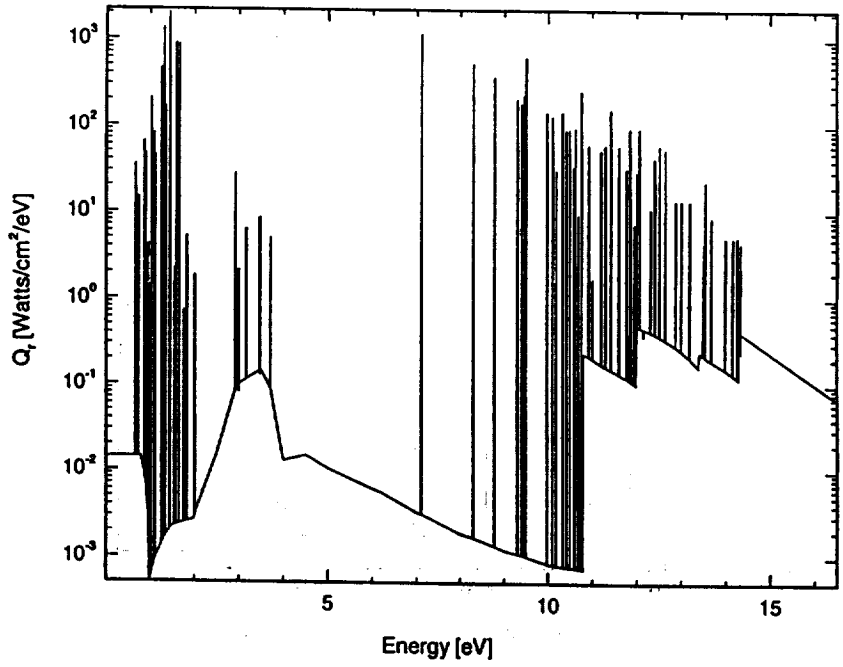

Figure 5: Stagnation Point Grouped and Detailed Radiative Spectra

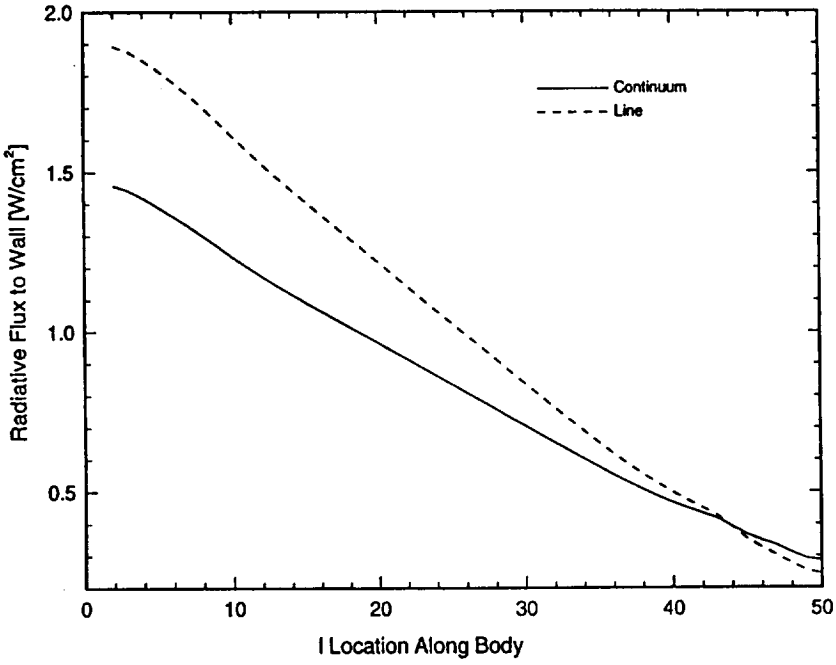

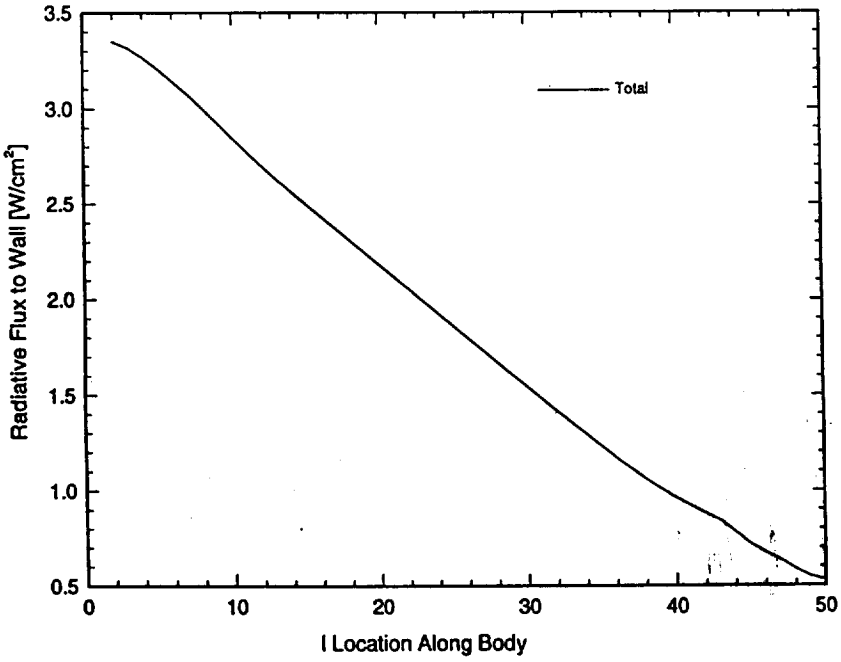

Figure 6: Line and Continuum Radiative Heat Transfer to Cylinder Surface

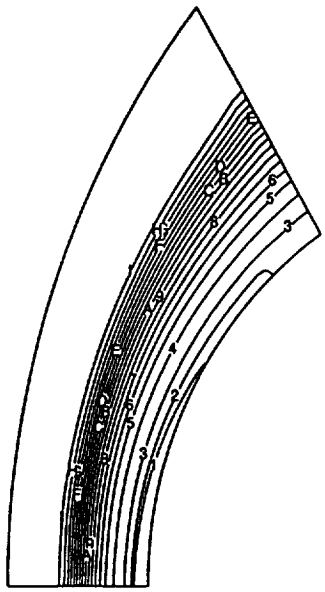

N_2 Mass Fraction

I	0.719136
H	0.671271
G	0.623407
F	0.575542
E	0.527678
D	0.479813
C	0.431949
B	0.384084
A	0.33622
9	0.288355
8	0.240491
7	0.192626
6	0.144761
5	0.0968969
4	0.0490324
3	0.0156727
2	0.00468656
1	0.00269442

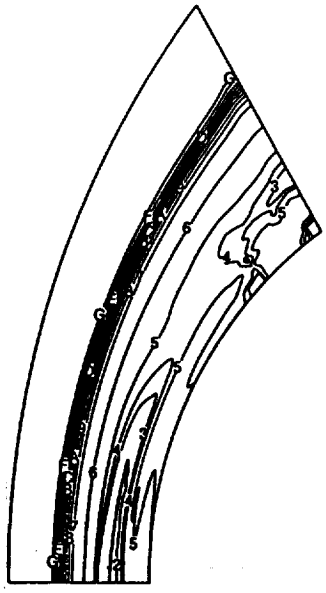

O_2 Mass Fraction

G	0.211818
F	0.190636
E	0.169454
D	0.148273
C	0.127091
B	0.105909
A	0.0847272
9	0.0635454
8	0.0423636
7	0.0211818
6	0.000767192
5	2.240E-5
4	8.681E-6
3	3.407E-6
2	2.5E-17
1	2.5E-17

Figure 7: N_2 and O_2 Mass Fraction Contour Plots

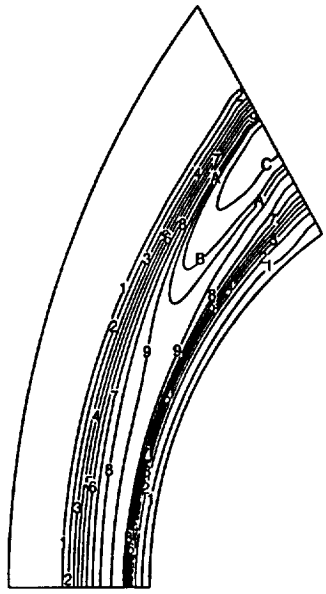

N_2^+ Mass Fraction

C	0.000242439
B	0.000218195
A	0.000207544
9	0.000193951
8	0.000169707
7	0.000145463
6	0.000121219
5	9.697E-5
4	7.273E-5
3	4.848E-5
2	2.424E-5
1	8.282E-6

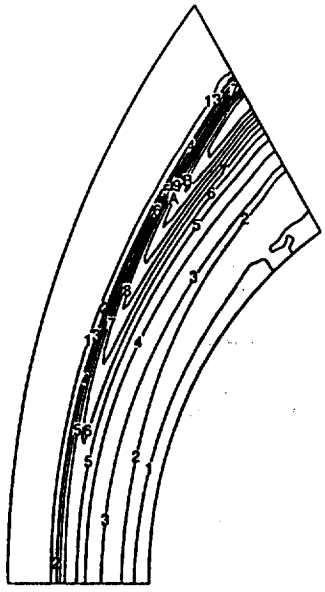

O_2^+ Mass Fraction

C	0.000109031
B	9.812E-5
A	8.722E-5
9	7.632E-5
8	6.541E-5
7	5.451E-5
6	4.361E-5
5	3.270E-5
4	2.180E-5
3	1.354E-5
2	1.090E-5
1	1.478E-6

Figure 8: N_2^+ and O_2^+ Mass Fraction Contour Plots

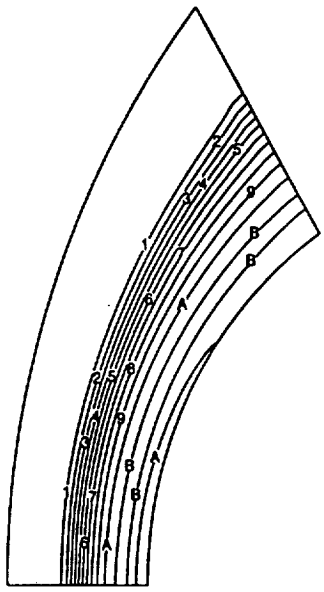

N Mass Fraction

B	0.702502
A	0.648984
9	0.584086
8	0.519187
7	0.454289
6	0.38939
5	0.324492
4	0.259594
3	0.194695
2	0.129797
1	0.0648984

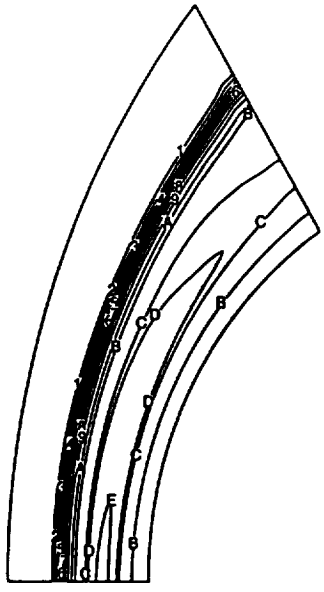

O Mass Fraction

E	0.232719
D	0.232538
C	0.232287
B	0.223413
A	0.211573
9	0.190416
8	0.169258
7	0.148101
6	0.126944
5	0.105787
4	0.0846292
3	0.0634719
2	0.0423146
1	0.0211573

Figure 9: *N* and *O* Mass Fraction Contour Plots

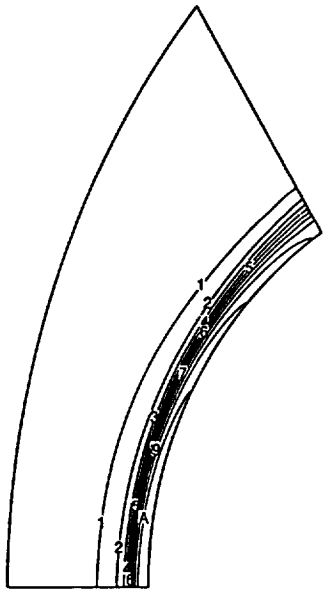

N^+ Mass Fraction

A	0.121219
9	0.109097
8	0.0969752
7	0.0848533
6	0.0727314
5	0.0606095
4	0.0484876
3	0.0363657
2	0.0242438
1	0.0121219

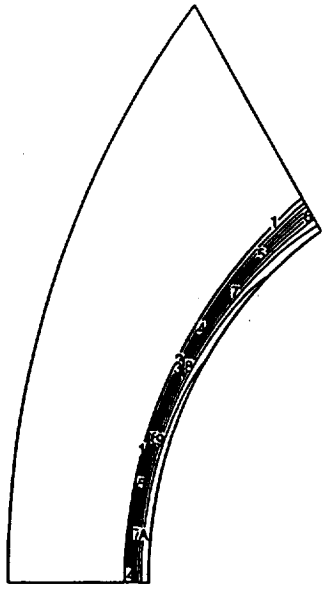

O^+ Mass Fraction

A	0.0181957
9	0.0163761
8	0.0145566
7	0.012737
6	0.0109174
5	0.00909785
4	0.00727828
3	0.00545871
2	0.00363914
1	0.00181957

Figure 10: N^+ and O^+ Mass Fraction Contour Plots

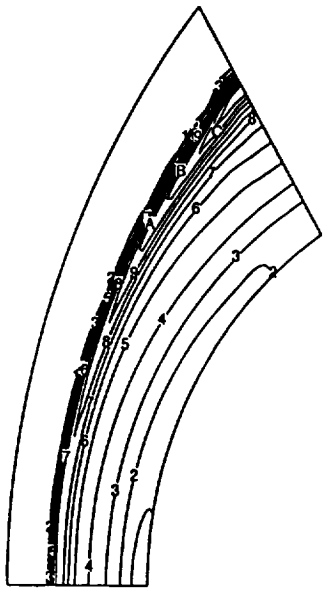

NO Mass Fraction

D	0.00216681
C	0.00195013
B	0.00173345
A	0.00151677
9	0.00130009
8	0.0010834
7	0.000866724
6	0.000650043
5	0.000433362
4	0.000216681
3	8.038E-5
2	2.191E-5
1	6.446E-6

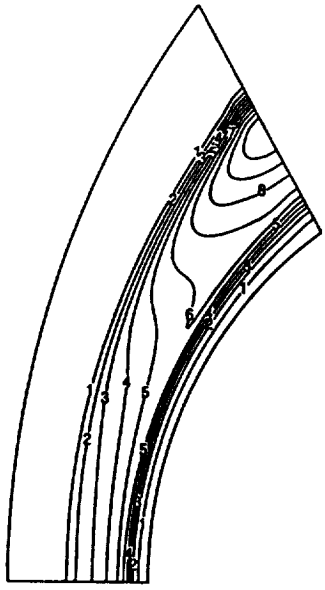

NO^+ Mass Fraction

A	0.000873875
9	0.000786487
8	0.0006991
7	0.000611712
6	0.000524325
5	0.000436937
4	0.00034955
3	0.000262163
2	0.000174775
1	8.738E-5

Figure 11: *NO* and NO^+ Mass Fraction Contour Plots

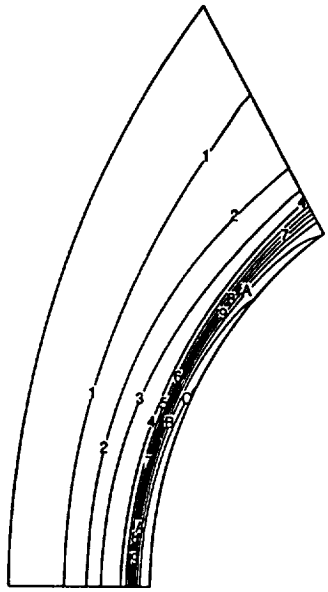

e⁻ Mass Fraction

C	5.402E-6
B	4.862E-6
A	4.321E-6
9	3.781E-6
8	3.241E-6
7	2.701E-6
6	2.160E-6
5	1.620E-6
4	1.080E-6
3	5.402E-7
2	2.552E-7
1	1.006E-8

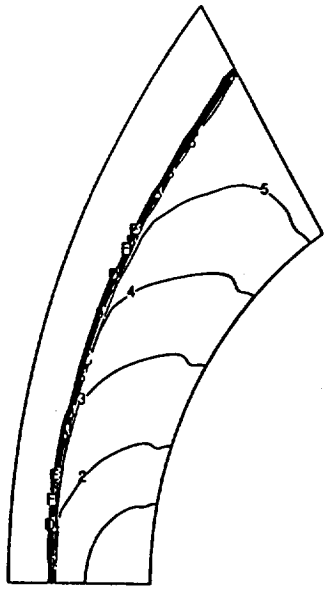

Mach Number

F	36.8934
E	33.2056
D	29.5177
C	25.8299
B	22.142
A	18.4542
9	14.7663
8	11.0785
7	7.39066
6	3.70282
5	1.271
4	0.967582
3	0.690863
2	0.419863
1	0.2395

Figure 12: Electron Mass Fraction and Mach Number Contour Plots

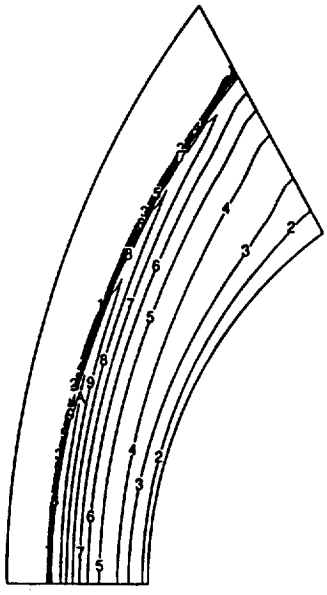

Translational Temperature

A	279.144
9	251.33
8	223.515
7	195.701
6	167.886
5	140.072
4	112.258
3	84.4432
2	56.6288
1	28.8144

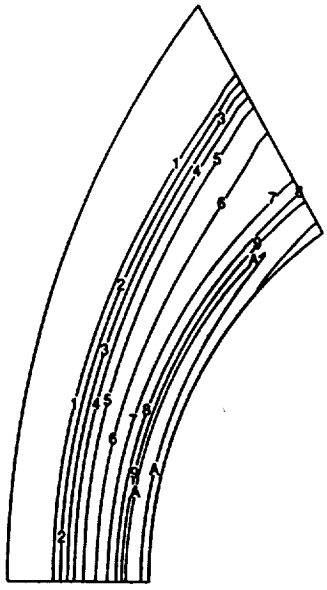

Vibrational Temperature

A	58.4109
9	52.6698
8	46.9287
7	41.1876
6	35.4465
5	29.7054
4	23.9644
3	18.2233
2	12.4822
1	6.74109

Figure 13: Translational and Vibrational Temperature Contour Plots

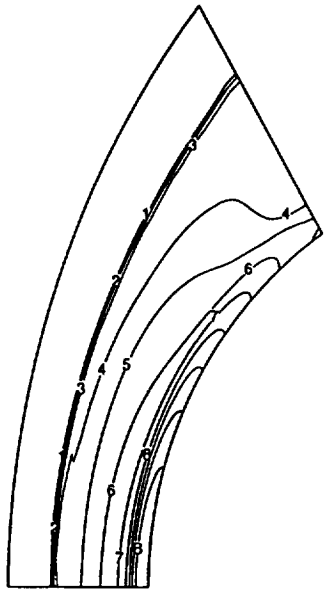

Density

B	15.4783
A	14.0305
9	12.5826
8	11.1348
7	9.68698
6	8.23915
5	6.79132
4	6.0036
3	5.34349
2	3.89566
1	2.44783

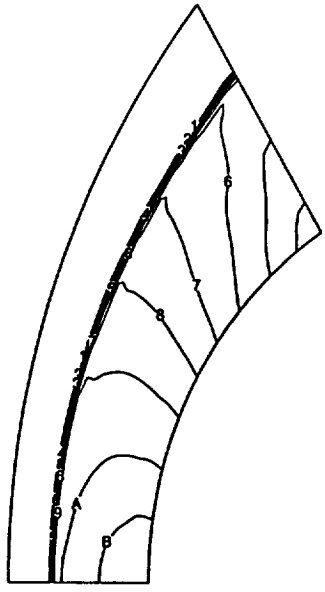

Pressure

B	2123.41
A	1988.32
9	1789.59
8	1590.86
7	1392.12
6	1193.39
5	994.66
4	795.928
3	597.196
2	398.464
1	199.732

Figure 14: Density and Pressure Contour Plots

9 Appendices

9.1 Input Files

9.1.1 Standard Input File

```
T F F F T F
T F T F F
T T F T F
   11   51
   50   70    2    1    00001  01000    200  10
    4    2    5    3   42   42
    4    1    4
1.0          1.0          1.0
6.6044E-6  -1.0          0.000000     0.00          0.00
37270.34  0.0436488    351.0         0.00         1.E6
1.40         0.73         1.50         8.30
firechem11
150.       65000.
    1    6    4   10
N2                  28.016     0.767       3395.
   .00000000+00    .35000000+01  -.16975380+04    .44721828+01
   .12032274-09    .14426096+04
   .10000000+01    .30000000+01    .60000000+01
   .00000000+00    .72233000+05    .85779000+05
O2                  32.0        0.233       2270.
   .00000000+00    .35000000+01  -.11361170+04    .55353971+01
  -.48120335-09   -.25376565+04
   .30000000+01    .20000000+01    .10000000+01
   .00000000+00    .11392000+05    .18985000+05
NO                  30.008                  2740.
   .30126055+07    .35000000+01  -.13755000+04    .58700914+01
  -.41428552-09    .82585556+02
   .40000000+01    .80000000+01    .20000000+01
   .00000000+00    .55835000+05    .63258000+05
NO+                 30.008                  2740.     .82
   .33098773+08    .35000000+01  -.17221480+04    .59047489+01
  -.54070696-10   -.29496701+03
   .10000000+01    .30000000+01    .60000000+01
   .00000000+00    .75090000+05    .85234000+05
N2+                 28.016                  3395.     .85
   .54532343+08    .35000000+01  -.38106880+04    .45195608+01
  -.50423765-09   -.38411001+04
   .20000000+01    .40000000+01    .40000000+01
   .00000000+00    .13189000+05    .36633000+05
O2+                 32.0                    2270.     .68
   .36637444+08    .35000000+01  -.13162570+04    .62894244+01
  -.77702160-09   -.98986157+03
   .40000000+01    .80000000+01    .40000000+01
   .00000000+00    .47428000+05    .58514000+05
N+                  14.008                             .59
   .13439875+09    .25000000+01    .45850000+02    .54147677+01
   .96467356-09    .56648418+04
   .90000000+01    .50000000+01    .10000000+01
   .00000000+00    .22000000+05    .47000000+05
O+                  16.0                               .60
   .98027720+08    .25000000+01    .42710000+02    .43968968+01
   .47954040-09   -.55391609+02
   .40000000+01    .10000000+02    .60000000+01
   .00000000+00    .38600000+05    .58200000+05
N                   14.008                            .1475
   .33756213+08    .25000000+01    .45890000+02    .51772995+01
   .37479202-08   -.10928045+03
```

```
   .40000000+01   .10000000+02   .60000000+01
   .00000000+00   .27665000+05   .41495000+05
O                   16.0                          .15
   .15570756+08   .25000000+01   .13429000+02   .60255466+01
   .38245505-08   .54019395+04
   .90000000+01   .50000000+01   .10000000+01
   .00000000+00   .22831000+05   .48619600+05
E-                  .0005486
   .00000000+00   .25000000+01  -.67087492+03  -.11687078+02
   .00000000+00   .00000000+00
   .00000000+00   .00000000+00   .00000000+00
   .00000000+00   .00000000+00   .00000000+00
N2    N           N     N     N
3  0          3.0E22  113200.     -1.6
N2    NO          N     N     NO
3  0          7.0E21  113200.     -1.6
N2    N2          N     N     N2
3  0         7.00E21  113200.     -1.6
N2    O           N     N     O
3  0         3.00E22  113200.     -1.6
N2    O2          N     N     O2
3  0          7.0E21  113200.     -1.6
N2    N+          N     N     N+
3  0         3.00E22  113200.     -1.60
N2    O+          N     N     O+
3  0         3.00E22  113200.     -1.60
N2    N2+         N     N     N2+
3  0         7.00E21  113200.     -1.60
N2    O2+         N     N     O2+
3  0         7.00E21  113200.     -1.60
N2    NO+         N     N     NO+
3  0         7.00E21  113200.     -1.60
O2    N+          O     O     N+
3  0         1.00E22  59500.      -1.50
O2    O+          O     O     O+
3  0         1.00E22  59500.      -1.50
O2    N2+         O     O     N2+
3  0         2.00E21  59500.      -1.50
O2    O2+         O     O     O2+
3  0         2.00E21  59500.      -1.50
O2    NO+         O     O     NO+
3  0         2.00E21  59500.      -1.50
O2    N           O     O     N
3  0          1.0E22  59500.      -1.5
O2    NO          O     O     NO
3  0          2.0E21  59500.      -1.5
O2    N2          O     O     N2
3  0          2.0E21  59500.      -1.5
O2    O           O     O     O
3  0          1.0E22  59500.      -1.5
O2    O2          O     O     O2
3  0         2.00E21  59500.      -1.5
NO    N+          N     O     N+
3  0         1.10E17  75500.       0.00
NO    O+          N     O     O+
3  0         1.10E17  75500.       0.00
NO    N2+         N     O     N2+
3  0         5.00E15  75500.       0.00
NO    O2+         N     O     O2+
3  0         5.00E15  75500.       0.00
NO    NO+         N     O     NO+
3  0         5.00E15  75500.       0.00
NO    N           N     O     N
3  0          1.1E17  75500.       0.0
NO    NO          N     O     NO
```

```
3  0          1.1E17  75500.        0.0
NO     N2          N     O     N2
3  0          5.0E15  75500.        0.0
NO     O           N     O     O
3  0          1.1E17  75500.        0.0
NO     O2          N     O     O2
3  0         5.00E15  75500.        0.0
NO     O           O2    N
1  0          8.4E12  19450.        0.0
N2     O           NO    N
1  0          6.4E17  38400.       -1.0
O      O2+         O2    O+
1  0         4.00E12  18000.       -0.09
N2     N+          N     N2+
1  0         1.00E12  12200.        0.50
N2     O+          O     N2+
1  0         9.10E11  22800.        0.36
O2     NO+         NO    O2+
1  0         2.30E13  32600.        0.41
O      NO+         O2    N+
1  0         1.00E12  77200.        0.50
N      NO+         O     N2+
1  0         7.20E13  35500.        0.00
O+     NO          N+    O2
1  0         1.40E05  26600.        1.90
NO+    N           O+    N2
1  0         3.40E13  12800.       -1.08
O2+    N           N+    O2
1  0         8.70E13  28600.        0.14
O2+    N2          N2+   O2
1  0         9.90E12  40700.        0.00
NO+    O           O2+   N
1  0         7.20E12  48600.        0.29
N      N           N+    E-    N
3  0         2.34E11  120000.       0.50
N      N+          N+    E-    N+
3  0         2.34E11  120000.       0.50
N      O           NO+   E-
1  0          5.3E12  31900.        0.0
N      N           N2+   E-
1  0         2.00E13  67500.        0.0
O      O           O2+   E-
1  0         1.10E13  80600.        0.00
N2     E-          N     N     E-
3  0         3.00E24  113100.      -1.6
N      E-          N+    E-    E-
3  1         5.08E16  121000.       0.00  13.57
O      E-          O+    E-    E-
3  2         6.35E15  106200.       0.00  14.60
```

9.1.2 Secondary Input File (*fort.88*)

```
**RADIATION COUPLING VARIABLES**
 T   T
 04001    1000    10.    70.
**CHEMICAL RATE TIME RELAXATION VARIABLE**
 0.3
**PARK'S TTV EFFECTIVE TEMP MODEL**
 T
 0.3    30    49
**GNOFFO'S T-E COUPLING:  CURVE FIT CONSTANTS FOR NEUTRALS**
 T
 5
```

```
1       7.5E-20         5.5E-24         -1.E-28
2       2.E-20          6.E-24           0.
3       1.E-19          0.               0.
9       5.E-20          0.               0.
10      1.2E-20         1.7E-24         -2.E-29
```

9.1.3 Molecular Collision Cross Section Data (*mexcite.dat*)

```
N2+           28.010    4    6    5    4    0
    2.000      0.000  2207.190    16.136    -0.040     0.000   1.93220 2.020E-02
    4.000   9168.400  1902.840    14.910     0.000     0.000   1.72200 1.800E-02
    2.000  25461.500  2419.840    23.190    -0.538     0.000   2.08300 1.950E-02
    4.000  51663.2     907.71     11.91      0.016     0.       1.113   0.020
    2.000  64622.199  2050.000     0.000     0.000     0.000   1.65000 5.000E-02
N  4S      1.401E+01 7.040E+04 4.000E+00 1.500E+00 0.000E+00
N+ 3P      1.401E+01 7.040E+04 9.000E+00 1.000E+00 1.000E+00
CROSS-SECTIONS ASSUMED TO BE THE SAME AS FOR X-B OF CRANDALL ET AL *0.1
70398.
8.727     11.01     16.52     22.03     27.54     41.30     55.07     82.61
2.950E-17 2.830E-17 2.380E-17 1.900E-17 1.550E-17 1.100E-17 0.890E-17 0.680E-17
CROSS-SECTIONS ASSUMED TO BE THE SAME AS FOR X-B OF CRANDALL ET AL *0.1
70398.
7.610     9.604     14.41     19.21     24.01     36.01     48.02     72.03
2.950E-17 2.830E-17 2.380E-17 1.900E-17 1.550E-17 1.100E-17 0.890E-17 0.680E-17
CROSS-SECTIONS ASSUMED TO BE THE SAME AS FOR X-B OF CRANDALL ET AL *0.1
70398.
5.558     7.014     10.52     14.03     17.54     26.30     35.07     52.61
2.950E-17 2.830E-17 2.380E-17 1.900E-17 1.550E-17 1.100E-17 0.890E-17 0.680E-17
CROSS-SECTIONS ASSUMED TO BE THE SAME AS FOR X-B OF CRANDALL ET AL *0.1
70398.
2.323     2.931     4.397     5.863     7.328     10.99     14.66     21.98
2.950E-17 2.830E-17 2.380E-17 1.900E-17 1.550E-17 1.100E-17 0.890E-17 0.680E-17
N2+MEI        1    2   10
 0  0 4.751E-01  0  1 3.798E-01  0  2 1.226E-01  0  3 2.055E-02  0  4 1.914E-03
 0  5 9.822E-05  1  0 3.255E-01  1  1 3.115E-01  1  2 3.358E-01  1  3 2.368E-01
 1  4 6.236E-02  1  5 7.946E-03  1  6 5.163E-04  2  0 1.360E-01  2  1 2.245E-01
 2  2 2.137E-02  2  3 1.851E-01  2  4 2.946E-01  2  5 1.171E-03  2  6 1.972E-03
 2  7 1.581E-03  3  0 4.526E-02  3  1 1.990E-01  3  2 7.974E-01  3  3 1.049E-01
 3  4 6.274E-02  3  5 2.929E-01  3  6 1.738E-01  3  7 3.793E-02  3  8 3.685E-03
 4  0 1.329E-02  4  1 1.032E-01  4  2 1.745E-01  4  3 7.195E-03  4  4 1.553E-01
 4  5 5.808E-03  4  6 2.479E-01  4  7 2.230E-01  4  8 6.228E-02  4  9 7.238E-03
 5  0 3.624E-03  5  1 4.145E-02  5  2 1.395E-01  5  3 1.078E-01  5  4 6.918E-03
 5  5 1.509E-01  5  6 5.609E-03  5  7 1.816E-01  5  8 2.578E-01  5  9 9.165E-02
CROSS-SECTIONS ASSUMED TO BE THE SAME  AS FOR X-B OF CRANDALL ET AL
1.118     1.411     2.116     2.821     3.527     5.289     7.053     10.58
2.950E-16 2.830E-16 2.380E-16 1.900E-16 1.550E-16 1.100E-16 0.890E-16 0.680E-16
0.
N2+ 1-        1    3   36
 0  0 6.509E-01  1  0 3.014E-01  2  0 4.537E-02  3  0 2.248E-03  4  0 1.452E-05
 0  1 2.588E-01  1  1 2.226E-01  2  1 4.060E-01  3  1 1.056E-01  4  1 6.935E-03
 5  1 3.986E-05  0  2 7.016E-02  1  2 2.860E-01  2  2 5.065E-02  3  2 4.137E-01
 4  2 1.660E-01  5  2 1.340E-02  6  2 5.729E-05  7  2 1.132E-05  0  3 1.600E-02
 1  3 1.324E-01  2  3 2.290E-01  3  3 2.101E-03  4  3 3.792E-01  5  3 2.205E-01
 6  3 2.069E-02  7  3 4.930E-05  8  3 3.006E-05  0  4 3.297E-03  1  4 4.273E-02
 2  4 1.654E-01  3  4 1.557E-01  4  4 6.726E-03  5  4 3.310E-01  6  4 2.673E-01
 7  4 2.789E-02  8  4 1.807E-05  9  4 6.420E-05  0  5 6.342E-04  1  5 1.140E-02
 2  5 7.113E-02  3  5 1.706E-01  4  5 9.290E-02  5  5 2.925E-02  6  5 2.830E-01
 7  5 3.068E-01  8  5 3.419E-02 10  5 1.161E-04  0  6 1.165E-04  1  6 2.700E-03
 2  6 2.362E-02  3  6 9.451E-02  4  6 1.569E-01  5  6 4.815E-02  6  6 5.331E-02
 7  6 2.415E-01  8  6 3.401E-01  9  6 3.890E-02 10  6 8.094E-05 11  6 1.823E-04
 0  7 2.000E-05  1  7 5.861E-04  2  7 6.691E-03  3  7 3.801E-02  4  7 1.096E-01
 5  7 1.333E-01  6  7 2.044E-02  7  7 7.236E-02  8  7 2.083E-01  9  7 3.686E-01
10  7 4.153E-02 11  7 3.873E-04 12  7 2.509E-04 13  7 1.172E-05  1  8 1.185E-04
 2  8 1.695E-03  3  8 1.261E-02  4  8 5.236E-02  5  8 1.161E-01  6  8 1.065E-01
```

```
 7  8 5.931E-03  8  8 8.468E-02  9  8 1.837E-01 10  8 3.933E-01 11  8 4.170E-02
12  8 1.087E-03 13  8 3.010E-04 14  8 3.005E-05  1  9 2.239E-05  2  9 3.934E-04
 8  9 4.743E-04  9  9 9.065E-02 10  9 1.672E-01 11  9 4.149E-01 12  9 3.928E-02
13  9 2.361E-03 14  9 3.071E-04 15  9 6.400E-05  2 10 8.445E-05  3 10 9.639E-04
 4 10 6.599E-03  5 10 2.826E-02  6 10 7.442E-02  7 10 1.084E-01  8 10 5.865E-02
 9 10 5.552E-04 10 10 9.141E-02 11 10 1.579E-01 12 10 4.338E-01 13 10 3.432E-02
14 10 4.364E-03 15 10 2.499E-04 16 10 1.171E-04  2 11 1.675E-05  3 11 2.324E-04
 4 11 1.942E-03  5 11 1.043E-02  6 11 3.652E-02  7 11 8.051E-02  8 11 9.821E-02
 9 11 4.075E-02 10 11 3.604E-03 11 11 8.818E-02 12 11 1.554E-01 13 11 4.496E-01
14 11 2.722E-02 15 11 7.165E-03 16 11 1.355E-04 17 11 1.867E-04  3 12 5.156E-05
 4 12 5.207E-04  5 12 3.406E-03  6 12 1.496E-02  7 12 4.411E-02  8 12 8.319E-02
 9 12 8.628E-02 10 12 2.710E-02 11 12 7.896E-03 12 12 8.205E-02 13 12 1.593E-01
14 12 4.615E-01 15 12 1.876E-02 16 12 1.068E-02 17 12 2.033E-05 18 12 2.587E-04
19 12 2.439E-05  3 13 1.044E-05  4 13 1.281E-04  5 13 1.007E-03  6 13 5.378E-03
 7 13 1.991E-02  8 13 5.053E-02  9 13 8.288E-02 10 13 7.393E-02 11 13 1.720E-02
12 13 1.238E-02 13 13 7.384E-02 14 13 1.697E-01 15 13 4.681E-01 16 13 1.018E-02
17 13 1.459E-02 18 13 3.550E-05 19 13 3.056E-04  4 14 2.877E-05  5 14 2.724E-04
 6 14 1.741E-03  7 14 7.823E-03  8 14 2.495E-02  9 14 5.544E-02 10 14 8.018E-02
11 14 6.208E-02 12 14 1.034E-02 13 14 1.651E-02 14 14 6.418E-02 15 14 1.866E-01
16 14 4.676E-01 17 14 3.207E-03 18 14 1.831E-02 19 14 3.955E-04  5 15 6.737E-05
CROSS-SECTINS MEASURED BY CRANDALL ET AL
3.17       4.00       5.0        6.0        8.0        10.        15.        20.
2.950E-16 2.830E-16 2.380E-16 1.900E-16 1.550E-16 1.100E-16 0.890E-16 0.680E-16
1.520E+07
N2+ DX        1    4   54
 0  4 1.579E-04  0  5 6.941E-04  0  6 2.501E-03  0  7 7.498E-03  0  8 1.888E-02
 0  9 4.020E-02  0 10 1.119E-01  0 11 1.469E-01  0 12 1.642E-01  0 13 1.556E-01
 0 14 8.237E-02  0 15 4.467E-02  0 16 6.454E-03  0 17 1.574E-03  1  3 2.379E-04
 1  4 1.105E-03  1  5 4.051E-03  1  6 1.193E-02  1  7 2.838E-02  1  8 5.433E-02
 1  9 8.246E-02  1 10 7.993E-02  1 11 3.886E-02  1 12 3.775E-03  1 13 9.785E-03
 1 14 1.231E-01  1 15 1.498E-01  1 16 7.868E-02  1 17 3.522E-02  1 18 2.220E-03
 2  2 2.055E-04  2  3 1.061E-03  2  4 4.119E-03  2  5 1.243E-02  2  6 2.937E-02
 2  7 5.383E-02  2  8 7.418E-02  2  9 7.166E-02  2 10 5.664E-03  2 11 6.219E-03
 2 12 4.435E-02  2 13 7.148E-02  2 14 5.578E-03  2 15 1.365E-02  2 16 1.467E-01
 2 17 1.458E-01  2 18 3.852E-02  2 19 1.260E-03  3  1 1.266E-04  3  2 7.873E-04
 3  3 3.383E-03  3  4 1.083E-02  3  5 2.642E-02  3  6 4.873E-02  3  7 6.544E-02
 3  8 5.822E-02  3  9 2.601E-02  3 10 1.461E-02  3 11 4.747E-02  3 12 4.558E-02
 3 13 9.981E-03  3 14 4.763E-02  3 15 6.338E-02  3 16 3.506E-03  3 17 7.154E-02
 3 18 1.543E-01  3 19 2.868E-02  3 20 2.104E-04  4  1 4.776E-04  4  2 2.441E-03
 4  3 8.604E-03  4  4 2.231E-02  4  5 4.286E-02  4  6 5.903E-02  4  7 5.284E-02
 4  8 2.278E-02  4  9 3.107E-04  4 10 4.162E-02  4 11 3.102E-02  4 12 2.057E-03
 4 13 1.384E-02  4 14 2.859E-02  4 16 6.297E-02  4 17 2.450E-02  4 18 8.839E-02
 4 19 1.494E-01  4 20 1.189E-02  5  0 2.140E-04  5  1 1.563E-03  5  2 6.463E-03
 5  3 1.834E-02  5  4 3.756E-02  5  5 5.462E-02  5  6 5.185E-02  5  7 2.462E-02
 5  8 8.863E-04  5  9 1.169E-02  5 10 2.555E-02  5 11 9.533E-04  5 12 1.462E-02
 5 13 3.651E-02  5 14 1.906E-03  5 15 3.396E-02  5 16 8.541E-04  5 17 2.805E-02
 5 18 1.584E-02  5 19 1.384E-01  5 20 1.102E-01  5 21 1.694E-03  6  0 8.007E-04
 6  1 4.533E-03  6  2 1.487E-02  6  3 3.315E-02  6  4 5.168E-02  6  5 5.310E-02
 6  6 2.909E-02  6  7 2.669E-03  6  8 7.266E-03  6  9 2.986E-02  6 10 1.364E-03
 6 11 1.171E-02  6 12 3.032E-02  6 13 1.091E-02  6 14 2.913E-02  6 15 2.045E-02
 6 16 2.965E-02  6 17 3.096E-02  6 18 3.761E-02  6 19 1.295E-03  6 20 2.057E-01
 6 21 4.502E-02  7  0 2.732E-03  7  1 1.163E-02  7  2 2.957E-02  7  3 4.991E-02
 7  4 5.571E-02  7  5 3.501E-02  7  6 5.910E-03  7  7 3.508E-03  7  8 2.451E-02
 7  9 2.438E-02  7 10 7.875E-03  7 11 2.579E-02  7 12 1.041E-02  7 13 1.982E-03
 7 14 1.547E-02  7 15 6.758E-04  7 16 1.859E-02  7 17 8.836E-04  7 18 2.156E-02
 7 19 5.653E-02  7 20 2.086E-02  7 21 2.030E-01  7 22 6.649E-03  8  0 2.272E-02
 8  1 4.752E-02  8  2 6.504E-02  8  3 4.986E-02  8  4 1.606E-02  8  6 1.551E-02
 8  7 2.468E-02  8  8 7.102E-03  8  9 2.077E-03  8 10 1.226E-02  8 11 1.357E-04
 8 12 1.509E-02  8 13 1.338E-02  8 14 1.572E-02  8 15 1.224E-02  8 16 1.958E-02
 8 17 8.542E-03  8 18 2.511E-02  8 19 2.164E-02  8 20 5.973E-03  8 21 5.069E-03
 8 22 2.433E-01  8 23 1.599E-02  9  0 5.255E-02  9  1 6.827E-02  9  2 6.214E-02
 9  3 2.240E-02  9  4 1.873E-04  9  5 1.256E-02  9  6 2.450E-02  9  7 9.697E-03
 9  8 6.955E-04  9  9 1.524E-02  9 11 1.157E-02  9 12 1.326E-02  9 14 1.165E-02
 9 15 2.491E-04  9 16 7.723E-03  9 17 3.467E-03  9 18 1.668E-03  9 19 1.614E-02
 9 20 3.486E-02  9 21 5.754E-02  9 22 6.642E-02  9 23 1.387E-01  9 24 1.769E-04
```

```
10  0 1.015E-01 10  1 6.956E-02 10  2 3.610E-02 10  3 9.781E-04 10  4 9.260E-03
10  5 2.566E-02 10  6 1.193E-02 10  8 1.277E-02 10  9 1.389E-02 10 10 8.671E-03
10 11 1.308E-02 10 12 4.079E-04 10 13 9.081E-03 10 15 1.218E-02 10 16 1.937E-03
10 17 1.562E-02 10 18 1.041E-02 10 19 2.075E-03 10 20 2.150E-04 10 21 5.829E-03
10 22 3.749E-02 10 23 2.378E-01 10 24 2.930E-03 11  0 2.010E-01 11  1 4.128E-03
11  2 9.081E-04 11  3 3.431E-02 11  4 1.479E-02 11  5 1.310E-03 11  6 1.013E-02
11  7 1.366E-02 11  8 2.956E-03 11  9 4.710E-03 11 10 2.317E-03 11 11 4.536E-03
11 12 1.066E-02 11 13 6.973E-04 11 14 8.468E-03 11 15 1.368E-04 11 16 3.669E-03
11 17 4.138E-03 11 19 2.462E-03 11 20 7.770E-03 11 21 1.372E-02 11 22 2.433E-02
11 23 6.579E-02 11 24 1.756E-01 12  0 1.293E-01 12  1 8.939E-02 12  2 5.961E-03
12  3 1.924E-02 12  4 1.544E-02 12  5 7.623E-03 12  6 1.198E-02 12  7 4.165E-03
12  8 7.042E-03 12  9 7.446E-03 12 10 7.521E-03 12 11 3.516E-03 12 12 3.584E-03
12 13 7.830E-03 12 14 6.465E-03 12 15 5.513E-03 12 16 9.053E-03 12 17 8.782E-04
12 18 5.483E-03 12 19 9.831E-03 12 20 1.299E-02 12 21 1.678E-02 12 22 2.334E-02
CROSS-SECTIONS ASSUMED TO BE THE SAME AS FOR B-X OF CRANDALL ET AL
6.405      8.083      12.12      16.17      20.21      30.31      40.42      60.62
2.950E-16 2.830E-16 2.380E-16 1.900E-16 1.550E-16 1.100E-16 0.890E-16 0.680E-16
0.
N2+MEI       2    3   61
 0  0 9.858E-02  0  1 2.010E-01  0  2 2.274E-01  0  3 1.897E-01  0  4 1.304E-01
 0  5 7.827E-02  0  6 4.202E-02  0  7 2.023E-02  0  8 8.537E-03  0  9 2.978E-03
 1  0 2.331E-01  1  1 1.645E-01  1  2 2.267E-02  1  3 1.090E-02  1  4 7.699E-02
 1  5 1.276E-01  1  6 1.324E-01  1  7 1.054E-01  1  8 6.863E-02  1  9 3.678E-02
 1 10 4.559E-03  1 11 6.144E-04  1 13 1.757E-04  2  0 2.739E-01  2  1 1.263E-02
 2  2 6.140E-02  2  3 1.150E-01  2  4 4.835E-02  2  5 3.454E-04  2  6 2.816E-02
 2  7 8.558E-02  2  8 1.196E-01  2  9 1.136E-01  2 10 4.217E-02  2 11 1.476E-02
 2 12 2.383E-03  2 14 7.023E-04  2 15 2.225E-04  3  0 2.110E-01  3  1 4.466E-02
 3  2 1.213E-01  3  3 9.749E-03  3  4 3.071E-02  3  5 8.135E-02  3  6 4.921E-02
 3  7 3.362E-03  3  8 1.564E-02  3  9 7.232E-02  3 10 1.179E-01  3 11 7.927E-02
 3 12 3.386E-02  3 13 6.730E-03  3 14 1.545E-03  3 15 1.969E-03  3 17 2.360E-04
 4  0 1.175E-01  4  1 1.690E-01  4  2 1.948E-02  4  3 5.468E-02  4  4 7.808E-02
 4  5 6.532E-03  4  6 2.003E-02  4  7 5.987E-02  4  8 3.954E-02  4  9 2.300E-03
 4 10 8.239E-02  4 11 1.290E-01  4 12 1.155E-01  4 13 6.142E-02  4 14 1.524E-04
 4 15 2.870E-03  4 16 1.669E-03  4 17 4.403E-04  4 18 1.643E-04  4 19 1.416E-04
 5  0 4.856E-02  5  1 2.020E-01  5  2 3.091E-02  5  3 9.172E-02  5  4 1.427E-04
 5  5 5.362E-02  5  6 5.327E-02  5  7 3.333E-03  5  8 1.674E-02  5  9 4.537E-02
 5 11 3.722E-02  5 12 1.109E-01  5 13 1.385E-01  5 14 2.914E-02  5 15 8.684E-04
 5 16 8.187E-03  5 18 1.376E-03  6  0 1.438E-02  6  1 1.359E-01  6  2 1.596E-01
 6  3 5.523E-03  6  4 6.783E-02  6  5 3.898E-02  6  6 3.357E-03  6  7 4.840E-02
 6  8 3.482E-02  6  9 6.546E-04  6 10 3.239E-02  6 11 8.087E-03  6 12 8.612E-03
 6 13 7.689E-02  6 14 1.222E-01  6 15 4.813E-02  6 16 5.028E-03  6 17 6.864E-03
 6 18 1.326E-03  6 19 9.596E-04  7  0 2.712E-03  7  1 5.621E-02  7  2 1.997E-01
 7  3 6.253E-02  7  4 5.351E-02  7  5 1.062E-02  7  6 5.970E-02  7  7 1.205E-02
 7  8 1.061E-02  7  9 4.128E-02  7 10 2.364E-04  7 11 1.802E-02  7 12 1.626E-02
 7 13 1.344E-04  7 14 1.267E-01  7 15 1.416E-01  7 16 7.417E-03  7 17 1.839E-02
 7 18 8.947E-04  7 19 4.369E-03  8  0 2.265E-04  8  1 1.307E-02  8  2 1.197E-01
 8  3 2.014E-01  8  4 5.484E-03  8  5 7.101E-02  8  6 3.963E-03  8  7 3.053E-02
 8  8 3.781E-02  8  9 1.110E-03  8 10 3.166E-02  8 11 6.858E-03  8 12 3.060E-03
 8 13 1.345E-02  8 14 2.037E-02  8 15 1.016E-01  8 16 9.138E-02  8 17 3.263E-03
 8 18 1.800E-02  8 19 1.632E-03  9  2 2.899E-03  9  3 6.683E-02  9  4 2.357E-01
 9  5 9.423E-02  9  6 2.519E-02  9  7 1.073E-02  9  8 4.088E-02  9  9 3.076E-03
 9 10 2.651E-02  9 11 2.462E-03  9 12 9.289E-03  9 13 2.262E-02  9 14 3.273E-04
 9 15 1.999E-03  9 16 5.189E-02  9 17 1.177E-01  9 19 3.142E-02 10  3 5.339E-03
10  4 1.066E-01 10  5 2.639E-01 10  6 4.767E-02 10  7 3.430E-02 10  9 3.080E-02
10 10 1.842E-03 10 11 2.221E-02 10 12 1.092E-02 10 13 9.910E-04 10 14 1.444E-02
10 15 1.188E-03 10 16 1.529E-03 10 17 1.059E-01 10 18 4.941E-02 10 19 1.990E-02
11  2 2.245E-04 11  3 5.422E-04 11  4 7.679E-03 11  5 1.488E-01 11  6 2.729E-01
11  7 2.125E-02 11  8 2.682E-02 11  9 7.368E-03 11 10 2.274E-02 11 11 7.674E-04
11 12 1.179E-02 11 13 1.601E-02 11 14 9.282E-03 11 15 1.739E-02 11 16 2.068E-04
11 17 2.478E-02 11 18 1.150E-01 11 19 3.166E-03 12  4 1.740E-03 12  5 6.393E-03
12  6 8.011E-03 12  7 2.178E-01 12  8 2.616E-01 12  9 6.698E-03 12 10 2.786E-02
12 12 1.370E-02 12 13 1.038E-02 12 14 1.144E-02 12 15 7.056E-03 12 16 1.222E-02
12 17 5.755E-03 12 18 1.538E-02 12 19 9.503E-02 13  5 3.214E-03 13  6 1.501E-02
13  7 4.955E-03 13  8 2.330E-01 13  9 2.522E-01 13 10 6.575E-04 13 11 3.209E-02
13 12 6.402E-04 13 13 7.041E-03 13 14 2.754E-04 13 15 7.066E-03 13 17 1.549E-02
```

```
13 18 5.836E-03 13 19 4.587E-02 14  5 5.767E-04 14  6 1.754E-03 14  7 4.791E-03
14  8 4.951E-02 14  9 3.759E-04 14 10 2.299E-01 14 11 2.551E-02 14 12 2.676E-02
14 13 3.778E-02 14 14 4.100E-04 14 15 1.029E-02 14 16 1.588E-03 14 17 1.967E-03
14 18 1.280E-02 14 19 1.100E-02 15  6 9.381E-04 15  7 5.386E-03 15  8 3.030E-03
15  9 7.132E-02 15 10 1.560E-01 15 11 2.100E-01 15 12 4.166E-02 15 13 5.199E-02
15 14 7.912E-04 15 16 3.713E-03 15 17 6.440E-03 15 18 8.720E-04 15 19 1.529E-02
16  6 1.202E-04 16  7 1.720E-03 16  8 3.403E-04 16  9 2.191E-02 16 10 8.807E-02
16 11 6.016E-02 16 12 4.443E-02 16 13 1.331E-01 16 14 1.157E-01 16 15 7.365E-02
16 16 3.836E-03 16 17 3.492E-03 16 18 4.125E-03 17  7 6.160E-04 17  9 6.856E-03
17 10 2.998E-02 17 11 3.679E-02 17 12 3.610E-02 17 13 1.144E-01 17 14 3.202E-02
17 15 5.362E-02 17 16 1.268E-01 17 17 1.735E-02 17 18 1.586E-03 17 19 2.835E-03
18  7 1.227E-04 18  8 4.722E-04 18  9 1.124E-03 18 10 4.144E-03 18 11 3.253E-02
18 12 3.762E-03 18 13 8.621E-02 18 14 6.917E-02 18 15 3.329E-02 18 16 4.071E-03
18 17 1.678E-01 18 18 5.230E-02 19  8 3.651E-04 19 10 7.526E-04 19 11 1.653E-02
19 12 6.207E-03 19 13 3.946E-02 19 14 3.596E-02 19 15 4.942E-02 19 16 1.820E-02
CROSS-SECTIONS ASSUMED TO BE THE SAME AS FOR X-B OF CRANDALL ETAL
2.052     2.589     3.884     5.179     6.473     9.709     12.95     19.42
2.950E-16 2.830E-16 2.380E-16 1.900E-16 1.550E-16 1.100E-16 0.890E-16 0.680E-16
0.
N2+JDI       2    4   14
 0  0 2.625E-06  0  2 3.782E-04  0  3 1.989E-03  0  4 7.451E-03  0  5 2.116E-02
 1  1 3.153E-04  1  2 2.208E-03  1  3 9.528E-03  1  4 2.820E-02  1  5 6.006E-02
 2  1 1.156E-03  2  2 6.808E-03  2  3 2.286E-02  2  4 5.450E-02  2  5 8.260E-02
 3  0 2.676E-04  3  1 2.992E-03  3  2 1.475E-02  3  3 4.141E-02  3  4 6.928E-02
 4  0 6.370E-04  4  1 6.138E-03  4  2 2.518E-02  4  3 5.561E-02  4  4 6.688E-02
 4  5 3.501E-02  5  0 1.282E-03  5  1 1.063E-02  5  2 3.603E-02  5  3 6.105E-02
 5  4 4.737E-02  5  5 7.281E-03  6  0 2.267E-03  6  1 1.617E-02  6  2 4.487E-02
 6  3 5.632E-02  6  4 2.363E-02  6  5 2.567E-04  7  0 3.621E-03  7  1 2.217E-02
 7  2 4.982E-02  7  3 4.401E-02  7  4 6.369E-03  7  5 9.586E-03  8  0 5.322E-03
 8  1 2.793E-02  8  2 5.016E-02  8  3 2.875E-02  8  4 5.422E-02  8  5 2.267E-02
 9  0 7.306E-03  9  1 3.282E-02  9  2 4.629E-02  9  3 1.493E-03  9  4 3.046E-03
 9  5 2.972E-02 10  0 9.470E-03 10  1 3.634E-02 10  2 3.939E-02 10  3 5.296E-03
10  4 1.062E-02 10  5 2.806E-02 11  0 1.169E-02 11  1 3.827E-02 11  2 3.098E-02
11  3 6.495E-04 11  4 1.808E-02 11  5 2.041E-02  0  1 4.563E-05  1  0 2.100E-05
CROSS-SECTIONS ASSUMED TO BE THE SAME AS FOR X-B OF CRANDALL ETAL
5.287     6.673     10.01     13.35     16.68     25.02     33.36     50.04
2.950E-16 2.830E-16 2.380E-16 1.900E-16 1.550E-16 1.100E-16 0.890E-16 0.680E-16
0.
N2+JDI       3    4   43
 0  7 1.400E-04  0  8 6.043E-04  0  9 7.837E-03  0 10 2.271E-02  0 11 5.541E-02
 0 12 1.799E-01  0 13 2.263E-01  0 14 1.314E-01  0 15 4.570E-02  1  6 2.347E-04
 1  7 9.487E-04  1  8 3.397E-03  1  9 2.759E-02  1 10 5.842E-02  1 11 9.454E-02
 1 12 6.349E-02  1 13 4.704E-03  1 14 1.817E-01  1 15 2.540E-01  1 16 1.953E-02
 1 17 4.728E-04  2  5 2.643E-04  2  6 1.016E-03  2  7 3.458E-03  2  8 1.021E-02
 2  9 5.059E-02  2 10 7.533E-02  2 11 7.295E-02  2 13 4.086E-02  2 14 1.873E-02
 2 15 4.644E-02  2 16 2.376E-01  2 17 1.340E-03  2 18 1.174E-03  3  4 2.611E-04
 3  5 9.672E-04  3  6 3.154E-03  3  7 8.963E-03  3  8 2.160E-02  3  9 6.202E-02
 3 10 5.959E-02  3 11 2.542E-02  3 12 2.943E-02  3 13 5.398E-02  3 14 2.494E-02
 3 15 7.028E-02  3 16 2.159E-01  3 17 4.280E-02  3 18 6.927E-03  3 19 1.089E-03
 4  3 2.491E-04  4  4 9.037E-04  4  5 2.846E-03  4  6 7.804E-03  4  7 1.832E-02
 4  8 3.544E-02  4  9 5.343E-02  4 10 2.664E-02  4 11 5.688E-04  4 12 4.220E-02
 4 13 1.237E-02  4 14 4.757E-02  4 15 2.575E-03  4 16 1.230E-02  4 17 3.780E-01
 4 18 3.457E-02  4 19 2.702E-04  5  2 2.367E-04  5  3 8.676E-04  5  4 2.671E-03
 5  5 7.086E-03  5  6 1.615E-02  5  7 3.080E-02  5  8 4.649E-02  5  9 2.979E-02
 5 10 3.001E-03  5 11 8.579E-03  5 12 1.775E-02  5 13 1.744E-03  5 14 1.063E-02
 5 15 1.880E-02  5 16 1.431E-02  5 17 1.539E-01  5 18 4.112E-01  5 19 3.821E-02
 6  1 2.178E-04  6  2 8.595E-04  6  3 2.654E-03  6  4 6.865E-03  6  5 1.516E-02
 6  6 2.822E-02  6  7 4.257E-02  6  8 4.771E-02  6  9 6.853E-03  6 10 2.828E-03
 6 11 2.488E-02  6 12 1.644E-04  6 13 1.976E-02  6 14 2.658E-03  6 15 3.042E-02
 6 16 3.599E-02  6 17 1.765E-02  6 18 1.712E-01  7  0 1.727E-04  7  1 8.435E-04
 7  2 2.765E-03  7  3 7.111E-03  7  4 1.526E-02  7  5 2.754E-02  7  6 4.079E-02
 7  7 4.643E-02  7  8 3.489E-02  7  9 3.820E-04  7 10 1.705E-02  7 11 2.399E-02
 7 12 8.803E-03  7 13 2.183E-02  7 14 1.994E-02  7 15 6.925E-03  7 16 7.100E-03
 7 17 9.588E-04  7 18 6.941E-03  7 19 3.421E-01  8  0 2.867E-03  8  1 8.360E-03
 8  2 1.825E-02  8  3 3.094E-02  8  4 4.274E-02  8  5 4.639E-02  8  6 3.593E-02
```

```
 8  7 1.472E-02  8  8 3.228E-04  8  9 2.106E-02  8 10 1.145E-02  8 11 1.462E-04
 8 12 1.049E-02  8 13 1.107E-03  8 14 9.045E-04  8 15 1.486E-02  8 16 1.706E-02
 8 17 1.621E-02  8 18 1.177E-02  8 19 7.529E-03  9  0 9.386E-03  9  1 2.003E-02
 9  2 3.486E-02  9  3 4.571E-02  9  4 4.740E-02  9  5 3.498E-02  9  6 1.414E-02
 9  7 4.308E-04  9  8 6.384E-03  9  9 1.362E-02  9 10 2.217E-04  9 11 9.246E-03
 9 12 1.145E-04  9 13 1.121E-02  9 14 5.186E-03  9 15 9.625E-03  9 16 7.202E-03
 9 17 3.854E-04  9 18 1.447E-02  9 19 1.089E-02 10  0 2.588E-02 10  1 3.808E-02
10  2 5.164E-02 10  3 4.874E-02 10  4 3.393E-02 10  5 1.229E-02 10  6 2.351E-04
10  7 6.373E-03 10  8 1.858E-02 10  9 1.047E-03 10 10 5.866E-03 10 11 1.372E-02
10 12 5.994E-03 10 13 9.979E-03 10 14 1.182E-02 10 16 4.727E-04 10 17 7.276E-03
10 18 7.282E-04 10 19 1.407E-02 11  0 1.113E-01 11  1 5.352E-02 11  2 3.960E-02
11  3 7.436E-03 11  5 9.672E-03 11  6 1.900E-02 11  7 1.508E-02 11  8 1.939E-03
11  9 1.243E-02 11 10 5.944E-03 11 11 6.697E-04 11 12 2.967E-03 11 13 3.581E-03
11 14 8.869E-04 11 15 8.174E-03 11 16 6.102E-03 11 17 5.154E-04 11 18 8.523E-03
12  0 1.993E-01 12  1 1.168E-03 12  2 4.138E-04 12  3 2.162E-02 12  4 1.619E-02
12  5 1.654E-02 12  6 6.967E-04 12  7 2.334E-03 12  8 1.279E-02 12 10 6.565E-03
12 11 6.843E-03 12 12 6.989E-03 12 13 2.334E-03 12 14 4.345E-03 12 15 2.758E-03
CROSS-SECTIONS ASSUMEDTO BE THE SAME AS FOR X-B OF CRANDALL ET AL
3.235      4.083      6.125      8.166      10.21      15.31      20.42      30.62
2.950E-16 2.830E-16 2.380E-16 1.900E-16 1.550E-16 1.100E-16 0.890E-16 0.680E-16
0.
N2           28.010    4    6    5    4
1.0        0.         2358.027   14.1351 -1.751E-02-1.144E-04 1.9980     1.772E-02
3.0        49754.8    1460.518   13.8313  5.999E-03 1.853E-03 1.45455    1.801E-02
6.0        59306.8    1733.391   14.1221 -5.688E-02-3.612E-03 1.6374     1.791E-02
2.0        68951.2    1694.208   13.9491  7.935E-03-2.911E-04 1.61688    1.793E-02
6.0        88977.9    2047.178   28.4450  2.08833   0.5350    1.82473    1.868E-02
N  4S      1.401E+01 7.872E+04 4.000E+00 1.500E+00 0.000E+00
N  4S      1.401E+01 7.872E+04 4.000E+00 1.500E+00 0.000E+00
CROSS-SECTIONS ASSUMED SAME AS FOR N2 1-3 OF CARTWRIGHT ET AL
78734.
9.7594     10.618     13.27      15.93      19.91      26.55      34.51      47.78
0.         0.054E-16 0.225E-16 0.299E-16 0.241E-16 0.156E-16 0.120E-16 0.076E-16
CROSS-SECTIONS ASSUMED SAME AS FOR N2 1-3 OF CARTWRIGHT ET AL
78734.
3.591      3.907      4.884      5.860      7.325      9.767      12.70      17.58
0.         0.054E-16 0.225E-16 0.299E-16 0.241E-16 0.156E-16 0.120E-16 0.076E-16
CROSS-SECTIONS ASSUMED SAME AS FOR N2 1-3 OF CARTWRIGHT ET AL
107559.
5.981      6.506      8.134      9.762      12.20      16.27      21.15      29.28
0.         0.054E-16 0.225E-16 0.299E-16 0.241E-16 0.156E-16 0.120E-16 0.076E-16
CROSS-SECTIONS ASSUMED SAME AS FOR N2 1-3 OF CARTWRIGHT ET AL
126787.
7.169      7.802      9.750      11.70      14.62      19.50      25.35      35.10
0.         0.054E-16 0.225E-16 0.299E-16 0.241E-16 0.156E-16 0.120E-16 0.076E-16
N2 VK        1    2   72
 0  0 5.900E-04  0  1 5.337E-03  0  2 2.286E-02  0  3 6.167E-02  0  4 1.176E-01
 0  5 1.688E-01  0  6 1.894E-01  0  7 1.704E-02  0  8 1.250E-01  0  9 7.578E-02
 0 10 3.828E-02  0 11 1.621E-02  0 12 5.780E-03  0 13 1.738E-03  0 14 4.411E-04
 1  0 3.319E-03  1  1 2.278E-02  1  2 6.919E-02  1  3 1.193E-01  1  4 1.216E-01
 1  5 6.383E-02  1  6 6.256E-03  1  7 1.395E-02  1  8 7.866E-02  1  9 1.370E-01
 1 10 1.450E-01  1 11 1.100E-01  1 12 6.404E-02  1 13 2.963E-02  1 14 1.110E-02
 2  0 9.975E-03  2  1 5.085E-02  2  2 1.035E-01  2  3 9.732E-02  2  4 2.922E-02
 2  5 2.161E-03  2  6 5.473E-02  2  7 8.924E-02  2  8 4.616E-02  2  9 8.840E-04
 2 10 2.955E-02  2 11 1.001E-01  2 12 1.378E-01  2 13 1.196E-01  2 14 7.472E-02
 3  0 2.133E-02  3  1 7.850E-02  3  2 9.768E-02  3  3 3.326E-02  3  4 2.589E-03
 3  5 5.617E-02  3  6 6.391E-02  3  7 8.564E-03  3  8 1.697E-02  3  9 7.318E-02
 3 10 6.181E-02  3 11 7.600E-03  3 12 1.520E-02  3 13 8.383E-02  3 14 1.315E-01
 4  0 3.642E-02  4  1 9.328E-02  4  2 5.998E-02  4  3 3.714E-04  4  4 4.107E-02
 4  5 5.758E-02  4  6 4.625E-03  4  7 2.554E-02  4  8 6.331E-02  4  9 1.916E-02
 4 10 7.127E-03  4 11 6.276E-02  4 12 6.314E-02  4 13 9.383E-03  4 14 1.379E-02
 5  0 5.290E-02  5  1 8.962E-02  5  2 2.011E-02  5  3 1.465E-02  5  4 5.868E-02
 5  5 1.223E-02  5  6 1.688E-02  5  7 5.462E-02  5  8 1.065E-02  5  9 1.643E-02
 5 10 5.871E-02  5 11 2.016E-02  5 12 6.585E-03  5 13 6.143E-02  5 14 5.832E-02
 6  0 6.799E-02  6  1 7.082E-02  6  2 8.381E-04  6  3 4.233E-02  6  4 3.400E-02
```

```
 6  5 2.630E-03  6  6 4.768E-02  6  7 1.641E-02  6  8 1.163E-02  6  9 5.008E-02
 6 10 9.734E-03  6 11 1.729E-02  6 12 5.579E-02  6 13 1.457E-02  6 14 1.131E-02
 7  0 7.939E-02  7  1 4.539E-02  7  2 5.264E-03  7  3 5.154E-02  7  4 5.402E-03
 7  5 2.805E-02  7  6 3.237E-02  7  7 1.710E-03  7  8 4.308E-02  7  9 1.308E-02
 7 10 1.409E-02  7 11 4.635E-02  7 12 4.785E-02  7 13 2.447E-02  7 14 5.170E-02
 8  0 8.588E-02  8  1 2.205E-02  8  2 2.231E-02  8  3 3.803E-02  8  4 1.933E-03
 8  5 4.203E-02  8  6 4.185E-03  8  7 2.701E-02  8  8 2.572E-02  8  9 4.073E-03
 8 10 4.148E-02  8 11 6.297E-03  8 12 2.185E-02  8 13 4.002E-02  8 14 3.600E-04
 9  0 8.730E-02  9  1 6.435E-03  9  2 3.838E-02  9  3 1.651E-02  9  4 1.815E-02
 9  5 2.890E-02  9  6 3.763E-03  9  7 3.696E-02  9  8 8.855E-04  9  9 3.109E-02
 9 10 1.592E-02  9 11 1.083E-02  9 12 3.765E-02  9 13 6.326E-04  9 14 3.284E-02
10  0 8.434E-02 10  1 2.053E-04 10  2 4.527E-02 10  3 2.254E-03 10  4 3.349E-02
10  5 8.054E-03 10  6 2.242E-02 10  7 1.837E-02 10  8 9.744E-03 10  9 3.026E-02
10 10 5.291E-04 10 11 3.475E-02 10 12 5.380E-03 10 13 2.218E-02 10 14 2.757E-02
11  0 7.812E-02 11  1 2.015E-03 11  2 4.180E-02 11  3 9.890E-04 11  4 3.530E-02
11  5 1.684E-05 11  6 3.257E-02 11  7 1.243E-03 11  8 2.835E-02 11  9 7.166E-02
11 10 1.963E-02 11 11 1.892E-02 11 12 7.224E-03 11 13 3.197E-02 11 14 5.829E-06
12  0 6.988E-02 12  1 9.015E-03 12  2 3.141E-02 12  3 9.423E-03 12  4 2.493E-02
12  5 7.426E-03 12  6 2.478E-02 12  7 4.205E-03 12  8 2.719E-02 12  9 9.855E-04
12 10 2.962E-02 12 11 2.597E-04 12 12 2.853E-02 12 13 5.872E-03 12 14 2.016E-02
13  0 6.071E-02 13  1 1.817E-02 13  2 1.899E-02 13  3 2.061E-02 13  4 1.116E-02
13  5 2.003E-02 13  6 9.630E-03 13  7 1.809E-02 13  8 1.114E-02 13  9 1.477E-02
13 10 1.519E-02 13 11 9.782E-03 13 12 2.152E-02 13 13 3.791E-03 13 14 2.831E-04
14  0 5.149E-02 14  1 2.707E-02 14  2 8.494E-03 14  3 2.870E-02 14  4 1.925E-03
14  5 2.732E-02 14  6 5.698E-04 14  7 2.605E-02 14  8 4.334E-04 14  9 2.527E-02
14 10 9.608E-04 14 11 2.437E-02 14 12 2.827E-03 14 13 2.209E-02 14 14 7.438E-03
15  0 4.280E-02 15  1 3.418E-02 15  2 2.038E-03 15  3 3.106E-02 15  4 2.871E-04
15  5 2.560E-02 15  6 2.212E-03 15  7 2.191E-02 15  8 3.623E-03 15  9 2.041E-02
15 10 3.825E-03 15 11 2.086E-02 15 12 2.852E-03 15 13 2.288E-02 15 14 1.148E-03
 2 15 3.567E-02  2 16 1.342E-02  2 17 4.046E-03  3 15 1.197E-01  3 16 7.543E-02
 3 17 3.543E-02  3 18 1.287E-02  3 19 3.690E-03  4 15 8.294E-02  4 16 1.299E-01
 4 17 1.152E-01  4 18 6.961E-02  4 19 3.095E-02  5 15 5.905E-03  5 16 1.982E-02
 5 17 9.210E-02  5 18 1.304E-01  5 19 1.066E-01  6 15 6.531E-02  6 16 4.826E-02
 6 17 1.141E-03  6 18 3.366E-02  6 19 1.068E-01  6 20 1.289E-01  5 20 5.938E-02
 6 21 9.341E-02  6 22 4.662E-02  6 23 1.704E-02  6 24 4.706E-03  7 20 5.591E-02
 7 15 6.143E-03  7 16 2.227E-02  7 17 6.887E-02  7 18 3.475E-02  7 21 1.216E-01
 7 22 1.217E-01  7 23 7.625E-02  7 24 3.334E-02  7 25 1.070E-02  8 15 3.610E-03
 8 16 4.227E-02  8 18 3.936E-02  8 19 6.567E-02  8 20 1.463E-02  8 21 1.114E-02
 8 22 8.420E-02  8 23 1.305E-01  8 24 1.069E-01  8 25 5.701E-02  8 26 2.147E-02
 9 15 2.810E-02  9 16 2.261E-03  9 17 4.748E-02  9 18 2.603E-02  9 19 3.787E-03
 9 20 5.775E-02  9 21 5.110E-02  9 22 1.516E-03  9 23 3.563E-02  9 24 1.120E-01
 9 25 1.284E-01  9 26 8.575E-02  9 27 3.813E-02 10 15 1.944E-03 10 16 4.137E-02
10 17 1.221E-02 10 18 1.464E-02 10 19 5.044E-02 10 21 2.086E-02 10 22 6.749E-02
10 23 2.717E-02 10 25 7.141E-02 10 26 1.302E-01 10 27 1.136E-01 11 15 3.333E-02
11 16 1.235E-02 11 17 1.382E-02 11 18 3.941E-02 11 20 3.440E-02 11 21 3.862E-02
11 23 4.661E-02 11 24 5.915E-02 11 26 2.730E-02 11 27 1.082E-01 12 15 1.998E-02
12 16 6.000E-03 12 17 3.526E-02 12 19 3.137E-02 12 20 2.308E-02 12 22 4.881E-02
12 23 1.619E-02 12 24 1.223E-02 12 25 6.568E-02 12 26 3.347E-02 13 16 3.060E-02
13 18 2.180E-02 13 19 2.293E-02 13 21 4.054E-02 13 23 2.521E-02 13 24 4.374E-02
13 26 4.106E-02 13 27 6.174E-02 14 15 1.686E-02 14 16 1.609E-02 14 18 2.250E-02
14 20 3.395E-02 14 22 2.305E-02 14 23 3.004E-02 14 25 4.613E-02 14 26 2.015E-02
15 15 2.563E-02 15 17 2.719E-02 15 19 2.415E-02 15 20 1.140E-02 15 21 1.370E-02
15 22 2.799E-02 15 24 3.891E-02 15 26 2.121E-02 15 27 4.501E-02 16 21 2.925E-02
CROSS-SECTIONS FROM CARTWRIGHT
6.1693     7.          9.         11.         14.         17.         20.         26.
0.          0.030E-16 0.094E-16 0.148E-16 0.204E-16 0.225E-16 0.183E-16 0.113E-16
0.
N2  BX        1    3   28
 0  0 6.117E-02  0  1 1.909E-01  0  2 2.753E-01  0  3 2.416E-01  0  4 1.442E-01
 0  5 6.185E-02  0  6 1.953E-02  0  7 4.555E-03  0  8 7.694E-04  1  0 1.487E-01
 1  1 1.921E-01  1  2 4.450E-02  1  3 1.658E-02  1  4 1.444E-01  1  5 2.072E-01
 1  6 1.509E-01  1  7 6.917E-02  1  8 2.138E-02  1  9 4.492E-03  1 10 6.123E-04
 2  0 1.999E-01  2  1 6.307E-02  2  2 2.445E-02  2  3 1.293E-01  2  4 4.565E-02
 2  5 1.167E-02  2  6 1.314E-01  2  7 1.908E-01  2  8 1.322E-01  2  9 5.475E-02
 2 10 1.434E-02  2 11 1.996E-04  3  0 1.969E-01  3  1 1.978E-04  3  2 1.039E-01
```

```
 3  3 3.337E-02  3  4 3.276E-02  3  5 1.086E-01  3  6 2.046E-02  3  7 3.142E-02
 3  8 1.547E-01  3  9 1.769E-01  3 10 1.006E-01  3 11 6.368E-03  3 12 6.241E-04
 4  0 1.585E-01  4  1 3.398E-02  4  2 7.628E-02  4  3 9.215E-03  4  4 8.940E-02
 4  5 4.742E-03  4  6 6.269E-02  4  7 8.009E-02  4  8 5.373E-04  4  9 7.885E-02
 4 10 1.807E-01  4 11 6.192E-02  4 12 1.426E-02  4 13 1.602E-03  5  0 1.099E-01
 5  1 9.570E-02  5  2 1.173E-02  5  3 6.681E-02  5  4 1.986E-02  5  5 4.484E-02
 5  6 5.414E-02  5  7 5.903E-03  5  8 8.773E-02  5  9 3.286E-02  5 10 1.764E-02
 5 11 1.796E-01  5 12 9.843E-02  5 13 2.745E-02  5 14 3.571E-03  6  0 6.681E-02
 6  1 1.298E-01  6  2 7.534E-03  6  3 6.134E-02  6  4 8.044E-03  6  5 6.331E-02
 6  6 1.317E-03  6  7 6.981E-02  6  8 9.108E-03  6  9 4.561E-02  6 10 7.154E-02
 6 11 8.608E-02  6 12 1.876E-01  6 13 1.375E-01  6 14 4.692E-02  6 15 2.910E-04
 7  0 3.542E-02  7  1 1.236E-01  7  2 6.025E-02  7  3 1.155E-02  7  4 5.031E-02
 7  5 8.094E-03  7  6 5.130E-02  7  7 1.502E-02  7  8 3.624E-02  7  9 4.307E-02
 7 10 7.110E-03  7 11 1.956E-02  7 12 3.391E-02  7 13 1.690E-01  7 14 1.718E-01
 7 15 1.304E-02  7 16 6.258E-04  8  0 1.578E-02  8  1 9.080E-02  8  2 1.133E-01
 8  3 7.048E-03  8  4 4.075E-02  8  5 1.139E-02  8  6 4.011E-02  8  7 1.422E-02
 8  8 4.374E-02  8  9 4.418E-03  8 10 5.827E-02  8 11 5.267E-02  8 12 4.908E-02
 8 13 4.720E-03  8 14 1.308E-01  8 15 1.030E-01  8 16 2.201E-02  8 17 1.265E-03
 9  0 5.388E-03  9  1 5.162E-02  9  2 1.249E-01  9  3 6.428E-02  9  4 2.636E-03
 9  5 3.857E-02  9  6 8.992E-04  9  7 5.011E-02  9  9 4.652E-02  9 10 3.142E-03
 9 11 2.077E-02  9 12 2.099E-02  9 13 6.614E-02  9 14 1.418E-03  9 15 2.013E-01
CROSS-SECTIONS FROM CARTWRIGHT
7.3529     8.          10.         12.         15.         20.         26          36.
0.          0.054E-16 0.225E-16 0.299E-16 0.241E-16 0.156E-16 0.120E-16 0.076E-16
0.
N2 LBH        1    4   38
 0  0 4.315E-02  1  0 1.162E-01  2  0 1.713E-01  3  0 1.835E-01  4  0 1.603E-01
 5  0 1.214E-01  6  0 8.287E-02  7  0 5.230E-02  8  0 3.109E-02  9  0 1.764E-02
10  0 9.661E-03 11  0 5.146E-03 12  0 2.684E-03 13  0 1.378E-03  0  1 1.517E-01
 1  1 1.932E-01  2  1 9.677E-02  3  1 1.212E-02  4  1 6.391E-03  5  1 4.706E-02
 6  1 8.542E-02  7  1 9.971E-02  8  1 9.216E-02  9  1 7.346E-02 10  1 5.285E-02
11  1 3.530E-02 12  1 2.230E-02 13  1 1.350E-02 14  1 7.917E-03  0  2 2.477E-01
 1  2 8.049E-02  2  2 3.276E-03  3  2 7.554E-02  4  2 9.661E-02  5  2 4.668E-02
 6  2 4.538E-03  7  2 5.796E-03  8  2 3.372E-02  9  2 6.105E-02 10  2 7.378E-02
11  2 7.163E-02 12  2 6.044E-02 13  2 4.625E-02 14  2 3.296E-02  0  3 2.492E-01
 2  3 1.074E-01  3  3 6.931E-02  4  3 5.812E-04  5  3 3.392E-02  6  3 7.289E-02
 7  3 5.658E-02  8  3 1.826E-02  9  3 1.314E-04 10  3 9.747E-03 11  3 3.200E-02
12  3 5.101E-02 13  3 5.954E-02 14  3 5.797E-02  0  4 1.731E-01  1  4 8.732E-02
 2  4 8.598E-02  3  4 3.606E-03  4  4 7.744E-02  5  4 5.670E-02  6  4 2.795E-03
 7  4 1.717E-02  8  4 5.340E-02  9  4 5.485E-02 10  4 2.795E-02 11  4 4.549E-03
12  4 1.158E-03 13  4 1.398E-02 14  4 3.142E-02  0  5 8.808E-02  1  5 1.851E-01
 3  5 9.511E-02  4  5 3.735E-02  5  5 8.364E-03  6  5 6.347E-02  7  5 4.694E-02
 8  5 4.209E-03  9  5 9.234E-03 10  5 3.918E-02 11  5 4.918E-02 12  5 3.299E-02
13  5 1.091E-02 14  5 2.538E-04  0  6 3.399E-02  1  6 1.752E-01  2  6 6.451E-02
 3  6 6.580E-02  4  6 1.689E-02  5  6 7.882E-02  6  6 1.485E-02  7  6 1.278E-02
11  6 4.904E-03 12  6 2.860E-02 13  6 4.237E-02 14  6 3.472E-02  0  7 1.017E-02
 1  7 1.032E-01  2  7 1.640E-01  4  7 9.667E-02  5  7 7.912E-03  6  7 4.042E-02
 7  7 5.731E-02  8  7 4.748E-03  9  7 1.587E-02 10  7 4.743E-02 11  7 3.446E-02
12  7 5.828E-03 13  7 2.321E-03 14  7 2.040E-02  0  8 2.392E-03  1  8 4.250E-02
 2  8 1.614E-01  3  8 7.840E-02  4  8 3.615E-02  5  8 4.675E-02  6  8 5.502E-02
 7  8 1.040E-03  8  8 5.031E-02  9  8 3.869E-02 11  8 1.742E-02 12  8 4.169E-02
13  8 3.071E-02 14  8 6.695E-03  0  9 4.454E-04  1  9 1.289E-02  2  9 9.406E-02
 3  9 1.632E-01  4  9 9.168E-03  5  9 8.536E-02  6  9 2.010E-03  7  9 6.765E-02
 8  9 1.751E-02  9  9 1.174E-02 10  9 4.934E-02 11  9 2.518E-02 13  9 1.758E-02
14  9 3.680E-02  1 10 2.968E-03  2 10 3.718E-02  3 10 1.431E-01  4 10 1.085E-01
 5 10 7.958E-03  6 10 7.874E-02  7 10 1.538E-02  8 10 3.144E-02  9 10 5.074E-02
10 10 1.843E-03 11 10 2.257E-02 12 10 4.332E-02 13 10 1.638E-02  1 11 5.266E-04
 2 11 1.060E-02  3 11 7.518E-02  4 11 1.626E-01  5 11 3.911E-02  6 11 5.144E-02
 7 11 3.210E-02  8 11 5.359E-02  9 11 1.246E-03 10 11 4.905E-02 11 11 2.698E-02
13 11 2.865E-02 14 11 3.626E-02  2 12 2.253E-03  3 12 2.675E-02  4 12 1.179E-01
 5 12 1.402E-01  6 12 1.628E-03  7 12 8.354E-02  8 12 1.043E-03  9 12 6.308E-02
10 12 1.151E-02 11 12 1.839E-02 12 12 4.567E-02 13 12 1.068E-02 14 12 4.524E-03
 3 13 6.824E-03  4 13 5.304E-02  5 13 1.499E-01  6 13 8.717E-02  7 13 1.195E-02
 8 13 7.317E-02  9 13 1.239E-02 10 13 3.555E-02 11 13 4.096E-02 13 13 3.303E-02
CROSS-SECTIONS FROM CARTWRIGHT
```

```
8.5489    9.        11.       13.       15.       18.       22.       30.
0.        0.019E-16 0.099E-16 0.180E-16 0.256E-16 0.297E-16 0.258E-16 0.204E-16
5880.
N2 1+        2    3   36
 0  0 3.382E-01  1  0 4.065E-01  2  0 1.975E-01  3  0 5.014E-02  4  0 7.191E-03
 5  0 5.871E-04  6  0 2.616E-05  0  1 3.248E-01  1  1 2.310E-03  2  1 2.120E-01
 3  1 2.987E-01  4  1 1.318E-01  5  1 2.729E-02  6  1 2.925E-03  7  1 1.613E-04
 0  2 1.900E-01  1  2 1.032E-01  2  2 1.132E-01  3  2 3.868E-02  4  2 2.738E-01
 5  2 2.107E-01  6  2 6.148E-02  7  2 8.462E-03  8  2 5.675E-04  9  2 1.719E-05
 0  3 8.857E-02  1  3 1.782E-01  2  3 1.205E-03  3  3 1.623E-01  4  3 1.807E-03
 5  3 1.808E-01  6  3 2.605E-01  7  3 1.065E-01  8  3 1.857E-02  9  3 1.495E-03
10  3 5.241E-05  0  4 3.649E-02  1  4 1.450E-01  2  4 7.724E-02  3  4 3.227E-02
 4  4 1.139E-01  5  4 4.780E-02  6  4 8.305E-02  7  4 2.706E-01  8  4 1.561E-01
 9  4 3.420E-02 10  4 3.274E-03 11  4 1.318E-04  0  5 1.399E-02  1  5 8.647E-02
 2  5 1.275E-01  3  5 9.050E-03  4  5 8.823E-02  5  5 4.262E-02  6  5 1.040E-01
 7  5 1.916E-02  8  5 2.438E-01  9  5 2.029E-01 10  5 5.569E-02 11  5 6.299E-03
12  5 2.890E-04  0  6 5.147E-03  1  6 4.367E-02  2  6 1.127E-01  3  6 6.910E-02
 4  6 5.227E-03  5  6 1.057E-01  6  6 3.171E-03  7  6 1.291E-01  8  6 2.766E-05
 9  6 1.919E-01 10  6 2.402E-01 11  6 8.265E-02 12  6 1.099E-02 13  6 5.717E-04
 0  7 1.851E-03  1  7 2.000E-02  2  7 7.496E-02  3  7 1.009E-01  4  7 1.798E-02
 5  7 3.829E-02  6  7 8.078E-02  7  7 6.748E-03  8  7 1.159E-01  9  7 1.694E-02
10  7 1.299E-01 11  7 2.630E-01 12  7 1.140E-01 13  7 1.777E-02 14  7 1.044E-03
 4  8 6.361E-02  6  8 6.967E-02  7  8 3.946E-02  8  8 3.633E-02  9  8 7.862E-02
10  8 5.219E-02 11  8 7.206E-02 12  8 2.688E-01 13  8 1.480E-01 14  8 2.702E-02
15  8 1.785E-03 16  8 3.480E-05  0  9 2.348E-04  1  9 3.589E-03  2  9 2.182E-02
 3  9 6.406E-02  4  9 8.349E-02  5  9 2.454E-02  6  9 1.289E-02  7  9 7.733E-02
 8  9 8.360E-03  9  9 6.773E-02 10  9 3.765E-02 11  9 8.779E-02 12  9 2.857E-02
13  9 2.575E-01 14  9 1.826E-01 15  9 3.902E-02 16  9 2.893E-03 17  9 6.131E-05
 0 10 8.403E-05  1 10 1.463E-03  2 10 1.053E-02  3 10 3.917E-02  4 10 7.511E-02
 5 10 5.820E-02  6 10 2.460E-03  7 10 3.833E-02  8 10 6.077E-02  9 10 3.194E-04
10 10 8.370E-02 11 10 9.012E-03 12 10 1.109E-01 13 10 4.687E-03 14 10 2.315E-01
15 10 2.154E-01 16 10 5.395E-02 17 10 4.480E-03 18 10 1.089E-04  0 11 3.038E-05
 1 11 5.907E-04  2 11 4.885E-03  3 11 2.187E-02  4 11 5.510E-02  5 11 7.056E-02
 6 11 2.810E-02  7 11 2.738E-03  8 11 5.721E-02  9 11 3.305E-02 10 11 1.307E-02
11 11 7.897E-02 12 11 2.617E-05 13 11 1.156E-01 14 11 7.733E-04 15 11 1.945E-01
16 11 2.443E-01 17 11 7.185E-02 18 11 6.675E-03 19 11 1.658E-04  0 12 1.114E-05
 1 12 2.380E-04  2 12 2.212E-03  3 12 1.151E-02  4 12 3.567E-02  5 12 6.338E-02
 6 12 5.261E-02  7 12 6.400E-03  8 12 1.852E-02  9 12 5.945E-02 10 12 9.576E-03
11 12 3.527E-02 12 12 5.846E-02 13 12 9.342E-03 14 12 1.029E-01 15 12 1.330E-02
16 12 1.516E-01 17 12 2.672E-01 18 12 9.261E-02 19 12 9.615E-03  1 13 9.627E-05
CROSS-SECTIONS ASSUMED SAME AS B-X OF CARTWRIGHT
1.1842    1.288     1.611     1.933     2.416     3.221     4.187     5.798
0.        0.054E-16 0.225E-16 0.299E-16 0.241E-16 0.156E-16 0.120E-16 0.076E-16
9.000E+04
N2 A1A       2    4   24
 0  0 7.827E-01  0  1 1.791E-01  0  2 3.059E-02  0  3 5.717E-03  0  4 5.717E-03
 0  5 1.303E-03  0  6 3.656E-04  0  7 1.238E-04  1  0 7.827E-01  1  1 1.791E-01
 1  2 3.059E-02  1  3 5.717E-03  1  4 5.717E-03  1  5 1.303E-03  1  6 3.656E-04
 1  7 1.238E-04  2  0 2.095E-01  2  1 5.035E-01  2  2 2.184E-01  2  3 5.205E-02
 2  4 5.205E-02  2  5 1.196E-02  2  6 3.080E-03  2  7 9.274E-04  2  8 3.263E-04
 2  9 3.263E-04  2 10 1.320E-04  3  0 7.735E-03  3  1 3.024E-01  3  2 3.595E-01
 3  3 2.312E-01  3  4 2.312E-01  3  5 7.099E-02  3  6 1.943E-02  3  7 5.626E-03
 3  8 1.826E-03  3  9 1.826E-03  3 10 6.737E-04  3 11 2.808E-04  3 12 1.305E-04
 4  0 7.735E-03  4  1 3.024E-01  4  2 3.595E-01  4  3 2.312E-01  4  4 2.312E-01
 4  5 7.099E-02  4  6 1.943E-02  4  7 5.626E-03  4  8 1.826E-03  4  9 1.826E-03
 4 10 6.737E-04  4 11 2.808E-04  4 12 1.305E-04  5  0 1.179E-04  5  1 1.479E-02
 5  2 3.693E-01  5  3 2.594E-01  5  4 2.594E-01  5  5 2.276E-01  5  6 8.641E-02
 5  7 2.778E-02  5  8 9.051E-03  5  9 9.051E-03  5 10 3.194E-03  5 11 1.248E-03
 5 12 5.408E-04  5 13 2.581E-04  6  1 1.910E-04  6  2 2.198E-02  6  3 4.228E-01
 6  4 4.228E-01  6  5 1.870E-01  6  6 2.121E-01  6  7 9.699E-02  6  8 3.623E-02
 6  9 3.623E-02  6 10 1.328E-02  6 11 5.125E-03  6 12 2.139E-03  6 13 9.724E-04
 6 14 2.558E-04  7  1 1.910E-04  7  2 2.198E-02  7  3 4.228E-01  7  4 4.228E-01
 7  5 1.870E-01  7  6 2.121E-01  7  7 9.699E-02  7  8 3.623E-02  7  9 3.623E-02
 7 10 1.328E-02  7 11 5.125E-03  7 12 2.139E-03  7 13 9.724E-04  7 14 2.558E-04
 8  2 1.834E-04  8  3 2.866E-02  8  4 2.866E-02  8  5 4.674E-01  8  6 1.355E-01
```

```
 8  7 1.896E-01  8  8 1.020E-01  8  9 1.020E-01  8 10 4.380E-02  8 11 1.803E-02
 8 12 7.629E-03  8 13 3.421E-03  8 14 8.450E-04  9  3 1.027E-04  9  4 1.027E-04
 9  5 3.385E-02  9  6 5.061E-01  9  7 9.970E-02  9  8 1.642E-01  9  9 1.642E-01
 9 10 1.016E-01  9 11 4.959E-02  9 12 2.280E-02  9 13 1.058E-02  9 14 2.605E-03
CROSS-SECTIONS ASSUMED SAME AS B-X OF CARTWRIGHT
2.3799     2.589      3.237      3.884      4.885      6.473      8.415      11.65
0.         0.054E-16 0.225E-16 0.299E-16 0.241E-16 0.156E-16 0.120E-16 0.076E-16
0.0
N2 A1B        3    4   11
 0  0 2.005E-03  0  1 9.979E-01  0  2 2.005E-03  1  0 2.005E-03  1  1 9.979E-01
 1  2 2.005E-03  2  0 9.942E-01  2  1 1.966E-03  2  2 9.942E-01  2  3 3.781E-03
 2  4 3.781E-03  3  0 3.652E-03  3  2 3.652E-03  3  3 9.907E-01  3  4 9.907E-01
 3  5 5.449E-03  3  6 1.042E-04  3  7 1.042E-04  4  0 3.652E-03  4  2 3.652E-03
 4  3 9.907E-01  4  4 9.907E-01  4  5 5.449E-03  4  6 1.042E-04  4  7 1.042E-04
 5  0 1.335E-04  5  2 1.335E-04  5  3 5.189E-03  5  4 5.189E-03  5  5 9.875E-01
 5  6 6.927E-03  5  7 6.927E-03  5  8 1.787E-04  6  3 2.431E-04  6  4 2.431E-04
 6  5 6.497E-03  6  6 9.848E-01  6  7 9.848E-01  6  8 8.129E-03  6  9 2.877E-04
 7  3 2.431E-04  7  4 2.431E-04  7  5 6.497E-03  7  6 9.848E-01  7  7 9.848E-01
 7  8 8.129E-03  7  9 2.877E-04  8  5 3.900E-04  8  6 7.497E-03  8  7 7.497E-03
 8  8 9.826E-01  8  9 8.985E-03  9  6 5.732E-04  9  7 5.732E-04  9  8 8.135E-03
CROSS-SECTION ASSUMED SAME AS B-X OF CARTWRIGHT
1.1956     1.301      1.626      1.951      2.439      3.252      4.228      5.854
0.         0.054E-16 0.225E-16 0.299E-16 0.241E-16 0.156E-16 0.120E-16 0.076E-16
0.
NO           30.010    3    3    6    3    0
    4.000     60.550  1903.855    13.970    -0.001     0.000   1.70460 1.780E-02
    2.000 43965.699   2371.300    14.480    -0.280     0.000   1.99520 1.640E-02
    4.000 45932.398   1037.680     7.603     0.097     0.000   1.12700 1.525E-02
    2.000 52148.000   2347.000     0.000     0.000     0.000   1.95500 0.000E+00
    2.000 53083.000   2327.000    23.000     0.000     0.000   1.99170 0.000E+00
    2.000 60628.500   2373.600    15.850     0.000     0.000   1.98630 1.820E-02
N  4S      1.401E+01 5.249E+04 4.000E+00 1.500E+00 0.000E+00
O  3P      1.600E+01 5.249E+04 9.000E+00 1.000E+00 1.000E+00
CROSS-SECTIONS ASSUMED AS SAME FOR NO 1-2 OF IMAMI ET AL
52490.
6.508      6.775      7.875      10.15      13.54      18.09      22.58      28.24
0.000E 00 3.370E-18 1.540E-17 2.450E-17 2.980E-17 3.030E-17 2.870E-17 2.700E-17
CROSS-SECTIONS ASSUMED AS SAME FOR NO 1-2 OF IMAMI ET AL
71718.
3.440      3.581      4.162      5.365      7.156      9.562      11.94      14.93
0.000E 00 3.370E-18 1.540E-17 2.450E-17 2.980E-17 3.030E-17 2.870E-17 2.700E-17
CROSS-SECTIONS ASSUMED AS SAME FOR NO 1-2 OF IMAMI ET AL
71718.
3.196      3.327      3.868      4.988      6.646      8.887      11.09      13.87
0.000E 00 3.370E-18 1.540E-17 2.450E-17 2.980E-17 3.030E-17 2.870E-17 2.700E-17
NO B          1    3   46
 3  0 1.000E-03  4  0 3.000E-03  5  0 5.000E-03  6  0 1.100E-02  7  0 1.700E-02
 8  0 2.200E-02  9  0 2.900E-02 10  0 3.200E-02 11  0 4.100E-02 12  0 5.100E-02
 1  1 1.000E-03  2  1 4.000E-03  3  1 9.000E-03  4  1 1.700E-02  5  1 3.200E-02
 6  1 4.400E-02  7  1 5.900E-02  8  1 5.800E-02  9  1 6.000E-02 10  1 5.700E-02
11  1 4.800E-02 12  1 3.400E-02  0  2 1.000E-03  1  2 6.000E-03  2  2 1.800E-02
 3  2 3.800E-02  4  2 5.400E-02  5  2 6.900E-02  6  2 7.000E-02  7  2 5.300E-02
 8  2 3.600E-02  9  2 1.900E-02 10  2 8.000E-03 11  2 1.000E-03 12  2 3.000E-03
 0  3 5.000E-03  1  3 2.400E-02  2  3 4.800E-02  3  3 7.600E-02  4  3 7.600E-02
 5  3 5.700E-02  6  3 3.200E-02  7  3 7.000E-03  9  3 1.400E-02 10  3 2.000E-02
11  3 3.100E-02 12  3 3.800E-02  0  4 1.700E-02  1  4 5.100E-02  2  4 8.500E-02
 3  4 8.400E-02  4  4 4.300E-02  5  4 6.000E-03  6  4 1.000E-03  7  4 2.400E-02
 8  4 3.400E-02  9  4 4.200E-02 10  4 3.400E-02 11  4 2.000E-02 12  4 1.000E-03
 0  5 4.100E-02  1  5 9.700E-02  2  5 9.200E-02  3  5 3.800E-02  4  5 1.000E-03
 5  5 1.200E-02  6  5 3.800E-02  7  5 4.600E-02  8  5 2.700E-02  9  5 6.000E-03
11  5 5.000E-03 12  5 2.600E-02  0  6 8.200E-02  1  6 1.170E-01  2  6 4.700E-02
 4  6 3.000E-02  5  6 5.300E-02  6  6 3.500E-02  7  6 5.000E-03  8  6 2.000E-03
 9  6 1.800E-02 10  6 3.200E-02 11  6 3.100E-02 12  6 1.100E-02  0  7 1.250E-01
 1  7 8.800E-02  2  7 2.000E-03  3  7 3.300E-02  4  7 6.000E-02  5  7 2.400E-02
 7  7 2.300E-02  8  7 3.800E-02  9  7 3.100E-02 10  7 1.000E-02 12  7 1.300E-02
```

```
 1  8 2.900E-02  2  8 2.100E-02  3  8 6.800E-02  4  8 2.100E-02  5  8 4.000E-03
 6  8 3.100E-02  7  8 3.600E-02  8  8 1.400E-02 10  8 1.400E-02 11  8 2.800E-02
12  8 2.000E-02  0  9 1.670E-01  2  9 7.300E-02  3  9 4.200E-02  4  9 3.000E-03
 5  9 4.600E-02  6  9 3.400E-02  7  9 1.000E-03  8  9 1.300E-02  9  9 3.000E-02
10  9 2.700E-02 11  9 9.000E-03 12  9 3.000E-03  0 10 1.520E-01  1 10 2.100E-02
 2 10 8.200E-02  3 10 1.000E-03  4 10 3.900E-02  5 10 3.700E-02  6 10 1.000E-03
 7 10 2.200E-02  8 10 3.500E-02  9 10 1.800E-02 11 10 8.000E-03 12 10 2.600E-02
 0 11 1.140E-01  1 11 7.400E-02  2 11 4.100E-02  3 11 2.400E-02  4 11 5.400E-02
 5 11 1.800E-02  6 11 2.500E-02  7 11 4.000E-02  8 11 2.000E-03  9 11 8.000E-03
10 11 2.400E-02 11 11 2.600E-02 12 11 1.000E-03  0 12 7.600E-02  1 12 1.260E-01
 3 12 7.200E-02  4 12 1.200E-02  5 12 2.500E-02  6 12 4.300E-02  7 12 2.000E-03
 8 12 1.700E-02  9 12 3.400E-02 10 12 1.400E-02 12 12 1.200E-02  0 13 3.300E-02
 1 13 1.390E-01  2 13 1.800E-02  3 13 5.400E-02  4 13 1.700E-02  5 13 5.200E-02
 6 13 2.000E-03  7 13 2.800E-02  8 13 2.700E-02  9 13 2.000E-03 10 13 1.400E-02
11 13 3.200E-02 12 13 7.000E-03  0 14 1.600E-02  1 14 1.050E-01  2 14 8.200E-02
 3 14 9.000E-03  4 14 6.600E-02  5 14 1.400E-02  6 14 1.800E-02  7 14 3.400E-02
 9 14 2.100E-02 10 14 2.700E-02 11 14 8.000E-03 12 14 8.000E-03  0 15 7.000E-03
 1 15 6.800E-02  2 15 1.260E-01  3 15 1.300E-02  4 15 5.600E-02  5 15 1.000E-02
 0 16 2.000E-03  1 16 2.800E-02  2 16 1.240E-01  3 16 8.600E-02  4 16 5.000E-03
 5 16 6.300E-02  6 16 6.000E-03  7 16 3.100E-02  8 16 2.200E-02 10 16 2.700E-02
11 16 2.200E-02 12 16 1.000E-03  1 17 1.200E-02  2 17 7.700E-02  3 17 1.340E-01
 4 17 2.900E-02  5 17 5.000E-02  6 17 1.800E-02  7 17 4.200E-02  9 17 3.200E-02
10 17 1.600E-02 11 17 2.000E-03 12 17 3.100E-02  1 18 4.000E-03  2 18 5.000E-02
 3 18 1.150E-01  4 18 7.700E-02  5 18 3.000E-03  6 18 6.200E-02  7 18 1.000E-03
 8 18 3.500E-02  9 18 2.200E-02 10 18 3.000E-03 11 18 2.900E-02 12 18 5.000E-03
 1 19 1.000E-03  2 19 1.000E-02  3 19 6.900E-02  4 19 1.290E-01  5 19 3.000E-02
 6 19 4.000E-02  7 19 3.800E-02  8 19 3.200E-02  9 19 8.000E-03 10 19 4.100E-02
CROSS-SECTIONS ASSUMED TO BE SAME AS FOR NO 1-2 OF IMAMI ET AL
5.687     6.        7.         9.        12.        16.       20.       25.
0.000E 00 3.370E-18 1.540E-17 2.450E-17 2.980E-17 3.030E-17 2.870E-17 2.700E-17
1.500E+06
NO G         1    2   38
 0  0 2.270E-01  1  0 3.670E-01  2  0 2.750E-01  3  0 9.900E-02  4  0 2.600E-02
 5  0 5.000E-03  6  0 2.000E-03  0  1 3.050E-01  1  1 5.600E-02  2  1 8.700E-02
 3  1 2.740E-01  4  1 1.930E-01  5  1 7.700E-02  6  1 1.000E-02  7  1 1.000E-03
 0  2 2.180E-01  1  2 2.400E-02  2  2 1.690E-01  3  2 1.000E-03  4  2 1.740E-01
 5  2 2.700E-01  6  2 1.050E-01  7  2 3.000E-02  8  2 3.000E-03  0  3 1.330E-01
 1  3 1.330E-01  2  3 1.500E-02  3  3 1.120E-01  4  3 5.300E-02  5  3 4.800E-02
 6  3 2.340E-01  7  3 1.920E-01  8  3 6.000E-02  9  3 1.600E-02 10  3 3.000E-03
 0  4 6.500E-02  1  4 1.600E-01  2  4 2.000E-02  3  4 9.400E-02  4  4 2.000E-02
 5  4 1.270E-01  6  4 6.000E-03  7  4 1.490E-01  8  4 2.210E-01  9  4 1.100E-01
10  4 2.400E-02 11  4 4.000E-03 12  4 1.000E-03  0  5 2.800E-02  1  5 1.260E-01
 2  5 9.200E-02  4  5 1.090E-01  6  5 1.270E-01  7  5 1.800E-02  8  5 5.200E-02
 9  5 2.300E-01 10  5 1.390E-01 11  5 6.100E-02 12  5 1.300E-02  0  6 1.000E-02
 1  6 7.000E-02  2  6 1.250E-01  3  6 2.600E-02  4  6 5.600E-02  5  6 6.200E-02
 6  6 2.200E-02  7  6 4.900E-02  8  6 9.300E-02  9  6 6.000E-03 10  6 1.790E-01
11  6 1.860E-01 12  6 9.300E-02  0  7 3.000E-03  1  7 3.400E-02  2  7 1.060E-01
 3  7 8.500E-02  5  7 8.200E-02  6  7 2.600E-02  7  7 7.700E-02  8  7 2.500E-02
 9  7 1.060E-01 10  7 2.000E-03 11  7 1.230E-01 12  7 2.040E-01  0  8 2.000E-03
 1  8 1.300E-02  2  8 6.100E-02  3  8 1.010E-01  4  8 3.100E-02  5  8 2.100E-02
 6  8 9.200E-02  7  8 5.000E-03  8  8 9.200E-02  9  8 3.000E-03 10  8 9.900E-02
 2  9 2.800E-02  3  9 8.300E-02  4  9 8.300E-02  6  9 3.600E-02  7  9 5.500E-02
 8  9 1.800E-02  9  9 7.500E-02 10  9 1.600E-02 11  9 8.000E-02 12  9 6.900E-02
 1 10 3.000E-03  2 10 1.400E-02  3 10 6.000E-02  4 10 8.900E-02  5 10 2.500E-02
 7 10 6.800E-02  8 10 1.100E-02  9 10 3.400E-02 10 10 5.300E-02 11 10 2.500E-02
12 10 4.500E-02  1 11 1.000E-03  2 11 7.000E-03  3 11 3.300E-02  4 11 6.700E-02
 5 11 7.100E-02  6 11 1.700E-02  7 11 3.000E-02  8 11 5.900E-02  9 11 3.000E-03
10 11 6.300E-02 11 11 2.400E-02 12 11 5.500E-02  2 12 4.000E-03  3 12 1.400E-02
 4 12 4.000E-02  5 12 7.500E-02  6 12 6.500E-02  8 12 1.700E-02  9 12 4.100E-02
10 12 2.000E-03 11 12 6.500E-02 12 12 2.000E-03  2 13 2.000E-03  3 13 7.000E-03
 4 13 3.200E-02  5 13 5.900E-02  6 13 7.400E-02  7 13 2.000E-02  8 13 4.100E-02
 9 13 5.300E-02 10 13 1.400E-02 11 13 3.200E-02 12 13 5.400E-02  2 14 1.000E-03
 3 14 3.000E-03  4 14 1.400E-02  5 14 3.800E-02  6 14 6.500E-02  7 14 6.100E-02
 8 14 2.100E-02  9 14 2.000E-02 10 14 5.000E-02 11 14 9.000E-03 12 14 2.900E-02
 3 15 1.000E-03  4 15 7.000E-03  5 15 2.400E-02  6 15 5.600E-02  7 15 7.100E-02
```

```
 8 15 1.300E-02  9 15 8.000E-03 10 15 3.400E-02 11 15 3.500E-02 12 15 3.000E-03
 4 16 5.000E-03  5 16 1.100E-02  6 16 3.200E-02  7 16 5.400E-02  8 16 5.200E-02
 9 16 4.000E-03 10 16 1.200E-02 11 16 4.800E-02 12 16 1.400E-02  4 17 1.000E-03
 5 17 7.000E-03  6 17 1.800E-02  7 17 4.400E-02  8 17 6.200E-02  9 17 3.400E-02
11 17 1.700E-02 12 17 3.200E-02  5 18 1.000E-03  6 18 6.000E-03  7 18 2.800E-02
FROM IMAMI ET AL
5.443      5.666      5.686      8.490      11.32      15.13      18.89      23.62
0.000E 00 3.370E-18 1.540E-17 2.450E-17 2.980E-17 3.030E-17 2.870E-17 2.700E-17
8.620E+06
NO A-B        2    3    1
 0  0 0.
CROSS-SECTIONS ASSUMED SAME AS AS FOR NO 1-2 OF IMAMI ET AL
0.2437     0.2537     0.2937     0.3802     0.5069     0.6775     0.8456     1.058
0.000E 00 3.370E-18 1.540E-17 2.450E-17 2.980E-17 3.030E-17 2.870E-17 2.700E-17
0.
02            32.0       0    0    5    0
    3.000      0.000  1580.361    12.073     0.055    -0.001   1.44567 1.579E-02
    2.000   7918.100  1509.300    12.900     0.000     0.000   1.42640 1.710E-02
    1.000  13195.220  1432.687    13.950    -0.011     0.000   1.40042 1.817E-02
    3.000  36096.000   819.000    22.500     0.000     0.000   1.05000 0.000E+00
    3.000  49802.102   700.360     8.002    -0.375     0.000   0.81900 1.100E-02
0  3P      1.600E+01 4.126E+04 9.000E+00 1.000E+00 1.000E+00
0  3P      1.600E+01 4.126E+04 9.000E+00 1.000E+00 1.000E+00
CN            26.020    3    3    3    3    0
    2.000      0.000  2068.745    13.134    -0.006     0.000   1.89900 1.701E-02
    4.000   9245.344  1812.555    12.609    -0.012     0.000   1.71510 1.708E-02
    2.000  25751.801  2168.610    20.200     0.000     0.000   1.97010 2.215E-02
C  3P      1.201E+01 6.364E+04 9.000E+00 1.000E+00 1.000E+00
N  4S      1.401E+01 6.363E+04 4.000E+00 1.500E+00 0.000E+00
CROSS-SECTIONS ASSUMED AS SAME FOR NO 1-2 OF IMAMI ET AL
63640.
7.89       8.213      9.547      12.31      16.41      21.93      27.38      34.24
0.000E 00 3.370E-18 1.540E-17 2.450E-17 2.980E-17 3.030E-17 2.870E-17 2.700E-17
CROSS-SECTIONS ASSUMED SAME AS SAME FOR NO 1-2 OF IMAMI ET AL
63640.
6.744      7.035      8.178      10.54      14.06      18.79      23.45      29.33
0.000E 00 3.370E-18 1.540E-17 2.450E-17 2.980E-17 3.030E-17 2.870E-17 2.700E-17
CROSS-SECTIONS ASSUMED SAME AS SAME FOR NO 1-2 OF IMAMI ET AL
63640.
4.697      4.884      5.677      7.320      9.759      13.04      16.28      20.36
0.000E 00 3.370E-18 1.540E-17 2.450E-17 2.980E-17 3.030E-17 2.870E-17 2.700E-17
CN VIO        1    3   13
 0  0 9.179E-01  1  0 8.090E-02  2  0 1.200E-03  0  1 7.600E-02  1  1 7.795E-01
 2  1 1.417E-01  3  1 2.800E-03  0  2 5.800E-03  1  2 1.240E-01  2  2 6.754E-01
 3  2 1.905E-01  4  2 4.300E-03  0  3 3.000E-04  1  3 1.430E-02  2  3 1.550E-01
 3  3 5.929E-01  4  3 2.318E-01  2  4 2.390E-02  3  4 1.745E-01  4  4 5.279E-01
 5  4 2.668E-01  3  5 3.420E-02  4  5 1.825E-01  5  5 4.824E-01  6  5 2.933E-01
 4  6 4.520E-02  5  6 1.781E-01  6  6 4.583E-01  7  6 3.095E-01  9  6 3.100E-03
 5  7 5.540E-02  6  7 1.640E-01  7  7 4.554E-01  8  7 3.122E-01 10  7 5.000E-03
 6  8 6.390E-02  8  8 4.750E-01  9  8 2.956E-01 11  8 6.700E-03  7  9 7.080E-02
 9  9 5.184E-01 10  9 2.537E-01  8 10 7.660E-02 10 10 5.801E-01 11 10 1.897E-01
12 10 4.810E-02 14 10 3.400E-03  7 11 3.100E-03  9 11 8.280E-02 11 11 6.447E-01
12 11 1.131E-01 13 11 8.540E-02 15 11 5.500E-03  8 12 3.700E-03 12 12 6.967E-01
14 12 1.203E-01  9 13 4.100E-03 13 13 7.127E-01 15 13 1.380E-01 18 13 4.000E-03
14 14 6.762E-01 16 14 1.234E-01 17 14 4.470E-02 15 15 5.786E-01 16 15 9.180E-02
CROSS-SECTIONS ASSUMED SAME AS FOR NO 1-2 OF IMAMI ET AL
3.193      3.329      3.870      4.989      6.652      8.890      11.10      13.88
0.000E 00 3.370E-18 1.540E-17 2.450E-17 2.980E-17 3.030E-17 2.870E-17 2.700E-17
1.180E+07
CN RED        1    2   50
 0  0 5.002E-01  1  0 3.179E-01  2  0 1.269E-01  3  0 4.020E-02  4  0 1.110E-02
 5  0 2.850E-03  6  0 7.500E-04  7  0 2.000E-04  8  0 5.000E-05  0  1 3.711E-01
 1  1 4.600E-02  2  1 2.409E-01  3  1 1.942E-01  4  1 9.410E-02  5  1 3.615E-02
 6  1 1.220E-02  7  1 3.800E-03  8  1 1.100E-03  9  1 3.500E-04 10  1 1.000E-04
 0  2 1.107E-01  1  2 3.528E-01  2  2 1.160E-02  3  2 9.950E-02  4  2 1.812E-01
```

```
 5  2 1.330E-01  6  2 6.755E-02  7  2 2.810E-02  8  2 1.040E-02  9  2 3.600E-03
10  2 1.150E-03 11  2 3.500E-04 12  2 1.500E-04 13  2 5.000E-05  0  3 1.670E-02
 1  3 2.234E-01  2  3 2.136E-01  3  3 8.780E-02  4  3 1.615E-02  5  3 1.228E-01
 6  3 1.416E-01  7  3 9.500E-02  8  3 4.855E-02  9  3 2.125E-02 10  3 8.450E-03
11  3 3.150E-03 12  3 1.100E-03 13  3 4.000E-04 14  3 1.500E-04 15  3 5.000E-05
 0  4 1.400E-03  1  4 5.355E-02  2  4 2.872E-01  3  4 8.785E-02  4  4 1.489E-01
 5  4 1.800E-03  6  4 5.870E-02  7  4 1.210E-01  8  4 1.088E-01  9  4 6.855E-02
10  4 3.530E-02 11  4 1.600E-02 12  4 6.650E-03 13  4 2.650E-03 14  4 1.000E-03
15  4 4.000E-04 16  4 1.500E-04 17  4 5.000E-05  0  5 1.000E-04  1  5 6.150E-03
 2  5 1.027E-01  3  5 2.994E-01  4  5 1.595E-02  5  5 1.591E-01  6  5 3.040E-02
 7  5 1.505E-02  8  5 8.440E-02  9  5 1.068E-01 10  5 8.305E-02 11  5 5.020E-02
12  5 2.590E-02 13  5 1.210E-02 14  5 5.300E-03 15  5 2.150E-03 16  5 8.500E-04
 1  6 4.000E-04  2  6 1.590E-02  3  6 1.567E-01  4  6 2.669E-01  5  6 7.500E-04
 6  6 1.287E-01  7  6 6.960E-02  8  6 1.500E-04  9  6 4.555E-02 10  6 9.010E-02
11  6 8.880E-02 12  6 6.315E-02 13  6 3.725E-02 14  6 1.940E-02 15  6 9.300E-03
16  6 4.200E-03 17  6 1.850E-03 18  6 7.500E-04  2  7 1.250E-03  3  7 3.130E-02
 4  7 2.067E-01  5  7 2.069E-01  6  7 2.400E-02  7  7 8.095E-02  8  7 9.770E-02
 9  7 9.450E-03 10  7 1.610E-02 11  7 6.515E-02 12  7 8.440E-02 13  7 7.165E-02
14  7 4.825E-02 15  7 2.805E-02 16  7 1.480E-02 17  7 7.300E-03 18  7 3.400E-03
 2  8 5.000E-05  3  8 2.950E-03  4  8 5.285E-02  5  8 2.455E-01  6  8 1.390E-01
 7  8 6.345E-02  8  8 3.650E-02  9  8 1.050E-01 10  8 3.190E-02 11  8 1.650E-03
12  8 3.835E-02 13  8 7.115E-02 14  8 7.365E-02 15  8 5.700E-02 16  8 3.705E-02
17  8 2.140E-02 18  8 1.145E-02  3  9 1.000E-04  4  9 6.000E-03  5  9 7.980E-02
 6  9 2.670E-01  7  9 7.770E-02  8  9 1.008E-01  9  9 8.250E-03 10  9 9.250E-02
11  9 5.585E-02 12  9 2.400E-03 13  9 1.650E-02 14  9 5.265E-02 15  9 6.860E-02
16  9 6.170E-02 17  9 4.505E-02 18  9 2.870E-02  4 10 3.500E-04  5 10 1.070E-02
 6 10 1.107E-01  7 10 2.728E-01  8 10 3.205E-02  9 10 1.242E-01 10 10 2.500E-04
11 10 6.780E-02 12 10 7.205E-02 13 10 1.425E-02 14 10 3.500E-03 15 10 3.275E-02
16 10 5.760E-02 17 10 6.145E-02 18 10 5.065E-02  5 11 6.500E-04  6 11 1.765E-02
 7 11 1.432E-01  8 11 2.606E-01  9 11 6.450E-03 10 11 1.297E-01 11 11 9.750E-03
12 11 3.975E-02 13 11 7.685E-02 14 11 3.125E-02 15 11 7.500E-04 16 11 1.575E-02
 6 12 1.250E-03  7 12 2.700E-02  8 12 1.762E-01  9 12 2.346E-01 10 12 5.500E-04
11 12 1.184E-01 12 12 2.990E-02 13 12 1.655E-02 14 12 6.985E-02 15 12 4.710E-02
16 12 6.700E-03 17 12 4.600E-03 18 12 2.705E-02  7 13 2.150E-03  8 13 3.910E-02
 9 13 2.066E-01 10 13 1.985E-01 11 13 6.075E-02 12 13 9.515E-02 13 13 5.275E-02
14 13 3.200E-03 15 13 5.435E-02 16 13 5.735E-02 17 13 1.830E-02 18 13 7.500E-04
 7 14 1.000E-04  8 14 3.550E-03  9 14 5.365E-02 10 14 2.326E-01 11 14 1.569E-01
12 14 3.170E-02 13 14 6.660E-02 14 14 7.175E-02 15 14 9.500E-04 16 14 3.565E-02
17 14 5.970E-02 18 14 3.145E-02  8 15 1.500E-04  9 15 5.500E-03 10 15 7.110E-02
11 15 2.520E-01 12 15 1.146E-01 13 15 5.755E-02 14 15 3.885E-02 15 15 8.250E-02
16 15 8.400E-03 17 15 1.815E-02 18 15 5.415E-02  9 16 2.500E-04 10 16 8.250E-03
11 16 9.090E-02 12 16 2.647E-01 13 16 7.545E-02 14 16 8.245E-02 15 16 1.700E-02
16 16 8.330E-02 17 16 2.195E-02 18 16 5.950E-03 10 17 3.500E-04 11 17 1.180E-02
12 17 1.128E-01 13 17 2.693E-01 14 17 4.340E-02 15 17 1.020E-01 16 17 4.200E-03
17 17 7.505E-02 18 17 3.715E-02 11 18 6.000E-04 12 18 1.635E-02 13 18 1.359E-01
CROSS-SECTIONS ASSUMED SAME AS NO 1-2 OF IMAMI ET AL
1.146      1.176      1.367      1.763      2.350      3.141      3.921      4.904
0.000E 00 3.370E-18 1.540E-17 2.450E-17 2.980E-17 3.030E-17 2.870E-17 2.700E-17
1.950E+05
CN AB        2    3   30
 1  0 2.248E-04  1  1 2.248E-04  1  2 1.833E-01  1  3 6.249E-01  1  4 6.249E-01
 1  5 1.442E-01  1  6 3.433E-02  1  7 8.821E-03  1  8 8.821E-03  1  9 2.609E-03
 1 10 8.926E-04  1 11 3.496E-04  1 12 3.496E-04  1 13 1.542E-04  2  0 8.909E-01
 2  1 8.909E-01  2  2 9.252E-02  2  3 1.300E-02  2  4 1.300E-02  2  5 2.521E-03
 2  6 6.437E-04  2  7 2.055E-04  2  8 2.055E-04  3  0 8.909E-01  3  1 8.909E-01
 3  2 9.252E-02  3  3 1.300E-02  3  4 1.300E-02  3  5 2.521E-03  3  6 6.437E-04
 3  7 2.055E-04  3  8 2.055E-04  4  0 1.088E-01  4  1 1.088E-01  4  2 7.239E-01
 4  3 1.339E-01  4  4 1.339E-01  4  5 2.530E-02  4  6 5.644E-03  4  7 1.530E-03
 4  8 1.530E-03  4  9 4.975E-04  4 10 1.894E-04  5  0 2.248E-04  5  1 2.248E-04
 5  2 1.833E-01  5  3 6.249E-01  5  4 6.249E-01  5  5 1.442E-01  5  6 3.433E-02
 5  7 8.821E-03  5  8 8.821E-03  5  9 2.609E-03  5 10 8.926E-04  5 11 3.496E-04
 5 12 3.496E-04  5 13 1.542E-04  6  0 2.248E-04  6  1 2.248E-04  6  2 1.833E-01
 6  3 6.249E-01  6  4 6.249E-01  6  5 1.442E-01  6  6 3.433E-02  6  7 8.821E-03
 6  8 8.821E-03  6  9 2.609E-03  6 10 8.926E-04  6 11 3.496E-04  6 12 3.496E-04
 6 13 1.542E-04  7  2 2.534E-04  7  3 2.281E-01  7  4 2.281E-01  7  5 5.836E-01
```

```
 7  6 1.320E-01  7  7 3.861E-02  7  8 3.861E-02  7  9 1.127E-02  7 10 3.657E-03
 7 11 1.335E-03  7 12 1.335E-03  7 13 5.469E-04  7 14 2.487E-04  8  2 2.534E-04
 8  3 2.281E-01  8  4 2.281E-01  8  5 5.836E-01  8  6 1.320E-01  8  7 3.861E-02
 8  8 3.861E-02  8  9 1.127E-02  8 10 3.657E-03  8 11 1.335E-03  8 12 1.335E-03
 8 13 5.469E-04  8 14 2.487E-04  9  5 2.428E-01  9  6 5.930E-01  9  7 1.051E-01
 9  8 1.051E-01  9  9 3.865E-02  9 10 1.255E-02  9 11 4.462E-03  9 12 4.462E-03
 9 13 1.748E-03  9 14 7.549E-04 10  5 1.531E-03 10  6 2.259E-01 10  7 6.444E-01
10  8 6.444E-01 10  9 7.020E-02 10 10 3.617E-02 10 11 1.266E-02 10 12 1.266E-02
10 13 4.907E-03 10 14 2.062E-03 11  6 8.358E-03 11  7 1.780E-01 11  8 1.780E-01
11  9 7.241E-01 11 10 3.468E-02 11 11 3.320E-02 11 12 3.320E-02 11 13 1.185E-02
11 14 4.989E-03 12  6 8.358E-03 12  7 1.780E-01 12  8 1.780E-01 12  9 7.241E-01
12 10 3.468E-02 12 11 3.320E-02 12 12 3.320E-02 12 13 1.185E-02 12 14 4.989E-03
13  7 2.205E-02 13  8 2.205E-02 13  9 1.088E-01 13 10 8.092E-01 13 11 7.994E-03
13 12 7.994E-03 13 13 3.150E-02 13 14 1.046E-02 14  7 1.136E-03 14  8 1.136E-03
14  9 3.815E-02 14 10 4.041E-02 14 11 8.689E-01 14 12 8.689E-01 14 13 4.843E-04
CROSS-SECTIONS ASSUMED SAME AS FOR NO 1-2 OF IMAMI ET AL
2.046     2.153     2.502     3.226     4.301     5.749     7.176     8.975
0.000E 00 3.370E-18 1.540E-17 2.450E-17 2.980E-17 3.030E-17 2.870E-17 2.700E-17
0.
```

9.1.4 Radiation Line Information (*rad.dat*)

```
2056
   0.40  +01   0.10  +02   0.60  +01   0.18  +02   0.54  +02   0.90  +02
   0.00  +00   0.00  +00   0.90  +01   0.50  +01   0.10  +01   0.50  +01
   0.30  +01   1.50  +01   0.90  +01   0.40  +02   0.90  +01   0.50  +01
   0.10  +01   0.50  +01   0.12  +02   0.15  +02   0.36  +02   0.00  +00
   0.20  +01   0.80  +01   0.18  +02   0.32  +02   0.00  +00   0.00  +00
   0.00  +00   0.00  +00   0.10  +01   0.30  +01   0.50  +01   0.50  +01
   0.10  +01   0.50  +01   0.00  +00   0.00  +00   0.40  +01   0.00  +00
   0.00  +00   0.00  +00   0.00  +00   0.00  +00   0.00  +00   0.00  +00
   0.60  +01   0.00  +00   0.00  +00   0.00  +00   0.00  +00   0.00  +00
   0.00  +00   0.00  +00   0.00  +00   0.00  +00   0.00  +00   0.00  +00
   0.00  +00   0.2384+01   0.3576+01   0.1045+02   0.1188+02   0.1300+02
   0.00  +00   0.00  +00   0.96  -02   0.1967+01   0.4189+01   0.9144+01
   0.9519+01   0.1074+02   0.1099+02   0.1208+02   0.00  +00   1.2639+00
   2.6839+00   4.1825+00   7.5351+00   7.9461+00   8.6442+00   0.00  +00
   0.00  +00   0.1020+02   0.1208+02   0.1274+02   0.00  +00   0.00  +00
   0.00  +00   0.00  +00   0.00  +00   0.6075-02   0.1624-01   0.1899+01
   0.4052+01   0.5848+01   0.00  +00   0.00  +00



   0.60  +00   0.85  +00   0.96  +00   0.12  +01   0.14  +01   0.162 +01
   0.24  +01   0.34  +01   0.62  +01   0.80  +01   0.86  +01   0.90  +01
   0.97  +01   0.1045+02   0.1080+02   0.1170+02   0.1210+02   0.1280+02
   0.1340+02   0.1380+02   0.00  +00   0.00  +00   0.00  +00   0.00  +00
   0.80  +00   0.95  +00   0.12  +01   0.14  +01   0.16  +01   0.24  +01
   0.3340+01   0.40  +01   0.80  +01   0.86  +01   0.90  +01   0.97  +01
   0.1045+02   0.1080+02   0.1170+02   0.1210+02   0.1280+02   0.1340+02
   0.1380+02   0.1450+02   0.00  +00   0.00  +00   0.00  +00   0.00  +00
   0.69  +00   0.89  +00   0.1080+01   0.1290+01   0.1460+01   0.1850+01
   0.2850+01   0.3700+01   0.7110+01   0.8302+01   0.8781+01   0.94  +01
   0.1007+02   0.1062+02   0.1120+02   0.1190+02   0.1241+02   0.1304+02
   0.1358+02   0.1420+02     .    +      .    +      .    +      .    +
 3 4 5 4 4 4 3 2 1 1 1 4 5 6 7 7 7 3 3 4
16          0.685       0.196          110E-21 6.
 6          0.689       0.1597         187E-20 6.
 5          0.7525      0.0149         446E-21
 5          0.875       0.0366         380E-21 4.
15          0.8840      0.1570         367E-21
 4          0.9158      0.00847        739E-22
 6          0.9304      0.0253         387E-20 2.
 6          0.965       0.0262         387E-20 4.
```

16	0.991	0.0805	309E-20	2.
5	1.0355	0.0735	331E-21	7.
15	1.0980	0.7490	344E-21	
14	1.1320	0.2010	367E-21	
5	1.2610	0.118	312E-21	3.
4	1.3190	0.1833	984E-22	
14	1.3380	0.9130	342E-21	
5	1.3677	0.0387	292E-21	
4	1.4380	0.256	824E-22	3.
13	1.4670	0.9500	865E-22	
5	1.5527	0.0030	293E-20	
12	1.594	1.0300	709E-22	
4	1.6630	0.0923	958E-22	
15	1.767	0.0226	275E-20	3.
5	1.8357	0.00566	293E-20	5.
14	2.015	0.0258	275E-20	3.
4	2.925	0.0070	106E-20	3.
13	3.0	0.010	810E-21	2.
12	3.167	0.00826	520E-21	
4	3.4724	0.00861	452E-20	3.
12	3.7110	0.0143	110E-20	
3	07.111	0.0634	912E-22	6.
2	08.302	0.0740	912E-22	6.
3	08.781	0.0435	661E-22	
3	09.301	0.0166	446E-21	
3	09.394	0.0119	229E-21	
3	09.460	0.0360	336E-21	
09	9.5010	0.0471	548E-22	
2	09.973	0.0890	661E-22	
3	10.102	0.0374	293E-20	
11	10.182	0.1510	653E-22	
1	10.332	0.1840	621E-22	12.
3	10.418	0.0225	532E-20	
2	10.493	0.0187	446E-20	
3	10.585	0.0131	796E-20	
2	10.619	0.0533	312E-21	14.
3	10.682	0.00819	268E-19	
3	10.757	0.00518	437E-19	
10	10.761	0.1200	653E-22	
1	10.927	0.4540	161E-23	12.
11	11.007	0.0185	367E-21	
3	11.200	0.0200	446E-21	
2	11.293	0.0418	293E-20	
3	11.310	0.0254	323E-21	
33	11.424	0.2260	143E-23	
2	11.609	0.0250	532E-20	
2	11.776	0.0220	796E-20	
11	11.806	0.0049	145E-20	
09	11.852	0.0199	367E-21	
2	11.874	0.0091	268E-19	
2	11.948	0.00575	437E-19	
3	12.000	0.0269	299E-20	
09	12.067	0.0218	344E-21	
11	12.160	0.0019	128E-20	
3	12.316	0.0156	696E-20	
10	12.404	0.0461	653E-22	
2	12.414	0.0574	390E-21	
2	12.511	0.0279	337E-21	
09	12.521	0.0775	633E-22	
09	12.651	0.00524	145E-20	
1	12.877	0.0230	446E-21	
1	13.004	0.1320	294E-21	12.
2	13.190	0.0489	299E-20	
2	13.508	0.0291	696E-19	
33	13.543	0.1610	950E-24	

```
1          13.677      0.0957          293E-20
1          13.993      0.0584          532E-20
1          14.160      0.0342          796E-20
1          14.257      0.0212          268E-19
1          14.332      0.0138          437E-19
36
.02         .1          .2          .3          .5          .6
.8          1.0         1.5         2.0         2.5         3.0
3.5         4.0         4.5         5.0         6.0         6.2
7.0         8.0         9.0         10.0        10.79       10.81
11.25       11.27       11.99       12.01       13.39       13.41
13.59       13.61       14.29       14.31       15.0        16.5
10012010111201110000   FIRE II FLUX ABSORBED
01100
1.00        1.00        1.00        1.00        1.00        1.00
1.00        1.00        1.00        1.00        1.00        1.00
1.00        1.00        1.00        1.00        1.00        1.00
1.00        1.00        1.00        1.00        1.00        1.00
1.00        1.00        1.00        1.00        1.00        1.00
1.00        1.00        1.00        1.00        1.00        1.00
1.00        1.00        1.00        1.00        1.00        1.00
1.00        1.00        1.00        1.00        1.00        1.00
1.00        1.00
 .00         .00         .00         .00         .00         .00
 .00         .00         .00         .00         .00         .00
 .00         .00         .00         .00         .00         .00
 .00         .00         .00         .00         .00         .00
 .00         .00         .00         .00         .00         .00
 .00         .00         .00         .00         .00         .00
 .00         .00         .00         .00         .00         .00
 .00         .00         .00         .00         .00         .00
 .00         .00
  1  1  1  0  0  0  1  1  1  0  1  1  0  0  0  0  0  0  0  0
```

9.2 Radiation Output File (*fort.16*)

```
MOLECULAR BAND NAME=N2+     MOLECULAR WEIGHT=    28.010
NUMBER OF ELECTRON-IMPACT DISSOCIATION CROSS-SECTION SET= 4
NUMBER OF ELECTRON-IMPACT EXCITATION CROSS-SECTION SET  = 6
NUMBER OF ELECTRONIC LEVELS                             = 5
NUMBER OF LEVELS IN QUASI-STEADY-STATE CALC.            = 4
 DEGEN       TERM        WE        WEXE       WEYE       WEZE        BE       ALPHA
    2.000      0.000  2207.190    16.136    -0.040      0.000   1.93220 2.020E-02
    4.000   9168.400  1902.840    14.910     0.000      0.000   1.72200 1.800E-02
    2.000  25461.500  2419.840    23.190    -0.538      0.000   2.08300 1.950E-02
    4.000  51663.200   907.710    11.910     0.016      0.000   1.11300 2.000E-02
    2.000  64622.199  2050.000     0.000     0.000      0.000   1.65000 5.000E-02

DISSOCIATED STATE
N  4S    ATOM. WT.=  14.010  DISSOC. ENERGY=   70400. CM-1  STATISTICAL WT.=  4.0
N+ 3P    ATOM. WT.=  14.010  DISSOC. ENERGY=   70400. CM-1  STATISTICAL WT.=  9.0

ELECTRON-IMPACT DISSOCIATION CROSS-SECTIONS
CROSS-SECTIONS ASSUMED TO BE THE SAME AS FOR X-B OF CRANDALL ET AL *0.1
DISSOCIATION ENERGY =   70398.0 CM-1
ELECTRON ENERGY=      8.73     11.01     16.52     22.03     27.54     41.30     55.07     82.61
CROSS SECTION  = 2.950E-17 2.830E-17 2.380E-17 1.900E-17 1.550E-17 1.100E-17 8.900E-18 6.800E-18
CROSS-SECTIONS ASSUMED TO BE THE SAME AS FOR X-B OF CRANDALL ET AL *0.1
DISSOCIATION ENERGY =   70398.0 CM-1
ELECTRON ENERGY=      7.61      9.60     14.41     19.21     24.01     36.01     48.02     72.03
CROSS SECTION  = 2.950E-17 2.830E-17 2.380E-17 1.900E-17 1.550E-17 1.100E-17 8.900E-18 6.800E-18
```

```
CROSS-SECTIONS ASSUMED TO BE THE SAME AS FOR X-B OF CRANDALL ET AL *0.1
DISSOCIATION ENERGY =   70398.0 CM-1
ELECTRON ENERGY=      5.56      7.01     10.52     14.03     17.54     26.30     35.07     52.61
CROSS SECTION  = 2.950E-17 2.830E-17 2.380E-17 1.900E-17 1.550E-17 1.100E-17 8.900E-18 6.800E-18
CROSS-SECTIONS ASSUMED TO BE THE SAME AS FOR X-B OF CRANDALL ET AL *0.1
DISSOCIATION ENERGY =   70398.0 CM-1
ELECTRON ENERGY=      2.32      2.93      4.40      5.86      7.33     10.99     14.66     21.98
CROSS SECTION  = 2.950E-17 2.830E-17 2.380E-17 1.900E-17 1.550E-17 1.100E-17 8.900E-18 6.800E-18

FRANCK-CONDON FACTOR DATA
IORD=  1
N2+MEI   LOWER STATE= 1  UPPER STATE= 2   NUMBER OF CARDS= 10
  0  0 4.751E-01  0  1 3.798E-01  0  2 1.226E-01  0  3 2.055E-02  0  4 1.914E-03
  0  5 9.822E-05  1  0 3.255E-01  1  1 3.115E-01  1  2 3.358E-01  1  3 2.368E-01
  1  4 6.236E-02  1  5 7.946E-03  1  6 5.163E-04  2  0 1.360E-01  2  1 2.245E-01
  2  2 2.137E-02  2  3 1.851E-01  2  4 2.946E-01  2  5 1.171E-03  2  6 1.972E-03
  2  7 1.581E-03  3  0 4.526E-02  3  1 1.990E-01  3  2 7.974E-01  3  3 1.049E-01
  3  4 6.274E-02  3  5 2.929E-01  3  6 1.738E-01  3  7 3.793E-02  3  8 3.685E-03
  4  0 1.329E-02  4  1 1.032E-01  4  2 1.745E-01  4  3 7.195E-03  4  4 1.553E-01
  4  5 5.808E-03  4  6 2.479E-01  4  7 2.230E-01  4  8 6.228E-02  4  9 7.238E-03
  5  0 3.624E-03  5  1 4.145E-02  5  2 1.395E-01  5  3 1.078E-01  5  4 6.918E-03
  5  5 1.509E-01  5  6 5.609E-03  5  7 1.816E-01  5  8 2.578E-01  5  9 9.165E-02
CROSS-SECTIONS ASSUMED TO BE THE SAME  AS FOR X-B OF CRANDALL ET AL
ELECTRON ENERGY=      1.12      1.41      2.12      2.82      3.53      5.29      7.05     10.58
CROSS SECTION  = 2.950E-16 2.830E-16 2.380E-16 1.900E-16 1.550E-16 1.100E-16 8.900E-17 6.800E-17
RADIATIVE TRANSITION PROBABILITY= 0.000E+00
IORD=  2
N2+ 1-   LOWER STATE= 1  UPPER STATE= 3   NUMBER OF CARDS= 36
  0  0 6.509E-01  1  0 3.014E-01  2  0 4.537E-02  3  0 2.248E-03  4  0 1.452E-05
  0  1 2.588E-01  1  1 2.226E-01  2  1 4.060E-01  3  1 1.056E-01  4  1 6.935E-03
  5  1 3.986E-05  0  2 7.016E-02  1  2 2.860E-01  2  2 5.065E-02  3  2 4.137E-01
  4  2 1.660E-01  5  2 1.340E-02  6  2 5.729E-05  7  2 1.132E-05  0  3 1.600E-02
  1  3 1.324E-01  2  3 2.290E-01  3  3 2.101E-03  4  3 3.792E-01  5  3 2.205E-01
  6  3 2.069E-02  7  3 4.930E-05  8  3 3.006E-05  0  4 3.297E-03  1  4 4.273E-02
  2  4 1.654E-01  3  4 1.557E-01  4  4 6.726E-03  5  4 3.310E-01  6  4 2.673E-01
  7  4 2.789E-02  8  4 1.807E-05  9  4 6.420E-05  0  5 6.342E-04  1  5 1.140E-02
  2  5 7.113E-02  3  5 1.706E-01  4  5 9.290E-02  5  5 2.925E-02  6  5 2.830E-01
  7  5 3.068E-01  8  5 3.419E-02 10  5 1.161E-04  0  6 1.155E-04  1  6 2.700E-03
  2  6 2.362E-02  3  6 9.451E-02  4  6 1.569E-01  5  6 4.815E-02  6  6 5.331E-02
  7  6 2.415E-01  8  6 3.401E-01  9  6 3.890E-02 10  6 8.094E-05 11  6 1.823E-04
  0  7 2.000E-05  1  7 5.861E-04  2  7 6.691E-03  3  7 3.801E-02  4  7 1.096E-01
  5  7 1.333E-01  6  7 2.044E-02  7  7 7.236E-02  8  7 2.083E-01  9  7 3.686E-01
 10  7 4.153E-02 11  7 3.873E-04 12  7 2.509E-04 13  7 1.172E-05  1  8 1.185E-04
  2  8 1.695E-03  3  8 1.261E-02  4  8 5.236E-02  5  8 1.161E-01  6  8 1.065E-01
  7  8 5.939E-03  8  8 8.468E-02  9  8 1.837E-01 10  8 3.933E-01 11  8 4.170E-02
 12  8 1.087E-03 13  8 3.010E-04 14  8 3.005E-05  1  9 2.239E-05  2  9 3.934E-04
  8  9 4.743E-04  9  9 9.065E-02 10  9 1.672E-01 11  9 4.149E-01 12  9 3.928E-02
 13  9 2.361E-03 14  9 3.071E-04 15  9 6.400E-05  2 10 8.445E-05  3 10 9.639E-04
  4 10 6.599E-03  5 10 2.826E-02  6 10 7.442E-02  7 10 1.084E-01  8 10 5.865E-02
  9 10 5.552E-04 10 10 9.141E-02 11 10 1.579E-01 12 10 4.338E-01 13 10 3.432E-02
 14 10 4.364E-03 15 10 2.499E-04 16 10 1.171E-04  2 11 1.675E-05  3 11 2.824E-04
  4 11 1.942E-03  5 11 1.043E-02  6 11 3.652E-02  7 11 8.051E-02  8 11 9.821E-02
  9 11 4.075E-02 10 11 3.604E-03 11 11 8.818E-02 12 11 1.554E-01 13 11 4.496E-01
 14 11 2.722E-02 15 11 7.165E-03 16 11 1.355E-04 17 11 1.867E-04  3 12 5.156E-05
  4 12 5.207E-04  5 12 3.406E-03  6 12 1.496E-02  7 12 4.411E-02  8 12 8.319E-02
  9 12 8.628E-02 10 12 2.710E-02 11 12 7.896E-03 12 12 8.205E-02 13 12 1.593E-01
 14 12 4.615E-01 15 12 1.876E-02 16 12 1.068E-02 17 12 2.033E-05 18 12 2.587E-04
 19 12 2.439E-05  3 13 1.044E-05  4 13 1.281E-04  5 13 1.007E-03  6 13 5.378E-03
  7 13 1.991E-02  8 13 5.053E-02  9 13 8.288E-02 10 13 7.393E-02 11 13 1.720E-02
 12 13 1.238E-02 13 13 7.384E-02 14 13 1.697E-01 15 13 4.681E-01 16 13 1.018E-02
 17 13 1.459E-02 18 13 3.550E-05 19 13 3.056E-04  4 14 2.877E-05  5 14 2.724E-04
  6 14 1.741E-03  7 14 7.823E-03  8 14 2.495E-02  9 14 5.544E-02 10 14 8.018E-02
 11 14 6.208E-02 12 14 1.034E-02 13 14 1.651E-02 14 14 6.418E-02 15 14 1.866E-01
 16 14 4.676E-01 17 14 3.207E-03 18 14 1.831E-02 19 14 3.955E-04  5 15 6.737E-05
CROSS-SECTINS MEASURED BY CRANDALL ET AL
```

```
ELECTRON ENERGY=      3.17      4.00      5.00      6.00      8.00     10.00     15.00     20.00
CROSS SECTION  = 2.950E-16 2.830E-16 2.380E-16 1.900E-16 1.550E-16 1.100E-16 8.900E-17 6.800E-17
RADIATIVE TRANSITION PROBABILITY= 1.520E+07
IORD=  3
N2+ DX   LOWER STATE= 1  UPPER STATE= 4   NUMBER OF CARDS= 54
  0  4 1.579E-04  0  5 6.941E-04  0  6 2.501E-03  0  7 7.498E-03  0  8 1.888E-02
  0  9 4.020E-02  0 10 1.119E-01  0 11 1.469E-01  0 12 1.642E-01  0 13 1.556E-01
  0 14 8.237E-02  0 15 4.467E-02  0 16 6.454E-03  0 17 1.574E-03  1  3 2.379E-04
  1  4 1.105E-03  1  5 4.051E-03  1  6 1.193E-02  1  7 2.838E-02  1  8 5.433E-02
  1  9 8.246E-02  1 10 7.993E-02  1 11 3.886E-02  1 12 3.775E-03  1 13 9.785E-03
  1 14 1.231E-01  1 15 1.498E-01  1 16 7.868E-02  1 17 3.522E-02  1 18 2.220E-03
  2  2 2.055E-04  2  3 1.061E-03  2  4 4.119E-03  2  5 1.243E-02  2  6 2.937E-02
  2  7 5.383E-02  2  8 7.418E-02  2  9 7.166E-02  2 10 5.664E-03  2 11 6.219E-03
  2 12 4.435E-02  2 13 7.148E-02  2 14 5.578E-03  2 15 1.365E-02  2 16 1.467E-01
  2 17 1.458E-01  2 18 3.852E-02  2 19 1.260E-03  3  1 1.266E-04  3  2 7.873E-04
  3  3 3.383E-03  3  4 1.083E-02  3  5 2.642E-02  3  6 4.873E-02  3  7 6.544E-02
  3  8 5.822E-02  3  9 2.601E-02  3 10 1.461E-02  3 11 4.747E-02  3 12 4.558E-02
  3 13 9.981E-03  3 14 4.763E-02  3 15 6.338E-02  3 16 3.506E-03  3 17 7.154E-02
  3 18 1.543E-01  3 19 2.868E-02  3 20 2.104E-04  4  1 4.776E-04  4  2 2.441E-03
  4  3 8.604E-03  4  4 2.231E-02  4  5 4.286E-02  4  6 5.903E-02  4  7 5.284E-02
  4  8 2.278E-02  4  9 3.107E-04  4 10 4.162E-02  4 11 3.102E-02  4 12 2.057E-03
  4 13 1.384E-02  4 14 2.859E-02  4 16 6.297E-02  4 17 2.450E-02  4 18 8.839E-02
  4 19 1.494E-01  4 20 1.189E-02  5  0 2.140E-04  5  1 1.563E-03  5  2 6.463E-03
  5  3 1.834E-02  5  4 3.756E-02  5  5 5.462E-02  5  6 5.185E-02  5  7 2.462E-02
  5  8 8.863E-04  5  9 1.169E-02  5 10 2.555E-02  5 11 9.533E-04  5 12 1.462E-02
  5 13 3.651E-02  5 14 1.906E-03  5 15 3.396E-02  5 16 8.541E-04  5 17 2.805E-02
  5 18 1.584E-02  5 19 1.384E-01  5 20 1.102E-01  5 21 1.694E-03  6  0 8.007E-04
  6  1 4.533E-03  6  2 1.487E-02  6  3 3.315E-02  6  4 5.168E-02  6  5 5.310E-02
  6  6 2.909E-02  6  7 2.669E-03  6  8 7.266E-03  6  9 2.986E-02  6 10 1.364E-03
  6 11 1.171E-02  6 12 3.032E-02  6 13 1.091E-02  6 14 2.913E-02  6 15 2.045E-02
  6 16 2.965E-02  6 17 3.096E-02  6 18 3.761E-02  6 19 1.295E-03  6 20 0.000E+00
  6 21 4.502E-02  7  0 2.732E-03  7  1 1.163E-02  7  2 2.957E-02  7  3 4.991E-02
  7  4 5.571E-02  7  5 3.501E-02  7  6 5.910E-03  7  7 3.508E-03  7  8 2.451E-02
  7  9 2.438E-02  7 10 7.875E-03  7 11 2.579E-02  7 12 1.041E-02  7 13 1.982E-03
  7 14 1.547E-02  7 15 6.758E-04  7 16 1.859E-02  7 17 8.836E-04  7 18 2.166E-02
  7 19 5.653E-02  7 20 2.086E-02  7 21 2.030E-01  7 22 6.649E-03  8  0 2.272E-02
  8  1 4.752E-02  8  2 6.504E-02  8  3 4.986E-02  8  4 1.606E-02  8  6 1.551E-02
  8  7 2.468E-02  8  8 7.102E-03  8  9 2.077E-03  8 10 1.226E-02  8 11 1.357E-04
  8 12 1.509E-02  8 13 1.338E-02  8 14 1.572E-02  8 15 1.224E-02  8 16 1.958E-02
  8 17 8.542E-03  8 18 2.511E-02  8 19 2.164E-02  8 20 5.973E-03  8 21 0.000E+00
  8 22 2.433E-01  8 23 1.599E-02  9  0 5.255E-02  9  1 6.827E-02  9  2 6.214E-02
  9  3 2.240E-02  9  4 1.873E-04  9  5 1.256E-02  9  6 2.450E-02  9  7 9.697E-03
  9  8 6.955E-04  9  9 1.524E-02  9 11 1.157E-02  9 12 1.326E-02  9 14 1.165E-02
  9 15 2.491E-04  9 16 7.723E-03  9 17 3.467E-03  9 18 1.668E-03  9 19 1.614E-02
  9 20 3.486E-02  9 21 5.754E-02  9 22 6.642E-02  9 23 1.387E-01  9 24 0.000E+00
 10  0 1.015E-01 10  1 6.956E-02 10  2 3.610E-02 10  3 9.781E-04 10  4 9.260E-03
 10  5 2.566E-02 10  6 1.193E-02 10  8 1.277E-02 10  9 1.389E-02 10 10 8.671E-03
 10 11 1.308E-02 10 12 4.079E-04 10 13 9.081E-03 10 15 1.218E-02 10 16 1.937E-03
 10 17 1.562E-02 10 18 1.041E-02 10 19 2.075E-03 10 20 2.150E-04 10 21 0.000E+00
 10 22 3.749E-02 10 23 2.378E-01 10 24 2.930E-03 11  0 2.010E-01 11  1 4.128E-03
 11  2 9.081E-04 11  3 3.431E-02 11  4 1.479E-02 11  5 1.310E-03 11  6 1.013E-02
 11  7 1.366E-02 11  8 2.956E-03 11  9 4.710E-03 11 10 2.317E-03 11 11 4.536E-03
 11 12 1.066E-02 11 13 6.973E-04 11 14 8.468E-03 11 15 1.868E-04 11 16 3.669E-03
 11 17 4.138E-03 11 19 2.462E-03 11 20 7.770E-03 11 21 1.372E-02 11 22 0.000E+00
 11 23 6.579E-02 11 24 1.756E-01 12  0 1.293E-01 12  1 8.939E-02 12  2 5.961E-03
 12  3 1.924E-02 12  4 1.544E-02 12  5 7.623E-03 12  6 1.198E-02 12  7 4.165E-03
 12  8 7.042E-03 12  9 7.446E-03 12 10 7.521E-03 12 11 3.516E-03 12 12 3.584E-03
 12 13 7.830E-03 12 14 6.465E-03 12 15 5.513E-03 12 16 9.053E-03 12 17 8.782E-04
 12 18 5.483E-03 12 19 9.831E-03 12 20 1.299E-02 12 21 1.678E-02 12 22 0.000E+00
CROSS-SECTIONS ASSUMED TO BE THE SAME AS FOR B-X OF CRANDALL ET AL
ELECTRON ENERGY=      6.41      8.08     12.12     16.17     20.21     30.31     40.42     60.62
CROSS SECTION  = 2.950E-16 2.830E-16 2.380E-16 1.900E-16 1.550E-16 1.100E-16 8.900E-17 6.800E-17
RADIATIVE TRANSITION PROBABILITY= 0.000E+00
IORD=  4
N2+MEI   LOWER STATE= 2  UPPER STATE= 3   NUMBER OF CARDS= 61
```

```
 0  0 9.858E-02  0  1 2.010E-01  0  2 2.274E-01  0  3 1.897E-01  0  4 1.304E-01
 0  5 7.827E-02  0  6 4.202E-02  0  7 2.023E-02  0  8 8.537E-03  0  9 2.978E-03
 1  0 2.331E-01  1  1 1.645E-01  1  2 2.267E-02  1  3 1.090E-02  1  4 7.699E-02
 1  5 1.276E-01  1  6 1.324E-01  1  7 1.054E-01  1  8 6.863E-02  1  9 3.678E-02
 1 10 4.559E-03  1 11 6.144E-04  1 13 1.757E-04  2  0 2.739E-01  2  1 1.263E-02
 2  2 6.140E-02  2  3 1.150E-01  2  4 4.835E-02  2  5 3.454E-04  2  6 2.816E-02
 2  7 8.558E-02  2  8 1.196E-01  2  9 1.136E-01  2 10 4.217E-02  2 11 1.476E-02
 2 12 2.383E-03  2 14 7.023E-04  2 15 2.225E-04  3  0 2.110E-01  3  1 4.466E-02
 3  2 1.213E-01  3  3 9.749E-03  3  4 3.071E-02  3  5 8.135E-02  3  6 4.921E-02
 3  7 3.362E-03  3  8 1.564E-02  3  9 7.232E-02  3 10 1.179E-01  3 11 7.927E-02
 3 12 3.386E-02  3 13 6.730E-03  3 14 1.545E-03  3 15 1.969E-03  3 17 2.360E-04
 4  0 1.175E-01  4  1 1.690E-01  4  2 1.948E-02  4  3 5.468E-02  4  4 7.808E-02
 4  5 6.532E-03  4  6 2.003E-02  4  7 5.987E-02  4  8 3.954E-02  4  9 2.300E-03
 4 10 8.239E-02  4 11 1.290E-01  4 12 1.155E-01  4 13 6.142E-02  4 14 1.524E-04
 4 15 2.870E-03  4 16 1.669E-03  4 17 4.403E-04  4 18 1.643E-04  4 19 1.416E-04
 5  0 4.856E-02  5  1 2.020E-01  5  2 3.091E-02  5  3 9.172E-02  5  4 1.427E-04
 5  5 5.362E-02  5  6 5.327E-02  5  7 3.333E-03  5  8 1.674E-02  5  9 4.537E-02
 5 11 3.722E-02  5 12 1.109E-01  5 13 1.385E-01  5 14 2.914E-02  5 15 8.684E-04
 5 16 8.187E-03  5 18 1.376E-03  6  0 1.438E-02  6  1 1.359E-01  6  2 1.596E-01
 6  3 5.523E-03  6  4 6.783E-02  6  5 3.898E-02  6  6 3.357E-03  6  7 4.840E-02
 6  8 3.482E-02  6  9 6.546E-04  6 10 3.239E-02  6 11 8.087E-03  6 12 8.612E-03
 6 13 7.689E-02  6 14 1.222E-01  6 15 4.813E-02  6 16 5.028E-03  6 17 6.864E-03
 6 18 1.326E-03  6 19 9.596E-04  7  0 2.712E-03  7  1 5.621E-02  7  2 1.997E-01
 7  3 6.253E-02  7  4 5.351E-02  7  5 1.062E-02  7  6 5.970E-02  7  7 1.205E-02
 7  8 1.061E-02  7  9 4.128E-02  7 10 2.364E-04  7 11 1.802E-02  7 12 1.626E-02
 7 13 1.344E-04  7 14 1.267E-01  7 15 1.416E-01  7 16 7.417E-03  7 17 1.839E-02
 7 18 8.947E-04  7 19 4.369E-03  8  0 2.265E-04  8  1 1.307E-02  8  2 1.197E-01
 8  3 2.014E-01  8  4 5.484E-03  8  5 7.101E-02  8  6 3.963E-03  8  7 3.053E-02
 8  8 3.781E-02  8  9 1.110E-03  8 10 3.166E-02  8 11 6.858E-03  8 12 3.060E-03
 8 13 1.345E-02  8 14 2.037E-02  8 15 1.016E-01  8 16 9.138E-02  8 17 3.263E-03
 8 18 1.800E-02  8 19 1.632E-03  9  2 2.899E-03  9  3 6.683E-02  9  4 2.357E-01
 9  5 9.423E-02  9  6 2.519E-02  9  7 1.073E-02  9  8 4.088E-02  9  9 3.076E-03
 9 10 2.651E-02  9 11 2.462E-03  9 12 9.289E-03  9 13 2.262E-02  9 14 3.273E-04
 9 15 1.999E-03  9 16 5.189E-02  9 17 1.177E-01  9 19 3.142E-02 10  3 5.339E-03
10  4 1.066E-01 10  5 2.639E-01 10  6 4.767E-02 10  7 3.430E-02 10  9 3.080E-02
10 10 1.842E-03 10 11 2.221E-02 10 12 1.092E-02 10 13 9.910E-04 10 14 1.444E-02
10 15 1.188E-03 10 16 1.529E-03 10 17 1.059E-01 10 18 4.941E-02 10 19 1.990E-02
11  2 2.245E-04 11  3 5.422E-04 11  4 7.679E-03 11  5 1.488E-01 11  6 2.729E-01
11  7 2.125E-02 11  8 2.682E-02 11  9 7.368E-03 11 10 2.274E-02 11 11 7.674E-04
11 12 1.179E-02 11 13 1.601E-02 11 14 9.282E-03 11 15 1.739E-02 11 16 2.068E-04
11 17 2.478E-02 11 18 1.150E-01 11 19 3.166E-03 12  4 1.740E-03 12  5 6.393E-03
12  6 8.011E-03 12  7 2.178E-01 12  8 2.616E-01 12  9 6.698E-03 12 10 2.786E-02
12 12 1.370E-02 12 13 1.038E-02 12 14 1.144E-02 12 15 7.056E-03 12 16 1.222E-02
12 17 5.755E-03 12 18 1.538E-02 12 19 9.503E-02 13  5 3.214E-03 13  6 1.501E-02
13  7 4.955E-03 13  8 2.330E-01 13  9 2.522E-01 13 10 6.575E-04 13 11 3.209E-02
13 12 6.402E-04 13 13 7.041E-03 13 14 2.754E-04 13 15 7.066E-03 13 17 1.549E-02
13 18 5.836E-03 13 19 4.587E-02 14  5 5.767E-04 14  6 1.754E-03 14  7 4.791E-03
14  8 4.951E-02 14  9 3.759E-04 14 10 2.299E-01 14 11 2.551E-02 14 12 2.676E-02
14 13 3.778E-02 14 14 4.100E-04 14 15 1.029E-02 14 16 1.588E-03 14 17 1.967E-03
14 18 1.280E-02 14 19 1.100E-02 15  6 9.381E-04 15  7 5.386E-03 15  8 3.030E-03
15  9 7.132E-02 15 10 1.560E-01 15 11 2.100E-01 15 12 4.166E-02 15 13 5.199E-02
15 14 7.912E-04 15 16 3.713E-03 15 17 6.440E-03 15 18 8.720E-04 15 19 1.529E-02
16  6 1.202E-04 16  7 1.720E-03 16  8 3.403E-04 16  9 2.191E-02 16 10 8.807E-02
16 11 6.016E-02 16 12 4.443E-02 16 13 1.331E-01 16 14 1.157E-01 16 15 7.365E-02
16 16 3.836E-03 16 17 3.492E-03 16 18 4.125E-03 17  7 6.160E-04 17  9 6.856E-03
17 10 2.998E-02 17 11 3.679E-02 17 12 3.610E-02 17 13 1.144E-01 17 14 3.202E-02
17 15 5.362E-02 17 16 1.268E-01 17 17 1.735E-02 17 18 1.586E-03 17 19 2.835E-03
18  7 1.227E-04 18  8 4.722E-04 18  9 1.124E-03 18 10 4.144E-03 18 11 3.253E-02
18 12 3.762E-03 18 13 8.621E-02 18 14 6.917E-02 18 15 3.329E-02 18 16 4.071E-03
18 17 1.678E-01 18 18 5.230E-02 19  8 3.651E-04 19 10 7.526E-04 19 11 1.653E-02
19 12 6.207E-03 19 13 3.946E-02 19 14 3.596E-02 19 15 4.942E-02 19 16 1.820E-02
CROSS-SECTIONS ASSUMED TO BE THE SAME AS FOR X-B OF CRANDALL ETAL
ELECTRON ENERGY=       2.05       2.59       3.88       5.18       6.47       9.71      12.95      19.42
CROSS SECTION  = 2.950E-16 2.830E-16 2.380E-16 1.900E-16 1.550E-16 1.100E-16 8.900E-17 6.800E-17
RADIATIVE TRANSITION PROBABILITY= 0.000E+00
```

```
IORD=  5
N2+JDI   LOWER STATE= 2  UPPER STATE= 4   NUMBER OF CARDS= 14
  0  0 2.625E-06  0  2 3.782E-04  0  3 1.989E-03  0  4 7.451E-03  0  5 2.116E-02
  1  1 3.153E-04  1  2 2.208E-03  1  3 9.528E-03  1  4 2.820E-02  1  5 6.006E-02
  2  1 1.156E-03  2  2 6.808E-03  2  3 2.286E-02  2  4 5.450E-02  2  5 8.260E-02
  3  0 2.676E-04  3  1 2.992E-03  3  2 1.475E-02  3  3 4.141E-02  3  4 6.928E-02
  4  0 6.370E-04  4  1 6.138E-03  4  2 2.518E-02  4  3 5.561E-02  4  4 6.688E-02
  4  5 3.501E-02  5  0 1.282E-03  5  1 1.063E-02  5  2 3.603E-02  5  3 6.105E-02
  5  4 4.737E-02  5  5 7.281E-03  6  0 2.267E-03  6  1 1.617E-02  6  2 4.487E-02
  6  3 5.632E-02  6  4 2.363E-02  6  5 2.567E-04  7  0 3.621E-03  7  1 2.217E-02
  7  2 4.982E-02  7  3 4.401E-02  7  4 6.369E-03  7  5 9.586E-03  8  0 5.322E-03
  8  1 2.793E-02  8  2 5.016E-02  8  3 2.875E-02  8  4 5.422E-02  8  5 2.267E-02
  9  0 7.306E-03  9  1 3.282E-02  9  2 4.629E-02  9  3 1.493E-03  9  4 3.046E-03
  9  5 2.972E-02 10  0 9.470E-03 10  1 3.634E-02 10  2 3.939E-02 10  3 5.296E-03
 10  4 1.062E-02 10  5 2.806E-02 11  0 1.169E-02 11  1 3.827E-02 11  2 3.098E-02
 11  3 6.495E-04 11  4 1.808E-02 11  5 2.041E-02  0  1 4.563E-05  1  0 2.100E-05
CROSS-SECTIONS ASSUMED TO BE THE SAME AS FOR X-B OF CRANDALL ETAL
ELECTRON ENERGY=      5.29      6.67      10.01      13.35      16.68      25.02      33.36      50.04
CROSS SECTION  = 2.950E-16 2.830E-16 2.380E-16 1.900E-16 1.550E-16 1.100E-16 8.900E-17 6.800E-17
RADIATIVE TRANSITION PROBABILITY= 0.000E+00
IORD=  6
N2+JDI   LOWER STATE= 3  UPPER STATE= 4   NUMBER OF CARDS= 43
  0  7 1.400E-04  0  8 6.043E-04  0  9 7.837E-03  0 10 2.271E-02  0 11 5.541E-02
  0 12 1.799E-01  0 13 2.263E-01  0 14 1.314E-01  0 15 4.570E-02  1  6 2.347E-04
  1  7 9.487E-04  1  8 3.397E-03  1  9 2.759E-02  1 10 5.842E-02  1 11 9.454E-02
  1 12 6.349E-02  1 13 4.704E-03  1 14 1.817E-01  1 15 2.540E-01  1 16 1.953E-02
  1 17 4.728E-04  2  5 2.643E-04  2  6 1.016E-03  2  7 3.458E-03  2  8 1.021E-02
  2  9 5.059E-02  2 10 7.533E-02  2 11 7.295E-02  2 13 4.086E-02  2 14 1.873E-02
  2 15 4.644E-02  2 16 2.376E-01  2 17 1.340E-03  2 18 1.174E-03  3  4 2.611E-04
  3  5 9.672E-04  3  6 3.154E-03  3  7 8.963E-03  3  8 2.160E-02  3  9 6.202E-02
  3 10 5.959E-02  3 11 2.542E-02  3 12 2.943E-02  3 13 5.398E-02  3 14 2.494E-02
  3 15 7.028E-02  3 16 2.159E-01  3 17 4.280E-02  3 18 6.927E-03  3 19 1.089E-03
  4  3 2.491E-04  4  4 9.037E-04  4  5 2.846E-03  4  6 7.804E-03  4  7 1.832E-02
  4  8 3.544E-02  4  9 5.343E-02  4 10 2.664E-02  4 11 5.688E-04  4 12 4.220E-02
  4 13 1.237E-02  4 14 4.757E-02  4 15 2.575E-03  4 16 1.230E-02  4 17 3.780E-01
  4 18 3.457E-02  4 19 2.702E-04  5  2 2.367E-04  5  3 8.676E-04  5  4 2.671E-03
  5  5 7.086E-03  5  6 1.615E-02  5  7 3.080E-02  5  8 4.649E-02  5  9 2.979E-02
  5 10 3.001E-03  5 11 8.579E-03  5 12 1.775E-02  5 13 1.744E-03  5 14 1.063E-02
  5 15 1.880E-02  5 16 1.431E-02  5 17 1.539E-01  5 18 4.112E-01  5 19 3.821E-02
  6  1 2.178E-04  6  2 8.595E-04  6  3 2.654E-03  6  4 6.865E-03  6  5 1.516E-02
  6  6 2.822E-02  6  7 4.257E-02  6  8 4.771E-02  6  9 6.853E-03  6 10 2.823E-03
  6 11 2.488E-02  6 12 1.644E-04  6 13 1.976E-02  6 14 2.658E-03  6 15 3.042E-02
  6 16 3.599E-02  6 17 1.765E-02  6 18 1.712E-01  7  0 1.727E-04  7  1 8.435E-04
  7  2 2.765E-03  7  3 7.111E-03  7  4 1.526E-02  7  5 2.754E-02  7  6 4.079E-02
  7  7 4.643E-02  7  8 3.489E-02  7  9 3.820E-04  7 10 1.705E-02  7 11 2.399E-02
  7 12 8.803E-03  7 13 2.183E-02  7 14 1.994E-02  7 15 6.925E-03  7 16 7.100E-03
  7 17 9.588E-04  7 18 6.941E-03  7 19 3.421E-01  8  0 2.867E-03  8  1 8.360E-03
  8  2 1.825E-02  8  3 3.094E-02  8  4 4.274E-02  8  5 4.639E-02  8  6 3.593E-02
  8  7 1.472E-02  8  8 3.228E-04  8  9 2.106E-02  8 10 1.145E-02  8 11 1.462E-04
  8 12 1.049E-02  8 13 1.107E-03  8 14 9.045E-04  8 15 1.486E-02  8 16 1.706E-02
  8 17 1.621E-02  8 18 1.177E-02  8 19 7.529E-03  9  0 9.386E-03  9  1 2.003E-02
  9  2 3.486E-02  9  3 4.571E-02  9  4 4.740E-02  9  5 3.498E-02  9  6 1.414E-02
  9  7 4.308E-04  9  8 6.384E-03  9  9 1.362E-02  9 10 2.217E-04  9 11 9.246E-03
  9 12 1.145E-04  9 13 1.121E-02  9 14 5.186E-03  9 15 9.625E-03  9 16 7.202E-03
  9 17 3.854E-04  9 18 1.447E-02  9 19 1.089E-02 10  0 2.588E-02 10  1 3.808E-02
 10  2 5.164E-02 10  3 4.874E-02 10  4 3.393E-02 10  5 1.229E-02 10  6 2.351E-04
 10  7 6.373E-03 10  8 1.858E-02 10  9 1.047E-03 10 10 5.866E-03 10 11 1.372E-02
 10 12 5.994E-03 10 13 9.979E-03 10 14 1.182E-02 10 16 4.727E-04 10 17 7.276E-03
 10 18 7.282E-04 10 19 1.407E-02 11  0 1.113E-01 11  1 5.352E-02 11  2 3.960E-02
 11  3 7.436E-03 11  5 9.672E-03 11  6 1.900E-02 11  7 1.508E-02 11  8 1.939E-03
 11  9 1.243E-02 11 10 5.944E-03 11 11 6.697E-04 11 12 2.967E-03 11 13 3.581E-03
 11 14 8.869E-04 11 15 8.174E-03 11 16 6.102E-03 11 17 5.154E-04 11 18 8.523E-03
 12  0 1.993E-01 12  1 1.168E-03 12  2 4.138E-04 12  3 2.162E-02 12  4 1.619E-02
 12  5 1.654E-02 12  6 6.967E-04 12  7 2.334E-03 12  8 1.279E-02 12 10 6.565E-03
 12 11 6.843E-03 12 12 6.989E-03 12 13 2.334E-03 12 14 4.345E-03 12 15 2.758E-03
```

```
CROSS-SECTIONS ASSUMEDTO BE THE SAME AS FOR X-B OF CRANDALL ET AL
ELECTRON ENERGY=      3.23      4.08      6.13      8.17     10.21     15.31     20.42     30.62
CROSS SECTION  = 2.950E-16 2.830E-16 2.380E-16 1.900E-16 1.550E-16 1.100E-16 8.900E-17 6.800E-17
RADIATIVE TRANSITION PROBABILITY= 0.000E+00


MOLECULAR BAND NAME=N2      MOLECULAR WEIGHT=    28.010
NUMBER OF ELECTRON-IMPACT DISSOCIATION CROSS-SECTION SET= 4
NUMBER OF ELECTRON-IMPACT EXCITATION CROSS-SECTION SET  = 6
NUMBER OF ELECTRONIC LEVELS                             = 5
NUMBER OF LEVELS IN QUASI-STEADY-STATE CALC.            = 4
 DEGEN      TERM       WE       WEXE      WEYE      WEZE       BE      ALPHA
    1.000     0.000  2358.027    14.135    -0.018     0.000   1.99800 1.772E-02
    3.000 49754.800  1460.518    13.831     0.006     0.002   1.45455 1.801E-02
    6.000 59306.800  1733.391    14.122    -0.057    -0.004   1.63740 1.791E-02
    2.000 68951.200  1694.208    13.949     0.008     0.000   1.61688 1.793E-02
    6.000 88977.900  2047.178    28.445     2.088     0.535   1.82473 1.868E-02

DISSOCIATED STATE
N  4S    ATOM. WT.=  14.010  DISSOC. ENERGY=   78720. CM-1  STATISTICAL WT.=  4.0
N  4S    ATOM. WT.=  14.010  DISSOC. ENERGY=   78720. CM-1  STATISTICAL WT.=  4.0

ELECTRON-IMPACT DISSOCIATION CROSS-SECTIONS
CROSS-SECTIONS ASSUMED SAME AS FOR N2 1-3 OF CARTWRIGHT ET AL
DISSOCIATION ENERGY =   78734.0 CM-1
ELECTRON ENERGY=      9.76     10.62     13.27     15.93     19.91     26.55     34.51     47.78
CROSS SECTION  = 0.000E+00 5.400E-18 2.250E-17 2.990E-17 2.410E-17 1.560E-17 1.200E-17 7.600E-18
CROSS-SECTIONS ASSUMED SAME AS FOR N2 1-3 OF CARTWRIGHT ET AL
DISSOCIATION ENERGY =   78734.0 CM-1
ELECTRON ENERGY=      3.59      3.91      4.88      5.86      7.32      9.77     12.70     17.58
CROSS SECTION  = 0.000E+00 5.400E-18 2.250E-17 2.990E-17 2.410E-17 1.560E-17 1.200E-17 7.600E-18
CROSS-SECTIONS ASSUMED SAME AS FOR N2 1-3 OF CARTWRIGHT ET AL
DISSOCIATION ENERGY =  107559.0 CM-1
ELECTRON ENERGY=      5.98      6.51      8.13      9.76     12.20     16.27     21.15     29.28
CROSS SECTION  = 0.000E+00 5.400E-18 2.250E-17 2.990E-17 2.410E-17 1.560E-17 1.200E-17 7.600E-18
CROSS-SECTIONS ASSUMED SAME AS FOR N2 1-3 OF CARTWRIGHT ET AL
DISSOCIATION ENERGY =  126787.0 CM-1
ELECTRON ENERGY=      7.17      7.80      9.75     11.70     14.62     19.50     25.35     35.10
CROSS SECTION  = 0.000E+00 5.400E-18 2.250E-17 2.990E-17 2.410E-17 1.560E-17 1.200E-17 7.600E-18

FRANCK-CONDON FACTOR DATA
IORD=  7
N2 VK    LOWER STATE= 1  UPPER STATE= 2   NUMBER OF CARDS= 72
  0  0 5.900E-04  0  1 5.337E-03  0  2 2.286E-02  0  3 6.167E-02  0  4 1.176E-01
  0  5 1.688E-01  0  6 1.894E-01  0  7 1.704E-02  0  8 1.250E-01  0  9 7.578E-02
  0 10 3.828E-02  0 11 1.621E-02  0 12 5.780E-03  0 13 1.738E-03  0 14 4.411E-04
  1  0 3.319E-03  1  1 2.278E-02  1  2 6.919E-02  1  3 1.193E-01  1  4 1.216E-01
  1  5 6.383E-02  1  6 6.256E-03  1  7 1.395E-02  1  8 7.866E-02  1  9 1.370E-01
  1 10 1.450E-01  1 11 1.100E-01  1 12 6.404E-02  1 13 2.963E-02  1 14 1.110E-02
  2  0 9.975E-03  2  1 5.085E-02  2  2 1.035E-01  2  3 9.732E-02  2  4 2.922E-02
  2  5 2.161E-03  2  6 5.473E-02  2  7 8.924E-02  2  8 4.616E-02  2  9 8.840E-04
  2 10 2.955E-02  2 11 1.001E-01  2 12 1.378E-01  2 13 1.196E-01  2 14 7.472E-02
  3  0 2.133E-02  3  1 7.850E-02  3  2 9.768E-02  3  3 3.326E-02  3  4 2.539E-03
  3  5 5.617E-02  3  6 6.391E-02  3  7 8.564E-03  3  8 1.697E-02  3  9 7.318E-02
  3 10 6.181E-02  3 11 7.600E-03  3 12 1.520E-02  3 13 8.383E-02  3 14 1.315E-01
  4  0 3.642E-02  4  1 9.328E-02  4  2 5.998E-02  4  3 3.714E-04  4  4 4.107E-02
  4  5 5.758E-02  4  6 4.625E-03  4  7 2.554E-02  4  8 6.331E-02  4  9 1.916E-02
  4 10 7.127E-03  4 11 6.276E-02  4 12 6.314E-02  4 13 9.383E-03  4 14 1.379E-02
  5  0 5.290E-02  5  1 8.962E-02  5  2 2.011E-02  5  3 1.465E-02  5  4 5.868E-02
  5  5 1.223E-02  5  6 1.688E-02  5  7 5.462E-02  5  8 1.065E-02  5  9 1.643E-02
  5 10 5.871E-02  5 11 2.016E-02  5 12 6.585E-03  5 13 6.143E-02  5 14 5.832E-02
  6  0 6.799E-02  6  1 7.082E-02  6  2 8.381E-04  6  3 4.233E-02  6  4 3.400E-02
  6  5 2.630E-03  6  6 4.768E-02  6  7 1.641E-02  6  8 1.163E-02  6  9 5.008E-02
  6 10 9.734E-03  6 11 1.729E-02  6 12 5.579E-02  6 13 1.457E-02  6 14 1.131E-02
  7  0 7.939E-02  7  1 4.539E-02  7  2 5.264E-03  7  3 5.154E-02  7  4 5.402E-03
```

```
 7  5 2.805E-02  7  6 3.237E-02  7  7 1.710E-03  7  8 4.308E-02  7  9 1.308E-02
 7 10 1.409E-02  7 11 4.635E-02  7 12 4.785E-02  7 13 2.447E-02  7 14 5.170E-02
 8  0 8.588E-02  8  1 2.205E-02  8  2 2.231E-02  8  3 3.803E-02  8  4 1.933E-03
 8  5 4.203E-02  8  6 4.185E-03  8  7 2.701E-02  8  8 2.572E-02  8  9 4.073E-03
 8 10 4.148E-02  8 11 6.297E-03  8 12 2.185E-02  8 13 4.002E-02  8 14 3.600E-04
 9  0 8.730E-02  9  1 6.435E-03  9  2 3.838E-02  9  3 1.651E-02  9  4 1.815E-02
 9  5 2.890E-02  9  6 3.763E-03  9  7 3.696E-02  9  8 8.855E-04  9  9 3.109E-02
 9 10 1.592E-02  9 11 1.083E-02  9 12 3.765E-02  9 13 6.326E-04  9 14 3.284E-02
10  0 8.434E-02 10  1 2.053E-04 10  2 4.527E-02 10  3 2.254E-03 10  4 3.349E-02
10  5 8.054E-03 10  6 2.242E-02 10  7 1.837E-02 10  8 9.744E-03 10  9 3.026E-02
10 10 5.291E-04 10 11 3.475E-02 10 12 5.380E-03 10 13 2.218E-02 10 14 2.757E-02
11  0 7.812E-02 11  1 2.015E-03 11  2 4.180E-02 11  3 9.890E-04 11  4 3.530E-02
11  5 1.684E-05 11  6 3.257E-02 11  7 1.243E-03 11  8 2.835E-02 11  9 7.166E-02
11 10 1.963E-02 11 11 1.892E-02 11 12 7.224E-03 11 13 3.197E-02 11 14 5.829E-06
12  0 6.988E-02 12  1 9.015E-03 12  2 3.141E-02 12  3 9.423E-03 12  4 2.493E-02
12  5 7.426E-03 12  6 2.478E-02 12  7 4.205E-03 12  8 2.719E-02 12  9 9.855E-04
12 10 2.962E-02 12 11 2.597E-04 12 12 2.853E-02 12 13 5.872E-03 12 14 2.016E-02
13  0 6.071E-02 13  1 1.817E-02 13  2 1.899E-02 13  3 2.061E-02 13  4 1.116E-02
13  5 2.003E-02 13  6 9.630E-03 13  7 1.809E-02 13  8 1.114E-02 13  9 1.477E-02
13 10 1.519E-02 13 11 9.782E-03 13 12 2.152E-02 13 13 3.791E-03 13 14 2.831E-04
14  0 5.149E-02 14  1 2.707E-02 14  2 8.494E-03 14  3 2.870E-02 14  4 1.925E-03
14  5 2.732E-02 14  6 5.698E-04 14  7 2.605E-02 14  8 4.334E-04 14  9 2.527E-02
14 10 9.608E-04 14 11 2.437E-02 14 12 2.827E-03 14 13 2.209E-02 14 14 7.438E-03
15  0 4.280E-02 15  1 3.418E-02 15  2 2.038E-03 15  3 3.106E-02 15  4 2.871E-04
15  5 2.560E-02 15  6 2.212E-03 15  7 2.191E-02 15  8 3.623E-03 15  9 2.041E-02
15 10 3.825E-03 15 11 2.086E-02 15 12 2.852E-03 15 13 2.288E-02 15 14 1.148E-03
 2 15 3.567E-02  2 16 1.342E-02  2 17 4.046E-03  3 15 1.197E-01  3 16 7.543E-02
 3 17 3.543E-02  3 18 1.287E-02  3 19 3.690E-03  4 15 8.294E-02  4 16 1.299E-01
 4 17 1.152E-01  4 18 6.961E-02  4 19 3.095E-02  5 15 5.905E-03  5 16 1.982E-02
 5 17 9.210E-02  5 18 1.304E-01  5 19 1.066E-01  6 15 6.531E-02  6 16 4.826E-02
 6 17 1.141E-03  6 18 3.366E-02  6 19 1.068E-01  6 20 1.289E-01  5 20 0.000E+00
 6 21 9.341E-02  6 22 4.662E-02  6 23 1.704E-02  6 24 4.706E-03  7 20 0.000E+00
 7 15 6.143E-03  7 16 2.227E-02  7 17 6.887E-02  7 18 3.475E-02  7 21 0.000E+00
 7 22 1.217E-01  7 23 7.625E-02  7 24 3.334E-02  7 25 1.070E-02  8 15 3.610E-03
 8 16 4.227E-02  8 18 3.936E-02  8 19 6.567E-02  8 20 1.463E-02  8 21 0.000E+00
 8 22 8.420E-02  8 23 1.305E-01  8 24 1.069E-01  8 25 5.701E-02  8 26 0.000E+00
 9 15 2.810E-02  9 16 2.261E-03  9 17 4.748E-02  9 18 2.603E-02  9 19 3.787E-03
 9 20 5.775E-02  9 21 5.110E-02  9 22 1.516E-03  9 23 3.563E-02  9 24 0.000E+00
 9 25 1.284E-01  9 26 8.575E-02  9 27 3.813E-02 10 15 1.944E-03 10 16 4.137E-02
10 17 1.221E-02 10 18 1.464E-02 10 19 5.044E-02 10 21 2.086E-02 10 22 0.000E+00
10 23 2.717E-02 10 25 7.141E-02 10 26 1.302E-01 10 27 1.136E-01 11 15 3.333E-02
11 16 1.235E-02 11 17 1.382E-02 11 18 3.941E-02 11 20 3.440E-02 11 21 0.000E+00
11 23 4.661E-02 11 24 5.915E-02 11 26 2.730E-02 11 27 1.082E-01 12 15 1.998E-02
12 16 6.000E-03 12 17 3.526E-02 12 19 3.137E-02 12 20 2.308E-02 12 22 0.000E+00
12 23 1.619E-02 12 24 1.223E-02 12 25 6.568E-02 12 26 3.347E-02 13 16 3.060E-02
13 18 2.180E-02 13 19 2.293E-02 13 21 4.054E-02 13 23 2.521E-02 13 24 0.000E+00
13 26 4.106E-02 13 27 6.174E-02 14 15 1.686E-02 14 16 1.609E-02 14 18 2.250E-02
14 20 3.395E-02 14 22 2.305E-02 14 23 3.004E-02 14 25 4.613E-02 14 26 0.000E+00
15 15 2.563E-02 15 17 2.719E-02 15 19 2.415E-02 15 20 1.140E-02 15 21 0.000E+00
15 22 2.799E-02 15 24 3.891E-02 15 26 2.121E-02 15 27 4.501E-02 16 21 0.000E+00
CROSS-SECTIONS FROM CARTWRIGHT
ELECTRON ENERGY=      6.17      7.00      9.00     11.00     14.00     17.00     20.00     26.00
CROSS SECTION  = 0.000E+00 3.000E-18 9.400E-18 1.480E-17 2.040E-17 2.250E-17 1.830E-17 1.130E-17
RADIATIVE TRANSITION PROBABILITY= 0.000E+00
IORD=  8
N2  BX   LOWER STATE= 1  UPPER STATE= 3   NUMBER OF CARDS= 28
  0  0 6.117E-02  0  1 1.909E-01  0  2 2.753E-01  0  3 2.416E-01  0  4 1.442E-01
  0  5 6.185E-02  0  6 1.953E-02  0  7 4.555E-03  0  8 7.694E-04  1  0 1.487E-01
  1  1 1.921E-01  1  2 4.450E-02  1  3 1.658E-02  1  4 1.444E-01  1  5 2.072E-01
  1  6 1.509E-01  1  7 6.917E-02  1  8 2.138E-02  1  9 4.492E-03  1 10 6.123E-04
  2  0 1.999E-01  2  1 6.307E-02  2  2 2.445E-02  2  3 1.293E-01  2  4 4.565E-02
  2  5 1.167E-02  2  6 1.314E-01  2  7 1.908E-01  2  8 1.322E-01  2  9 5.475E-02
  2 10 1.434E-02  2 11 1.996E-04  3  0 1.969E-01  3  1 1.978E-04  3  2 1.039E-01
  3  3 3.337E-02  3  4 3.276E-02  3  5 1.086E-01  3  6 2.046E-02  3  7 3.142E-02
  3  8 1.547E-01  3  9 1.769E-01  3 10 1.006E-01  3 11 6.368E-03  3 12 6.241E-04
```

```
  4  0 1.585E-01  4  1 3.398E-02  4  2 7.628E-02  4  3 9.215E-03  4  4 8.940E-02
  4  5 4.742E-03  4  6 6.269E-02  4  7 8.009E-02  4  8 5.373E-04  4  9 7.885E-02
  4 10 1.807E-01  4 11 6.192E-02  4 12 1.426E-02  4 13 1.602E-03  5  0 1.099E-01
  5  1 9.570E-02  5  2 1.173E-02  5  3 6.681E-02  5  4 1.986E-02  5  5 4.484E-02
  5  6 5.414E-02  5  7 5.903E-03  5  8 8.773E-02  5  9 3.286E-02  5 10 1.764E-02
  5 11 1.796E-01  5 12 9.843E-02  5 13 2.745E-02  5 14 3.571E-03  6  0 6.681E-02
  6  1 1.298E-01  6  2 7.534E-03  6  3 6.134E-02  6  4 8.044E-03  6  5 6.331E-02
  6  6 1.317E-03  6  7 6.981E-02  6  8 9.108E-03  6  9 4.561E-02  6 10 7.154E-02
  6 11 8.608E-02  6 12 1.876E-01  6 13 1.375E-01  6 14 4.692E-02  6 15 2.910E-04
  7  0 3.542E-02  7  1 1.236E-01  7  2 6.025E-02  7  3 1.155E-02  7  4 5.031E-02
  7  5 8.094E-03  7  6 5.130E-02  7  7 1.502E-02  7  8 3.624E-02  7  9 4.307E-02
  7 10 7.110E-03  7 11 1.956E-02  7 12 3.391E-02  7 13 1.690E-01  7 14 1.718E-01
  7 15 1.304E-02  7 16 6.258E-04  8  0 1.578E-02  8  1 9.080E-02  8  2 1.133E-01
  8  3 7.048E-03  8  4 4.075E-02  8  5 1.139E-02  8  6 4.011E-02  8  7 1.422E-02
  8  8 4.374E-02  8  9 4.418E-03  8 10 5.827E-02  8 11 5.267E-02  8 12 4.908E-02
  8 13 4.720E-03  8 14 1.308E-01  8 15 1.030E-01  8 16 2.201E-02  8 17 1.265E-03
  9  0 5.388E-03  9  1 5.162E-02  9  2 1.249E-01  9  3 6.428E-02  9  4 2.636E-03
  9  5 3.857E-02  9  6 8.992E-04  9  7 5.011E-02  9  9 4.652E-02  9 10 3.142E-03
  9 11 2.077E-02  9 12 2.099E-02  9 13 6.614E-02  9 14 1.418E-03  9 15 2.013E-01
CROSS-SECTIONS FROM CARTWRIGHT
ELECTRON ENERGY=      7.35      8.00      10.00      12.00      15.00      20.00      0.03      36.00
CROSS SECTION  = 0.000E+00 5.400E-18 2.250E-17 2.990E-17 2.410E-17 1.560E-17 1.200E-17 7.600E-18
RADIATIVE TRANSITION PROBABILITY= 0.000E+00
IORD=  9
N2 LBH   LOWER STATE= 1  UPPER STATE= 4   NUMBER OF CARDS= 38
  0  0 4.315E-02  1  0 1.162E-01  2  0 1.713E-01  3  0 1.835E-01  4  0 1.603E-01
  5  0 1.214E-01  6  0 8.287E-02  7  0 5.230E-02  8  0 3.109E-02  9  0 1.764E-02
 10  0 9.661E-03 11  0 5.146E-03 12  0 2.684E-03 13  0 1.378E-03  0  1 1.517E-01
  1  1 1.932E-01  2  1 9.677E-02  3  1 1.212E-02  4  1 6.391E-03  5  1 4.706E-02
  6  1 8.542E-02  7  1 9.971E-02  8  1 9.216E-02  9  1 7.346E-02 10  1 5.285E-02
 11  1 3.530E-02 12  1 2.230E-02 13  1 1.350E-02 14  1 7.917E-03  0  2 2.477E-01
  1  2 8.049E-02  2  2 3.276E-03  3  2 7.554E-02  4  2 9.661E-02  5  2 4.668E-02
  6  2 4.538E-03  7  2 5.796E-03  8  2 3.372E-02  9  2 6.105E-02 10  2 7.378E-02
 11  2 7.163E-02 12  2 6.044E-02 13  2 4.625E-02 14  2 3.296E-02  0  3 2.492E-01
  2  3 1.074E-01  3  3 6.931E-02  4  3 5.812E-04  5  3 3.392E-02  6  3 7.289E-02
  7  3 5.658E-02  8  3 1.826E-02  9  3 1.314E-04 10  3 9.747E-03 11  3 3.200E-02
 12  3 5.101E-02 13  3 5.954E-02 14  3 5.797E-02  0  4 1.731E-01  1  4 8.732E-02
  2  4 8.598E-02  3  4 3.606E-03  4  4 7.744E-02  5  4 5.670E-02  6  4 2.795E-03
  7  4 1.717E-02  8  4 5.340E-02  9  4 5.485E-02 10  4 2.795E-02 11  4 4.549E-03
 12  4 1.158E-03 13  4 1.398E-02 14  4 3.142E-02  0  5 8.808E-02  1  5 1.851E-01
  3  5 9.511E-02  4  5 3.735E-02  5  5 8.364E-03  6  5 6.347E-02  7  5 4.694E-02
  8  5 4.209E-03  9  5 9.234E-03 10  5 3.918E-02 11  5 4.918E-02 12  5 3.299E-02
 13  5 1.091E-02 14  5 2.538E-04  0  6 3.399E-02  1  6 1.752E-01  2  6 6.451E-02
  3  6 6.580E-02  4  6 1.689E-02  5  6 7.882E-02  6  6 1.485E-02  7  6 1.278E-02
 11  6 4.904E-03 12  6 2.860E-02 13  6 4.237E-02 14  6 3.472E-02  0  7 1.017E-02
  1  7 1.032E-01  2  7 1.640E-01  4  7 9.667E-02  5  7 7.912E-03  6  7 4.042E-02
  7  7 5.731E-02  8  7 4.748E-03  9  7 1.587E-02 10  7 4.743E-02 11  7 3.446E-02
 12  7 5.828E-03 13  7 2.321E-03 14  7 2.040E-02  0  8 2.392E-03  1  8 4.250E-02
  2  8 1.614E-01  3  8 7.840E-02  4  8 3.615E-02  5  8 4.675E-02  6  8 5.502E-02
  7  8 1.040E-03  8  8 5.031E-02  9  8 3.869E-02 11  8 1.742E-02 12  8 4.169E-02
 13  8 3.071E-02 14  8 6.695E-03  0  9 4.454E-04  1  9 1.289E-02  2  9 9.406E-02
  3  9 1.632E-01  4  9 9.168E-03  5  9 8.536E-02  6  9 2.010E-03  7  9 6.755E-02
  8  9 1.751E-02  9  9 1.174E-02 10  9 4.934E-02 11  9 2.518E-02 13  9 1.758E-02
 14  9 3.680E-02  1 10 2.968E-03  2 10 3.718E-02  3 10 1.431E-01  4 10 1.085E-01
  5 10 7.958E-03  6 10 7.874E-02  7 10 1.538E-02  8 10 3.144E-02  9 10 5.074E-02
 10 10 1.843E-03 11 10 2.257E-02 12 10 4.332E-02 13 10 1.638E-02  1 11 5.266E-04
  2 11 1.060E-02  3 11 7.518E-02  4 11 1.626E-01  5 11 3.911E-02  6 11 5.144E-02
  7 11 3.210E-02  8 11 5.359E-02  9 11 1.246E-03 10 11 4.905E-02 11 11 2.698E-02
 13 11 2.865E-02 14 11 3.626E-02  2 12 2.253E-03  3 12 2.676E-02  4 12 1.179E-01
  5 12 1.402E-01  6 12 1.628E-03  7 12 8.354E-02  8 12 1.043E-03  9 12 6.308E-02
 10 12 1.151E-02 11 12 1.839E-02 12 12 4.567E-02 13 12 1.068E-02 14 12 4.524E-03
  3 13 6.824E-03  4 13 5.304E-02  5 13 1.499E-01  6 13 8.717E-02  7 13 1.195E-02
  8 13 7.317E-02  9 13 1.239E-02 10 13 3.555E-02 11 13 4.096E-02 13 13 3.303E-02
CROSS-SECTIONS FROM CARTWRIGHT
ELECTRON ENERGY=      8.55      9.00      11.00      13.00      15.00      18.00      22.00      30.00
```

```
CROSS SECTION  = 0.000E+00 1.300E-18 9.900E-18 1.800E-17 2.560E-17 2.970E-17 2.580E-17 2.040E-17
RADIATIVE TRANSITION PROBABILITY= 5.880E+03
IORD= 10
N2 1+    LOWER STATE= 2  UPPER STATE= 3   NUMBER OF CARDS= 36
  0  0 3.382E-01  1  0 4.065E-01  2  0 1.975E-01  3  0 5.014E-02  4  0 7.191E-03
  5  0 5.871E-04  6  0 2.616E-05  0  1 3.248E-01  1  1 2.310E-03  2  1 2.120E-01
  3  1 2.987E-01  4  1 1.318E-01  5  1 2.729E-02  6  1 2.925E-03  7  1 1.613E-04
  0  2 1.900E-01  1  2 1.032E-01  2  2 1.132E-01  3  2 3.868E-02  4  2 2.738E-01
  5  2 2.107E-01  6  2 6.148E-02  7  2 8.462E-03  8  2 5.675E-04  9  2 1.719E-05
  0  3 8.857E-02  1  3 1.782E-01  2  3 1.205E-03  3  3 1.623E-01  4  3 1.807E-03
  5  3 1.808E-01  6  3 2.605E-01  7  3 1.065E-01  8  3 1.857E-02  9  3 1.495E-03
 10  3 5.241E-05  0  4 3.649E-02  1  4 1.450E-01  2  4 7.724E-02  3  4 3.227E-02
  4  4 1.139E-01  5  4 4.780E-02  6  4 8.305E-02  7  4 2.706E-01  8  4 1.561E-01
  9  4 3.420E-02 10  4 3.274E-03 11  4 1.318E-04  0  5 1.399E-02  1  5 8.647E-02
  2  5 1.275E-01  3  5 9.050E-03  4  5 8.823E-02  5  5 4.262E-02  6  5 1.040E-01
  7  5 1.916E-02  8  5 2.438E-01  9  5 2.029E-01 10  5 5.569E-02 11  5 6.299E-03
 12  5 2.890E-04  0  6 5.147E-03  1  6 4.367E-02  2  6 1.127E-01  3  6 6.910E-02
  4  6 5.227E-03  5  6 1.057E-01  6  6 3.171E-03  7  6 1.291E-01  8  6 2.766E-05
  9  6 1.919E-01 10  6 2.402E-01 11  6 8.265E-02 12  6 1.099E-02 13  6 5.717E-04
  0  7 1.851E-03  1  7 2.000E-02  2  7 7.496E-02  3  7 1.009E-01  4  7 1.798E-02
  5  7 3.829E-02  6  7 8.078E-02  7  7 6.748E-03  8  7 1.159E-01  9  7 1.694E-02
 10  7 1.299E-01 11  7 2.630E-01 12  7 1.140E-01 13  7 1.777E-02 14  7 1.044E-03
  4  8 6.361E-02  6  8 6.967E-02  7  8 3.946E-02  8  8 3.633E-02  9  8 7.862E-02
 10  8 5.219E-02 11  8 7.206E-02 12  8 2.688E-01 13  8 1.480E-01 14  8 2.702E-02
 15  8 1.785E-03 16  8 3.480E-05  0  9 2.348E-04  1  9 3.589E-03  2  9 2.182E-02
  3  9 6.406E-02  4  9 8.349E-02  5  9 2.454E-02  6  9 1.289E-02  7  9 7.733E-02
  8  9 8.360E-03  9  9 6.773E-02 10  9 3.765E-02 11  9 8.779E-02 12  9 2.857E-02
 13  9 2.575E-01 14  9 1.826E-01 15  9 3.902E-02 16  9 2.893E-03 17  9 6.131E-05
  0 10 8.403E-05  1 10 1.463E-03  2 10 1.053E-02  3 10 3.917E-02  4 10 7.511E-02
  5 10 5.820E-02  6 10 2.460E-03  7 10 3.833E-02  8 10 6.077E-02  9 10 3.194E-04
 10 10 8.370E-02 11 10 9.012E-03 12 10 1.109E-01 13 10 4.687E-03 14 10 2.315E-01
 15 10 2.154E-01 16 10 5.395E-02 17 10 4.480E-03 18 10 1.089E-04  0 11 3.038E-05
  1 11 5.907E-04  2 11 4.885E-03  3 11 2.187E-02  4 11 5.510E-02  5 11 7.056E-02
  6 11 2.810E-02  7 11 2.738E-03  8 11 5.721E-02  9 11 3.305E-02 10 11 1.307E-02
 11 11 7.897E-02 12 11 2.617E-05 13 11 1.156E-01 14 11 7.733E-04 15 11 1.945E-01
 16 11 2.443E-01 17 11 7.185E-02 18 11 6.675E-03 19 11 1.658E-04  0 12 1.114E-05
  1 12 2.380E-04  2 12 2.212E-03  3 12 1.151E-02  4 12 3.567E-02  5 12 6.338E-02
  6 12 5.261E-02  7 12 6.400E-03  8 12 1.852E-02  9 12 5.945E-02 10 12 9.576E-03
 11 12 3.527E-02 12 12 5.846E-02 13 12 9.342E-03 14 12 1.029E-01 15 12 1.330E-02
 16 12 1.516E-01 17 12 2.672E-01 18 12 9.261E-02 19 12 9.615E-03  1 13 9.627E-05
CROSS-SECTIONS ASSUMED SAME AS B-X OF CARTWRIGHT
ELECTRON ENERGY=       1.18       1.29       1.61       1.93       2.42       3.22       4.19       5.80
CROSS SECTION  = 0.000E+00 5.400E-18 2.250E-17 2.990E-17 2.410E-17 1.560E-17 1.200E-17 7.600E-18
RADIATIVE TRANSITION PROBABILITY= 9.000E+04
IORD= 11
N2 A1A   LOWER STATE= 2  UPPER STATE= 4   NUMBER OF CARDS= 24
  0  0 7.827E-01  0  1 1.791E-01  0  2 3.059E-02  0  3 5.717E-03  0  4 5.717E-03
  0  5 1.303E-03  0  6 3.656E-04  0  7 1.238E-04  1  0 7.827E-01  1  1 1.791E-01
  1  2 3.059E-02  1  3 5.717E-03  1  4 5.717E-03  1  5 1.303E-03  1  6 3.656E-04
  1  7 1.238E-04  2  0 2.095E-01  2  1 5.035E-01  2  2 2.184E-01  2  3 5.205E-02
  2  4 5.205E-02  2  5 1.196E-02  2  6 3.080E-03  2  7 9.274E-04  2  8 3.263E-04
  2  9 3.263E-04  2 10 1.320E-04  3  0 7.735E-03  3  1 3.024E-01  3  2 3.595E-01
  3  3 2.312E-01  3  4 2.312E-01  3  5 7.099E-02  3  6 1.943E-02  3  7 5.626E-03
  3  8 1.826E-03  3  9 1.826E-03  3 10 6.737E-04  3 11 2.808E-04  3 12 1.305E-04
  4  0 7.735E-03  4  1 3.024E-01  4  2 3.595E-01  4  3 2.312E-01  4  4 2.312E-01
  4  5 7.099E-02  4  6 1.943E-02  4  7 5.626E-03  4  8 1.826E-03  4  9 1.826E-03
  4 10 6.737E-04  4 11 2.808E-04  4 12 1.305E-04  5  0 1.179E-04  5  1 1.479E-02
  5  2 3.693E-01  5  3 2.594E-01  5  4 2.594E-01  5  5 2.276E-01  5  6 8.641E-02
  5  7 2.778E-02  5  8 9.051E-03  5  9 9.051E-03  5 10 3.194E-03  5 11 1.248E-03
  5 12 5.408E-04  5 13 2.581E-04  6  1 1.910E-04  6  2 2.198E-02  6  3 4.228E-01
  6  4 4.228E-01  6  5 1.870E-01  6  6 2.121E-01  6  7 9.699E-02  6  8 3.623E-02
  6  9 3.623E-02  6 10 1.328E-02  6 11 5.125E-03  6 12 2.139E-03  6 13 9.724E-04
  6 14 2.558E-04  7  1 1.910E-04  7  2 2.198E-02  7  3 4.228E-01  7  4 4.228E-01
  7  5 1.870E-01  7  6 2.121E-01  7  7 9.699E-02  7  8 3.623E-02  7  9 3.623E-02
  7 10 1.328E-02  7 11 5.125E-03  7 12 2.139E-03  7 13 9.724E-04  7 14 2.558E-04
```

```
  8  2 1.834E-04  8  3 2.866E-02  8  4 2.866E-02  8  5 4.674E-01  8  6 1.355E-01
  8  7 1.896E-01  8  8 1.020E-01  8  9 1.020E-01  8 10 4.380E-02  8 11 1.803E-02
  8 12 7.629E-03  8 13 3.421E-03  8 14 8.450E-04  9  3 1.027E-04  9  4 1.027E-04
  9  5 3.385E-02  9  6 5.061E-01  9  7 9.970E-02  9  8 1.642E-01  9  9 1.642E-01
  9 10 1.016E-01  9 11 4.959E-02  9 12 2.280E-02  9 13 1.058E-02  9 14 2.605E-03
CROSS-SECTIONS ASSUMED SAME AS B-X OF CARTWRIGHT
ELECTRON ENERGY=      2.38      2.59      3.24      3.88      4.88      6.47      8.42      11.65
CROSS SECTION  = 0.000E+00 5.400E-18 2.250E-17 2.990E-17 2.410E-17 1.560E-17 1.200E-17 7.600E-18
RADIATIVE TRANSITION PROBABILITY= 0.000E+00
IORD= 12
N2 A1B   LOWER STATE= 3  UPPER STATE= 4   NUMBER OF CARDS= 11
  0  0 2.005E-03  0  1 9.979E-01  0  2 2.005E-03  1  0 2.005E-03  1  1 9.979E-01
  1  2 2.005E-03  2  0 9.942E-01  2  1 1.966E-03  2  2 9.942E-01  2  3 3.781E-03
  2  4 3.781E-03  3  0 3.652E-03  3  2 3.652E-03  3  3 9.907E-01  3  4 9.907E-01
  3  5 5.449E-03  3  6 1.042E-04  3  7 1.042E-04  4  0 3.652E-03  4  2 3.652E-03
  4  3 9.907E-01  4  4 9.907E-01  4  5 5.449E-03  4  6 1.042E-04  4  7 1.042E-04
  5  0 1.335E-04  5  2 1.335E-04  5  3 5.189E-03  5  4 5.189E-03  5  5 9.875E-01
  5  6 6.927E-03  5  7 6.927E-03  5  8 1.787E-04  6  3 2.431E-04  6  4 2.431E-04
  6  5 6.497E-03  6  6 9.848E-01  6  7 9.848E-01  6  8 8.129E-03  6  9 2.877E-04
  7  3 2.431E-04  7  4 2.431E-04  7  5 6.497E-03  7  6 9.848E-01  7  7 9.848E-01
  7  8 8.129E-03  7  9 2.877E-04  8  5 3.900E-04  8  6 7.497E-03  8  7 7.497E-03
  8  8 9.826E-01  8  9 8.985E-03  9  6 5.732E-04  9  7 5.732E-04  9  8 8.135E-03
CROSS-SECTION ASSUMED SAME AS B-X OF CARTWRIGHT
ELECTRON ENERGY=      1.20      1.30      1.63      1.95      2.44      3.25      4.23      5.85
CROSS SECTION  = 0.000E+00 5.400E-18 2.250E-17 2.990E-17 2.410E-17 1.560E-17 1.200E-17 7.600E-18
RADIATIVE TRANSITION PROBABILITY= 0.000E+00


MOLECULAR BAND NAME=NO      MOLECULAR WEIGHT=    30.010
NUMBER OF ELECTRON-IMPACT DISSOCIATION CROSS-SECTION SET= 3
NUMBER OF ELECTRON-IMPACT EXCITATION CROSS-SECTION SET  = 3
NUMBER OF ELECTRONIC LEVELS                             = 6
NUMBER OF LEVELS IN QUASI-STEADY-STATE CALC.            = 3
 DEGEN      TERM       WE       WEXE      WEYE      WEZE       BE      ALPHA
    4.000    60.550  1903.855    13.970    -0.001     0.000   1.70460 1.780E-02
    2.000 43965.699  2371.300    14.480    -0.280     0.000   1.99520 1.640E-02
    4.000 45932.398  1037.680     7.603     0.097     0.000   1.12700 1.525E-02
    2.000 52148.000  2347.000     0.000     0.000     0.000   1.95500 0.000E+00
    2.000 53083.000  2327.000    23.000     0.000     0.000   1.99170 0.000E+00
    2.000 60628.500  2373.600    15.850     0.000     0.000   1.98630 1.820E-02

DISSOCIATED STATE
N  4S    ATOM. WT.=  14.010  DISSOC. ENERGY=   52490. CM-1  STATISTICAL WT.=  4.0
O  3P    ATOM. WT.=  16.000  DISSOC. ENERGY=   52490. CM-1  STATISTICAL WT.=  9.0

ELECTRON-IMPACT DISSOCIATION CROSS-SECTIONS
CROSS-SECTIONS ASSUMED AS SAME FOR NO 1-2 OF IMAMI ET AL
DISSOCIATION ENERGY =   52490.0 CM-1
ELECTRON ENERGY=      6.51      6.78      7.88     10.15     13.54     18.09     22.58     28.24
CROSS SECTION  = 0.000E+00 3.370E-18 1.540E-17 2.450E-17 2.980E-17 3.030E-17 2.870E-17 2.700E-17
CROSS-SECTIONS ASSUMED AS SAME FOR NO 1-2 OF IMAMI ET AL
DISSOCIATION ENERGY =   71718.0 CM-1
ELECTRON ENERGY=      3.44      3.58      4.16      5.37      7.16      9.56     11.94     14.93
CROSS SECTION  = 0.000E+00 3.370E-18 1.540E-17 2.450E-17 2.980E-17 3.030E-17 2.870E-17 2.700E-17
CROSS-SECTIONS ASSUMED AS SAME FOR NO 1-2 OF IMAMI ET AL
DISSOCIATION ENERGY =   71718.0 CM-1
ELECTRON ENERGY=      3.20      3.33      3.87      4.99      6.65      8.89     11.09     13.87
CROSS SECTION  = 0.000E+00 3.370E-18 1.540E-17 2.450E-17 2.980E-17 3.030E-17 2.870E-17 2.700E-17

FRANCK-CONDON FACTOR DATA
IORD= 13
NO B     LOWER STATE= 1  UPPER STATE= 3   NUMBER OF CARDS= 46
  3  0 1.000E-03  4  0 3.000E-03  5  0 5.000E-03  6  0 1.100E-02  7  0 1.700E-02
  8  0 2.200E-02  9  0 2.900E-02 10  0 3.200E-02 11  0 4.100E-02 12  0 5.100E-02
  1  1 1.000E-03  2  1 4.000E-03  3  1 9.000E-03  4  1 1.700E-02  5  1 3.200E-02
```

```
 6  1 4.400E-02  7  1 5.900E-02  8  1 5.800E-02  9  1 6.000E-02 10  1 5.700E-02
11  1 4.800E-02 12  1 3.400E-02  0  2 1.000E-03  1  2 6.000E-03  2  2 1.800E-02
 3  2 3.800E-02  4  2 5.400E-02  5  2 6.900E-02  6  2 7.000E-02  7  2 5.300E-02
 8  2 3.600E-02  9  2 1.900E-02 10  2 8.000E-03 11  2 1.000E-03 12  2 3.000E-03
 0  3 5.000E-03  1  3 2.400E-02  2  3 4.800E-02  3  3 7.600E-02  4  3 7.600E-02
 5  3 5.700E-02  6  3 3.200E-02  7  3 7.000E-03  9  3 1.400E-02 10  3 2.000E-02
11  3 3.100E-02 12  3 3.800E-02  0  4 1.700E-02  1  4 5.100E-02  2  4 8.500E-02
 3  4 8.400E-02  4  4 4.300E-02  5  4 6.000E-03  6  4 1.000E-03  7  4 2.400E-02
 8  4 3.400E-02  9  4 4.200E-02 10  4 3.400E-02 11  4 2.000E-02 12  4 1.000E-03
 0  5 4.100E-02  1  5 9.700E-02  2  5 9.200E-02  3  5 3.800E-02  4  5 1.000E-03
 5  5 1.200E-02  6  5 3.800E-02  7  5 4.600E-02  8  5 2.700E-02  9  5 6.000E-03
11  5 5.000E-03 12  5 2.600E-02  0  6 8.200E-02  1  6 1.170E-01  2  6 4.700E-02
 4  6 3.000E-02  5  6 5.300E-02  6  6 3.500E-02  7  6 5.000E-03  8  6 2.000E-03
 9  6 1.800E-02 10  6 3.200E-02 11  6 3.100E-02 12  6 1.100E-02  0  7 1.250E-01
 1  7 8.800E-02  2  7 2.000E-03  3  7 3.300E-02  4  7 6.000E-02  5  7 2.400E-02
 7  7 2.300E-02  8  7 3.800E-02  9  7 3.100E-02 10  7 1.000E-02 12  7 1.300E-02
 1  8 2.900E-02  2  8 2.100E-02  3  8 6.800E-02  4  8 2.100E-02  5  8 4.000E-03
 6  8 3.100E-02  7  8 3.600E-02  8  8 1.400E-02 10  8 1.400E-02 11  8 2.800E-02
12  8 2.000E-02  0  9 1.670E-01  2  9 7.300E-02  3  9 4.200E-02  4  9 3.000E-03
 5  9 4.600E-02  6  9 3.400E-02  7  9 1.000E-03  8  9 1.300E-02  9  9 3.000E-02
10  9 2.700E-02 11  9 9.000E-03 12  9 3.000E-03  0 10 1.520E-01  1 10 2.100E-02
 2 10 8.200E-02  3 10 1.000E-03  4 10 3.900E-02  5 10 3.700E-02  6 10 1.000E-03
 7 10 2.200E-02  8 10 3.500E-02  9 10 1.800E-02 11 10 8.000E-03 12 10 2.600E-02
 0 11 1.140E-01  1 11 7.400E-02  2 11 4.100E-02  3 11 2.400E-02  4 11 5.400E-02
 5 11 1.800E-02  6 11 2.500E-02  7 11 4.000E-02  8 11 2.000E-03  9 11 8.000E-03
10 11 2.400E-02 11 11 2.600E-02 12 11 1.000E-03  0 12 7.600E-02  1 12 1.260E-01
 3 12 7.200E-02  4 12 1.200E-02  5 12 2.500E-02  6 12 4.300E-02  7 12 2.000E-03
 8 12 1.700E-02  9 12 3.400E-02 10 12 1.400E-02 12 12 1.200E-02  0 13 3.300E-02
 1 13 1.390E-01  2 13 1.800E-02  3 13 5.400E-02  4 13 1.700E-02  5 13 5.200E-02
 6 13 2.000E-03  7 13 2.800E-02  8 13 2.700E-02  9 13 2.000E-03 10 13 1.400E-02
11 13 3.200E-02 12 13 7.000E-03  0 14 1.600E-02  1 14 1.050E-01  2 14 8.200E-02
 3 14 9.000E-03  4 14 6.600E-02  5 14 1.400E-02  6 14 1.800E-02  7 14 3.400E-02
 9 14 2.100E-02 10 14 2.700E-02 11 14 8.000E-03 12 14 8.000E-03  0 15 7.000E-03
 1 15 6.800E-02  2 15 1.260E-01  3 15 1.300E-02  4 15 5.600E-02  5 15 1.000E-02
 0 16 2.000E-03  1 16 2.800E-02  2 16 1.240E-01  3 16 8.600E-02  4 16 5.000E-03
 5 16 6.300E-02  6 16 6.000E-03  7 16 3.100E-02  8 16 2.200E-02 10 16 2.700E-02
11 16 2.200E-02 12 16 1.000E-03  1 17 1.200E-02  2 17 7.700E-02  3 17 1.340E-01
 4 17 2.900E-02  5 17 5.000E-02  6 17 1.800E-02  7 17 4.200E-02  9 17 3.200E-02
10 17 1.600E-02 11 17 2.000E-03 12 17 3.100E-02  1 18 4.000E-03  2 18 5.000E-02
 3 18 1.150E-01  4 18 7.700E-02  5 18 3.000E-03  6 18 6.200E-02  7 18 1.000E-03
 8 18 3.500E-02  9 18 2.200E-02 10 18 3.000E-03 11 18 2.900E-02 12 18 5.000E-03
 1 19 1.000E-03  2 19 1.000E-02  3 19 6.900E-02  4 19 1.290E-01  5 19 3.000E-02
 6 19 4.000E-02  7 19 3.800E-02  8 19 3.200E-02  9 19 8.000E-03 10 19 4.100E-02
CROSS-SECTIONS ASSUMED TO BE SAME AS FOR NO 1-2 OF IMAMI ET AL
ELECTRON ENERGY=      5.69      6.00      7.00      9.00     12.00     16.00     20.00     25.00
CROSS SECTION  = 0.000E+00 3.370E-18 1.540E-17 2.450E-17 2.980E-17 3.030E-17 2.870E-17 2.700E-17
RADIATIVE TRANSITION PROBABILITY= 1.500E+06
IORD= 14
NO G     LOWER STATE= 1  UPPER STATE= 2   NUMBER OF CARDS= 38
 0  0 2.270E-01  1  0 3.670E-01  2  0 2.750E-01  3  0 9.900E-02  4  0 2.600E-02
 5  0 5.000E-03  6  0 2.000E-03  0  1 3.050E-01  1  1 5.600E-02  2  1 8.700E-02
 3  1 2.740E-01  4  1 1.930E-01  5  1 7.700E-02  6  1 1.000E-02  7  1 1.000E-03
 0  2 2.180E-01  1  2 2.400E-02  2  2 1.690E-01  3  2 1.000E-03  4  2 1.740E-01
 5  2 2.700E-01  6  2 1.050E-01  7  2 3.000E-02  8  2 3.000E-03  0  3 1.330E-01
 1  3 1.330E-01  2  3 1.500E-02  3  3 1.120E-01  4  3 5.300E-02  5  3 4.800E-02
 6  3 2.340E-01  7  3 1.920E-01  8  3 6.000E-02  9  3 1.600E-02 10  3 3.000E-03
 0  4 6.500E-02  1  4 1.600E-01  2  4 2.000E-02  3  4 9.400E-02  4  4 2.000E-02
 5  4 1.270E-01  6  4 6.000E-03  7  4 1.490E-01  8  4 2.210E-01  9  4 1.100E-01
10  4 2.400E-02 11  4 4.000E-03 12  4 1.000E-03  0  5 2.800E-02  1  5 1.260E-01
 2  5 9.200E-02  4  5 1.090E-01  6  5 1.270E-01  7  5 1.800E-02  8  5 5.200E-02
 9  5 2.300E-01 10  5 1.390E-01 11  5 6.100E-02 12  5 1.300E-02  0  6 1.000E-02
 1  6 7.000E-02  2  6 1.250E-01  3  6 2.600E-02  4  6 5.600E-02  5  6 6.200E-02
 6  6 2.200E-02  7  6 4.900E-02  8  6 9.300E-02  9  6 6.000E-03 10  6 1.790E-01
11  6 1.860E-01 12  6 9.300E-02  0  7 3.000E-03  1  7 3.400E-02  2  7 1.060E-01
 3  7 8.500E-02  5  7 8.200E-02  6  7 2.600E-02  7  7 7.700E-02  8  7 2.500E-02
```

```
 9  7 1.060E-01 10  7 2.000E-03 11  7 1.230E-01 12  7 2.040E-01  0  8 2.000E-03
 1  8 1.300E-02  2  8 6.100E-02  3  8 1.010E-01  4  8 3.100E-02  5  8 2.100E-02
 6  8 9.200E-02  7  8 5.000E-03  8  8 9.200E-02  9  8 3.000E-03 10  8 9.900E-02
 2  9 2.800E-02  3  9 8.300E-02  4  9 8.300E-02  6  9 3.600E-02  7  9 5.500E-02
 8  9 1.800E-02  9  9 7.500E-02 10  9 1.600E-02 11  9 8.000E-02 12  9 6.900E-02
 1 10 3.000E-03  2 10 1.400E-02  3 10 6.000E-02  4 10 8.900E-02  5 10 2.500E-02
 7 10 6.800E-02  8 10 1.100E-02  9 10 3.400E-02 10 10 5.300E-02 11 10 2.500E-02
12 10 4.500E-02  1 11 1.000E-03  2 11 7.000E-03  3 11 3.300E-02  4 11 6.700E-02
 5 11 7.100E-02  6 11 1.700E-02  7 11 3.000E-02  8 11 5.900E-02  9 11 3.000E-03
10 11 6.300E-02 11 11 2.400E-02 12 11 5.500E-02  2 12 4.000E-03  3 12 1.400E-02
 4 12 4.000E-02  5 12 7.500E-02  6 12 6.500E-02  8 12 1.700E-02  9 12 4.100E-02
10 12 2.000E-03 11 12 6.500E-02 12 12 2.000E-03  2 13 2.000E-03  3 13 7.000E-03
 4 13 3.200E-02  5 13 5.900E-02  6 13 7.400E-02  7 13 2.000E-02  8 13 4.100E-02
 9 13 5.300E-02 10 13 1.400E-02 11 13 3.200E-02 12 13 5.400E-02  2 14 1.000E-03
 3 14 3.000E-03  4 14 1.400E-02  5 14 3.800E-02  6 14 6.500E-02  7 14 6.100E-02
 8 14 2.100E-02  9 14 2.000E-02 10 14 5.000E-02 11 14 9.000E-03 12 14 2.900E-02
 3 15 1.000E-03  4 15 7.000E-03  5 15 2.400E-02  6 15 5.600E-02  7 15 7.100E-02
 8 15 1.300E-02  9 15 8.000E-03 10 15 3.400E-02 11 15 3.500E-02 12 15 3.000E-03
 4 16 5.000E-03  5 16 1.100E-02  6 16 3.200E-02  7 16 5.400E-02  8 16 5.200E-02
 9 16 4.000E-03 10 16 1.200E-02 11 16 4.800E-02 12 16 1.400E-02  4 17 1.000E-03
 5 17 7.000E-03  6 17 1.800E-02  7 17 4.400E-02  8 17 6.200E-02  9 17 3.400E-02
11 17 1.700E-02 12 17 3.200E-02  5 18 1.000E-03  6 18 6.000E-03  7 18 2.800E-02
FROM IMAMI ET AL
ELECTRON ENERGY=      5.44      5.67      5.69      8.49     11.32     15.13     18.89     23.62
CROSS SECTION  = 0.000E+00 3.370E-18 1.540E-17 2.450E-17 2.980E-17 3.030E-17 2.870E-17 2.700E-17
RADIATIVE TRANSITION PROBABILITY= 8.620E+06
IORD= 15
NO A-B   LOWER STATE= 2  UPPER STATE= 3   NUMBER OF CARDS=  1
  0  0 0.000E+00  0  0 0.000E+00  0  0 0.000E+00  0  0 0.000E+00  0  0 0.000E+00
CROSS-SECTIONS ASSUMED SAME AS AS FOR NO 1-2 OF IMAMI ET AL
ELECTRON ENERGY=      0.24      0.25      0.29      0.38      0.51      0.68      0.85      1.06
CROSS SECTION  = 0.000E+00 3.370E-18 1.540E-17 2.450E-17 2.980E-17 3.030E-17 2.870E-17 2.700E-17
RADIATIVE TRANSITION PROBABILITY= 0.000E+00


MOLECULAR BAND NAME=O2      MOLECULAR WEIGHT=    32.000
NUMBER OF ELECTRON-IMPACT DISSOCIATION CROSS-SECTION SET= 0
NUMBER OF ELECTRON-IMPACT EXCITATION CROSS-SECTION SET  = 0
NUMBER OF ELECTRONIC LEVELS                             = 5
NUMBER OF LEVELS IN QUASI-STEADY-STATE CALC.            = 0
 DEGEN       TERM       WE       WEXE      WEYE      WEZE       BE      ALPHA
    3.000      0.000  1580.361   12.073     0.055    -0.001   1.44567 1.579E-02
    2.000   7918.100  1509.300   12.900     0.000     0.000   1.42640 1.710E-02
    1.000  13195.220  1432.687   13.950    -0.011     0.000   1.40042 1.817E-02
    3.000  36096.000   819.000   22.500     0.000     0.000   1.05000 0.000E+00
    3.000  49802.102   700.360    8.002    -0.375     0.000   0.81900 1.100E-02

DISSOCIATED STATE
O  3P    ATOM. WT.=  16.000  DISSOC. ENERGY=   41260. CM-1  STATISTICAL WT.=  9.0
O  3P    ATOM. WT.=  16.000  DISSOC. ENERGY=   41260. CM-1  STATISTICAL WT.=  9.0


MOLECULAR BAND NAME=CN      MOLECULAR WEIGHT=    26.020
NUMBER OF ELECTRON-IMPACT DISSOCIATION CROSS-SECTION SET= 3
NUMBER OF ELECTRON-IMPACT EXCITATION CROSS-SECTION SET  = 3
NUMBER OF ELECTRONIC LEVELS                             = 3
NUMBER OF LEVELS IN QUASI-STEADY-STATE CALC.            = 3
 DEGEN       TERM       WE       WEXE      WEYE      WEZE       BE      ALPHA
    2.000      0.000  2068.745   13.134    -0.006     0.000   1.89900 1.701E-02
    4.000   9245.344  1812.655   12.609    -0.012     0.000   1.71510 1.708E-02
    2.000  25751.801  2168.610   20.200     0.000     0.000   1.97010 2.215E-02

DISSOCIATED STATE
C  3P    ATOM. WT.=  12.010  DISSOC. ENERGY=   63640. CM-1  STATISTICAL WT.=  9.0
N  4S    ATOM. WT.=  14.010  DISSOC. ENERGY=   63630. CM-1  STATISTICAL WT.=  4.0
```

```
ELECTRON-IMPACT DISSOCIATION CROSS-SECTIONS
CROSS-SECTIONS ASSUMED AS SAME FOR NO 1-2 OF IMAMI ET AL
DISSOCIATION ENERGY =   63640.0 CM-1
ELECTRON ENERGY=      7.89      8.21      9.55     12.31     16.41     21.93     27.38     34.24
CROSS SECTION  = 0.000E+00 3.370E-18 1.540E-17 2.450E-17 2.980E-17 3.030E-17 2.870E-17 2.700E-17
CROSS-SECTIONS ASSUMED SAME AS SAME FOR NO 1-2 OF IMAMI ET AL
DISSOCIATION ENERGY =   63640.0 CM-1
ELECTRON ENERGY=      6.74      7.03      8.18     10.54     14.06     18.79     23.45     29.33
CROSS SECTION  = 0.000E+00 3.370E-18 1.540E-17 2.450E-17 2.980E-17 3.030E-17 2.870E-17 2.700E-17
CROSS-SECTIONS ASSUMED SAME AS SAME FOR NO 1-2 OF IMAMI ET AL
DISSOCIATION ENERGY =   63640.0 CM-1
ELECTRON ENERGY=      4.70      4.88      5.68      7.32      9.76     13.04     16.28     20.36
CROSS SECTION  = 0.000E+00 3.370E-18 1.540E-17 2.450E-17 2.980E-17 3.030E-17 2.870E-17 2.700E-17

FRANCK-CONDON FACTOR DATA
IORD= 16
CN VIO   LOWER STATE= 1  UPPER STATE= 3   NUMBER OF CARDS= 13
  0  0 9.179E-01  1  0 8.090E-02  2  0 1.200E-03  0  1 7.600E-02  1  1 7.795E-01
  2  1 1.417E-01  3  1 2.800E-03  0  2 5.800E-03  1  2 1.240E-01  2  2 6.754E-01
  3  2 1.905E-01  4  2 4.300E-03  0  3 3.000E-04  1  3 1.430E-02  2  3 1.550E-01
  3  3 5.929E-01  4  3 2.318E-01  2  4 2.390E-02  3  4 1.745E-01  4  4 5.279E-01
  5  4 2.668E-01  3  5 3.420E-02  4  5 1.825E-01  5  5 4.824E-01  6  5 2.933E-01
  4  6 4.520E-02  5  6 1.781E-01  6  6 4.583E-01  7  6 3.095E-01  9  6 3.100E-03
  5  7 5.540E-02  6  7 1.640E-01  7  7 4.554E-01  8  7 3.122E-01 10  7 5.000E-03
  6  8 6.390E-02  8  8 4.750E-01  9  8 2.956E-01 11  8 6.700E-03  7  9 7.080E-02
  9  9 5.184E-01 10  9 2.537E-01  8 10 7.660E-02 10 10 5.801E-01 11 10 1.897E-01
 12 10 4.810E-02 14 10 3.400E-03  7 11 3.100E-03  9 11 8.280E-02 11 11 6.447E-01
 12 11 1.131E-01 13 11 8.540E-02 15 11 5.500E-03  8 12 3.700E-03 12 12 6.967E-01
 14 12 1.203E-01  9 13 4.100E-03 13 13 7.127E-01 15 13 1.380E-01 18 13 4.000E-03
 14 14 6.762E-01 16 14 1.234E-01 17 14 4.470E-02 15 15 5.786E-01 16 15 9.180E-02
CROSS-SECTIONS ASSUMED SAME AS FOR NO 1-2 OF IMAMI ET AL
ELECTRON ENERGY=      3.19      3.33      3.87      4.99      6.65      8.89     11.10     13.88
CROSS SECTION  = 0.000E+00 3.370E-18 1.540E-17 2.450E-17 2.980E-17 3.030E-17 2.870E-17 2.700E-17
RADIATIVE TRANSITION PROBABILITY= 1.180E+07
IORD= 17
CN RED   LOWER STATE= 1  UPPER STATE= 2   NUMBER OF CARDS= 50
  0  0 5.002E-01  1  0 3.179E-01  2  0 1.269E-01  3  0 4.020E-02  4  0 1.110E-02
  5  0 2.850E-03  6  0 7.500E-04  7  0 2.000E-04  8  0 5.000E-05  0  1 3.711E-01
  1  1 4.600E-02  2  1 2.409E-01  3  1 1.942E-01  4  1 9.410E-02  5  1 3.615E-02
  6  1 1.220E-02  7  1 3.800E-03  8  1 1.100E-03  9  1 3.500E-04 10  1 1.000E-04
  0  2 1.107E-01  1  2 3.528E-01  2  2 1.160E-02  3  2 9.950E-02  4  2 1.812E-01
  5  2 1.330E-01  6  2 6.755E-02  7  2 2.810E-02  8  2 1.040E-02  9  2 3.600E-03
 10  2 1.150E-03 11  2 3.500E-04 12  2 1.500E-04 13  2 5.000E-05  0  3 1.670E-02
  1  3 2.234E-01  2  3 2.136E-01  3  3 8.780E-02  4  3 1.615E-02  5  3 1.228E-01
  6  3 1.416E-01  7  3 9.500E-02  8  3 4.855E-02  9  3 2.125E-02 10  3 8.450E-03
 11  3 3.150E-03 12  3 1.100E-03 13  3 4.000E-04 14  3 1.500E-04 15  3 5.000E-05
  0  4 1.400E-03  1  4 5.355E-02  2  4 2.872E-01  3  4 8.785E-02  4  4 1.489E-01
  5  4 1.800E-03  6  4 5.870E-02  7  4 1.210E-01  8  4 1.088E-01  9  4 6.855E-02
 10  4 3.530E-02 11  4 1.600E-02 12  4 6.650E-03 13  4 2.650E-03 14  4 1.000E-03
 15  4 4.000E-04 16  4 1.500E-04 17  4 5.000E-05  0  5 1.000E-04  1  5 6.150E-03
  2  5 1.027E-01  3  5 2.994E-01  4  5 1.595E-02  5  5 1.591E-01  6  5 3.040E-02
  7  5 1.505E-02  8  5 8.440E-02  9  5 1.068E-01 10  5 8.305E-02 11  5 5.020E-02
 12  5 2.590E-02 13  5 1.210E-02 14  5 5.300E-03 15  5 2.150E-03 16  5 8.500E-04
  1  6 4.000E-04  2  6 1.590E-02  3  6 1.567E-01  4  6 2.669E-01  5  6 7.500E-04
  6  6 1.287E-01  7  6 6.960E-02  8  6 1.500E-04  9  6 4.555E-02 10  6 9.010E-02
 11  6 8.880E-02 12  6 6.315E-02 13  6 3.725E-02 14  6 1.940E-02 15  6 9.300E-03
 16  6 4.200E-03 17  6 1.850E-03 18  6 7.500E-04  2  7 1.250E-03  3  7 3.130E-02
  4  7 2.067E-01  5  7 2.069E-01  6  7 2.400E-02  7  7 8.095E-02  8  7 9.770E-02
  9  7 9.450E-03 10  7 1.610E-02 11  7 6.515E-02 12  7 8.440E-02 13  7 7.165E-02
 14  7 4.825E-02 15  7 2.805E-02 16  7 1.480E-02 17  7 7.300E-03 18  7 3.400E-03
  2  8 5.000E-05  3  8 2.950E-03  4  8 5.285E-02  5  8 2.455E-01  6  8 1.390E-01
  7  8 6.345E-02  8  8 3.650E-02  9  8 1.050E-01 10  8 3.190E-02 11  8 1.650E-03
 12  8 3.835E-02 13  8 7.115E-02 14  8 7.365E-02 15  8 5.700E-02 16  8 3.705E-02
 17  8 2.140E-02 18  8 1.145E-02  3  9 1.000E-04  4  9 6.000E-03  5  9 7.980E-02
```

```
 6  9 2.670E-01  7  9 7.770E-02  8  9 1.008E-01  9  9 8.250E-03 10  9 9.250E-02
11  9 5.585E-02 12  9 2.400E-03 13  9 1.650E-02 14  9 5.265E-02 15  9 6.860E-02
16  9 6.170E-02 17  9 4.505E-02 18  9 2.870E-02  4 10 3.500E-04  5 10 1.070E-02
 6 10 1.107E-01  7 10 2.728E-01  8 10 3.205E-02  9 10 1.242E-01 10 10 2.500E-04
11 10 6.780E-02 12 10 7.205E-02 13 10 1.425E-02 14 10 3.500E-03 15 10 3.275E-02
16 10 5.760E-02 17 10 6.145E-02 18 10 5.065E-02  5 11 6.500E-04  6 11 1.765E-02
 7 11 1.432E-01  8 11 2.606E-01  9 11 6.450E-03 10 11 1.297E-01 11 11 9.750E-03
12 11 3.975E-02 13 11 7.685E-02 14 11 3.125E-02 15 11 7.500E-04 16 11 1.575E-02
 6 12 1.250E-03  7 12 2.700E-02  8 12 1.762E-01  9 12 2.346E-01 10 12 5.500E-04
11 12 1.184E-01 12 12 2.990E-02 13 12 1.655E-02 14 12 6.985E-02 15 12 4.710E-02
16 12 6.700E-03 17 12 4.600E-03 18 12 2.705E-02  7 13 2.150E-03  8 13 3.910E-02
 9 13 2.066E-01 10 13 1.985E-01 11 13 6.075E-02 12 13 9.515E-02 13 13 5.275E-02
14 13 3.200E-03 15 13 5.435E-02 16 13 5.735E-02 17 13 1.830E-02 18 13 7.500E-04
 7 14 1.000E-04  8 14 3.550E-03  9 14 5.365E-02 10 14 2.326E-01 11 14 1.569E-01
12 14 3.170E-02 13 14 6.660E-02 14 14 7.175E-02 15 14 9.500E-04 16 14 3.565E-02
17 14 5.970E-02 18 14 3.145E-02  8 15 1.500E-04  9 15 5.500E-03 10 15 7.110E-02
11 15 2.520E-01 12 15 1.146E-01 13 15 5.755E-02 14 15 3.885E-02 15 15 8.250E-02
16 15 8.400E-03 17 15 1.815E-02 18 15 5.415E-02  9 16 2.500E-04 10 16 8.250E-03
11 16 9.090E-02 12 16 2.647E-01 13 16 7.545E-02 14 16 8.245E-02 15 16 1.700E-02
16 16 8.330E-02 17 16 2.195E-02 18 16 5.950E-03 10 17 3.500E-04 11 17 1.180E-02
12 17 1.128E-01 13 17 2.693E-01 14 17 4.340E-02 15 17 1.020E-01 16 17 4.200E-03
17 17 7.505E-02 18 17 3.715E-02 11 18 6.000E-04 12 18 1.635E-02 13 18 1.359E-01
CROSS-SECTIONS ASSUMED SAME AS NO 1-2 OF IMAMI ET AL
ELECTRON ENERGY=      1.15      1.18      1.37      1.76      2.35      3.14      3.92      4.90
CROSS SECTION  = 0.000E+00 3.370E-18 1.540E-17 2.450E-17 2.980E-17 3.030E-17 2.870E-17 2.700E-17
RADIATIVE TRANSITION PROBABILITY= 1.950E+05
IORD= 18
CN AB    LOWER STATE= 2  UPPER STATE= 3   NUMBER OF CARDS= 30
 1  0 2.248E-04  1  1 2.248E-04  1  2 1.833E-01  1  3 6.249E-01  1  4 6.249E-01
 1  5 1.442E-01  1  6 3.433E-02  1  7 8.821E-03  1  8 8.821E-03  1  9 2.609E-03
 1 10 8.926E-04  1 11 3.496E-04  1 12 3.496E-04  1 13 1.542E-04  2  0 8.909E-01
 2  1 8.909E-01  2  2 9.252E-02  2  3 1.300E-02  2  4 1.300E-02  2  5 2.521E-03
 2  6 6.437E-04  2  7 2.055E-04  2  8 2.055E-04  3  0 8.909E-01  3  1 8.909E-01
 3  2 9.252E-02  3  3 1.300E-02  3  4 1.300E-02  3  5 2.521E-03  3  6 6.437E-04
 3  7 2.055E-04  3  8 2.055E-04  4  0 1.088E-01  4  1 1.088E-01  4  2 7.239E-01
 4  3 1.339E-01  4  4 1.339E-01  4  5 2.530E-02  4  6 5.644E-03  4  7 1.530E-03
 4  8 1.530E-03  4  9 4.975E-04  4 10 1.894E-04  5  0 2.248E-04  5  1 2.248E-04
 5  2 1.833E-01  5  3 6.249E-01  5  4 6.249E-01  5  5 1.442E-01  5  6 3.433E-02
 5  7 8.821E-03  5  8 8.821E-03  5  9 2.609E-03  5 10 8.926E-04  5 11 3.496E-04
 5 12 3.496E-04  5 13 1.542E-04  6  0 2.248E-04  6  1 2.248E-04  6  2 1.833E-01
 6  3 6.249E-01  6  4 6.249E-01  6  5 1.442E-01  6  6 3.433E-02  6  7 8.821E-03
 6  8 8.821E-03  6  9 2.609E-03  6 10 8.926E-04  6 11 3.496E-04  6 12 3.496E-04
 6 13 1.542E-04  7  2 2.534E-04  7  3 2.281E-01  7  4 2.281E-01  7  5 5.836E-01
 7  6 1.320E-01  7  7 3.861E-02  7  8 3.861E-02  7  9 1.127E-02  7 10 3.657E-03
 7 11 1.335E-03  7 12 1.335E-03  7 13 5.469E-04  7 14 2.487E-04  8  2 2.534E-04
 8  3 2.281E-01  8  4 2.281E-01  8  5 5.836E-01  8  6 1.320E-01  8  7 3.861E-02
 8  8 3.861E-02  8  9 1.127E-02  8 10 3.657E-03  8 11 1.335E-03  8 12 1.335E-03
 8 13 5.469E-04  8 14 2.487E-04  9  5 2.428E-01  9  6 5.930E-01  9  7 1.051E-01
 9  8 1.051E-01  9  9 3.865E-02  9 10 1.255E-02  9 11 4.462E-03  9 12 4.462E-03
 9 13 1.748E-03  9 14 7.549E-04 10  5 1.531E-03 10  6 2.259E-01 10  7 6.444E-01
10  8 6.444E-01 10  9 7.020E-02 10 10 3.617E-02 10 11 1.266E-02 10 12 1.266E-02
10 13 4.907E-03 10 14 2.062E-03 11  6 8.358E-03 11  7 1.780E-01 11  8 1.780E-01
11  9 7.241E-01 11 10 3.468E-02 11 11 3.320E-02 11 12 3.320E-02 11 13 1.185E-02
11 14 4.989E-03 12  6 8.358E-03 12  7 1.780E-01 12  8 1.780E-01 12  9 7.241E-01
12 10 3.468E-02 12 11 3.320E-02 12 12 3.320E-02 12 13 1.185E-02 12 14 4.989E-03
13  7 2.205E-02 13  8 2.205E-02 13  9 1.088E-01 13 10 8.092E-01 13 11 7.994E-03
13 12 7.994E-03 13 13 3.150E-02 13 14 1.046E-02 14  7 1.136E-03 14  8 1.136E-03
14  9 3.815E-02 14 10 4.041E-02 14 11 8.689E-01 14 12 8.689E-01 14 13 4.843E-04
CROSS-SECTIONS ASSUMED SAME AS FOR NO 1-2 OF IMAMI ET AL
ELECTRON ENERGY=      2.05      2.15      2.60      3.23      4.30      5.75      7.18      8.98
CROSS SECTION  = 0.000E+00 3.370E-18 1.540E-17 2.450E-17 2.980E-17 3.030E-17 2.870E-17 2.700E-17
RADIATIVE TRANSITION PROBABILITY= 0.000E+00
VSLNIC=60.
VSLDEL=2.362488934719
VSLTW=2000.
```

VSLNI=1.
1

INEQ3D FLOWFIELD PROPERTIES

Y	PRESSURE	TEMP(ELEC)	TEMP(TRAN)	TOT. # DENS
0.0000E+00	0.4511E-01	0.1096E+05	0.1090E+05	0.3037E+17
0.7193E-02	0.4511E-01	0.1096E+05	0.1090E+05	0.3037E+17
0.2158E-01	0.4511E-01	0.1098E+05	0.1091E+05	0.3034E+17
0.3596E-01	0.4511E-01	0.1102E+05	0.1094E+05	0.3025E+17
0.5035E-01	0.4509E-01	0.1109E+05	0.1099E+05	0.3011E+17
0.6473E-01	0.4508E-01	0.1118E+05	0.1106E+05	0.2991E+17
0.7912E-01	0.4508E-01	0.1131E+05	0.1116E+05	0.2964E+17
0.9350E-01	0.4508E-01	0.1147E+05	0.1131E+05	0.2926E+17
0.1079	0.4508E-01	0.1167E+05	0.1151E+05	0.2874E+17
0.1223	0.4506E-01	0.1190E+05	0.1181E+05	0.2802E+17
0.1367	0.4504E-01	0.1213E+05	0.1222E+05	0.2705E+17
0.1510	0.4503E-01	0.1234E+05	0.1280E+05	0.2582E+17
0.1654	0.4501E-01	0.1249E+05	0.1355E+05	0.2438E+17
0.1798	0.4498E-01	0.1253E+05	0.1447E+05	0.2282E+17
0.1942	0.4498E-01	0.1246E+05	0.1550E+05	0.2131E+17
0.2086	0.4490E-01	0.1225E+05	0.1655E+05	0.1992E+17
0.2230	0.4484E-01	0.1194E+05	0.1757E+05	0.1874E+17
0.2374	0.4479E-01	0.1157E+05	0.1850E+05	0.1777E+17
0.2517	0.4474E-01	0.1118E+05	0.1930E+05	0.1701E+17
0.2661	0.4469E-01	0.1079E+05	0.1998E+05	0.1642E+17
0.2805	0.4465E-01	0.1043E+05	0.2056E+05	0.1594E+17
0.2949	0.4460E-01	0.1010E+05	0.2105E+05	0.1555E+17
0.3092	0.4456E-01	9799.	0.2148E+05	0.1522E+17
0.3236	0.4452E-01	9528.	0.2187E+05	0.1494E+17
0.3379	0.4447E-01	9282.	0.2224E+05	0.1468E+17
0.3523	0.4443E-01	9057.	0.2259E+05	0.1444E+17
0.3667	0.4439E-01	8850.	0.2294E+05	0.1420E+17
0.3812	0.4435E-01	8656.	0.2329E+05	0.1398E+17
0.3957	0.4430E-01	8473.	0.2365E+05	0.1375E+17
0.4103	0.4425E-01	8300.	0.2403E+05	0.1351E+17
0.4250	0.4420E-01	8134.	0.2443E+05	0.1328E+17
0.4398	0.4415E-01	7974.	0.2485E+05	0.1304E+17
0.4547	0.4409E-01	7820.	0.2530E+05	0.1279E+17
0.4697	0.4403E-01	7670.	0.2578E+05	0.1254E+17
0.4849	0.4397E-01	7525.	0.2628E+05	0.1228E+17
0.5002	0.4390E-01	7382.	0.2682E+05	0.1201E+17
0.5158	0.4382E-01	7242.	0.2739E+05	0.1174E+17
0.5315	0.4374E-01	7103.	0.2800E+05	0.1147E+17
0.5474	0.4366E-01	6966.	0.2865E+05	0.1118E+17
0.5636	0.4357E-01	6829.	0.2934E+05	0.1090E+17
0.5800	0.4347E-01	6692.	0.3008E+05	0.1061E+17
0.5966	0.4337E-01	6554.	0.3088E+05	0.1031E+17
0.6135	0.4326E-01	6413.	0.3173E+05	0.1001E+17
0.6307	0.4314E-01	6268.	0.3264E+05	0.9702E+16
0.6482	0.4302E-01	6117.	0.3362E+05	0.9392E+16
0.6660	0.4290E-01	5958.	0.3468E+05	0.9079E+16
0.6840	0.4276E-01	5789.	0.3580E+05	0.8765E+16
0.7019	0.4261E-01	5610.	0.3700E+05	0.8454E+16
0.7200	0.4245E-01	5416.	0.3826E+05	0.8144E+16
0.7385	0.4230E-01	5203.	0.3959E+05	0.7840E+16
0.7575	0.4214E-01	4965.	0.4102E+05	0.7541E+16
0.7774	0.4199E-01	4697.	0.4255E+05	0.7243E+16
0.7984	0.4181E-01	4392.	0.4422E+05	0.6940E+16
0.8207	0.4161E-01	4047.	0.4606E+05	0.6630E+16
0.8448	0.4139E-01	3660.	0.4810E+05	0.6315E+16
0.8711	0.4121E-01	3235.	0.5040E+05	0.6002E+16
0.9003	0.4107E-01	2778.	0.5300E+05	0.5687E+16
0.9334	0.4095E-01	2285.	0.5597E+05	0.5370E+16

0.9685	0.4066E-01	1763.	0.5894E+05	0.5063E+16
1.000	0.3831E-01	1307.	0.6068E+05	0.4634E+16

1

INEQ3D MOLE FRACTIONS

Y	O+	O	N+	N	e-	O2	N2	NO	N2+
0.0000E+00	0.1563E-01	0.1663	0.1189	0.5641	0.1346	0.8156E-06	0.5218E-03	0.2230E-05	0.2777E-06
0.7193E-02	0.1563E-01	0.1663	0.1189	0.5641	0.1346	0.8156E-06	0.5218E-03	0.2230E-05	0.2777E-06
0.2158E-01	0.1565E-01	0.1664	0.1187	0.5645	0.1343	0.7764E-06	0.5199E-03	0.2197E-05	0.2812E-06
0.3696E-01	0.1540E-01	0.1667	0.1183	0.5653	0.1337	0.7418E-06	0.5225E-03	0.2157E-05	0.2892E-06
0.5035E-01	0.1516E-01	0.1671	0.1176	0.5667	0.1328	0.7048E-06	0.5321E-03	0.2117E-05	0.3030E-06
0.6473E-01	0.1484E-01	0.1677	0.1166	0.5688	0.1315	0.6646E-06	0.5498E-03	0.2078E-05	0.3244E-06
0.7912E-01	0.1442E-01	0.1685	0.1152	0.5716	0.1298	0.6216E-06	0.5789E-03	0.2044E-05	0.3567E-06
0.9350E-01	0.1388E-01	0.1696	0.1132	0.5756	0.1271	0.5785E-06	0.6254E-03	0.2029E-05	0.4055E-06
0.1079	0.1323E-01	0.1710	0.1104	0.5810	0.1236	0.5416E-06	0.6890E-03	0.2041E-05	0.4806E-06
0.1223	0.1243E-01	0.1728	0.1066	0.5883	0.1191	0.5199E-06	0.8144E-03	0.2096E-05	0.5981E-06
0.1367	0.1146E-01	0.1750	0.1016	0.5978	0.1131	0.5187E-06	0.9927E-03	0.2211E-05	0.7861E-06
0.1510	0.1033E-01	0.1778	0.9508E-01	0.6100	0.1055	0.5437E-06	0.1264E-02	0.2404E-05	0.1088E-04
0.1654	0.9028E-02	0.1811	0.8718E-01	0.6246	0.9630E-01	0.6178E-06	0.1644E-02	0.2696E-05	0.1565E-04
0.1798	0.7617E-02	0.1848	0.7812E-01	0.6412	0.8598E-01	0.8307E-06	0.2238E-02	0.3099E-05	0.2282E-04
0.1942	0.6188E-02	0.1887	0.6857E-01	0.6585	0.7491E-01	0.5842E-06	0.2978E-02	0.3534E-05	0.3268E-04
0.2086	0.4839E-02	0.1924	0.5937E-01	0.6749	0.6440E-01	0.2658E-06	0.3863E-02	0.4069E-05	0.4680E-04
0.2230	0.3642E-02	0.1958	0.5113E-01	0.6892	0.5500E-01	0.5216E-06	0.5007E-02	0.4828E-05	0.5826E-04
0.2374	0.2646E-02	0.1987	0.4423E-01	0.7006	0.4714E-01	0.5550E-06	0.6362E-02	0.5751E-05	0.7145E-04
0.2517	0.1864E-02	0.2011	0.3875E-01	0.7092	0.4090E-01	0.5055E-06	0.7830E-02	0.6785E-05	0.8301E-04
0.2661	0.1290E-02	0.2030	0.3455E-01	0.7153	0.3613E-01	0.4159E-06	0.9414E-02	0.7847E-05	0.9206E-04
0.2805	0.8606E-03	0.2046	0.3138E-01	0.7192	0.3256E-01	0.2983E-06	0.1113E-01	0.9259E-05	0.9837E-04
0.2949	0.5703E-03	0.2058	0.2900E-01	0.7214	0.2989E-01	0.1718E-06	0.1298E-01	0.1074E-04	0.1023E-03
0.3092	0.3762E-03	0.2069	0.2716E-01	0.7224	0.2786E-01	0.7013E-06	0.1504E-01	0.1240E-04	0.1043E-03
0.3236	0.2472E-03	0.2078	0.2570E-01	0.7224	0.2627E-01	0.1049E-06	0.1730E-01	0.1427E-04	0.1050E-03
0.3379	0.1650E-03	0.2087	0.2449E-01	0.7216	0.2497E-01	0.1122E-16	0.1978E-01	0.1634E-04	0.1049E-03
0.3523	0.1131E-03	0.2096	0.2345E-01	0.7202	0.2387E-01	0.1126E-16	0.2254E-01	0.1864E-04	0.1044E-03
0.3667	0.8073E-04	0.2104	0.2250E-01	0.7182	0.2288E-01	0.1131E-16	0.2560E-01	0.2118E-04	0.1037E-03
0.3812	0.6068E-04	0.2113	0.2162E-01	0.7157	0.2196E-01	0.1136E-16	0.2902E-01	0.2398E-04	0.1029E-03
0.3957	0.4826E-04	0.2123	0.2078E-01	0.7125	0.2113E-01	0.1141E-16	0.3284E-01	0.2710E-04	0.1020E-03
0.4103	0.4049E-04	0.2134	0.1998E-01	0.7088	0.2031E-01	0.1146E-16	0.3711E-01	0.3064E-04	0.1012E-03
0.4250	0.3554E-04	0.2146	0.1920E-01	0.7045	0.1952E-01	0.1153E-16	0.4188E-01	0.3432E-04	0.1003E-03
0.4398	0.3228E-04	0.2159	0.1843E-01	0.6994	0.1874E-01	0.1159E-16	0.4720E-01	0.3845E-04	0.9947E-04
0.4547	0.3005E-04	0.2173	0.1768E-01	0.6936	0.1798E-01	0.1167E-16	0.5309E-01	0.4295E-04	0.9858E-04
0.4697	0.2845E-04	0.2188	0.1693E-01	0.6871	0.1723E-01	0.1175E-16	0.5961E-01	0.4784E-04	0.9763E-04
0.4849	0.2725E-04	0.2205	0.1620E-01	0.6797	0.1649E-01	0.1184E-16	0.6680E-01	0.5311E-04	0.9661E-04
0.5002	0.2632E-04	0.2223	0.1546E-01	0.6715	0.1575E-01	0.1194E-16	0.7470E-01	0.5877E-04	0.9548E-04
0.5158	0.2559E-04	0.2243	0.1473E-01	0.6623	0.1501E-01	0.1204E-16	0.8334E-01	0.6485E-04	0.9427E-04
0.5315	0.2499E-04	0.2264	0.1399E-01	0.6522	0.1427E-01	0.2648E-06	0.9284E-01	0.7137E-04	0.9292E-04
0.5474	0.2451E-04	0.2287	0.1324E-01	0.6410	0.1352E-01	0.2675E-06	0.1032	0.7835E-04	0.9142E-04
0.5634	0.2413E-04	0.2313	0.1249E-01	0.6286	0.1275E-01	0.6577E-06	0.1145	0.8585E-04	0.8977E-04
0.5800	0.2385E-04	0.2340	0.1172E-01	0.6150	0.1198E-01	0.1246E-04	0.1269	0.9391E-04	0.8796E-04
0.5966	0.2364E-04	0.2370	0.1093E-01	0.6001	0.1119E-01	0.2210E-04	0.1404	0.1026E-03	0.8592E-04
0.6135	0.2352E-04	0.2402	0.1012E-01	0.5836	0.1038E-01	0.3897E-04	0.1553	0.1122E-03	0.8366E-04
0.6307	0.2348E-04	0.2438	0.9292E-02	0.5654	0.9543E-02	0.6945E-04	0.1716	0.1226E-03	0.8111E-04
0.6482	0.2351E-04	0.2476	0.8444E-02	0.5453	0.8691E-02	0.1252E-03	0.1894	0.1343E-03	0.7823E-04
0.6660	0.2359E-04	0.2517	0.7578E-02	0.5231	0.7821E-02	0.2268E-03	0.2091	0.1476E-03	0.7495E-04
0.6840	0.2370E-04	0.2561	0.6707E-02	0.4989	0.6945E-02	0.4092E-03	0.2306	0.1627E-03	0.7120E-04
0.7019	0.2383E-04	0.2605	0.5850E-02	0.4726	0.6083E-02	0.7332E-03	0.2538	0.1801E-03	0.6693E-04
0.7200	0.2398E-04	0.2649	0.5014E-02	0.4442	0.5240E-02	0.1300E-02	0.2789	0.2005E-03	0.6204E-04
0.7385	0.2381E-04	0.2690	0.4205E-02	0.4138	0.4424E-02	0.2257E-02	0.3058	0.2249E-03	0.5658E-04
0.7575	0.2344E-04	0.2725	0.3432E-02	0.3811	0.3642E-02	0.3830E-02	0.3350	0.2547E-03	0.5048E-04
0.7774	0.2263E-04	0.2748	0.2706E-02	0.3458	0.2905E-02	0.6387E-02	0.3669	0.2921E-03	0.4375E-04
0.7984	0.2120E-04	0.2749	0.2041E-02	0.3078	0.2225E-02	0.1051E-01	0.4020	0.3399E-03	0.3654E-04
0.8207	0.1898E-04	0.2714	0.1453E-02	0.2671	0.1618E-02	0.1707E-01	0.4408	0.4020E-03	0.2911E-04
0.8448	0.1582E-04	0.2620	0.9583E-03	0.2238	0.1100E-02	0.2739E-01	0.4841	0.4837E-03	0.2185E-04
0.8711	0.1200E-04	0.2438	0.5693E-03	0.1785	0.6841E-03	0.4326E-01	0.5325	0.5918E-03	0.1524E-04
0.9003	0.8010E-05	0.2127	0.2907E-03	0.1320	0.3754E-03	0.6700E-01	0.5868	0.7275E-03	0.9631E-05
0.9334	0.4292E-05	0.1635	0.1156E-03	0.8548E-01	0.1682E-03	0.1016	0.6481	0.9543E-03	0.5181E-05
0.9685	0.1614E-05	0.1000	0.3100E-04	0.4416E-01	0.5512E-04	0.1445	0.7104	0.9561E-03	0.2160E-05
1.000	0.4433E-06	0.4714E-01	0.6003E-06	0.1751E-01	0.1399E-04	0.1795	0.7563	0.6164E-03	0.6876E-06

1

SUMMARY OF RESULTS

TOTAL WALL ABSORPTION = 3.349

Y	QT+	QC+	QL+	QT-	QC-	QL-	QW	Te	Tr
0.0000E+00	3.349	1.458	1.891	92.60	92.60	-0.6529E-13	-89.25	0.1096E+06	0.1090E+06
0.2158E-01	3.039	1.258	1.681	93.50	92.80	0.7006	-90.56	0.1098E+06	0.1091E+06
0.5035E-01	2.366	0.9958	1.370	94.17	93.07	1.106	-91.81	0.1109E+06	0.1098E+06
0.7912E-01	1.790	0.7496	1.041	94.66	93.31	1.346	-92.87	0.1131E+06	0.1118E+06
0.1079	1.344	0.5331	0.7109	94.99	93.52	1.465	-93.74	0.1167E+06	0.1151E+06
0.1367	0.7800	0.3623	0.4177	95.16	93.68	1.478	-94.38	0.1213E+06	0.1222E+06
0.1654	0.4670	0.2477	0.2193	95.20	93.77	1.424	-94.73	0.1249E+06	0.1355E+06
0.1942	0.2997	0.1806	0.1191	95.17	93.82	1.348	-94.87	0.1246E+06	0.1550E+06
0.2230	0.2166	0.1396	0.7701E-01	95.13	93.84	1.298	-94.91	0.1194E+06	0.1767E+06
0.2517	0.1703	0.1097	0.6061E-01	95.11	93.86	1.249	-94.94	0.1118E+06	0.1930E+06
0.2805	0.1410	0.8627E-01	0.5474E-01	95.10	93.87	1.225	-94.96	0.1043E+06	0.2056E+06
0.3092	0.1215	0.6787E-01	0.5359E-01	95.09	93.89	1.209	-94.97	9789.	0.2148E+06
0.3379	0.1083	0.5342E-01	0.5490E-01	95.09	93.89	1.199	-94.98	9282.	0.2224E+06
0.3667	0.9966E-01	0.4192E-01	0.5774E-01	95.09	93.90	1.193	-94.99	8850.	0.2294E+06
0.3957	0.9418E-01	0.3266E-01	0.6152E-01	95.09	93.90	1.188	-94.99	8473.	0.2365E+06
0.4250	0.9071E-01	0.2514E-01	0.6557E-01	95.08	93.90	1.184	-94.99	8134.	0.2443E+06
0.4547	0.8807E-01	0.1903E-01	0.6904E-01	95.08	93.90	1.178	-94.99	7820.	0.2530E+06
0.4849	0.8508E-01	0.1408E-01	0.7100E-01	95.07	93.90	1.169	-94.98	7525.	0.2628E+06
0.5158	0.8087E-01	0.1011E-01	0.7076E-01	95.05	93.89	1.152	-94.97	7242.	0.2739E+06
0.5474	0.7507E-01	0.6988E-02	0.6808E-01	95.02	93.89	1.130	-94.95	6966.	0.2865E+06
0.5800	0.6785E-01	0.4580E-02	0.6327E-01	94.99	93.89	1.106	-94.93	6692.	0.3008E+06
0.6135	0.5928E-01	0.2787E-02	0.5649E-01	94.97	93.88	1.089	-94.91	6413.	0.3173E+06
0.6482	0.4713E-01	0.1516E-02	0.4562E-01	94.95	93.88	1.077	-94.91	6117.	0.3362E+06

```
 0.6840    0.2472E-01  0.6863E-03  0.2404E-01   94.94     93.87     1.075     -94.92     5789.     0.3500E+06
 0.7200    0.4736E-03  0.2558E-03  0.4480E-02   94.93     93.86     1.068     -94.83     5416.     0.3026E+06
 0.7575    0.4529E-03  0.7582E-04  0.3770E-03   94.91     93.86     1.058     -94.81     4965.     0.4102E+06
 0.7964    0.2217E-04  0.1333E-04  0.8837E-05   94.90     93.85     1.052     -94.90     4382.     0.4422E+06
 0.8448    0.8527E-06  0.8335E-06  0.1924E-07   94.89     93.84     1.048     -94.89     3660.     0.4810E+06
 0.9003    0.7847E-08  0.7866E-08  0.4182E-12   94.89     93.84     1.048     -94.88     2778.     0.5300E+06
 0.9685    0.6458E-10  0.6458E-10  -0.7292E-18  94.88     93.83     1.047     -94.88     1763.     0.5894E+06
1


1


     RADIATION CORRECTION FACTORS

     Y          Hg          H+       H-SOURCE       Dg          O+       O-SOURCE
 0.0000E+00   1.000      0.3834      0.3834       1.000      0.2763      0.2763
 0.2158E-01   1.000      0.3701      0.3701       1.000      0.2661      0.2661
 0.5035E-01   1.000      0.3055      0.3055       1.000      0.2171      0.2171
 0.7912E-01   1.000      0.2070      0.2070       1.000      0.1441      0.1441
 0.1078       1.000      0.1100      0.1100       1.000      0.7435E-01  0.7435E-01
 0.1367       1.000      0.4683E-01  0.4683E-01   1.000      0.3035E-01  0.3035E-01
 0.1654       1.000      0.1926E-01  0.1926E-01   1.000      0.1165E-01  0.1165E-01
 0.1942       1.000      0.1012E-01  0.1012E-01   1.000      0.5397E-02  0.5397E-02
 0.2230       1.000      0.8684E-02  0.8684E-02   1.000      0.3647E-02  0.3647E-02
 0.2517       1.000      0.1225E-01  0.1225E-01   1.000      0.3389E-02  0.3389E-02
 0.2805       1.000      0.2329E-01  0.2329E-01   1.000      0.3533E-02  0.3533E-02
 0.3092       1.000      0.5012E-01  0.5012E-01   1.000      0.3652E-02  0.3652E-02
 0.3379       1.000      0.1089      0.1089       1.000      0.3672E-02  0.3672E-02
 0.3667       1.000      0.2296      0.2296       1.000      0.3902E-02  0.3902E-02
 0.3957       1.000      0.4705      0.4705       1.000      0.4874E-02  0.4874E-02
 0.4250       1.000      0.9488      0.9488       1.000      0.7336E-02  0.7336E-02
 0.4547       1.000       1.906       1.906       1.000      0.1257E-01  0.1257E-01
 0.4849       1.000       3.851       3.851       1.000      0.2315E-01  0.2315E-01
 0.5158       1.000       7.908       7.908       1.000      0.4468E-01  0.4468E-01
 0.5474       1.000       16.70       16.70       1.000      0.9029E-01  0.9029E-01
 0.5800       1.000       36.84       36.84       1.000      0.1935      0.1935
 0.6135       1.000       87.32       87.32       1.000      0.4526      0.4526
 0.6482       1.000       234.1       234.1       1.000      1.217       1.217
 0.6840       1.000       780.7       780.7       1.000      4.132       4.132
 0.7200       1.000       1000.       1000.       1.000      20.40       20.40
 0.7575       1.000       1000.       1000.       1.000      200.3       200.3
 0.7964       1.000       1000.       1000.       1.000      1000.       1000.
 0.8448       1.000       1000.       1000.       1.000      1000.       1000.
 0.9003       1.000       1000.       1000.       1.000      1000.       1000.
 0.9685       1.000       1000.       1000.       1.000      1000.       1000.
1


     Y          N2+(I)      N2+(B)      N2(I)       N2(A)       N2(B)       N2(C)       NO(I)       NO(A)       NO(B)       O2(I)       O2(A)

 0.0000E+00   1.000      0.9986      1.007       0.5723      0.6033      0.1170      1.003      0.3772      0.8361      1.000      0.7352E-02
 0.2158E-01   1.000      0.9988      1.007       0.5723      0.6033      0.1170      1.003      0.3772      0.8361      1.000      0.7352E-02
 0.5035E-01   1.000      0.9988      1.008       0.5804      0.5910      0.1043      1.003      0.3747      0.8293      1.000      0.7794E-02
 0.7912E-01   1.000      0.9988      1.009       0.5360      0.5667      0.9003E-01  1.003      0.3611      0.8074      1.000      0.8168E-02
 0.1078       1.000      0.9989      1.012       0.4974      0.5308      0.4992E-01  1.005      0.3308      0.7629      1.000      0.8255E-02
 0.1367       1.000      0.9989      1.017       0.4534      0.4886      0.2468E-01  1.007      0.2821      0.6934      1.000      0.7261E-02
 0.1654       1.001      0.9989      1.022       0.4120      0.4498      0.1096E-01  1.009      0.2281      0.6164      1.000      0.5110E-02
 0.1942       1.001      0.9986      1.023       0.3763      0.4187      0.5670E-02  1.010      0.1905      0.5581      1.000      0.4831E-02
 0.2230       1.001      0.9992      1.019       0.3623      0.4018      0.4258E-02  1.009      0.1710      0.5312      1.000      0.5486E-02
 0.2517       1.000      0.9985      1.012       0.3685      0.4067      0.4404E-02  1.006      0.1653      0.5341      1.000      0.6510E-02
 0.2805       1.000      0.9978      1.007       0.3651      0.4309      0.5501E-02  1.004      0.1640      0.5600      1.000      0.1356E-01
 0.3092       1.000      0.9973      1.004       0.3990      0.4701      0.7193E-02  1.002      0.1634      0.5981      1.000      0.7213E-01
 0.3379       1.000      0.9968      1.002       0.4425      0.5164      0.9249E-02  1.001      0.1629      0.6381      1.000      0.5381
 0.3667       1.000      0.9964      1.001       0.4923      0.5668      0.1161E-01  1.001      0.1623      0.6804      1.000      0.5381
 0.3957       1.000      0.9959      1.001       0.5484      0.6211      0.1430E-01  1.001      0.1613      0.7264      1.000      0.5381
 0.4250       1.000      0.9954      1.001       0.6101      0.6783      0.1730E-01  1.000      0.1601      0.7697      1.000      0.5381
 0.4547       1.000      0.9948      1.000       0.6762      0.7372      0.2107E-01  1.000      0.1586      0.8106      1.000      0.5381
 0.4849       1.000      0.9940      1.000       0.7457      0.7962      0.2567E-01  1.000      0.1567      0.8439      1.000      0.5381
 0.5158       1.000      0.9931      1.000       0.8164      0.8529      0.3158E-01  1.000      0.1546      0.8778      1.000      0.5381
 0.5474       1.000      0.9918      1.000       0.8775      0.8990      0.3963E-01  1.000      0.1521      0.9044      1.000      0.1049
 0.5800       1.000      0.9901      1.000       0.9266      0.9342      0.5112E-01  1.000      0.1492      0.9277      1.000      0.2926E-01
 0.6135       1.000      0.9878      1.000       0.9603      0.9575      0.6907E-01  1.000      0.1460      0.9466      1.000      0.1258E-01
 0.6482       1.000      0.9841      1.000       0.9817      0.9733      0.1006      1.000      0.1424      0.9623      1.000      0.5567E-02
 0.6840       1.000      0.9782      1.000       0.9936      0.9847      0.1662      1.000      0.1385      0.9751      1.000      0.3651E-02
 0.7200       1.000      0.9680      1.000       0.9986      0.9932      0.3558      1.000      0.1342      0.9852      1.000      0.1492E-02
 0.7575       1.000      0.9486      1.000       1.000       0.9980      1.188       1.000      0.1300      0.9927      1.000      0.1158E-02
 0.7964       1.000      0.9054      1.000       1.000       0.9997      9.778       1.000      0.1257      0.9977      1.000      0.1553E-02
 0.8448       1.000      0.7908      1.000       1.001       1.000       533.6       1.000      0.1225      0.9997      1.000      0.5455E-02
 0.9003       1.000      0.4868      1.000       1.030       1.000      0.1760E+07   1.000      0.1358      0.9999      1.000      0.1826
 0.9685       0.8600      23.95      1.000      0.1787E+06  0.1468E+07  0.1231E+16  1.000       13.68       1.358      1.000       1842.
1
```

9.3 Batch File (*cylinder.bat*)

```
# QSUB -A S480BM -eo -o cpl.cylinder.lst -s /bin/sh
# QSUB -lT 6800 -lM 3.2Mw -lF 50Mb
ja -m
PATH=$PATH:.;export PATH
rcp -p roy@aero15:./coupled/rad_src/\*.f /tmp
rcp -p roy@aero15:./coupled/rad_coupling/rad_src/\*.f /tmp
```

```
rcp -p roy@aero15:./coupled/rad_obj_cpl_cylinder/\*.o /tmp
#rcp -p roy@aero15:/usr3/roy/ineq3d_run/radical.cpl.cylinder.a /tmp/radical.a
rcp -p roy@aero15:./coupled/rad_src/Makefile /tmp
rcp -p roy@aero15:./coupled/rad_coupling/ineq3d_src/\*.inc /tmp
cd /tmp
make
rm Makefile
rcp -p *.o roy@aero15:./coupled/rad_obj_cpl_cylinder
rm *.o
#rcp -p radical.a roy@aero15:/usr3/roy/ineq3d_run/radical.cpl.cylinder.a
#
rcp -p roy@aero15:./coupled/ineq3d_src/\*.f /tmp
rcp -p roy@aero15:./coupled/rad_coupling/ineq3d_src/\*.f /tmp
rcp -p roy@aero15:./coupled/ineq3d_obj_cpl_cylinder/\*o /tmp
rcp -p roy@aero15:./coupled/rad_coupling/ineq3d_src/dum.o /tmp
rcp -p roy@aero15:./coupled/ineq3d_src/Makefile /tmp
#rcp -p roy@aero15:/usr3/roy/ineq3d_run/ineq3d.cpl.cylinder.exe /tmp/ineq3d.exe
make
rcp -p *.o roy@aero15:./coupled/ineq3d_obj_cpl_cylinder
rm *.o
#rcp -p ineq3d.exe roy@aero15:/usr3/roy/ineq3d_run/ineq3d.cpl.cylinder.exe
#
rcp roy@aero15:./coupled/input_files/spec11.cpl.cylinder.dat /tmp/inputfile.dat
rcp roy@aero15:./coupled/input_files/input2.cpl.cylinder.dat /tmp/fort.88
rcp roy@aero15:./coupled/input_files/rad.dat /tmp
rcp roy@aero15:./coupled/input_files/mexcite.dat /tmp
rcp roy@aero15:./coupled/grids/grid50x70c.cylinder.dat /tmp/fire2.dat
rcp roy@aero15:/usr3/roy/ineq3d_run/convert.i50.1634.f /tmp/convert.f
cf77 -o convert.exe convert.f
#rcp roy@aero15:/usr3/roy/ineq3d_run/fort.cpl.cylinder.42 /tmp/fort.20
rcp roy@aero15:/usr3/roy/ineq3d_run/fort.42 /tmp/fort.20
mkdir run
ineq3d.exe < inputfile.dat > tv40000.wdot_elec.50x70c.cylinder.0pt0625.out
rm core
mv tv40000*.out run
#rcp fort.42 roy@aero15:/usr3/roy/ineq3d_run/fort.cpl.cylinder.42
rcp fort.42 roy@aero15:/usr3/roy/ineq3d_run/fort.42
convert.exe
cp inputfile.dat run
mv fort.4* run
mv fort.1* run
mv fort.5* run
mv fort.26 run
mv fort.? run
mv radiation.out run/fort.25
mv temp*.dat run
mv molefrac1.dat run/molefrac.dat
mv molefrac30.dat run/molefr30.dat
mv molefr50.dat run
mv molefr75.dat run
mv molefr90.dat run
```

```
mv massfr1.dat run
mv j*.dat run
mv flow.dat run
mkdir augd40cp0625
mv run/* augd40cp0625
rcp -r augd40cp0625 roy@aero15:/usr3/roy/output_files
ja -cfs
```

9.4 Post-processing Files

9.4.1 Flowfield Post-processing File (*convert.f*)

```
      PROGRAM CONVERT
C
C*************************************************************************
C**********CONVERT UNFORMATTED OUTPUT FROM INEQ3D TO FORMATTED***********
C**************OUTPUT ALONG CONSTANT I OR CONSTANT J LINES***************
C*************************************************************************
C
      DIMENSION P(100,100,2),T(100,100,2),TV(100,100,2),
     1          X(100,100,2),Y(100,100,2),Z(100,100,2),
     2          A(100,100,2),B(100,100,2),
     3          Q(100,100,2,17),
     4          RMOL(11),FRAC(11)
C
SCALE=1.0
C
C   SET MOLECULAR WEIGHTS
      RMOL(1)=28.016
      RMOL(2)=32.0
      RMOL(3)=30.008
      RMOL(4)=30.008
      RMOL(5)=28.016
      RMOL(6)=32.0
      RMOL(7)=14.008
      RMOL(8)=16.0
      RMOL(9)=14.008
      RMOL(10)=16.0
      RMOL(11)=0.0005486
C
C********READ IN BINARY GRID FILE**********************************
C
      IUNIT=8
      OPEN (UNIT=IUNIT, FILE="fire2.dat", FORM='UNFORMATTED')
      READ(IUNIT) IDIM,JDIM,KDIM
      READ(IUNIT) (((X(I,J,K),I=1,IDIM),J=1,JDIM),K=1,KDIM),
     +             (((Y(I,J,K),I=1,IDIM),J=1,JDIM),K=1,KDIM),
     +             (((Z(I,J,K),I=1,IDIM),J=1,JDIM),K=1,KDIM)
      CLOSE(IUNIT)
C
```

```
C********READ IN INEQ3D BINARY FLOWFIELD VARIABLE FILES********
C
      READ(43) NII,NJJ,NKK
      READ(43) ACH,ALPHA2,RE,TLAST
      READ(43) (((P(I,J,K),I=1,NII),J=1,NJJ),K=1,NKK),
     +         (((T(I,J,K),I=1,NII),J=1,NJJ),K=1,NKK),
     +         (((TV(I,J,K),I=1,NII),J=1,NJJ),K=1,NKK),
     +         (((A(I,J,K),I=1,NII),J=1,NJJ),K=1,NKK),
     +         (((B(I,J,K),I=1,NII),J=1,NJJ),K=1,NKK)
C
      READ(44) NII,NJJ,NKK
      READ(44) ACH,ALPHA2,RE,TLAST
      READ(44) ((((Q(I,J,K,L),I=1,NII),J=1,NJJ),K=1,NKK),L=1,11)
C
      READ(45) NII,NJJ,NKK
      READ(45) ACH,ALPHA2,RE,TLAST
      READ(45) ((((Q(I,J,K,L),I=1,NII),J=1,NJJ),K=1,NKK),L=12,16)
C
C**************RIN is free stream density in gm/cm^3*****************
C*****RIN=3.72E-8 is for fireII 1634*****
      RIN=3.72E-8
C*****RIN=1.9964E-8 is for 9 km/sec case*****
C     RIN=1.9964E-8
C*****RIN=4.2930E-8 is for AFE 4 case*****
C     RIN=4.2930E-8
C
C     ******CONVERT ELECTRONS TO MASS FRACTION************************
      DO 10 I=1,IDIM
      DO 10 J=1,JDIM
      DO 10 K=1,KDIM
 10   Q(I,J,K,11)=10**Q(I,J,K,11)*RMOL(11)/(6.022E23*Q(I,J,K,12)*RIN)
C
C     ******CALCULATE MOLE FRACTIONS FROM MASS FRACTIONS**************
C     ********I=1********
      OPEN (UNIT=22, FILE="molefr1.dat", FORM='FORMATTED')
      I=1
      K=1
      DO 30 J=1,JDIM
        D=((X(I,J,K)-X(I,1,K))**2.+(Z(I,J,K)-Z(I,1,K))**2.)**0.5
        D=D/SCALE
        RMBAR=0.0
        DO 35 JJ=1,11
          RMBAR=RMBAR+Q(I,J,K,JJ)/RMOL(JJ)
 35     CONTINUE
        RMBAR=1./RMBAR
        DO 37 JJ=1,11
          FRAC(JJ)=RMBAR*Q(I,J,K,JJ)/RMOL(JJ)
 37     CONTINUE
        WRITE(22,99)D,(FRAC(JJ),JJ=1,11)
 99     FORMAT(1X,E11.5,1X,E11.5,1X,E11.5,1X,E11.5,1X,E11.5,1X,E11.5,
     1         1X,E11.5,1X,E11.5,1X,E11.5,1X,E11.5,1X,E11.5,1X,E11.5)
```

```
 30   CONTINUE
      CLOSE(22)
C
C     ********I=15********
      OPEN (UNIT=24, FILE="molefr15.dat", FORM='FORMATTED')
      I=15
      K=1
      DO 34 J=1,JDIM
        D=((X(I,J,K)-X(I,1,K))**2.+(Z(I,J,K)-Z(I,1,K))**2.)**0.5
        D=D/SCALE
        RMBAR=0.0
        DO 33 JJ=1,11
          RMBAR=RMBAR+Q(I,J,K,JJ)/RMOL(JJ)
 33     CONTINUE
        RMBAR=1./RMBAR
        DO 39 JJ=1,11
          FRAC(JJ)=RMBAR*Q(I,J,K,JJ)/RMOL(JJ)
 39     CONTINUE
        WRITE(24,99)D,(FRAC(JJ),JJ=1,11)
 34   CONTINUE
      CLOSE(24)
C
C     ********I=30********
      OPEN (UNIT=25, FILE="molefr30.dat", FORM='FORMATTED')
      I=30
      K=1
      DO 54 J=1,JDIM
        D=((X(I,J,K)-X(I,1,K))**2.+(Z(I,J,K)-Z(I,1,K))**2.)**0.5
        D=D/SCALE
        RMBAR=0.0
        DO 53 JJ=1,11
          RMBAR=RMBAR+Q(I,J,K,JJ)/RMOL(JJ)
 53     CONTINUE
        RMBAR=1./RMBAR
        DO 59 JJ=1,11
          FRAC(JJ)=RMBAR*Q(I,J,K,JJ)/RMOL(JJ)
 59     CONTINUE
        WRITE(25,99)D,(FRAC(JJ),JJ=1,11)
 54   CONTINUE
      CLOSE(25)
C
C     ********I=40********
      OPEN (UNIT=26, FILE="molefr40.dat", FORM='FORMATTED')
      I=40
      K=1
      DO 64 J=1,JDIM
        D=((X(I,J,K)-X(I,1,K))**2.+(Z(I,J,K)-Z(I,1,K))**2.)**0.5
        D=D/SCALE
        RMBAR=0.0
        DO 63 JJ=1,11
          RMBAR=RMBAR+Q(I,J,K,JJ)/RMOL(JJ)
```

```
 63     CONTINUE
        RMBAR=1./RMBAR
        DO 69 JJ=1,11
          FRAC(JJ)=RMBAR*Q(I,J,K,JJ)/RMOL(JJ)
 69     CONTINUE
        WRITE(26,99)D,(FRAC(JJ),JJ=1,11)
 64   CONTINUE
      CLOSE(26)
C
C     ********I=50********
C
      OPEN (UNIT=27, FILE="molefr50.dat", FORM='FORMATTED')
      I=50
      K=1
      DO 74 J=1,JDIM
        D=((X(I,J,K)-X(I,1,K))**2.+(Z(I,J,K)-Z(I,1,K))**2.)**0.5
        D=D/SCALE
        RMBAR=0.0
        DO 73 JJ=1,11
          RMBAR=RMBAR+Q(I,J,K,JJ)/RMOL(JJ)
 73     CONTINUE
        RMBAR=1./RMBAR
        DO 79 JJ=1,11
          FRAC(JJ)=RMBAR*Q(I,J,K,JJ)/RMOL(JJ)
 79     CONTINUE
        WRITE(27,99)D,(FRAC(JJ),JJ=1,11)
 74   CONTINUE
      CLOSE(27)
C
C     *************OTHER FILES*****************************************
C
      K=1
      OPEN (UNIT=39, FILE="diag.dat", FORM='FORMATTED')
      WRITE(39,*) 'title="DIAGNOSTIC"'
      WRITE(39,*) 'variables=x,y,n2,o2,no,no+,n2+,o2+,n+,o+,n,o,e-,',
     1            'rho,p,t,tv,mach,gamma'
      WRITE(39,*) 'zone t="z1",i=',IDIM,',j=',JDIM,',f=point'
      WRITE(39,*) ((X(I,J,K),Z(I,J,K),(Q(I,J,K,NNN),NNN=1,12),
     1            P(I,J,K),T(I,J,K),TV(I,J,K),A(I,J,K),B(I,J,K),
     1            I=1,IDIM),J=1,JDIM)
      CLOSE(39)
C
      JE=16
      JRH=12
      JU=13
      JV=14
      JW=15
C
      OPEN (UNIT=11, FILE="temp1.dat")
      I=1
      K=1
```

```
      DO 200 J=1,JDIM
        D=((X(I,J,K)-X(I,1,K))**2.+(Z(I,J,K)-Z(I,1,K))**2.)**0.5
        D=D/SCALE
        H=Q(I,J,K,JE)/Q(I,J,K,JRH)+P(I,J,K)/Q(I,J,K,JRH)
        WRITE(11,999) D,T(I,J,K),P(I,J,K),TV(I,J,K),Q(I,J,K,12)
     +               ,A(I,J,K),B(I,J,K),H
 200  CONTINUE
      CLOSE(11)
C
      OPEN (UNIT=12, FILE="temp15.dat")
      I=15
      K=1
      DO 300 J=1,JDIM
        D=((X(I,J,K)-X(I,1,K))**2.+(Z(I,J,K)-Z(I,1,K))**2.)**0.5
        D=D/SCALE
        H=Q(I,J,K,JE)/Q(I,J,K,JRH)+P(I,J,K)/Q(I,J,K,JRH)
       WRITE(12,999) D,T(I,J,K),P(I,J,K),TV(I,J,K),Q(I,J,K,12)
     +               ,A(I,J,K),B(I,J,K),H
 300  CONTINUE
      CLOSE(12)
C
      OPEN (UNIT=13, FILE="temp30.dat")
      I=30
      K=1
      DO 500 J=1,JDIM
        D=((X(I,J,K)-X(I,1,K))**2.+(Z(I,J,K)-Z(I,1,K))**2.)**0.5
        D=D/SCALE
        H=Q(I,J,K,JE)/Q(I,J,K,JRH)+P(I,J,K)/Q(I,J,K,JRH)
        WRITE(13,999) D,T(I,J,K),P(I,J,K),TV(I,J,K),Q(I,J,K,12)
     +               ,A(I,J,K),B(I,J,K),H
 500  CONTINUE
      CLOSE(13)
C
      OPEN (UNIT=36, FILE="temp40.dat")
      I=40
      K=1
      DO 525 J=1,JDIM
        D=((X(I,J,K)-X(I,1,K))**2.+(Z(I,J,K)-Z(I,1,K))**2.)**0.5
D=D/SCALE
        H=Q(I,J,K,JE)/Q(I,J,K,JRH)+P(I,J,K)/Q(I,J,K,JRH)
        WRITE(36,999) D,T(I,J,K),P(I,J,K),TV(I,J,K),Q(I,J,K,12)
     +               ,A(I,J,K),B(I,J,K),H
 525  CONTINUE
      CLOSE(36)
C
      OPEN (UNIT=33, FILE="temp50.dat")
      I=50
      K=1
      DO 550 J=1,JDIM
        D=((X(I,J,K)-X(I,1,K))**2.+(Z(I,J,K)-Z(I,1,K))**2.)**0.5
        D=D/SCALE
```

```
        H=Q(I,J,K,JE)/Q(I,J,K,JRH)+P(I,J,K)/Q(I,J,K,JRH)
        WRITE(33,999) D,T(I,J,K),P(I,J,K),TV(I,J,K),Q(I,J,K,12)
     +              ,A(I,J,K),B(I,J,K),H
 550  CONTINUE
      CLOSE(33)
C
      K=1
      OPEN (UNIT=14, FILE="jouter.dat")
      DO 600 I=1,IDIM
        WRITE(14,*) I,T(I,JDIM,K),P(I,JDIM,K),TV(I,JDIM,K),
     +              Q(I,JDIM,K,12),A(I,JDIM,K),B(I,JDIM,K)
 600  CONTINUE
      CLOSE(14)
C
      K=1
      OPEN (UNIT=37, FILE="j1.dat")
      DO 620 I=1,IDIM
        WRITE(37,*) I,T(I,1,K),P(I,1,K),TV(I,1,K),Q(I,1,K,12)
     +              ,A(I,1,K),B(I,1,K)
 620  CONTINUE
      CLOSE(37)
 999  FORMAT(1X,7(2X,E15.5),2X,E20.10)
      STOP
      END
```

9.4.2 Radiation Post-processing File (*radnew.f*)

```
      PROGRAM RAD
C
C     RADIATION POST-PROCESSING FILE  UPDATED 6/94
C
      IANS = 1
C
      CALL PLOT(IANS)
 40   CONTINUE
      STOP
      END
C
C
C
      SUBROUTINE PLOT(IPLT)
      DIMENSION GV(200),GQ(200,4),DV(5050),DQ(5050,4)
      DIMENSION IPKRAY(400)
      L = 1
      GMAX = 0.0
      CALL READIN(L)
      CALL GROUP(NG,GV,GQ(1,L),GMAX1)
      IF(GMAX1.GT.GMAX) GMAX = GMAX1
      CALL DETAIL(ND,DV,DQ(1,L))
 801  CONTINUE
```

```
      WRITE(*,*) ' Calculated GMAX = ',GMAX
C     ****OUTPUT RADIATIVE INTENSITY TO FILES 65 AND 66****
c      WRITE(65,*) NG, GMAX
      DO 950 I=1,NG
 950    WRITE(65,*)GV(I),GQ(I,L)
c      WRITE(66,*) ND
      DO 960 I=1,ND
 960    WRITE(66,*)DV(I),DQ(I,L)
C      ************************************************
 999  RETURN
      END
c
      subroutine readin(ll)
      common /datain/ ncont,nline,vcont(50),qcont(50),qcent(20),
     1 vline(5000),qline(5000),l1(5000),l2(5000),l3(5000)
      character first*1,rest*80,star*1
      data star/'*'/
      ncont = 36
      mm = 24 + ll
      do 10 i=1,ncont
 10     read(mm,1000) vcont(i),qcont(i)
      k = 0
      nline = 0
 20   read(mm,1010,end=999) first,rest
      if(first .eq. star) then
        k=k+1
        read(rest,1020) qcent(k)
       else
        nline=nline+1
        l = nline
        read(rest,1030) vline(l),qline(l),l1(l),l2(l),l3(l)
      endif
      goto 20
 999  return
1000  format(2F15.4,3I5)
1010  format(A1,A80)
1020  format(25X,F15.4)
1030  format(F14.4,F15.4,3I5)
      end
c
      subroutine group(ng,gv,gq,gmax)
      common /datain/ ncont,nline,vcont(50),qcont(50),qcent(20),
     1 vline(5000),qline(5000),l1(5000),l2(5000),l3(5000)
      dimension gv(200),gq(200)
      dimension vmin(20),vmax(20)
      data ncent/20/
      data vmin/0.60,0.85,0.96,1.2,1.4,1.62,2.4,3.4,6.2,8.0,8.6,
     1 9.0,9.7,10.45,10.80,11.70,12.10,12.80,13.40,13.8/
      data vmax/0.80,0.95,1.2,1.4,1.6,2.4,3.34,4.0,8.0,8.6,9.0,
     1 9.7,10.45,10.80,11.70,12.10,12.80,13.40,13.80,14.50/
c
```

```
      do 10 i=1,ncent
       qcent(i) = qcent(i) / (vmax(i)-vmin(i))
10    continue
c
      i = 1
      k = 1
      j = 0
15    j = j+1
20      if(vcont(i) .ge. vmin(j)) goto 30
          gv(k) = vcont(i)
          gq(k) = qcont(i)
          k=k+1
          i=i+1
          goto 20
30      ratio = (vmin(j) - vcont(i-1))/(vcont(i) - vcont(i-1))
        q = qcont(i-1) * (1.-ratio) + qcont(i)*ratio
        gv(k) = vmin(j)
        gq(k) = q
        k=k+1
35      q = q + qcent(j)
        gv(k) = vmin(j)
        gq(k) = q
        k=k+1
        if(vcont(i) .eq. vmin(j)) i=i+1
40      if(vcont(i) .ge. vmax(j)) goto 50
          q = qcent(j) + qcont(i)
          gv(k) = vcont(i)
          gq(k) = q
          k=k+1
          i=i+1
          goto 40
50      ratio = (vmax(j) - vcont(i-1))/(vcont(i) - vcont(i-1))
        q = qcent(j) + qcont(i-1) * (1.-ratio) + qcont(i)*ratio
        gv(k) = vmax(j)
        gq(k) = q
        k=k+1
        q = q - qcent(j)
        if(j.ne.ncent .and. vmin(j+1) .eq. vmax(j)) then
          j=j+1
          goto 35
        endif
        gv(k) = vmax(j)
        gq(k) = q
        k=k+1
        if(vcont(i) .eq. vmax(j)) i=i+1
      if(j.lt.ncent) goto 15
      if(i .lt. ncont) then
        do 110 j=i,ncont
          gv(k) = vcont(j)
          gq(k) = qcont(j)
          k=k+1
```

```
110     continue
      endif
      ng = k - 1
      gmax = 0.0
      do 120 j=1,ng
120     if(gq(j).gt.gmax) gmax = gq(j)
      return
      end
c
      subroutine detail(nd,dv,dq)
      common /datain/ ncont,nline,vcont(50),qcont(50),qcent(20),
     1 vline(5000),qline(5000),l1(5000),l2(5000),l3(5000)
      dimension dv(5050),dq(5050)
c
      ii = 1
      v = vline(ii)
      q = qline(ii)
      i1 = l1(ii)
      i2 = l2(ii)
      i3 = l3(ii)
      i = 1
      k = 1
2     j1 = i1
      j2 = i2
      if(vcont(i) .lt. v) then
        dv(k) = vcont(i)
        dq(k) = qcont(i)
        i=i+1
        k=k+1
        goto 2
      endif
      ratio = (v - vcont(i-1))/(vcont(i) - vcont(i-1))
      qq = qcont(i-1)*(1.-ratio) + qcont(i)*ratio
      dv(k) = v
      dq(k) = qq
      k=k+1
3     vold = v
      dv(k) = v
      dq(k) = q
      k=k+1
      ii=ii+1
      if(ii.gt.nline) goto 999
      v = vline(ii)
      q = qline(ii)
      i1 = l1(ii)
      i2 = l2(ii)
      i3 = l3(ii)
      if(j1.eq.i1 .and. j2.eq.i2) goto 3
4     if(vcont(i) .lt. vold) then
        i=i+1
        goto 4
```

```
      endif
      ratio = (vold - vcont(i-1))/(vcont(i) - vcont(i-1))
      qq = qcont(i-1)*(1.-ratio) + qcont(i)*ratio
      dv(k) = vold
      dq(k) = qq
      k=k+1
      goto 2
999   if(vcont(i) .lt. vold) then
        i=i+1
        goto 999
      endif
      ratio = (vold - vcont(i-1))/(vcont(i) - vcont(i-1))
      qq = qcont(i-1)*(1.-ratio) + qcont(i)*ratio
      dv(k) = vold
      dq(k) = qq
      k=k+1
      do 20 j=i,ncont
        dv(k) = vcont(j)
        dq(k) = qcont(j)
20      k=k+1
      nd = k - 1
      return
      end
```

9.5 Listing of Modified Subroutines and Include Files

9.5.1 *indx1.inc*

This include file was modified to pass the four new parameter variables (IICPL, JJCPL, KKCPL, and JSPEC) as well as the variable TCH (chemical time-step modification) for use in the restart file.

```
C file indx.inc-----------------------------------------------
      COMMON/I/ JTRN,JC,JCF,JCL,JADD,JE1,JE2,JRH,JU,JV,JW,JE,JEV,
     1 JVF,JVL,NS1,NSL,NJRH,NJU,NJV,NJW,NJE,NJEV,NJVF,NJVL,
     1 JN2,JO2,JNO,JNOP,JN2P,JO2P,JNP,JOP,JN,JO,JECC,
     2 TCH,IICPL,JJCPL,KKCPL,JSPEC
C     file end-----------------------------------------------
```

9.5.2 *main.f*

Modification to *main.f* include:

- the addition of four new parameters which are dependent on the size of the grid as well as the number of species (IRCPL, JRCPL, KRCPL, and JRSPEC)
- reading in two addtional flags (RSTAG and RBODY) from the first line of the input file
- adding loops to allow radiative frequency spectra to be calculated along both the stagnation streamline and the body

```
      PROGRAM MAIN
C
C file btyp1.inc-------------------------------------------
C     COMMON/B/BDX1,BDXN,BDY1,BDYN,BDZ1,BDZN
C     INTEGER  BDX1,BDXN,BDY1,BDYN,BDZ1,BDZN
C     file end---------------------------------------------
C
C file cont1.inc-------------------------------------------
C     COMMON/C/ACH,ALPHA,GAMMA,GA,FUIN,FVIN,FWIN,PIN,TIN,RIN,
C    1         TW,SCALE,CONS,EVIBIN,GBNEQ,FRAC(11)
C     file end---------------------------------------------
C
C file indx1.inc-------------------------------------------
C     COMMON/I/ JTRN,JC,JCF,JCL,JADD,JE1,JE2,JRH,JU,JV,JW,JE,JEV,
C    1 JVF,JVL,NS1,NSL,NJRH,NJU,NJV,NJW,NJE,NJEV,NJVF,NJVL,
C    1 JN2,JO2,JNO,JNOP,JN2P,JO2P,JNP,JOP,JN,JO,JECC,
C    2 TCH,IICPL,JJCPL,KKCPL,JSPEC
C     file end---------------------------------------------
C
C file reac1.inc-------------------------------------------
C     COMMON/R/NRCT,KIONF,ITYPE(30),KIONR(30),IPR(30,6),COEFA(30),
C    1 COEFB(30),ETA(30),EION(30)
C     file end---------------------------------------------
C
C file therm1.inc------------------------------------------
C     COMMON/T1/WMOL(11),RMOL(11),COEF(8,11),CVIB(11),
C    1 GDEGER(3,11),CELRON(3,11),ELCRS(11)
C     file end---------------------------------------------
C
C file tlim1.inc-------------------------------------------
C     COMMON/T2/TLOW,THIGH,TSLOW,TSHIGH,ETRMAX(11),ETRMIN(11),
C    1 EVBMAX(11),EVBMIN(11)
C     file end---------------------------------------------
      include 'btyp1.inc'
      include 'cont1.inc'
      include 'indx1.inc'
      include 'reac1.inc'
      include 'therm1.inc'
      include 'tlim1.inc'
      PARAMETER(NFDIM=1950000, NIDIM=17000)
C ***New parameters for radiative coupling (corresp. to grid size)***
      PARAMETER(IRCPL=60,JRCPL=100,KRCPL=3,JRSPEC=11)
      DIMENSION F(NFDIM),IAF(NIDIM),WOLD(IRCPL,JRCPL,KRCPL,JRSPEC),
     2 DQDY(100)
      INTEGER Q,QOLD,DELQ,P,A,B,PHI,T,TV,CJAB,DT,X,Y,Z,VOL,
     1 DFMX,DFMX1,CSR,RSR,PSR,TSR,TVSR,ASR,RUSR,RVSR,RWSR,RESR,
     1 EVSR,W,EGION,DUM1,FSTP,
     1 F1,F2,F3,F4,F5,F6,F7,F8,F9,F10,F11,F12,
     1 F13,F14,F15,F16,F17,F18,F19,F20,F21,F22,F23,F24,
     1 F25,F26,F27,F28,F29,F30,F31,F32,F33,F34,F35,F36,
```

```
     1 F37,F38,F39,F40,F41,F42,F43,F44,F45,F46,F47,F48,F49,
     1 F50,F51,F52,F53,F54,F55,F56,F57,F58,F59,F60,F61,F62,
     1 F63,F64,F65,F66,F67,F68,F69,F70,F71,F72,F73,F74,F75,
     1 F76,F77,F78,F79,F80,F81,F82,F83,F84,F85,F86,F87,F88,
     1 F89,F90,F91,F92,F93,F94,F95,F96,F97,F98,F99,F100,
     1 F101,F102,F103,F104,F105,F106,F107,F108,F109,F110,
     1 F111,F112,F113,F114,F115,F116,F117,F118,F119,F120,
     1 F121,F122,F123,F124,F125,F126,F127,F128,F129,F130,
     1 F131,F132,F133,F134,F135,F136,F137,F138,F139,F140
      REAL LEWIS
      LOGICAL NSTOKE,MULTM,HADJ,HFLXI,HFLX,AVG,RESTA,GFDUM,GDUM,
     1 FDUM,IGRID,OUTP7,THIN,ADIAB,NORML,RSTAG,RBODY
C
      IICPL=IRCPL
      JJCPL=JRCPL
      KKCPL=KRCPL
      JSPEC=JRSPEC
C*****************************************************************
      READ(5,*) MULTM,NSTOKE,THIN,ADIAB,RSTAG,RBODY
      READ(5,*) HFLXI,NORML,HADJ,IGRID,AVG
      READ(5,*) RESTA,GFDUM,GDUM,FDUM,OUTP7
      READ(5,*) NS,NR
      READ(5,*) NI,NJ,NK,KTEST,FSTP,LSTP,NSTP,KMOD
      READ(5,*) BDX1,BDXN,BDY1,BDYN,BDZ1,BDZN
      READ(5,*) IFILE,ITVD,ILIM
      READ(5,*) RLIM1,RLIM2,FAV
      READ(5,*) CFLO,ORDER,ESPI,ESPJ,ESPK
      READ(5,*) UO,PIN,TIN,ALPHA1,TLAST
      READ(5,*) GAMMA,PRTL,LEWIS,TW
      DATA XREF,YREF,ZREF,AREF,CREF/3*.0,2*1./
C*****************************************************************
      CALL CHEM(MULTM,KTEST,NS,NR,NSLP,NLST,JCP,JLST)
C
      NIM=NI-1
      NIP=NI+1
      NJM=NJ-1
      NJP=NJ+1
      NKM=NK-1
      NKP=NK+1
      NAX=MAXO(NJ,NK)
      MAX=MAXO(NIP,NJP,NKP)
      NIP2=NI+2
      NJP2=NJ+2
      NKP2=NK+2
      NIJ=NI*NJ
      NIJK=NIJ*NK
      NIJKM=NIM*NJM*NKM
      NIJKP=NIP*NJP*NKP
      NIK=NI*NK
      NIKP=NIP*NKP
C
```

```
      KPL=NI+NJ+NK-5
      JMJ=1
      KMK=JMJ+NJ
      JMJP=KMK+NK
      KMKP=JMJP+NJ
      NPT=KMKP+NK
      NPTO=NPT+KPL
      KPT=NPTO+KPL
      KPTO=KPT+NIJKM
      IS=KPTO+NIJKM
      JTOTAL=IS+NR*6
C
      CALL INDX(NI,NJ,NK,NIP,NJP,NIJ,NIJKM,
     1 KPL,IAF(JMJ),IAF(KMK),IAF(JMJP),IAF(KMKP),
     1 IAF(NPT),IAF(NPTO),IAF(KPT),IAF(KPTO),IPMAX)
C
      WRITE(6,*) 'JTOTAL  IPMAX'
      WRITE(6,*) JTOTAL,IPMAX
C
      Q=1
      DELQ= Q+JLST*NIJKP
      P=DELQ +NLST*NIJKP
      T =P+NIJKP
      TV=T
      IF(MULTM) TV=T+NIJKP
      B   =TV +NIJKP
      PHI =B  +NIJKP
      A   =PHI+NIJKP
      CJAB=A  +NIJKP
      QOLD=B
      DT=CJAB +NSLP*NIJKP
      X=DT+NIJK
      Y=X+NIJK
      Z=Y+NIJK
      VOL =Z+NIJK
      DFMX=VOL+NIJKP
      DFMX1= DFMX +NLST
      CSR  = DFMX1+NLST
      RSR  = CSR  +JC*NIKP
      PSR  = RSR  +NIKP
      TSR  = PSR  +NIKP
      TVSR=TSR+NIKP
      ASR  = TVSR +NIKP
      RUSR = ASR  +NIKP
      RVSR = RUSR +NIKP
      RWSR = RVSR +NIKP
      RESR = RWSR +NIKP
      EVSR = RESR +NIKP
      W    = EVSR +NIKP
      EGION= W+NIJ*JCP
      DUM1 = EGION+NIJ
```

```
C
      F1=DUM1
      F2=DUM1
      F3=F2+NI*4
      F4=F3+NI*4
      NUM1=12*NI
C
      F5 = DUM1
      F6 = F5+NAX*NI*JLST
      F7 = F6+NAX*NI
      F8 = F7+NAX*NI
      F9 = F8+NAX*NI
      F10= F9+NAX*NI
      F11=F10+NAX*NI
      F12=F11+NAX*NI
      F13=F12+NAX*NI
      F14=F13+NAX*NI
      F15=F14+NAX*NI
      F16=F15+NAX*NI*NLST
      F17=F16+NAX*NI
      F18=F17+NAX*NI
      F19=F18+NAX*NI
      F20=F19+NAX*NI
      F21=F16
      F22=F17
      F23=F18
      F24=F19
      F25=F20+NAX*NI*JLST
      F26=F25+NAX*NI
      F27=F26+NAX*NI
      F28=F27+MAX
      F29=F28+MAX
      F30=F29+MAX
      F31=F30+MAX
      F32=F31+MAX
      F33=F32+MAX
      F34=F33+MAX
      F35=F34+NAX*NI
      F36=F35+NAX*NI*NS
      NUMM=F36+NAX*NI*NS - DUM1
      F38 =F20+3*MAX
      F39 =F38+3*MAX
      F40 =F39+MAX
      F41 =F40+MAX
      F42 =F41+MAX
      F43 =F42+MAX
      F44 =F43+MAX
      F45 =F44+MAX
      F46 =F45+MAX
      F47 =F46+MAX
      F48 =F47+MAX*NS
```

```
      F49 =F48+MAX*NLST
      F50 =F49+MAX*NLST
      F51 =F50+MAX*NLST*NLST
      NUMM2=F51+MAX*NLST*NLST - DUM1
      NUM2 =MAXO(NUMM,NUMM2)
C
      F52=DUM1
      F53=F52+NLST*NLST*IPMAX
      F54=F53+       NS*IPMAX
      F55=F54+     NLST*IPMAX
      F56=F55+        3*IPMAX
      F57=F56+        4*IPMAX
      NUM3=IPMAX*(NLST*NLST+NLST+NS+8)
C
      F37=DUM1
      F58=F37+MAX
      F59=F58+MAX
      F60=F59+MAX
      F61=F60+MAX
      F62=F61+MAX
      F63=F62+MAX
      F64=F63+MAX
      F65=F64+NIJ
      F66=F65+NIJ
      F67=F66+NIJ
      F68=F67+NIJ*NS
      F69=F68+NIJ*NS
      F70=F69+NIJ*NS
      F71=F70+NIJ*NS
      NUM4=7*MAX+3*NIJ+5*NS*NIJ
C
      F72=DUM1
      F73=F72+JLST
      F74=F73+NI
      F75=F74+NI
      F76=F75+NI
      F77=F76+NI
      F78=F77+NI
      F79=F78+NI
      F80=F79+NI
      F81=F80+NI
      F82=F81+NI
      F83=F82+3*NI
      F84=F83+3*NI
      F85=F84+3*NI
      F86=F85+3*NI
      F87=F86+3*NI
      F88=F87+3*NI
      F89=F88+3*NI
      F90=F89+3*NI
      F91=F90+3*NI
```

```
      F92=F91+3*NI
      F93=F92+3*NI
      F94=F93+NS*NI
      F95=F94+NS*NI
      F96=F95+NS*NI
      F97=F96+NIK
      F98=F97+NIK
      F99=F98+NIK
      F100=F99+NIK
      F101=F100+NIK
      F102=F101+NIK
      F103=F102+MAX
      F104=F103+MAX
      NUM5=JLST+42*NI+3*NS*NI+6*NIK+3*MAX
C
      F105=DUM1
      F106=F105+NI
      F107=F106+NI
      F108=F107+NI
      F109=F108+NI
      F110=F109+NI
      F111=F110+NI
      F112=F111+NI
      F113=F112+NI
      F114=F113+NI
      F115=F114+NI
      F116=F115+NI
      F117=F116+NI
      F118=F117+NI
      F119=F118+NI
      F120=F119+NR*6
      F121=F120+NR*6
      F122=F121+NR*6
      F123=F122+NR*6
      F124=F123+JCP*NR
      F125=F124+NR*NI
      F126=F125+NR*NI
      F127=F126+NR*NI
      F128=F127+NR*NI
      F129=F128+NR*NI
      F130=F129+JCP*NI
      F131=F130+JCP*NI
      F132=F131+JCP*NI
      NUM6=14*NI+(24+JCP+5*NI)*NR+4*JCP*NI
C
      F133=DUM1
      F134=F133+MAX
      F135=F134+NIP*NJP*JLST
      F136=F135+NIP*NJP
      F137=F136+NIP*NJP
      F138=F137+NIP*NJP
```

```
      F139=F138+NIP*NJP
      NUM7=NS+MAX+(JLST+4)*NIP*NJP
      NTOTAL=DUM1+MAXO(NUM1,NUM2,NUM3,NUM4,NUM5,NUM6,NUM7)
      WRITE(6,*) 'DUM1,NUM1,NUM2,NUM3,NUM4,NUM5,NUM6,NUM7,NTOTAL'
      WRITE(6,*)  DUM1,NUM1,NUM2,NUM3,NUM4,NUM5,NUM6,NUM7,NTOTAL
C
C
C*************************************************************
      CALL GRID(NI,NJ,NK,F(X),F(Y),F(Z),XREF,YREF,ZREF,AREF,CREF,
     1 SCALE)
C
      CALL START(RESTA,MULTM,NI,NIM,NIP,NJ,NJM,NJP,NK,NKM,NKP,
     1 JLST,UO,ALPHA1,CFLO,CFL,RE,TLAST,F(Q),F(P),F(A),F(B),
     1 F(PHI),F(T),F(TV),F(X),F(Y),F(Z),F(VOL),WOLD)
C
      IF(.NOT.RESTA) THEN
      CALL INIT(NIP,NJP,NKP,JLST,NS,F(Q),F(P),F(A),F(B),F(PHI),
     1 F(T),F(TV))
      ENDIF
C
C*************************************************************
      DO 10 ISTP=FSTP,LSTP
C
      CALL LOCDT(NI,NJ,NK,NIP,NJP,NKP,JLST,CFL,F(Q),
     1 F(P),F(B),F(X),F(Y),F(Z),F(DT),F(F2),F(F3),F(F4))
C
      CALL INVRHS(MULTM,RESTA,HFLXI,HFLX,ISTP,NSTP,NI,NJ,NK,
     1 NIP,NJP,NKP,NIM,NJM,NKM,NAX,MAX,NS,NLST,JLST,
     1 ITVD,ILIM,RLIM1,RLIM2,ORDER,F(Q),F(DELQ),F(P),F(T),F(TV),
     1 F(B),F(DT),F(X),F(Y),F(Z),F(F5),F(F6),F(F7),F(F8),F(F9),
     1 F(F10),F(F11),F(F12),F(F13),F(F14),F(F15),F(F16),F(F17),
     1 F(F18),F(F19),F(F21),F(F22),F(F23),F(F24),F(F20),
     1 F(F25),F(F26),F(F27),F(F28),F(F29),F(F30),F(F31),F(F32),
     1 F(F33),F(F34),F(F35),F(F36),
     1 F(F20),F(F38),F(F39),F(F40),F(F41),F(F42),F(F43),F(F44),
     1 F(F45),F(F46),F(F47),F(F48),F(F49),F(F50),F(F51))
C
C
      CALL SOURCE(MULTM,ISTP,NI,NJ,NK,NIP,NJP,NKP,NS,NSLP,JCP,
     1 JLST,NLST,NR,IAF(IS),F(Q),F(DELQ),F(P),F(T),F(TV),F(CJAB),
     1 F(DT),F(X),F(Y),F(Z),F(VOL),F(W),
     1 F(EGION),F(F105),F(F106),F(F107),F(F108),F(F109),F(F110),
     1 F(F111),F(F112),F(F113),F(F114),F(F115),F(F116),F(F117),
     1 F(F118),F(F119),F(F120),F(F121),F(F122),F(F123),F(F124),
     1 F(F125),F(F126),F(F127),F(F128),F(F129),F(F130),F(F131),
     1 F(F132),RESTA,FSTP,WOLD)
C
      CALL SOLVC(MULTM,NI,NJ,NK,NIP,NJP,NKP,NKP2,NIJ,NIJK,
     1 NIJKM,NIJKP,NS,NSLP,NLST,JLST,KPL,IAF(NPT),IAF(NPTO),
     1 IPMAX,IAF(KPT),IAF(KPTO),F(Q),F(DELQ),F(DELQ),F(P),
     1 F(T),F(TV),F(B),F(PHI),F(CJAB),F(DT),F(X),F(Y),F(Z),
```

```
     1 F(F52),F(F53),F(F54),F(F55),F(F56),F(F57))
C
      CALL ADVCE(MULTM,NSTOKE,HADJ,AVG,NI,NJ,NK,NIP,NJP,NKP,JLST,NS,
     1 NLST,FAV,F(Q),F(DELQ),F(P),F(QOLD),F(F72),F(F73),F(F74),
     1 F(F75))
C
      CALL TEMP(MULTM,NSTOKE,NI,NJ,NK,NIP,NJP,NKP,MAX,NS,JLST,NLST,
     1 F(Q),F(P),F(T),F(TV),F(B),F(PHI),F(A),F(QOLD),F(F37),F(F58),
     1 F(F59),F(F60),F(F61),F(F62),F(F63),F(F64),F(F65),F(F66),
     1 F(F67),F(F68),F(F69),F(F70),F(F71))
C
      CALL BNDY(MAX,NI,NJ,NK,NIM,NIP,NJP,NKP,NKP2,JLST,NS,
     1 F(Q),F(P),F(T),F(TV),F(B),F(PHI),F(A),F(X),F(Y),
     1 F(Z),F(F37))
C
      IF(BDY1.EQ.5) THEN
      IF(NK.EQ.2) THEN
      CALL YWL2D(MULTM,NORML,AVG,ISTP,MAX,NI,NJ,NK,NIM,NIP,NJP,NKP,
     1 NKP2,NS,JLST,FAV,F(Q),F(P),F(T),F(TV),F(B),F(PHI),F(A),F(X),
     1 F(Y),F(Z),F(VOL),F(CSR),F(RSR),F(PSR),F(TSR),F(TVSR),
     1 F(ASR),F(RUSR),F(RVSR),F(RWSR),F(RESR),F(EVSR),F(F72),
     1 F(F73),F(F74),F(F75),F(F76),F(F77),F(F78),F(F79),F(F80),
     1 F(F81),F(F82),F(F83),F(F84),F(F85),F(F86),F(F87),F(F88),
     1 F(F89),F(F90),F(F91),F(F92),F(F93),F(F94),F(F95),F(F96),
     1 F(F97),F(F98),F(F99),F(F100),F(F101),F(F102),F(F103),
     1 F(F104))
      ELSE
      CALL YWALL(MULTM,NORML,AVG,ISTP,MAX,NI,NJ,NK,NIM,NIP,NJP,NKP,
     1 NKP2,NS,JLST,FAV,F(Q),F(P),F(T),F(TV),F(B),F(PHI),F(A),F(X),
     1 F(Y),F(Z),F(VOL),F(CSR),F(RSR),F(PSR),F(TSR),F(TVSR),
     1 F(ASR),F(RUSR),F(RVSR),F(RWSR),F(RESR),F(EVSR),F(F72),
     1 F(F73),F(F74),F(F75),F(F76),F(F77),F(F78),F(F79),F(F80),
     1 F(F81),F(F82),F(F83),F(F84),F(F85),F(F86),F(F87),F(F88),
     1 F(F89),F(F90),F(F91),F(F92),F(F93),F(F94),F(F95),F(F96),
     1 F(F97),F(F98),F(F99),F(F100),F(F101),F(F102),F(F103),
     1 F(F104))
        ENDIF
        ENDIF
C
      ISTPO=ISTP-FSTP
      IF(MOD(ISTPO,KMOD).EQ.0) THEN
      CALL REROR(MULTM,FSTP,ISTP,IFILE,MAX,NI,NJ,NK,NIP,NJP,
     1 NKP,NLST,F(DELQ),F(DFMX),F(DFMX1),F(A),F(F37),F(DT))
      ENDIF
C
   10 CONTINUE
C
C     ****radiative post-processing:  STAGNATION STREAMLINE****
C
      IF(RSTAG) THEN
        I=2
```

```
        K=2
        CALL RADCALC(DQDY,I,K,NI,NJ,NK,NIP,NJP,NKP,F(Q),F(P),
     1   F(T),F(TV),F(X),F(Y),F(Z),JC,JLST,JRH,1)
       ENDIF
C
C      ****radiative post-processing:  ALONG BODY****
C
       IF(RBODY) THEN
         K=2
         DO 600 I=2,NI
           CALL RADCALC(DQDY,I,K,NI,NJ,NK,NIP,NJP,NKP,F(Q),F(P),
     1      F(T),F(TV),F(X),F(Y),F(Z),JC,JLST,JRH,1)
 600     CONTINUE
       ENDIF
C
       IF(OUTP7) THEN
       CALL OUT(NI,NJ,NK,NIP,NJP,NKP,JLST,F(Q),F(P),F(VOL))
       ENDIF
C
       IF(GDUM .OR. FDUM .OR. GFDUM) THEN
C
       CALL DUM(MULTM,IGRID,GFDUM,GDUM,FDUM,MAX,IFILE,NI,NIM,NIP,
      1 NJ,NJM,NJP,NK,NKM,NKP,NKP2,JLST,NS,XREF,YREF,ZREF,AREF,CREF,
      1 RE,TLAST,F(Q),F(P),F(T),F(TV),F(B),F(PHI),F(A),F(X),
      1 F(Y),F(Z),F(VOL),F(CSR),F(RSR),F(PSR),F(TSR),F(TVSR),F(ASR),
      1 F(RUSR),F(RVSR),F(RWSR),F(RESR),F(EVSR),F(F133),F(F134),
      1 F(F135),F(F136),F(F137),F(F138),F(F139),WOLD)
C
       ENDIF
C
       STOP
       END
```

9.5.3 *diss.f*

This subroutine was modified to include Park's TTV effective temperature model and chemical rate relaxation.

```
C*************************************************************
       SUBROUTINE DISS(MULTM,ISTP,K,NI,NJ,NK,NIP,NJP,
      1 NKP,NS,NSLP,JLST,JCP,NR,IS,Q,TT,TV,CJAB,W,EGION,
      1 DUM1,DUM2,DUM3,DUM4,DUM5,DUM6,DUM7,DUM8,DUM9,DUM10,
      1 RHO,T,TTV,WM,STRN,SVIB,SELC,CMFC,FDW,WDEL,DSDF,GDUM1,
      1 GDUM2,GDUM3,GRT,GRVB,CM,DW,WOLD,WFAC,RESTA,
      2 TMODEL,QPARK,IPARK1,IPARK2)
       LOGICAL MULTM,RESTA,TMODEL
       DIMENSION KREX(53),CJAB(NIP,NJP,NKP,NSLP),
      1 Q(NIP,NJP,NKP,JLST),TT(NIP,NJP,NKP),
      1 TV(NIP,NJP,NKP),EGION(NI,NJ),W(NI,NJ,JCP),
      1 GRT(JCP,NI),CMFC(NR,6),STRN(NR,6),SVIB(NR,6),SELC(NR,6),
```

```
     1 IS(NR,6),FDW(NR,JCP),WDEL(NR,NI),
     1 DSDF(NR,NI),GDUM1(NR,NI),GDUM2(NR,NI),GDUM3(NR,NI),
     1 DW(JCP,NI),GRVB(JCP,NI),CM(JCP,NI),
     1 DUM1(NI),DUM2(NI),DUM3(NI),DUM4(NI),DUM5(NI),
     1 DUM6(NI),DUM7(NI),DUM8(NI),DUM9(NI),DUM10(NI),
     1 WM(NI),T(NI),TTV(NI),RHO(NI),
     2 TA(100),WOLD(IICPL,JJCPL,KKCPL,JSPEC)
      include 'cont1.inc'
      include 'indx1.inc'
      include 'reac1.inc'
      include 'therm1.inc'
C*************************************************************
      DATA GAS1/82.07835/
      DATA III/0/
      IF(III.EQ.0) THEN
      IF(MULTM) JRL=JCF-1
      THIRD=1./3.
      RHOC=32.2*454./(12.*2.54)**3. *RIN
      CONV=SCALE*SQRT(RIN/PIN)/RHOC
      CONVJ=CONV*RHOC
      TINC=TIN/1.8
      DO 1 KR=1,NRCT
    1 KREX(KR)=0
      DO 3 ICON=1,6
      DO 2 KR=1,NRCT
      IF(IPR(KR,ICON).EQ.0) THEN
      IF(ICON.LE.3) THEN
      KREX(KR)=KREX(KR)+1
      ELSE
      KREX(KR)=KREX(KR)-1
      ENDIF
      ENDIF
    2 CONTINUE
    3 CONTINUE
C
C   ****initialize WOLD array for chemical rate time relaxation****
      IF (.NOT.RESTA) THEN
        DO 777 IRF=1,NI
        DO 777 JRF=1,NJ
        DO 777 KRF=1,NK
        DO 777 JRRF=1,JC
 777    WOLD(IRF,JRF,KRF,JRRF)=0.
      ENDIF
C*****************************************************************
C*****CHECK TO SEE IF EXPLICIT PARAMETERS ARE SET HIGH ENOUGH******
C*****(IICPL,JJCPL,KKCPL,JSPEC)**********************************
C*****************************************************************
C
C
      III=1
      ENDIF
```

```
C
      DO 200 J=2,NJ
C
      DO 7 I=2,NI
      RHO(I)=Q(I,J,K,JRH)*RHOC
      T  (I)=TT(I,J,K)*TINC
      TTV(I)=TV(I,J,K)*TINC
      TA(I)=(TTV(I)**QPARK) * (T(I)**(1.-QPARK))
    7 CONTINUE
C
C
      DO 16 JR=1,JTRN
      DO 16 I=2,NI
   16 GRT(JR,I)=COEF(1,JR)*(1.-ALOG(T(I)))+COEF(2,JR)/T(I)
     1         -COEF(3,JR)
C
      IF(MULTM) THEN
C
      IF(JC.GT.5) THEN
      DO 11 I=2,NI
   11 GRT(JC,I)=COEF(1,JC)*(1.-ALOG(TTV(I)))+COEF(2,JC)/TTV(I)
     1          -COEF(3,JC)
      ENDIF
      DO 12 JR=1,JCL
      DO 12 I=2,NI
   12 GRVB(JR,I)=.0
      DO 13 JR=JVF,JVL
      DO 13 I=2,NI
      TTT=CVIB(JR)/TTV(I)
      TERM=EXP(TTT)
   13 GRVB(JR,I)=ALOG(1.-1./TERM)
      DO 15 JR=1,JCL
      DO 15 I=2,NI
      RTV=1./TTV(I)
      SUMQ=GDEGER(1,JR)+EXP(-CELRON(2,JR)*RTV)*GDEGER(2,JR)
     1                 +EXP(-CELRON(3,JR)*RTV)*GDEGER(3,JR)
      GRVB(JR,I)=GRVB(JR,I)-ALOG(SUMQ/GDEGER(1,JR))
   15 CONTINUE
C
      ELSE
C
      DO 17 JR=JVF,JVL
      DO 17 I=2,NI
      TTT=CVIB(JR)/T(I)
      TERM=EXP(TTT)
   17 GRT(JR,I)=GRT(JR,I)+ALOG(1.-1./TERM)
      DO 20 JR=1,JCL
      DO 20 I=2,NI
      RTT=1./T(I)
      SUMQ=GDEGER(1,JR)+EXP(-CELRON(2,JR)*RTT)*GDEGER(2,JR)
     1                 +EXP(-CELRON(3,JR)*RTT)*GDEGER(3,JR)
```

```
      GRT(JR,I)=GRT(JR,I)-ALOG(SUMQ/GDEGER(1,JR))
   20 CONTINUE
      ENDIF
C
C
      DO 33 KR=1,NRCT
      DO 32 I=2,NI
      GDUM1(KR,I)=(STRN(KR,1)*GRT(IS(KR,1),I)
     1   +STRN(KR,2)*GRT(IS(KR,2),I)+STRN(KR,3)*GRT(IS(KR,3),I))
     1  -(STRN(KR,4)*GRT(IS(KR,4),I)+STRN(KR,5)*GRT(IS(KR,5),I)
     1   +STRN(KR,6)*GRT(IS(KR,6),I))
      GDUM2(KR,I)=(SVIB(KR,1)*GRVB(IS(KR,1),I)
     1   +SVIB(KR,2)*GRVB(IS(KR,2),I)+SVIB(KR,3)*GRVB(IS(KR,3),I))
     1  -(SVIB(KR,4)*GRVB(IS(KR,4),I)+SVIB(KR,5)*GRVB(IS(KR,5),I)
     1   +SVIB(KR,6)*GRVB(IS(KR,6),I))
      GDUM3(KR,I)=(SELC(KR,1)*GRT(IS(KR,1),I)
     1   +SELC(KR,2)*GRT(IS(KR,2),I)+SELC(KR,3)*GRT(IS(KR,3),I))
     1  -(SELC(KR,4)*GRT(IS(KR,4),I)+SELC(KR,5)*GRT(IS(KR,5),I)
     1   +SELC(KR,6)*GRT(IS(KR,6),I))
   32 CONTINUE
   33 CONTINUE
C
      DO 8 JR=1,JC
      DO 8 I=2,NI
      CM(JR,I)=RHOC*AMAX1(1.E-18,Q(I,J,K,JR)*RMOL(JR))
      GRT(JR,I)=1.E-20
    8 DW(JR,I)=1.E-20
C
      DO 36 KR=1,NRCT
      DO 35 I=2,NI
      TRAT =TTV(I)/T(I)
      GDVIB=(ABS(GDUM2(KR,I))+ABS(GDUM3(KR,I)))*TRAT
      GDTRN= AMAX1(1.E-10,ABS(GDUM1(KR,I)))
      FAC1 = AMAX1(.0,AMIN1(1.,GDTRN/(GDTRN+GDVIB)))
      TEQV=TTV(I)/(FAC1*TRAT+(1.-FAC1))
C   ****assign appropriate temperature to TEQV2 according to Park****
      IF (TMODEL) THEN
        TEQV2=TA(I)
        IF (KR.GT.IPARK1) THEN
          TEQV2=T(I)
          IF (KR.GE.IPARK2) TEQV2=TTV(I)
        ENDIF
      TEQV=TEQV2
      ENDIF
C   ********************************************************************
      GDUM =AMAX1(-50.,
     1      AMIN1(50.,(GDUM1(KR,I)+GDUM2(KR,I)+GDUM3(KR,I))))
      ETERM=AMAX1(-50.,AMIN1(50.,COEFB(KR)/TEQV))
      AKF =COEFA(KR)*EXP(-ETERM)*TEQV**ETA(KR)
      AKB =AKF*EXP(-GDUM)*(GAS1*TEQV)**KREX(KR)
      AKF1=AKF*CM(IS(KR,1),I)
```

```
C
      P23 =CM(IS(KR,2),I)*CM(IS(KR,3),I)
      AKB1=AKB*CM(IS(KR,4),I)
      P56 =CM(IS(KR,5),I)*CM(IS(KR,6),I)
      DSDF(KR,I)=
     1   AKF1*(CM(IS(KR,2),I)*CMFC(KR,3)+CM(IS(KR,3),I)*CMFC(KR,2))
     1  +AKF *P23*CMFC(KR,1)
     1  +AKB1*(CM(IS(KR,5),I)*CMFC(KR,6)+CM(IS(KR,6),I)*CMFC(KR,5))
     1  +AKB *P56*CMFC(KR,4)
      WDEL(KR,I)=AKF1*P23-AKB1*P56
   35 CONTINUE
   36 CONTINUE
C
C
      DO 44 JR=JCF,JCL
      DO 43 KR=1,NRCT
      DO 42 I=2,NI
      GRT(JR,I)=GRT(JR,I)+    FDW(KR,JR) *WDEL(KR,I)
   42 DW (JR,I)=DW (JR,I)+ABS(FDW(KR,JR))*DSDF(KR,I)
   43 CONTINUE
   44 CONTINUE
C
      DO 51 JR=JCF,JCL
      NJR=JR-JADD
      DO 50 I=2,NI
        IFAC=MIN0(1,IFIX(5.E-3*T(I)))
        CJAB(I,J,K,NJR)=IFAC* DW(JR,I)*CONVJ
C*******modified W for chemical rate time relaxation******
        W(I,J,   JR)=IFAC*GRT(JR,I)*WMOL(JR)*CONV
        W(I,J,JR)=WFAC*W(I,J,JR)+(1.-WFAC)*WOLD(I,J,K,JR)
   50   WOLD(I,J,K,JR)=W(I,J,JR)
   51 CONTINUE
C
C
      IF(MULTM) THEN
C
      IF(JRL.GT.1) THEN
      DO 54 JR=1,JRL
      DO 53 KR=1,NRCT
      DO 52 I=2,NI
      GRT(JR,I)=GRT(JR,I)+    FDW(KR,JR) *WDEL(KR,I)
   52 DW (JR,I)=DW (JR,I)+ABS(FDW(KR,JR))*DSDF(KR,I)
   53 CONTINUE
   54 CONTINUE
      DO 56 JR=1,JRL
      DO 55 I=2,NI
                IFAC=MIN0(1,IFIX(5.E-3*T(I)))
   55    W(I,J,   JR)=IFAC*GRT(JR,I)*WMOL(JR)*CONV
   56 CONTINUE
      ENDIF
C
```

```
      DO 61 I=2,NI
   61 EGION(I,J)=.0
C
      IF(KIONF.LE.NRCT) THEN
      DO 65 KR=KIONF,NRCT
      JION=KIONR(KR)
      DO 64  I=2,NI
   64 EGION(I,J)=EGION(I,J)+CONV*EION(KR)*FDW(KR,JION)*WDEL(KR,I)
   65 CONTINUE
      ENDIF
      ENDIF
C
C
  200 CONTINUE
      RETURN
      END
```

9.5.4 *disq.f*

This subroutine was modified to inclued Appleton and Bray's translational coupling between heavy particles and free electrons.

```
C*********************************************************
      SUBROUTINE DISQ(K,NI,NJ,NIP,NJP,NKP,NS,NSLP,JLST,JCP,NR,
     1 Q,P,T,TTV,CJAB,W,EGION,EDIF,SUM1,SUM2,SUM3,SUM4,SUM5,
     1 SUM6,SUMWEV,SUM,PRESS,RHO,TT,TV,
     1 DUM1,DUM2,DUM3,DUM4,DUM5,DUM6,DUM7,DUM8,DUM9,DUM10,
     1 DUM11,DUM12,DUM13,DUM14,DUM15)
      DIMENSION RHO(NI),PRESS(NI),TT(NI),TV(NI),SUM1(NI),
     1 SUM2(NI),SUM3(NI),SUM4(NI),SUM5(NI),SUM6(NI),SUMWEV(NI),
     1 SUM(NI),EDIF(NI),CJAB(NIP,NJP,NKP,NSLP),W(NI,NJ,JCP),
     1 DUM5(NR,6),Q(NIP,NJP,NKP,JLST),P(NIP,NJP,NKP),
     1 DUM6(NR,JCP),T(NIP,NJP,NKP),TTV(NIP,NJP,NKP),EGION(NI,NJ),
     1 DUM1(NI),DUM2(NR,6),DUM3(NR,6),DUM4(NR,6),DUM7(NR,NI),
     1 DUM8(NR,NI),DUM9(NR,NI),DUM10(NR,NI),DUM11(NR,NI),
     1 DUM12(JCP,NI),DUM13(JCP,NI),DUM14(JCP,NI),DUM15(JCP,NI),
     1 ICCS(10),CCS(3,10),SUMNEW(100)
c*****NOTE: dimension on SUMNEW assumes NI<=100*****
      LOGICAL TECPL
      include 'cont1.inc'
      include 'indx1.inc'
      include 'therm1.inc'
C*************************************************************
      DATA III/0/
      IF(III.EQ.0) THEN
      THIRD=1./3.
      CONS18=1.8*CONS
      TCON  =TIN/1.8
      TSKCON=5000./TCON
      ELCON=1.5*28.853*RMOL(JC)
```

```
      RHCON=1000.*32.2*454.*RIN/(12.*2.54)**3
      PCON =PIN/2116.8
      CONV =SQRT(RIN/PIN)*SCALE
      CONEE=6.02E26*SQRT(WMOL(JC)*8.*8314./3.14159)
      C1   =5.9E-12
      C2   =SQRT(WMOL(JC))/(CONEE*2.5E-12)/RHCON
      TSK  =(1.+2.*GAMMA*(ACH**2-1.)/(GAMMA+1.))
     1     *(2./((GAMMA+1.)*ACH**2)+(GAMMA-1.)/(GAMMA+1.))
      TVSK=1.
      DTSK=TSK-TVSK
      SKPOW=3.5*EXP(-TSKCON/TSK)-1.
      WRITE(6,*) ELCON,RHCON,PCON,CONV
      WRITE(6,*) CONEE,C1,C2
C***********added in DATA loop for Gnoffo's T-E coupling***********
C***********-->TECPL is the flag for trans.-electron coupling
C***********-->TECPL=TRUE for Gnoffo's version of trans-elecr. cpling.
C***********-->TECPL=FALSE for Tam's version
      READ(88,*)
      READ(88,*)TECPL
      IF (TECPL) THEN
        BOLTZ=1.380622E-23 * 1.E24
        ESU=1.5188E-14 * 1.E12
        PI=3.14159
        AVOG=6.02E26/1.E8
c        write(*,*)' k,e,N = ',BOLTZ,ESU,AVOG
        A1=(ESU**4)*AVOG*8.*THIRD
        A2=SQRT(PI*AVOG*RMOL(JC)/8./BOLTZ**3)
        B1=(BOLTZ/PI**THIRD/ESU/ESU)**3
c        write(*,*)'A1,A2,B1= ',A1,A2,B1
        READ(88,*) KMAX
        DO 200 KK=1,KMAX
 200    READ(88,*) ICCS(KK),(CCS(J,ICCS(KK)),J=1,3)
        CLOSE(88)
c
        WRITE(*,*) KMAX
        DO 1000 KK=1,KMAX
 1000   WRITE(*,*) KK,ICCS(KK),(CCS(J,ICCS(KK)),J=1,3)
C
C************indexing for collision frequency of ions*************
C**NOTE: fix indexing for species sets with no electrons maybe????
        write(*,*) '********KMAX = ', KMAX
        KPNTR=KMAX
        DO 210 JR=1,JC-1
          KKFLAG=1
          DO 205 KK=1,KMAX
 205         IF (JR.EQ.ICCS(KK)) KKFLAG=0
          IF (KKFLAG.EQ.1) THEN
            KPNTR=KPNTR+1
            ICCS(KPNTR)=JR
          ENDIF
 210    CONTINUE
```

```
C
c        do 1001 KK=KMAX+1,JC-1
c 1001   write(*,*) KK,ICCS(KK)
c        write(*,*)KPNTR,JC,'       KPNTR,JC'
      ENDIF
C
      III  =1
C*****************************
      ENDIF
C--------------------VIBRATIONAL COUPLING
      DO 100 J=2,NJ
      DO 1 I=2,NI
      TT(I)=T(I,J,K)*TCON
      TV(I)=TTV(I,J,K)*TCON
      RHO(I)=Q(I,J,K,JRH)*RHCON
      PRESS(I)=P(I,J,K)*PCON
      SUMWEV(I)=.0
      SUM1(I)=.0
      SUM2(I)=.0
      SUM3(I)=.0
      SUM4(I)=.0
      SUM5(I)=.0
    1 SUM6(I)=.0
C
      IF(JC.GT.5) THEN
      DO 2 I=2,NI
      SUM5(I)=Q(I,J,K,JC)*(COEF(1,JC)+COEF(2,JC)/TV(I)-1.)
     1       *TV(I)*RMOL(JC)
    2 SUM6(I)=Q(I,J,K,JC)*(COEF(1,JC)+COEF(2,JC)/TT(I)-1.)
     1       *TT(I)*RMOL(JC)
      ENDIF
C
      DO 3 JR=JVF,JVL
      DO 3 I=2,NI
      XCC=Q(I,J,K,JR)*RMOL(JR)
      SUM1(I)=SUM1(I)+XCC
      SUM2(I)=SUM2(I)+XCC*XCC*SQRT(RMOL(JR))
      TTT=.5*CVIB(JR)/TT(I)
      TERM=EXP(TTT)
      RTERM=1./TERM
      TERM1=2.*TTT/(TERM-RTERM)
    3 SUM3(I)=SUM3(I)+Q(I,J,K,JR)*(TTT+TERM1*RTERM)*TT(I)*RMOL(JR)
      DO 4 JR=JVF,JVL
      DO 4 I=2,NI
      TTT=.5*CVIB(JR)/TV(I)
      TERM=EXP(TTT)
      RTERM=1./TERM
      TERM1=2.*TTT/(TERM-RTERM)
      ERB=(TTT+TERM1*RTERM)*TV(I)*RMOL(JR)
      SUM4(I)=SUM4(I)+Q(I,J,K,JR)*ERB
    4 SUMWEV(I)=SUMWEV(I)+ERB*W(I,J,JR)
```

```
C
      DO 5 JR=1,JCL
      DO 5 I=2,NI
      RTV=1./TV(I)
      GEX2=EXP(-CELRON(2,JR)*RTV)*GDEGER(2,JR)
      GEX3=EXP(-CELRON(3,JR)*RTV)*GDEGER(3,JR)
      SUMQ=GDEGER(1,JR)+GEX2+GEX3
      SUMCQ=GEX2*CELRON(2,JR)+GEX3*CELRON(3,JR)
      ERB=(SUMCQ/SUMQ+COEF(4,JR)*THIRD*TV(I)**3-COEF(5,JR)*RTV)
     1    *RMOL(JR)
      SUM5(I)=SUM5(I)+Q(I,J,K,JR)*ERB
      SUMWEV(I)=SUMWEV(I)+ERB*W(I,J,JR)
    5 CONTINUE
      DO 7 JR=1,JCL
      DO 7 I=2,NI
      RTT=1./TT(I)
      GEX2=EXP(-CELRON(2,JR)*RTT)*GDEGER(2,JR)
      GEX3=EXP(-CELRON(3,JR)*RTT)*GDEGER(3,JR)
      SUMQ=GDEGER(1,JR)+GEX2+GEX3
      SUMCQ=GEX2*CELRON(2,JR)+GEX3*CELRON(3,JR)
      SUM6(I)=SUM6(I)+Q(I,J,K,JR)*(SUMCQ/SUMQ
     1       +COEF(4,JR)*THIRD*TT(I)**3-COEF(5,JR)*RTT)*RMOL(JR)
    7 CONTINUE
C
      DO 10 I=2,NI
      DTCL=ABS(TSK-TTV(I,J,K))
      CORRL=(DTCL/DTSK)**SKPOW
      DEVIB=(SUM3(I)-SUM4(I))*CORRL*CONS18
      TSCLE=C1*EXP(220./TT(I)**.33333)/PRESS(I)
     1     +C2*SUM1(I)*TT(I)**1.5/SUM2(I)
      EDIF(I)=((SUM4(I)-SUM3(I))+(SUM5(I)-SUM6(I)))*CONS18
      EDIF(I)=EDIF(I)+SIGN(1.E-10,EDIF(I))
      CWES=AMIN1(.0,SUMWEV(I)*CONS18/EDIF(I))
      CONST1=CONV/TSCLE
      W(I,J,JCP)      = CONST1*DEVIB + CWES*EDIF(I)
      CJAB(I,J,K,NSLP)= CONST1 - CWES
   10 CONTINUE
C
C--------------------ELECTRON IMPACT
C
      IF(JE1.GT.0) THEN
      DO 21 I=2,NI
   21 SUM(I)=.0
      DO 22 JR=JE1,JE2
      DO 22 I=2,NI
   22 SUM(I)=SUM(I)+ELCRS(JR)*Q(I,J,K,JR)*RMOL(JR)**2
C********Gnoffo's T-E coupling************************************
      IF (TECPL) THEN
      DO 821 I=2,NI
  821 SUMNEW(I)=0.
C*******neutral particles*******
```

```
      DO 822 KK=1,KMAX
      JR=ICCS(KK)
      DO 822 I=2,NI
        SIGMAE=CCS(1,JR)+CCS(2,JR)*TV(I)+CCS(3,JR)*TV(I)*TV(I)
        CFREQP=RMOL(JR)*RMOL(JC)*SIGMAE*CONEE*SQRT(TV(I))
        SUMNEW(I)=SUMNEW(I)+Q(I,J,K,JR)*CFREQP*RMOL(JR)
 822  CONTINUE
C
C*******charged particles*******
      DO 823 KK=KMAX+1,JC-1
      JR=ICCS(KK)
      DO 823 I=2,NI
        DELEC=AMAX1(1.E-18,Q(I,J,K,JC))
        B2=WMOL(JC)*TV(I)**3/AVOG/1.E8/RHCON/DELEC
        CFREQP=A1*A2*RMOL(JR)/TV(I)**1.5
     +         *ALOG(B1*B2)
 823    SUMNEW(I)=SUMNEW(I)+Q(I,J,K,JR)*CFREQP*RMOL(JR)
      ENDIF
C
      DO 25 I=2,NI
      CONST2=2.*CONV*RHCON*SUM(I)*TV(I)*SQRT(TV(I))
c
      DTTV=(T(I,J,K)-TTV(I,J,K))
      IF (TECPL) THEN
C       **CONST3 is for Gnoffo's T-E coupling & shoud have**
C       **the same basic form and units as Tam's CONST2**
        CONST3=2.*CONV*RHCON*SUMNEW(I)*WMOL(JC)
        CONST2=CONST3
C
      ENDIF
      WSOR=CONST2*Q(I,J,K,JC)*ELCON*DTTV
      W(I,J,JCP)      =W(I,J,JCP)   +WSOR - EGION(I,J)
      CJAB(I,J,K,NSLP)=CJAB(I,J,K,NSLP) + CONST2
     1                +ABS(EGION(I,J)/EDIF(I))
   25 CONTINUE
      ENDIF
  100 CONTINUE
      RETURN
      END
```

9.5.5 *dum.f*

The only modification to this subroutine was to include the variable TCH (chemical time-step modification) in the restart file.

9.5.6 *radcalc.f*

This subroutine was added to call the radiation routines from INEQ3D.

```
      SUBROUTINE RADCALC(DQDY,I,K,NI,NJ,NK,NIP,NJP,NKP,Q,P,T,
```

```
     1 TV,X,Y,Z,JC,JLST,JRH,IPRAD)
      include 'therm1.inc'
      include 'cont1.inc'
      COMMON /INEQVARS/ PRSR(99),TE(99),TTRANS(99),DIST(99),QQ(99,12)
      COMMON /WALRAD/ FIPI1, TLCP1
      DIMENSION DQDY(100),Q(NIP,NJP,NKP,JLST),P(NIP,NJP,NKP),
     1 T(NIP,NJP,NKP),TV(NIP,NJP,NKP),X(NI,NJ,NK),Y(NI,NJ,NK),
     1 Z(NI,NJ,NK)
C*********************************************************************
C
C***IPRAD = 0 for supressed output and coupled version of Qi,j,k,jr***
C***IPRAD = 1 for radiation output and post-proc. vers. of Qi,j,k,jr**
      DIST(1)=0.
      IM=I-1
      KM=K-1
      DO 100 J=1,NJ
        DQDY(J)=0.
        JM=MAXO(1,J-1)
        PRSR(J)=P(I,JM+1,K)
        TE(J)=TV(I,JM+1,K)
        TTRANS(J)=T(I,JM+1,K)
        XK=.25*(X(I,J,K)+X(IM,J,K)+X(I,JM,K)+X(IM,JM,K))
        YK=.25*(Y(I,J,K)+Y(IM,J,K)+Y(I,JM,K)+Y(IM,JM,K))
        ZK=.25*(Z(I,J,K)+Z(IM,J,K)+Z(I,JM,K)+Z(IM,JM,K))
        XKM=.25*(X(I,J,KM)+X(IM,J,KM)+X(I,JM,KM)+X(IM,JM,KM))
        YKM=.25*(Y(I,J,KM)+Y(IM,J,KM)+Y(I,JM,KM)+Y(IM,JM,KM))
        ZKM=.25*(Z(I,J,KM)+Z(IM,J,KM)+Z(I,JM,KM)+Z(IM,JM,KM))
        XC=.5*(XK+XKM)
        YC=.5*(YK+YKM)
ZC=.5*(ZK+ZKM)
        IF (J.GT.1) THEN
          DD=((XC-XCOLD)**2.+(YC-YCOLD)**2.+(ZC-ZCOLD)**2.)**0.5
          DIST(J)=DIST(JM) +DD
        ENDIF
        XCOLD=XC
        YCOLD=YC
        ZCOLD=ZC
        DO 150 JR=1,JC
          QQ(J,JR)=Q(I,JM+1,K,JR)/Q(I,JM+1,K,JRH)
 150    CONTINUE
        QQ(J,JRH)=Q(I,JM+1,K,JRH)
 100  CONTINUE
C
      CALL RADHEAT(DQDY,NJ,JC,JLST,PIN,TIN,RIN,SCALE,IPRAD)
C
C     WRITE RADIATIVE HEATING VALUES AT WALL TO FILE
C     FIPI1 IS THE CONTINUUM HEAT FLUX TO THE WALL
C     TLCP1 IS THE TOTAL LINE CONTRIBUTION TO THE HEAT FLUX TO THE WALL
C     FIPI1+TLCP1 IS THE TOTAL RADIATIVE HEAT FLUX TO THE WALL
      IF (IPRAD.EQ.1) WRITE(55,*) I,FIPI1,TLCP1,FIPI1+TLCP1
      RETURN
```

```
      END
```

9.5.7 *reror.f*

This subroutine was modified to output the RMS difference of the solution vector, the value and location of the maximum difference, and the maximum and minimum time steps.

```
C*****************************************************************
      SUBROUTINE REROR(MULTM,FSTP,ISTP,IFILE,MAX,NI,NJ,NK,
     1 NIP,NJP,NKP,NLST,DELQ,DIFMAX,DIFMX1,A,DUM,DT)
      INTEGER FSTP,FSTP1
      LOGICAL MULTM
      DIMENSION DELQ(NIP,NJP,NKP,NLST),DIFMAX(NLST),DRMS(20),
     1 DUM(MAX),A(NIP,NJP,NKP),DIFMX1(NLST),IDM(20),JDM(20),
     2 DT(NI,NJ,NK)
      include 'cont1.inc'
      include 'indx1.inc'
C*****************************************************************
      DATA III/0/
      IF(III.EQ.0) THEN
      JCNSL=JC-NSL
      FSTP1=FSTP+20
      HINFY=1.+GBNEQ+.5*GAMMA*ACH**2
      PST=(1.-GAMMA+2.*GAMMA*ACH**2)*((1.+GAMMA)**2*ACH**2/
     1    (4.*GAMMA*ACH**2-2.*(GAMMA-1.)))**GA/(1.+GAMMA)
      RST=GA*PST/HINFY
      RRST=1./RST
      RSTHIN=1./(RST*HINFY)
      ACHSGM=1./(ACH*SQRT(GAMMA))
      DO 1 NJR=1,NLST
    1 DIFMAX(NJR)=.0
      III=1
      ENDIF

C****************ADDED TO FIND MAX AND MIN TIME STEP VALUES**********
      DTMAX=0.
      DTMIN=9999.
      DO 600 J=2,NJ
        DTMAX=AMAX1(DTMAX,DT(2,J,2))
        DTMIN=AMIN1(DTMIN,DT(2,J,2))
  600 CONTINUE
C*************WRITE DTMAX AND DTMIN TO OUTPUT FILE***************
      WRITE(8,*)'ITER,DTMAX,DTMIN:  ',ISTP,DTMAX,DTMIN
C*****************************************************************
C
C*****************ADDED LINES FOR RMS OF THE CHANGE IN Q*********
      DO 3 NJR=1,NLST
      DRMS(NJR)=0.0
      DO 2 K=2,NK
      DO 2 J=2,NJ
```

```
  495 DT(I,J,K)=DT(I,J,K)*TCH*RMAX/(.5+RMAX)
C
      DO 490 NJR=NS1,NSL
      JR=NJR+JADD
      DO 490 J=2,NJ
      DO 490 I=2,NI
      IFAC1=MIN0(1,IFIX(Q(I,J,K,JRH)*1.E6 -1.))
      IFAC2=10*MIN0(1,IFIX(Q(I,J,K,JR )*1.E4/Q(I,J,K,JRH)-1.))
      TERM =IFAC1*DT(I,J,K)*VOL(I,J,K)*W(I,J,JR)
      CRHO=Q(I,J,K,JR)+1.E-4
      TCHN=AMIN1(TCHN,CRHO/(CRHO+IFAC2*ABS(TERM)))
  490 W(I,J,JR)=TERM
C
      DO 496 NJR=1,NLST
      DO 496 J=2,NJ
      DO 496 I=2,NI
  496 DELQ(I,J,K,NJR)=-DT(I,J,K)*DELQ(I,J,K,NJR)
      DO 497 NJR=NS1,NSL
      JR=NJR+JADD
      DO 497 J=2,NJ
      DO 497 I=2,NI
      CJAB(I,J,K,NJR)=CJAB(I,J,K,NJR)*VOL(I,J,K)
  497 DELQ(I,J,K,NJR)=(DELQ(I,J,K,NJR)+W(I,J,JR))
      IF(MULTM) THEN
      DO 498 J=2,NJ
      DO 498 I=2,NI
      IFAC1=MIN0(1,IFIX(Q(I,J,K,JRH)*1.E6-1.))
      DELQ(I,J,K,NJEV)=DELQ(I,J,K,NJEV)
     1                 +IFAC1*DT(I,J,K)*VOL(I,J,K)*W(I,J,JCP)
  498 CJAB(I,J,K,NSLP)=CJAB(I,J,K,NSLP)*VOL(I,J,K)
      ENDIF
C
C********RADIATION COUPLING FOR THE GLOBAL ENERGY EQUATION********
      IF (RAD2) THEN
        DO 920 J=2,NJ
        DO 920 I=1,NI
          IFAC1=MIN0(1,IFIX(Q(I,J,K,JRH)*1.E6 - 1.))
 920      DELQ(I,J,K,NJE)=DELQ(I,J,K,NJE)+IFAC1*DT(I,J,K)*VOL(I,J,K)
     +                    *RADFLX(I,J,K)
C
C****RADIATION CPLNG FOR VIB-ELECRON-ELECTRONIC ENERGY EQUATION****
        IF (MULTM.AND.RADVEE) THEN
          DO 940 J=2,NJ
          DO 940 I=2,NI
            IFAC1=MIN0(1,IFIX(Q(I,J,K,JRH)*1.E6 - 1.))
 940        DELQ(I,J,K,NJEV)=DELQ(I,J,K,NJEV)+IFAC1*DT(I,J,K)
     +                       *VOL(I,J,K)*RADFLX(I,J,K)
        ENDIF
      ENDIF
C
  500 CONTINUE
```

```
TCH=TCHN
RETURN
END
```

9.5.9 *start.f*

The only modification to this subroutine was to include the variable TCH (chemical time step modification) in the restart file.